

THE MOTION OF A GLOW DISCHARGE  
UNDER THE INFLUENCE OF A TRANSVERSE MAGNETIC FIELD

A thesis submitted for  
the degree of Doctor of Philosophy  
in the Australian National University

I.S. FALCONER

SAVANNAH  
GEORGIA  
MAY 1865

## INTRODUCTION

This thesis describes an experimental study of the motion of a glow discharge under the influence of a strong transverse magnetic field, at moderate gas pressures. Conditions were generally such that  $\omega_e T_e$  was of the order of 1, where  $\omega_e$  is the electron cyclotron frequency, and  $T_e$  the mean time between the collisions of an electron with neutral gas molecules. Experiments were mostly performed with discharge currents of the order of tens of milliamperes, so that the directed velocity given to the gas by the ions and electrons of the moving discharge was negligible compared with the velocity of the discharge.

It was found that the nature of the motion of the discharge underwent a radical change at pressures such that  $\omega_e T_e$  was of the order of 1. At pressures above that at which this transition occurs the velocity of the discharge is determined largely by the cathode region of the discharge. However this region is pulled along by the remainder of the discharge at a velocity greater than that which it would have if it alone determined the velocity of the discharge. A theoretical study, (along with a suggestive, but not conclusive, experimental result) indicates that the negative glow region controls the velocity of the discharge under these conditions.

There is some evidence that at pressures below the

transition pressure, the velocity is controlled by the anode region of the discharge.

Candidate's Contribution to this Project

Chapter 1

The candidate is entirely responsible for selection of the work discussed, and any criticism of this work.

Chapter 2

The candidate was jointly responsible with Dr. A.H. MORTON, and G.F. CAWSEY, for the design and construction of the apparatus described in this chapter. The experimental work, and the interpretation of this work, was the candidate's responsibility, although Dr. MORTON closely supervised this work, and planned much of the experimental work described in this chapter.

Chapter 3

The discharge chamber and ancillary equipment were designed by the candidate, at Dr. MORTON'S suggestion. The experimental program was planned and carried out entirely by the candidate.

Chapter 4

The equipment was designed and the experimental work carried out entirely by the candidate.

Chapter 5

The theory was developed by the candidate from suggestions by J.W. BLAMEY (Sections 5.2 and 5.3) and Dr. MORTON (Section 5.4).

It should be pointed out that at no stage of this project was the candidate working entirely alone. Assistance, advice and criticism were freely asked for, and freely given.

---

98 Falconer  
4/4/63

### ACKNOWLEDGEMENTS

The candidate wishes to express his thanks to the following, whose assistance and encouragement contributed greatly to the completion of this project.

The AUSTRALIAN NATIONAL UNIVERSITY for the opportunity to study under an A.N.U. Research Scholarship.

Professor SIR MARK OLIPHANT for his interest in, and encouragement of, this research project.

J.W. BLAMEY, and Dr. A.H. MORTON, for guidance, assistance, and helpful criticism.

The technical and academic staff of the Research School of Physical Sciences, for assistance willingly given. Particular thanks must be given to R.G. GOLDBERG, L. DOWEN, and P. EGENER.

Fellow students, R.H. HOSKING, A.G. PULFORD, and P.W. SEYMOUR, and G.F. CAWSEY, a Public Service Fellow of the University (1959), for assistance, and helpful discussion.

Miss M. MACKIE, for her careful typing of this thesis.

*I.S. Falconer.*

(I.S. Falconer)  
4th April, 1963

## CONTENTS

|  | <u>Page No.</u> |
|--|-----------------|
| <u>INTRODUCTION</u>  | i               |
| <u>ACKNOWLEDGEMENTS</u>  | iv              |
| <u>CONTENTS</u>  | v               |
| <u>CHAPTER 1. THE GAS DISCHARGE IN A TRANSVERSE<br/>MAGNETIC FIELD - A REVIEW OF THEORY AND<br/>EXPERIMENT</u> | 1               |
| 1. 1 <u>General references</u>   | 4               |
| 1. 2 <u>The Glow Discharge and the Arc Discharge</u>   | 6               |
| 1. 3 <u>The Glow Discharge</u>   | 10              |
| 1. 3. 1   The cathode region   | 10              |
| 1. 3. 2   The negative glow and the Faraday dark space   | 18              |
| 1. 3. 3   The positive column  | 19              |
| 1. 3. 4   The anode region   | 22              |
| 1. 4 <u>The Arc Discharge</u>  | 22              |
| 1. 4. 1   The cathode region   | 22              |
| 1. 4. 2   The positive column  | 26              |
| 1. 4. 3   The anode region   | 27              |
| 1. 5 <u>Early Studies of the Motion of a Glow Discharge<br/>in a Transverse Magnetic Field</u>                 | 28              |
| 1. 6 <u>The Work of Guye</u>   | 33              |
| 1. 6. 1   Experimental results   | 36              |
| 1. 6. 2   Theory of the rotation of the discharge  | 40              |
| 1. 7 <u>The Arc Discharge in a Transverse Magnetic Field:<br/>Retrograde Motion</u>                            | 44              |

|       |  |    |
|-------|--|----|
| 1.8   | <u>Recent Work on the Glow Discharge in a Transverse Magnetic Field</u>  | 55 |
| 1.9   | <u>A Critical Summary of the Previous Work on the Motion of a Gas Discharge in a Transverse Magnetic Field</u> | 63 |
| 1.9.1 | Experimental studies of the moving glow discharge  | 63 |
| 1.9.2 | The theory of the motion of the glow discharge   | 67 |
| 1.9.3 | The motion of the arc  | 68 |
| 1.9.4 | The relationship between the work described in this thesis, and the previous work                              | 69 |

CHAPTER 2. INITIAL STUDIES OF THE MOTION OF THE GLOW DISCHARGE IN A TRANSVERSE MAGNETIC FIELD: EXPERIMENTS WITH THE "RACETRACK"

CHAMBER 71

|       |  |     |
|-------|--|-----|
| 2.1   | <u>Experimental Apparatus</u>                                      | 71  |
| 2.1.1 | The discharge chamber  | 71  |
| 2.1.2 | The power supply   | 78  |
| 2.1.3 | The magnet   | 78  |
| 2.1.4 | The vacuum system  | 86  |
| 2.1.5 | Light detection and velocity measurement                           | 94  |
| 2.2   | <u>Early Experiments: Lack of Reproduceability, and its Causes</u> | 96  |
| 2.3   | <u>The Source of the Motion</u>                                    | 101 |
| 2.4   | <u>The Shape of the Moving Discharge</u>                           | 103 |
| 2.5   | <u>Conclusions</u>   | 124 |

CHAPTER 3. THE EFFECT OF THE LENGTH OF THE DISCHARGE, AND THE ELECTRODE GEOMETRY ON THE MOTION OF THE DISCHARGE

126

|  | <u>Page No.</u> |
|--|-----------------|
| 3.1 <u>Experimental Apparatus</u>  | 126             |
| 3.1.1 The discharge chamber  | 126             |
| 3.1.2 The vacuum system  | 133             |
| 3.1.3 The power supply, the magnet, and the<br>velocity measuring equipment  | 135             |
| 3.2 <u>Lack of Reproduceability - Further Observations</u>   | 136             |
| 3.3 <u>The Two Modes of Rotation of the Discharge</u>  | 141             |
| 3.3.1 The nature of the transition   | 142             |
| 3.3.2 Dependence of the transition pressure on<br>the experimental gas   | 165             |
| 3.4 <u>The Influence of the Radii of the Electrodes, and<br/>        the Polarity of the Centre Electrode, on the<br/>        Behaviour of the Discharge</u> | 168             |
| 3.4.1 The motion of a long discharge   | 174             |
| 3.4.2 The motion of short discharges   | 181             |
| 3.4.3 The motion of a discharge of medium length   | 185             |
| 3.4.4 The shape of a long discharge  | 190             |
| 3.5 <u>The Dependence of the Transition Pressure on the<br/>        Magnetic Field</u>   | 194             |
| 3.6 <u>The Dependence of the Period of Rotation on the<br/>        Discharge Current</u>   | 195             |
| 3.7 <u>The Electric Field in the Positive Column of the<br/>        Discharge</u>  | 200             |
| 3.8 <u>The Influence of Electrode Shape on the Motion<br/>        of the Discharge</u>   | 207             |
| 3.9 <u>"Spokes"</u>  | 212             |
| 3.10 <u>Conclusions</u>  | 214             |

|   |     |
|---|-----|
| <u>CHAPTER 4. EXPERIMENTS WITH<br/>SPECTROSCOPICALLY PURE GASES</u>   | 216 |
| 4.1 <u>Experimental Apparatus</u>   | 216 |
| 4.1.1 The discharge chamber   | 216 |
| 4.1.2 The vacuum system   | 219 |
| 4.1.3 The magnet, power supply, and light detection<br>equipment  | 222 |
| 4.2 <u>The Cleanliness of the Electrodes</u>  | 222 |
| 4.3 <u>Experimental Results</u>   | 223 |
| <u>CHAPTER 5. SOME THEORETICAL ASPECTS OF THE<br/>MOTION OF A GLOW DISCHARGE IN A TRANSVERSE<br/>MAGNETIC FIELD</u> | 227 |
| 5.1 <u>The Motion of Charged Particles in Steady Electric<br/>            and Magnetic Fields</u>                   | 227 |
| 5.1.1 Motion in a magnetic field - no collisions  | 227 |
| 5.1.2 Motion in crossed electric and magnetic<br>fields - no collisions   | 228 |
| 5.1.3 The effect of collisions  | 230 |
| 5.1.4 Drift velocity  | 232 |
| 5.2 <u>The Velocity of an Unconstrained Positive Column</u>   | 234 |
| 5.2.1 Theory of the motion of a positive column   | 235 |
| 5.2.2 Comparison of this theory with experiment   | 238 |
| 5.3 <u>The Negative Glow as the Velocity Controlling<br/>            Region of the Discharge</u>                    | 245 |
| 5.4 <u>Control of the Velocity of the Discharge by the<br/>            Cathode Fall Region</u>                      | 246 |

APPENDICES

|     |  |     |
|-----|--|-----|
| A 1 | <u>The Shape of the Discharge - Further Contour<br/>Diagrams</u> | 253 |
| A 2 | <u>Liquid Air Level Controller</u>                               | 258 |
| A 3 | <u>The Rail Discharge Experiment</u>                             | 263 |

BIBLIOGRAPHY

|      |  |     |
|------|--|-----|
| B. 1 | <u>Papers Referred to in this Thesis</u>   | 270 |
| B. 2 | <u>The Motion of an Arc in a Transverse Magnetic<br/>Field - Papers Published Since 1944</u> | 279 |

---

## Chapter 1

### THE GAS DISCHARGE IN A TRANSVERSE MAGNETIC FIELD - A REVIEW OF THEORY AND EXPERIMENT

A gas at reduced pressure is, under normal conditions, a non-conductor of electricity. However, if the electric field between a pair of electrodes in the gas is suitably high, the gas can break down, and a current can be carried through the gas by the ions and electrons of the now ionized gas.

This chapter will review studies of the effect of a magnetic field perpendicular to the direction of the flow of current in such a discharge, on the behaviour of the discharge. Attention will be focussed on geometries such that the magnetic field is perpendicular to the current flow between long parallel electrodes, or coaxial electrodes, and the discharge is driven along the electrodes by the interaction of the discharge current and this transverse magnetic field. Conditions are such that the region of gas that carries the current is small compared with the length of the electrodes.

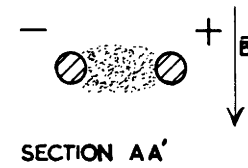
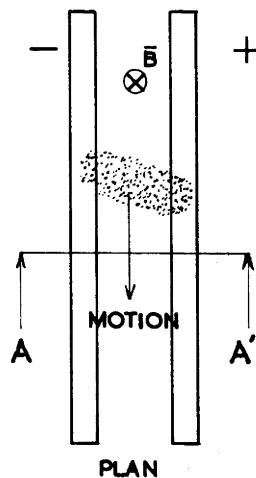
Figure 1.1 shows the three geometries of interest, and, for each geometry, the direction of the electromagnetic driving force - the "Lorentz" or "Amperian" force, which is given by

$$d\mathbf{F} = i (dl \times \mathbf{B}) \quad (1.1)$$

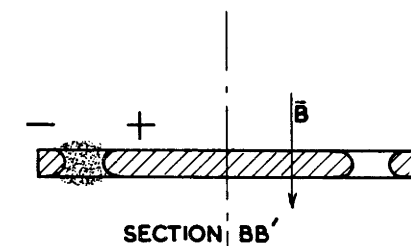
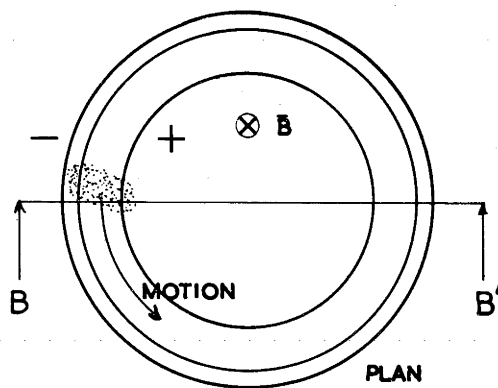
where dF is the force acting on an element of length dl of a current,

FIG 1.1 GEOMETRIES OF INTEREST

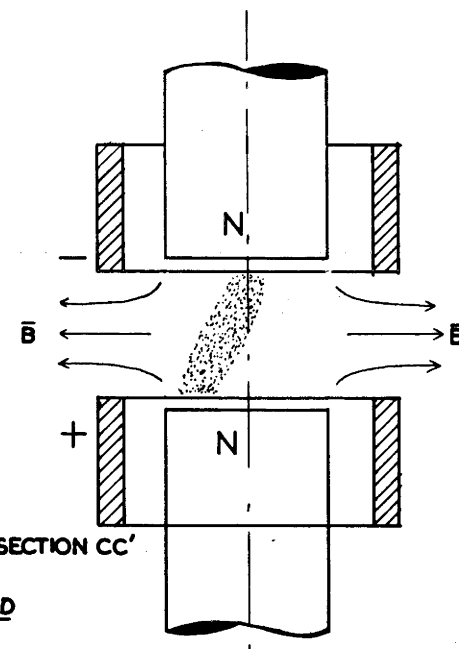
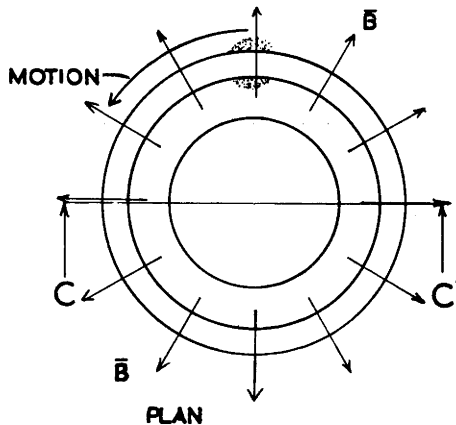
- (a) Straight parallel electrodes. Magnetic field perpendicular to the plane of the electrodes.
- (b) Concentric circular electrodes. The axial magnetic field drives the discharge around the radial gap between the electrodes.
- (c) Coaxial circular electrodes of the same diameter. The radial magnetic field, generally produced by the adjacent like poles of iron-cored electromagnets, drives the discharge around the axial gap between these electrodes.



(a) LINEAR



(b) CIRCULAR- AXIAL MAGNETIC FIELD



(c) CIRCULAR- RADIAL MAGNETIC FIELD

**FIG 1-1 GEOMETRIES OF INTEREST**

i, in a magnetic field, B.

Equation 1.1 is more conveniently expressed in terms of current density if it is to be applied to the finite current-carrying region of a gas discharge. In a form suitable for this application

$$\underline{dF} = (\underline{j} \times \underline{B}) dV \quad (1.2)$$

$dV$  = volume element.

Studies of the effect of a transverse magnetic field on transient discharges (e.g., a spark discharge), r.f. discharges, or the Townsend discharge (a discharge where the current density is so low that the distortion of the electric field by the charge flowing between the electrodes is negligible) will not be reviewed.

### 1.1 GENERAL REFERENCES

The following books and papers were much referred to during the course of the candidate's researches, and the writing of this thesis, especially this chapter of the thesis. This list includes the more important reviews of the Physics of Gas Discharges. A full bibliography listing these, and other references, is given at the back of this thesis. The code used to refer to a particular paper gives the first two letters of the senior author's name, followed by two numbers giving the year of publication. Lower-case letters after this code are used to distinguish between papers should an author publish more than one paper in a year.

### General references

Books by von ENGEL (En 55) (one of the most recent, and a most useful general reference on this subject), COBINE (Co 41), EMELEUS (Em 51), LOEB (Lo 39) and PENNING (Pe 57). Review papers by DRUYVESTEYN and PENNING (Dr 40), and LLEWELLYN-JONES (L1 53).

The physics of the positive column of gas discharges was discussed by ALLIS (Al 56) in two of a series of lectures given at the Los Alamos Scientific Laboratory. A transcript of this series of lectures has been published as a U.S.A.E.C. report (LA-2055).

### The Glow Discharge

FRANCIS (Fr 56) "The Glow Discharge at Low Pressure" in "Handbuch der Physik" Vol. 22. A most important and comprehensive review.

### The Arc Discharge

A book by Somerville (So 59) and review papers by ECKER (Ec 61), MAECKER (Ma 51), and FINKELNBURG and MAECKER (Fi 56).

### The Gas Discharge in a Magnetic Field

SOMERVILLE'S D.Sc. thesis (So 53), from the University of Sydney discusses the effect of magnetic fields (particularly transverse magnetic fields) on low pressure glow discharges, and surveys the literature relevant to this subject.

The work described in GUTHRIE and WAKERLING'S book (Gu 49), a summary of wartime work at the University of California Radiation Laboratory, is not particularly relevant to the work described in this thesis.

### Fundamental Processes

(Collisions, mobility, diffusion, ionization, velocity distributions, etc.) BROWN (Br 59) gives a comprehensive summary of experimental and theoretical results. LOEB'S books (Lo 39, Lo 55) were also very useful.

In this chapter, where no specific reference is made to the literature, the phenomenon described will be found to be discussed in one or more of the above references.

### 1.2 THE GLOW DISCHARGE AND THE ARC DISCHARGE

Under d.c. conditions a current passes through a gas in the form of a GLOW DISCHARGE, or an ARC DISCHARGE. The former occurs characteristically when the current is low (less than 1 ampere, approximately), the latter at higher currents.

The d.c. gas discharge consists of three main regions: the cathode region, the positive column, and the anode region. Most of the current in a discharge is carried by electrons, which originate in the cathode region and flow out of the discharge at the anode. Conditions in the cathode region are such as to eject suf-

ficient electrons from the cathode or produce sufficient electrons in the cathode region to maintain the discharge current. The anode region acts as an electron sink, and produces enough ions to provide the positive ion component of the current in the positive column. The positive column is a conducting path connecting these two regions.

The natures of anode region and positive column of arc and glow discharges do not differ greatly if the currents and pressures are of the same order of magnitude in both cases. However the nature of the cathode region is markedly different for these two types of discharge, both in appearance, and the physical processes involved in their maintenance. It is this difference in cathode region properties that is generally used to distinguish between the glow discharge and the arc discharge.

Because of the wide range of conditions under which a discharge can occur - variables are currents, gas pressure and composition, electrode material and geometry, container geometry, and external heating or irradiation of the discharge - the properties, and mechanisms of maintenance of discharges can vary greatly. This gives rise to difficulty in giving a definition of the glow, and especially the arc discharge that will cover all cases. (So 59)

The generally accepted definition of a glow discharge is:  
a discharge which is maintained by electrons removed from the cathode

by particle (and photon) bombardment (En 55). It is implied that the current density is large enough so that the electric field between the electrodes is distorted by the charge flowing between the electrodes.

Figure 1.2 shows the potential distribution along the axis of a typical glow discharge, and a typical low pressure arc discharge. The cathode fall voltage (or cathode fall) is defined as the voltage relative to the cathode, of the "knee" at the cathode end of these curves. The region of high electric field between the cathode and the knee is referred to as the cathode fall region of the discharge. The glow discharge is characterized by a large cathode fall voltage - in the range of 100 to 500 volts.

There is no generally accepted definition of the arc discharge (So 59). Definitions in current use are:

- (1) A discharge characterized by a small cathode fall voltage - generally of the order of the ionization or minimum excitation potential of the gas in which the discharge runs (Co 27a). This is probably the most widely used definition of the arc.
- (2) A discharge characterized by a high current density at the cathode (So 59).
- (3) A discharge where electrons are produced at the cathode by a method other than secondary emission by particle or photon bombardment (Dr 40).

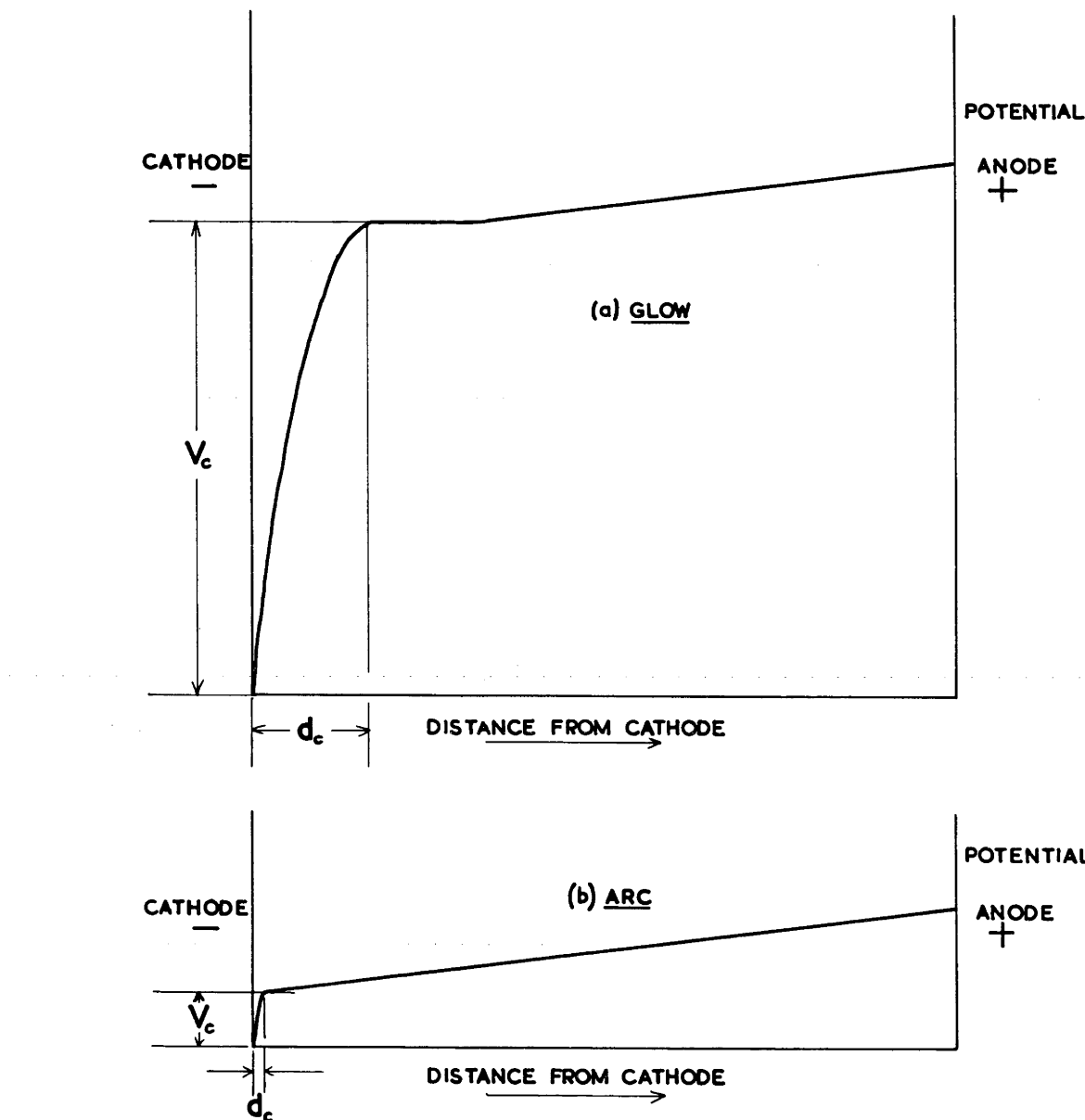


FIG 1.2 POTENTIAL DISTRIBUTION along the axes of a typical low pressure glow discharge, and a typical low pressure arc discharge

(a) Glow discharge      (b) Arc discharge

$V_c$  - Cathode fall voltage

$d_c$  - Length of the cathode fall region.

(4) A discharge where the temperatures of the ions, electrons and the neutral gas molecules in the positive column are such that these species are approximately in thermal equilibrium (Ma 51). In this type of column the charge carriers do not use the energy they gain from the electric field to produce ionization directly, but heat the gas so that thermal ionization occurs (see sections 1.4.1 and 1.4.2). This definition is often expressed in terms of the occurrence of thermal ionization, rather than thermal equilibrium (Ec 61). It should be noted that the arc is defined in terms of processes occurring in the positive column, rather than phenomena occurring in the cathode region.

### 1.3 THE GLOW DISCHARGE (Fr 56, En 55, Co 41)

#### 1.3.1 The cathode region

Figure 1.3 shows schematically the variation of voltage, electric field, charge density and light intensity along the axis of a glow discharge at a pressure of approximately 1 mm Hg. Also shown are the names given to the characteristic regions of the discharge.

The region between the cathode, and the cathode end of the negative glow (the cathode fall region) is the region where the electrons that constitute much of the discharge current in the remainder of the discharge are produced. The majority of the electrons are produced by ionization in the cathode fall region; the remainder are ejected from the cathode.

FIG 1.3 AXIAL VARIATION OF GLOW DISCHARGE  
PARAMETERS - SCHEMATIC

(a) Appearance of the discharge

|      |   |                    |
|------|---|--------------------|
| AsDS | - | Aston dark space   |
| CL   | - | Cathode layer      |
| CDS  | - | Cathode dark space |
| NG   | - | Negative glow      |
| FDS  | - | Faraday dark space |
| PC   | - | Positive column    |
| AnDS | - | Anode dark space   |
| AG   | - | Anode glow         |

(b) Potential

(c) Electric field

(d) Charge density  $\rho_+$  - positive ion density

$\rho_-$  - electron density

$\rho_{Nett}$  - Nett charge density  
(Dotted line)

(e) Intensity of the emitted light.

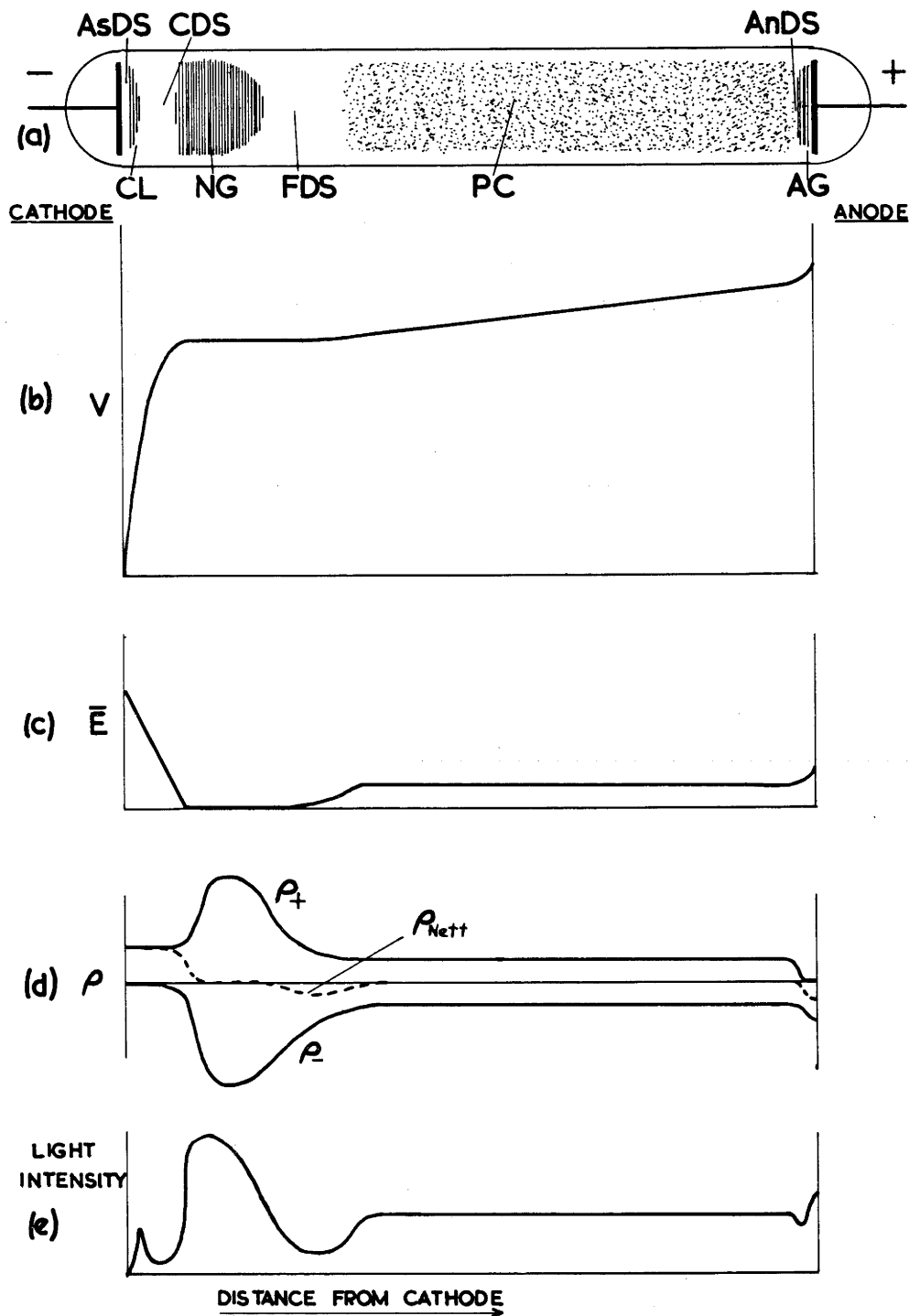


FIG I-3 GLOW DISCHARGE PARAMETERS

The dominant electron ejection mechanism at the cathode of a glow discharge is secondary emission by positive ion bombardment, although for certain geometries or conditions, secondary emission due to bombardment by metastable excited atoms, or photons, can be of importance.

An electron ejected from the cathode is accelerated by the high electric field near the cathode, gains ionization energy, and initiates a Townsend avalanche (En 55), (the process of cumulative ionization that occurs when an electron is accelerated by a high electric field. The electron producing an ionization, and that produced by the ionization are both accelerated by the electric field, to produce further ionization). The positive ions produced by this avalanche, drift back to the cathode. Conditions in the cathode fall region are such that each electron ejected from the cathode will initiate a Townsend avalanche that produces in the cathode fall region, the number of ions necessary to eject a single electron from the cathode, when these ions strike the cathode.

This maintenance condition, a necessary condition for the self-sustained existence of the cathode fall region, is expressed mathematically

$$\gamma(M-1) = 1 \quad (1.3)$$

where  $\gamma$  = mean number of secondary electrons ejected from the

cathode per incident positive ion.  $\gamma$  is not the secondary emission coefficient that would be obtained from measurements of the electron current from a surface bombarded by positive ions in vacuo. It is an effective secondary emission coefficient, corrected for the backscattering of electrons into the cathode by collisions with gas molecules (Bl 58).

M = number of electrons that leave the cathode fall for each electron ejected from the cathode. M is called the multiplication factor.

M-1 = number of ions produced per ejected electron.

In the case where the Townsend avalanche is the multiplication process

$$\gamma \left( \exp \int_0^d \alpha dx - 1 \right) = 1 \quad (1.4)$$

where  $\alpha$  = Townsend's first ionization coefficient, i.e., the number of ion pairs produced per cm. by a single electron.

d = thickness of the cathode fall region.

The positive ions produced in the cathode fall region which drift slowly towards the cathode, produce the large electric field observed at the cathode end of the discharge tube. This field accelerates the electrons to energies such that they can ionize efficiently in this region. In most cases  $\gamma$  is considerably less than 1, so that the current at the cathode is primarily a positive ion current. However, due to the multiplication of the

electron number in the cathode fall region, the current entering the negative glow from this region is primarily an electron current.

When the discharge current is so low that the cathode glow does not cover the entire cathode, the discharge is of a type referred to as the normal glow discharge. In the cathode region of this discharge:

(1) The normal cathode fall voltage  $V_n$  is independent of current and pressure, but depends on the gas, and the cathode material.

(2) When the current is increased, the normal cathode current density,  $j_n$ , remains constant, the cross sectional area of the cathode region increasing.

(3) For a fixed gas and cathode material and plane electrodes,

$$j_n/p^2 = \text{Constant} \quad (1.5)$$

( $p$  = gas pressure).

(4) For a fixed gas and cathode material

$$d_n p = \text{Constant} \quad (1.6)$$

( $d_n$  = normal cathode fall thickness).

(5) The electric field falls linearly from the edge of the cathode to the edge of the cathode fall region. This implies a uniform positive ion space charge, which could be obtained by the uniform generation of ions, provided the drift velocity of the

positive ions is proportional to the electric field.

No satisfactory theory of the normal cathode fall region, that predicts the above behaviour, has been developed to date. The theory, up to mid-1955, is reviewed by Francis (Fr 56).

The cathode fall region is described by the following three sets of equations:

- (1) Poisson's equation.
- (2) The equations of current continuity for ions and electrons. These equations include terms that account for ionization.
- (3) Mobility equations for ions and electrons. These relate the charge densities to the ion and electron currents.

with the boundary conditions:

- (1) The total current density is related to the secondary emission processes at the cathode through

$$j = j_+ (1 + \gamma) \quad (1.7)$$

where  $j$  = total current density at the cathode

$j_+$  = positive ion current density at the cathode.

- (2) The end of the cathode fall region is defined as being the point where the electric field falls to zero.

Several workers have derived expressions describing the cathode fall region, using the above general equations (Mo 28, Ro 32, Ro 39, We 39 a,b,c, Wa 62, Wa 58). Different assumptions are made about the dependence of the positive ion drift velocity,

and  $\alpha$ , on the electric field, and the contribution of the negative glow to the properties of the cathode fall region. However not all theories involve the use of the general equations. COMPTON and MORSE (Co 27 b) use equation 1.4 explicitly (equation 1.4 is implicit in the equations of continuity) and made use of STEENBECK'S Minimum Energy Principle (St 32). Von ENGEL and STEENBECK (En 34) omit the equations of continuity, use equation 1.4, and make use of the experimentally observed linear dependence of the electric field on distance from the cathode. None of the above theories make predictions in agreement with observations, basically because of our lack of understanding of ionization and mobility in non-uniform electric fields (Mo 46, Jo 48).

Although it is customary when developing a theory of the cathode fall region to ignore the contribution to the cathode current of electrons ejected from the cathode by photoelectric emission, this effect may have an important influence on the behaviour of the cathode region of the discharge. Indeed, LITTLE and von ENGEL (Li 54) have suggested that photoelectric emission due to ultra-violet radiation from the negative glow, could be an important secondary emission mechanism, not only for the hollow cathode discharge for which their theory was primarily developed, but also for the glow discharge between plane electrodes.

### 1.3.2 The negative glow and the Faraday dark space

In these regions high energy electrons from the cathode fall region lose energy and become randomized by collisions prior to entering the positive column. The electrons become randomized in the negative glow, and diffuse into the Faraday dark space (F.D.S.); they are accelerated through the F.D.S. to the positive column by a small electric field. This field results from a small negative charge excess in the F.D.S. due to electrons diffusing from the negative glow more rapidly than positive ions. The electric field is zero in the negative glow, and increases through the F.D.S. to the positive column value.

The rate of ionization per unit volume at the cathode end of the negative glow is high. This ionization is due to fast electrons from the cathode fall region. Because the axial field in the negative glow is zero the charged particles can only diffuse out of this region. For this reason positive ion and electron density are very high in the negative glow, being perhaps one or two orders of magnitude greater than in the positive column (Ud 52).

At the negative glow end of the F.D.S., the electrons have little energy, and hence the probability of recombination is high in this region. The decrease of ion and electron density through this region is largely the result of recombination.

The properties of these regions are close to those of an ideal plasma. The cathode fall region, with its large excess of positive ions, cannot be considered as a region of plasma.

### 1.3.3 The positive column (Al 56, Fr 56)

This plasma region is merely a conducting path between the cathode and anode regions. The current flows throughout the entire space between the electrodes except at pressures greater than a few cm. Hg., where the current carrying region tends to become restricted. The remarks in this section apply particularly to the glow discharge running axially between electrodes at the end of a long cylindrical discharge tube.

Electrons in the high velocity "tail" of the electrons' Maxwellian velocity distribution with energies above ionization energy can ionize gas molecules on collision. The electron temperature in the column is such that enough electrons and ions are produced by this process to replace those lost to the wall by diffusion. The electron temperature is of the order of a few electron volts, which is considerably greater than the temperature of the ions. The ions and the neutral gas molecules are in good "thermal" contact, and are at a temperature not greatly in excess of room temperature.

The axial electric field is such that an electron gains as

as much energy between collisions as it loses per collision. The charge density at the axis of the discharge tube is determined by the current flowing through the tube. The mechanism of diffusion of ions and electrons to the walls determines the radial electric field, and the radial charge density distribution. At pressures at which the mean-free-path of electrons is considerably less than the dimensions of the tube, the SCHOTTKY theory (Sc 24 a,b) applies. The diffusion mechanism is "ambipolar diffusion" (Al 56). Ambipolar diffusion is characterized by a radial electric field such that at any radius the radial ion and electron current densities are equal.

There is still some doubt as to the reason for the contraction of the positive column at high pressures (Fr 56). "Pinching" due to the self magnetic field of the column is obviously not the cause, for the contraction occurs even for very small currents (Fo 55). Various improvements to the simple Schottky theory (Fo 55) - second order approximations, more sophisticated boundary conditions (Al 54), introduction of two-stage ionization (Sp 50) and volume recombination (Se 53) - give charge density distributions that are somewhat more peaked than the distribution obtained from the simple Schottky theory, but which are still not peaked enough to explain the contraction.

It is difficult to assess whether an increase of gas temperature at the axis of the discharge could cause a contraction of the

positive column (El 51, Fo 55). However the contraction occurs at a density range well below that at which temperature gradients will be significant, indicating that gas heating is not of importance.

FOWLER (Fo 55) proposes that the contraction is due to the loss of electron energy in inelastic collisions. This energy loss is equivalent to a force acting radially inwards on the electrons, which flow outwards at a reduced velocity. This theory gives fair agreement with experiment.

At high pressures, according to the Schottky theory, the electron temperature and the voltage between the wall and the axis of the discharge tube are both reduced below the low pressure values. Von ENGEL (En 55, p. 224) suggests, in addition, that the higher current density near the axis of the discharge tube leads to a reduction of gas density near the axis. The partial pressure of the electron gas will be relatively high because its temperature is much greater than the gas temperature. The electrons and ions thus move radially outwards at reduced speed into a region of higher gas density. These conditions favour recombination, away from the central region of the positive column, which results in the observed contraction of the column. \*

---

\* No reference or calculations are given, and I have been unable to locate any other reference to this theory. Because of this, and Fowler's comments on recombination as an explanation of the contraction (Fo 55 - see above), I suggest that this theory be treated with a certain amount of caution until further work is published.

#### 1.3.4 The anode region

This region collects electrons from the positive column, and transfers them to the anode. Electrons are attracted to, positive ions repelled from the anode, producing an electron space charge layer just in front of this electrode. This gives a sharp drop of voltage between the anode and the positive column. Electrons are accelerated from the positive column by this field so that they can ionize the gas near the anode. Conditions are such that the number of positive ions produced is equal to the positive ion current in the positive column.

### 1.4 THE ARC DISCHARGE (So 59, Ec 61, Ma 51, Fi 56)

#### 1.4.1 The cathode region

This region is characterized by a low cathode fall, a very high current density at the cathode, and a brightly-glowing cathode spot where the current enters the cathode. Several possible mechanisms exist for the extraction of electrons from the cathode.

(1) Thermionic emission. Energy dissipated in the cathode fall region causes the cathode to heat so that it can emit thermionically, enough electrons to maintain the discharge. This mechanism can explain the behaviour of arcs running at moderate pressures (1 atmosphere and lower) on high melting point cathodes.

(2) Field emission. A positive charge close to the cathode

produces a strong electric field which pulls electrons from the cathode. The space charge is assumed to be due to the positive ions drifting from the positive column to the cathode. However, if this is the case, the current density required to give the electric field necessary to produce the observed emission, is much greater than the observed current density. Surface irregularities which increase the effective field, or surface layers of oxide, will increase the emission, but still not to the extent necessary to explain the experimental results. HULL (Hu 62) suggests that the observed spot consists of a number of rapidly moving emission regions, the current density in these regions being great enough to explain the observed emission. HERNQVIST (He 58) suggests that for some types of arc, the ions originate not in the positive column, but at the cathode. Excited neutral atoms diffuse from the plasma, and are ionized at the cathode. The ionization process is resonance ionization - a process in which an electron is transferred directly from the excited atom into the cathode.

(3) T - F (thermal-field) emission. ECKER (Ec 54), and more recently LEE (Le 57, Le 59) have investigated the field emission of electrons from a hot cathode as a possible mechanism of electron emission from the cathode. The increased emission from the hot cathode may be pictured as being due to (a) the width

of the potential barrier through which the electrons must tunnel to leave the cathode decreasing as their thermal energy increases, or (b) enhanced thermionic emission due to the depression of this potential barrier by the electric field. The actual mechanism has properties midway between those of these two extreme cases.

(4) The I - F (Individual-field) mechanism of ECKER and MÜLLER (Ec 59 a,b). The space charge near the cathode is due to the presence of a large number of positive ions. The random motion of these ions causes the field at any point on the cathode surface to fluctuate about a mean value, which is the value used for calculation of the field emission current density from the simple field emission theory. Because the field emission depends exponentially on the field at the cathode, the current density calculated for a model that takes account of these fluctuations is greater than that calculated from the simple field emission theory under equivalent conditions.

(5) Secondary electron emission due to the impact of metastable excited neutral atoms. This is the basis of a recent theory developed by ROBSON and von ENGEL (Ro 55, Ro 57), of the cathode region of the mercury arc.

(6) Secondary electron emission due to the impact of positive ions on the cathode. This is unimportant in the cathode region of

an arc because the energy of ions striking the cathode, which is determined by the cathode fall of the arc, is low. At these energies the secondary emission coefficient is small compared with the value at the much higher positive ion energies encountered in the cathode fall region of the glow discharge.

The discharge current at the cathode may be carried partly by positive ions flowing from the positive column to the cathode, in addition to the electron current flowing from the cathode. It has been suggested that the current to the cathode is carried entirely by positive ions (Sl 26 a, b, We 40) but energy balance considerations (Ro 57) indicate that a large part of the current must be carried by electrons.

To date, no entirely satisfactory theory of the cathode region of the arc has been developed. The development of such a theory has been hindered by the difficulty in making an experimental study of the cathode region because of its small size, and the extreme conditions encountered in this region.

ECKER (Ec 61), in a recent paper, gives an extensive discussion of the physics of the electrode regions of the arc, and, on the basis of known electron emission mechanisms, endeavours to explain the behaviour of the cathode region. He suggests that I - F emission is the important emission mechanism and that, under

certain conditions, a large proportion of the cathode current may be carried by positive ions. These ions are produced by thermal ionization in the region of very hot gas where the plasma region "contracts" towards the cathode spot. Thermal ionization is a general term used to describe the ionization that occurs in a system of electrons, ions, and neutral molecules in thermal equilibrium. It may be regarded as ionization resulting from the collision of two energetic gas molecules in a very hot gas (Co 41). This process is described by SAHA'S equation (Al 56).

#### 1.4.2 The positive column (Al 56, Ma 51)

At low pressures and moderate currents the mechanism of the positive column of the arc differs little from that of the glow discharge (see section 1.3.3). However, because of the greater current, and hence electron density in the arc column, the electron temperature required to maintain this density is somewhat lower. Ionization is more readily accomplished because of the larger number of excited molecules and dissociated molecules in the column.

At low pressures most of the energy dissipated by the passage of the current through the column is transferred directly to the walls by the diffusion of charged particles to the walls. As pressure increases radiation from excited atoms, and then transfer

of heat through the neutral gas, become the major channels of power dissipation. At high pressures the equation used to describe the arc column (the Elenbaas-Heller differential equation) relates the energy input to the energy lost by conduction through the gas, and radiation (Ma 51). The column at high pressures is characterized by local thermal equilibrium of electrons, ions, and neutral molecules.

As the current is increased the electron temperature falls until about 1% of the molecules of the gas are ionized, when the electron temperature begins to rise. This increase commences at a degree of ionization at which the number of collisions between two charged particles becomes approximately equal to the number of collisions between a charged particle and a neutral (i.e., neutral molecules are becoming scarce). At higher pressures the ionization under these conditions is described by Saha's equation (Al 56).

#### 1.4.3 The anode region

This region performs the same function as the anode region of the glow discharge, in substantially the same manner. However because of the higher currents encountered in an arc, which give rise to thermal effects, including the emission of electrons and the ejection of vapour jets from the anode, the physics of the anode region of the arc is much more complicated than that of the glow. ECKER (Ec 61) has modified his "contraction" theory of the cathode region

of the arc in order to explain the behaviour of the anode region.

### 1.5 EARLY STUDIES OF THE MOTION OF A GLOW DISCHARGE IN A TRANSVERSE MAGNETIC FIELD

Possibly the first observation of the motion of a gas discharge due to a transverse magnetic field was made by Sir Humphrey DAVY (Da 21) who, in 1821 reported observations of the "repulsion and rotation" of a low pressure carbon arc when a powerful magnet was brought near to the arc.

The first systematic study of the motion of a gas discharge in a transverse magnetic field (T. M. F.) was made by de la RIVE (Ri 66) who studied the motion of a glow discharge with the apparatus shown in figure 1.4(a). The discharge is driven around the circumference of the central glass tube containing the iron rod by the radial component of the magnetic field of this rod. De la RIVE and SARASIN (Ri 71, Ri 72) found that:

- (1) The velocity of rotation of the glow discharge increased as the gas pressure was decreased, but more slowly than would be the case if the velocity was inversely proportional to the pressure.
- (2) At a particular gas pressure the velocity is approximately inversely proportional to the density of the gas in the tube.
- (3) The velocity decreased as the discharge current was increased.

In the first two decades of this century the motion of the glow discharge in a T. M. F. was studied further, using apparatus similar

FIG 1.4 DISCHARGE TUBES USED BY THE EARLY WORKERS

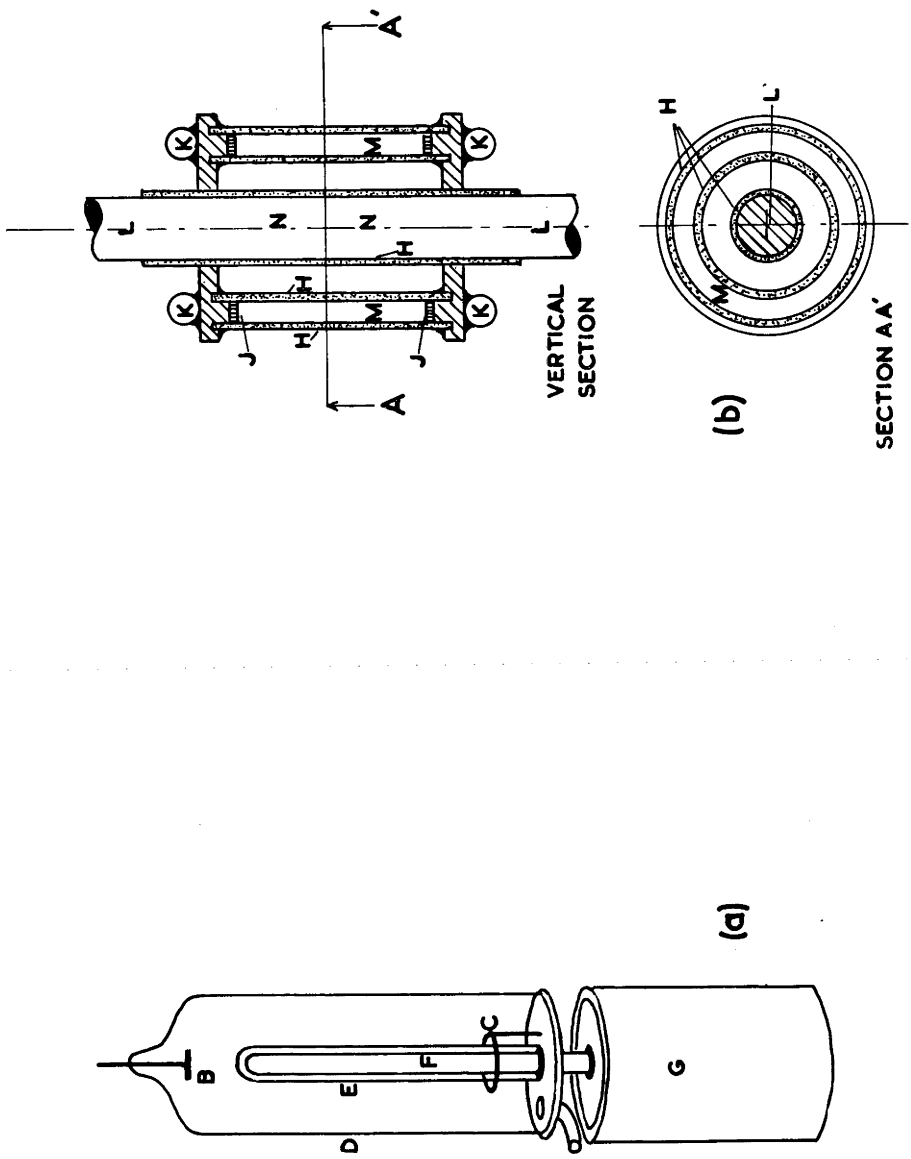
(a) DE LA RIVES DISCHARGE TUBE

- B - Aluminium disk electrode
- C - Aluminium ring electrode
- D - Outer glass wall of the evacuated envelope
- E - Glass tube. Inner wall of the evacuated envelope
- F - Soft iron rod. A "pole" of the electromagnet
- G - Coil of the electromagnet.

(b) WILSON and MARTYN'S DISCHARGE TUBE

- H - Glass tubes
- J - Ring electrodes
- K - Cooling tubes
- L - Soft iron rod
- M - Discharge channel
- N - North poles of the magnetized iron rod.

FIG 1.4 DISCHARGE TUBES OF (a) DE LA RIVE  
 (b) WILSON & MARTYN



to that of de la Rive. WILSON and MARTYN (Wi 07) performed experiments with a discharge tube so designed that its geometry is a closer approximation to the ideal "crossed fields" geometry (current and magnetic field perpendicular) than the unsymmetrical geometry used by de la Rive. The arrangement for their experiment is shown in figure 1.4(b). A bank of storage batteries was used to supply the discharge current, rather than the induction coil used by de la Rive. The use of a direct current power supply instead of an intermittent supply is a desirable simplification of the experiment. Wilson and Martyn found that the velocity of rotation of the discharge

$$v \propto B/p \quad (1.8)$$

where  $B$  = magnetic flux density (at the centre of the discharge)

$p$  = pressure

for nitrogen, air, and hydrogen. The velocity was found to be approximately inversely proportional to the molecular weight (density) of the gas. At low discharge currents the velocity decreased sharply as current increased, but above 12 mA was substantially independent of the discharge current.

A theory, based on the concept of the mobility (En 55) of charged particles in a gas, gives

$$v = BEk_1 k_2 \quad (1.9)$$

where  $E$  = electric field along the discharge

$k_1, k_2$  = mobility of positive and "negative ions" respectively.

This theory assumes that conditions are uniform along the length of the discharge (i.e., between the electrodes).

From the results of these measurements, and measurements of the Hall effect in a gas discharge, which gives  $k_1 - k_2$ , Wilson and Martyn calculated the mobilities of the positive and negative ions. Only the positive ion mobility is in order of magnitude agreement with the values obtained by other methods. Measurements of the velocity of the rotating discharge, and the Hall e.m.f. were made at different pressures. The range of extrapolation, and the nature of the measurements were such that these workers considered the calculated values of  $k_1$  and  $k_2$  were "fairly reliable" only in air, at the lowest pressures at which the velocity of the moving discharge was measured.

Shortly after the publication of Wilson and Martyn's work MALLIK (Ma 08) published a paper describing experiments on the rotation of a glow discharge in a discharge tube with the same geometry as that of de la Rive. The discharge was powered by an induction coil. This work confirmed, for air and  $N_2O$ , the dependence of velocity on pressure, magnetic field, and gas density observed by Wilson and Martyn. However for  $CO_2$ ,  $CCl_4$ , and  $SO_2$ , which tend to be decomposed by the discharge,  $pV$  was not constant, but increased with pressure.

The velocity was found to increase when the number of cells in the primary of the induction coil was increased. This apparently contradicts the observation of Wilson and Martyn that the velocity decreased as the current was increased. However it should be remembered that in Mallik's experiment the discharge current is much lower, and intermittent.

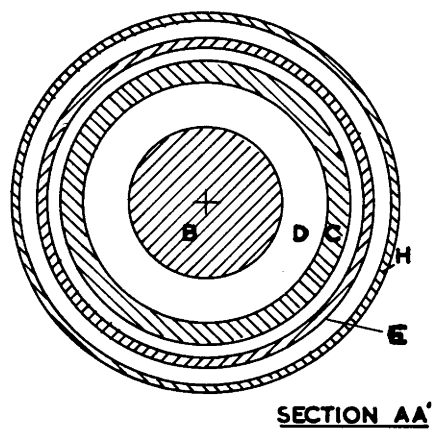
#### 1.6 THE WORK OF GUYE (Gu 21 a,b, Gu 23 a,b,c,d, Gu 27, Gu 17)

In the 1920's a group of researchers at Geneva, under C.E. GUYE, made a systematic study of the motion of a glow discharge in a T.M.F. The discharge current, supplied by an Influence Machine flowed radially between concentric electrodes, and was driven around the electrodes by an axial magnetic field. The geometry of the apparatus used for these experiments is shown in figure 1.5. The experimental results of this group show significant differences from those of the earlier workers.

These workers experienced difficulty in obtaining reproducible results. However if care was taken to use pure gases, the discharge chamber was flushed frequently with pure gas during the course of an experiment, and the electrodes "gilded", repeatable results could be obtained with this apparatus for most gases. Argon and hydrogen did not give regular rotation, except over a limited pressure range. Gas purity was checked spectroscopically. The

FIG 1.5 GUYE'S DISCHARGE TUBE

- B - Inner electrode.
- C - Outer electrode. This electrode may be moved to adjust the electrodes for concentricity.
- D - Discharge gap.
- E - Inner wall of the discharge chamber. The outer electrode is supported in this wall.
- F - Glass tube. Insulation between the inner electrode, and the remainder of the discharge chamber.
- G - Glass cover plate.
- H - Outer wall of the discharge chamber.



SECTION AA'

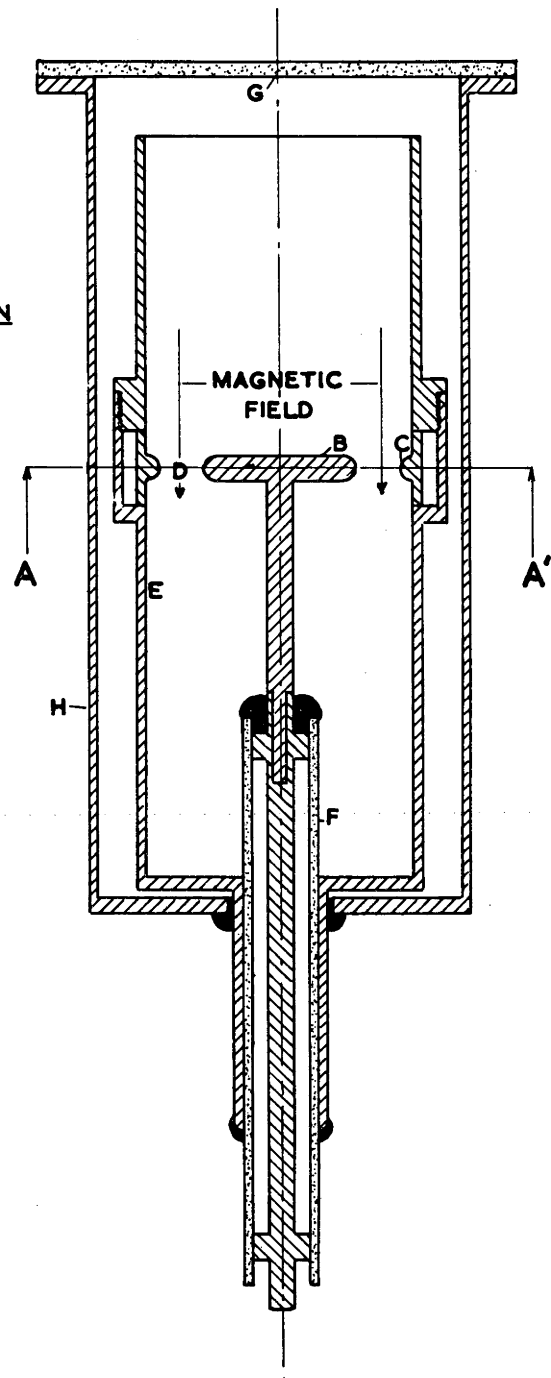


FIG 1·5 GUYE'S DISCHARGE TUBE

spectroscope always showed mercury lines, the mercury contamination originating in the manometer used for the measurement of gas pressure. Gilding the electrodes prevented the formation of a non-conducting layer that slowed the rotating discharge.

The velocity changed slowly after establishing the discharge, attaining an equilibrium value after some minutes. It was suggested that this change was due to adsorbed impurities being ejected from the electrodes and perhaps the walls of the discharge tube by the action of the discharge.

Under good conditions results reproduceable to within 3% were obtained for most of the gases used in these experiments.

#### 1.6.1 Experimental Results

- (1) The discharge velocity is proportional to the magnetic field.
- (2) Experiments in nitrogen, with the centre electrode the cathode, showed that the discharge velocity was proportional to the discharge current.
- (3) Variation of velocity with gas pressure.

##### Oxygen, centre electrode the anode (see figure 1.6).

Velocity is inversely proportional to pressure, at all but the lowest pressures.

Centre electrode the cathode (see figure 1.6). Velocity decreases as pressure increases. However the curvature of the

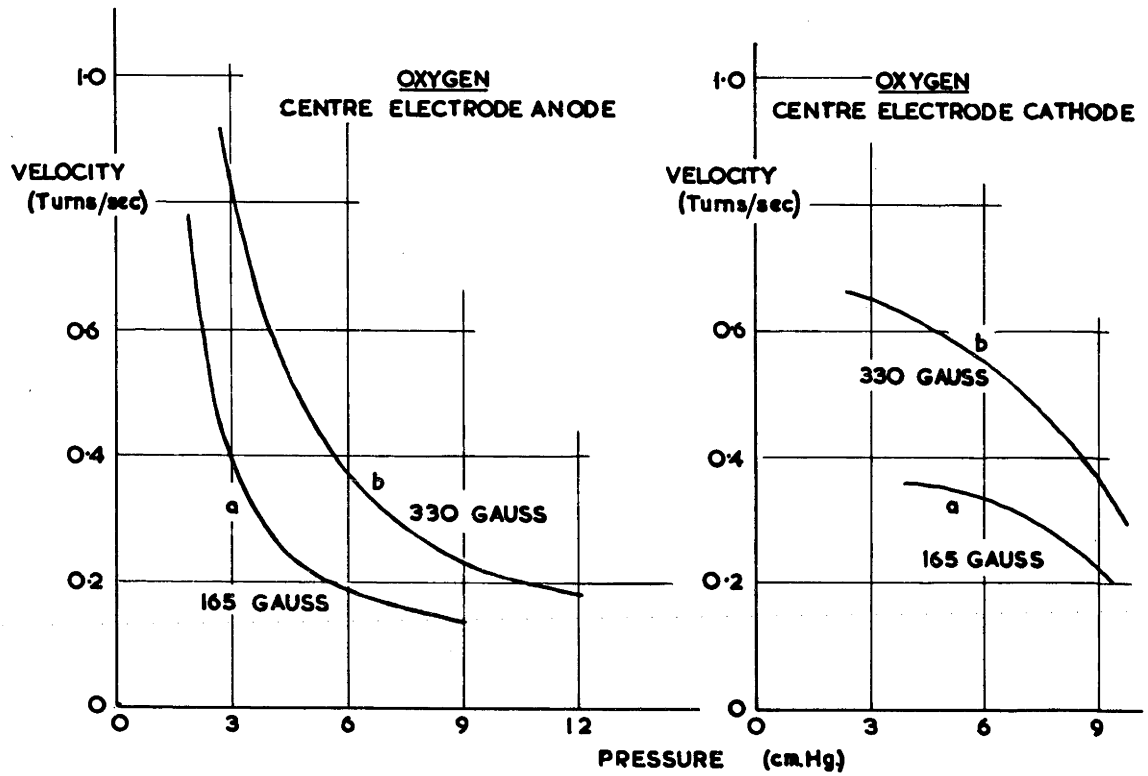


FIG 1.6 GUYE'S EXPERIMENTAL RESULTS - OXYGEN

velocity-pressure curve is opposite to that obtained with the centre electrode the anode (see figure 1.6).

Nitrogen, centre electrode the anode (see figure 1.7).

As pressure increases, then velocity decreases; then, (at about 5 cm. Hg with a magnetic field of 165 gauss) increases suddenly, and then more slowly. Above this sharp transition, the discharge is bright, and narrow, and the motion is irregular. The current falls when passing through the transition, with pressure increasing.

Centre electrode the cathode. Under these conditions, at pressures between 7 and 11 cm. Hg, the discharge in nitrogen shows the phenomenon of "spontaneous rotation" - i.e., if the magnetic field is decreased to zero, the discharge continues to rotate. If the velocity of the spontaneous rotation is subtracted from that observed in the presence of the magnetic field, the resultant velocity is inversely proportional to pressure (at all but the lowest pressures) (see figure 1.7).

Argon, centre electrode anode. This gas shows two different modes of rotation, similar to those observed in nitrogen.

Centre electrode cathode. The rotation is irregular, and occurs only for a limited range of pressures.

Other gases. Experiments with CO, CO<sub>2</sub>, N<sub>2</sub>O and CH<sub>4</sub> showed that discharges in these gases rotate only for a limited range of pressures. At higher pressures the velocity is inversely

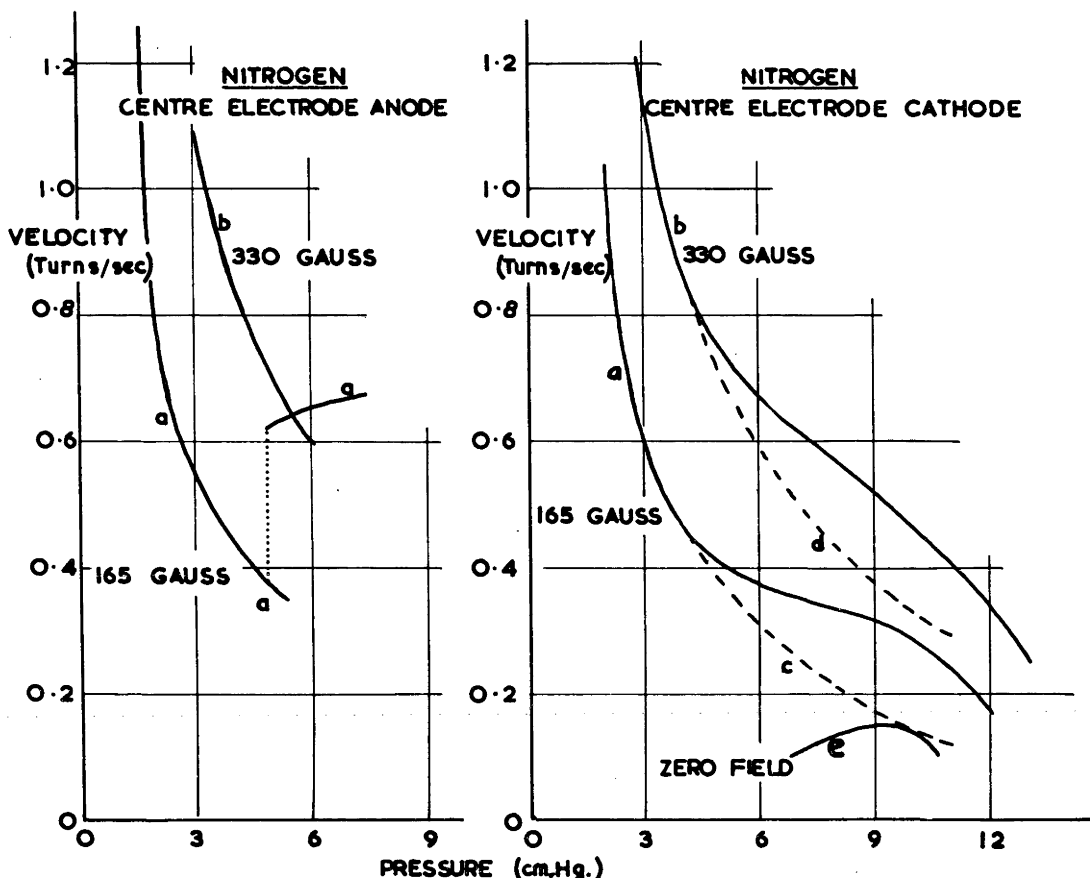


FIG 1.7 GUYE'S EXPERIMENTAL RESULTS - NITROGEN

Centre Electrode the Anode - Note "jump" in curve "a".

Centre Electrode the Cathode - Dotted curves "c" and "d" are the differences between curves "a" and "e" and "b" and "e" respectively. i.e., they are the experimental velocities less the velocity of the spontaneous rotation.

proportional to the pressure.

(4) The above experiments were performed in a discharge tube with an outer electrode of 5.7 cm. i.d., and an inner electrode of 2.55 cm. diameter. Attempts were made to measure the velocity of rotation with inner electrodes of 1.52 and 3.52 cm. diameter. With the 1.52 cm. electrode in nitrogen, the motion was too irregular to make measurements, the discharge tending to "stick" to the centre electrode. With the larger electrode the discharge tended to move more rapidly than with the 2.55 cm. electrode. However the nature of the power supply used for this experiment (two influence machines were used) was such that the results could not be compared with those of the experiments with the 2.55 cm. electrode.

#### 1.6.2 Theory of the rotation of the discharge

The following individual particle theory was developed to explain the observed dependence of the discharge velocity on pressure, and magnetic field.

If an electric field,  $E$ , acts in the  $y$  direction, and a magnetic field,  $B$ , in the  $z$  direction, as in figure 1.8, the equations describing the motion of a particle of mass  $m$ , charge  $e$ , in these crossed fields are:

$$u = - \frac{E}{B} \left( 1 - \cos \frac{Be}{m} t \right) \quad (1.10)$$

$$v = - \frac{E}{B} \sin \frac{Be}{m} t \quad (1.11)$$

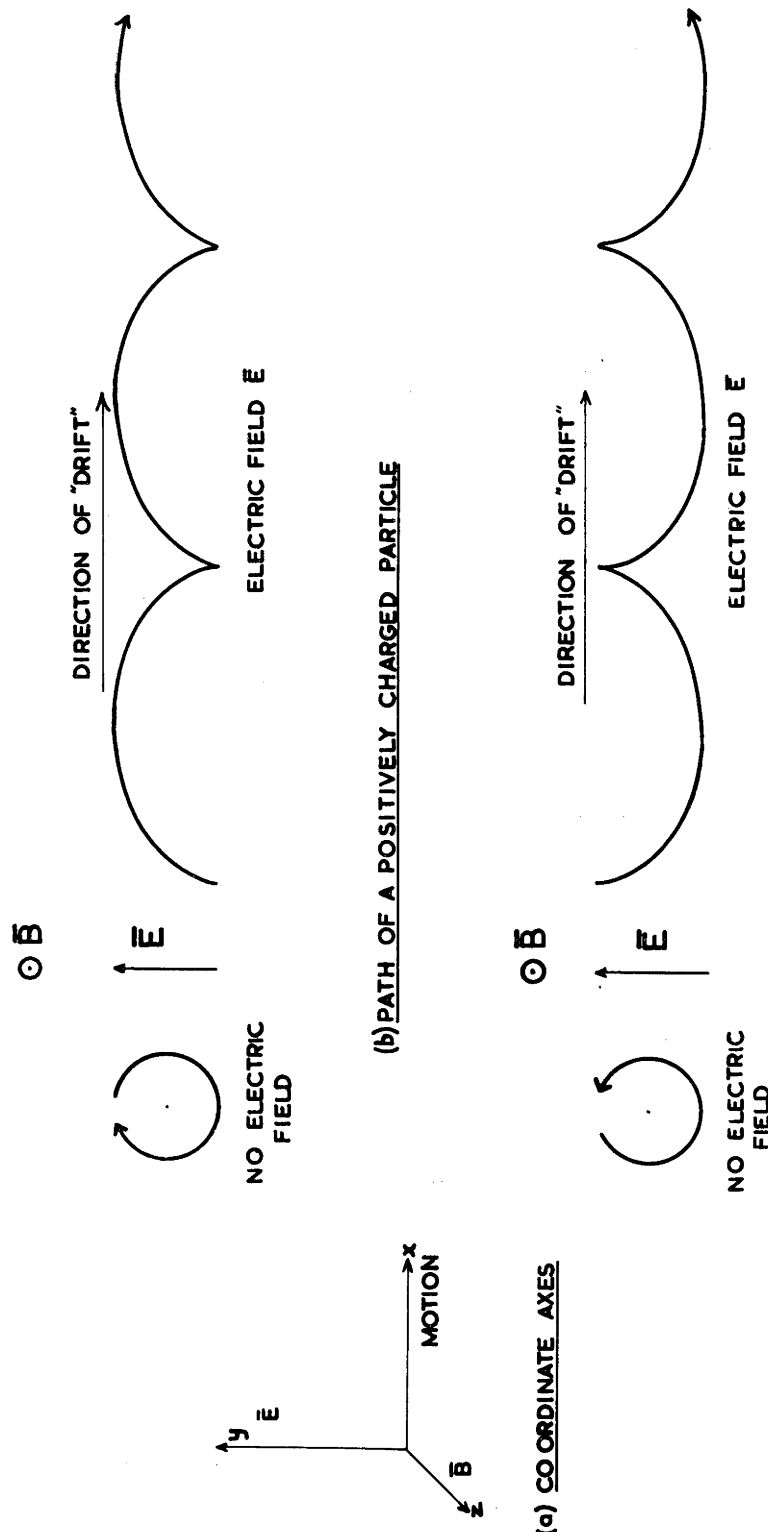


FIG 1.8 THE MOTION OF CHARGED PARTICLES IN "CROSSED" FIELDS

where  $u$ ,  $v$  are the instantaneous velocities of the particles in the  $x$  and  $y$  directions, respectively, at a time  $t$ . (For a derivation of these equations, see TOWNSEND (To 12). The motion of charged particles in crossed electric and magnetic fields is discussed in section 5.1 of this thesis).

The mean drift velocity of the particles in the  $x$  direction,  $u'$  is given by dividing the mean distance a particle moves in the  $x$  direction between collisions, by the mean time between collisions,  $T$ .

$$\text{i.e., } u' = \frac{1}{T} \int_0^T u dt \\ = -\frac{E}{B} \left\{ 1 - \left( \sin \frac{BeT}{m} \right) \middle/ \frac{BeT}{m} \right\} \quad (1.12)$$

The mean velocity of a particle in the  $y$  direction,  $v'$ , may be similarly obtained

$$v' = \frac{E}{B} \left\{ 1 - \cos \frac{BeT}{m} \right\} \frac{m}{BeT} \quad (1.13)$$

It is assumed that the mean distance a particle moves in the  $y$  direction between collisions is equal to the mean free path, i.e., the particles are not greatly deflected by the magnetic field between collisions.

Then  $\lambda = Tv'$

$$= \frac{E}{B} \frac{m}{Be} \left\{ 1 - \cos \frac{BeT}{m} \right\} \quad (1.14)$$

Expanding the cosine, and ignoring terms in the expansion of order greater than the square of  $B_e T / m$

$$\ell = \frac{Ee}{2m} T^2 \quad (1.15)$$

Therefore  $E = 2m\ell/eT^2 \quad (1.16)$

Substituting for E in equation 1.12, and expanding the sine, as above,

$$u' = \frac{1}{3} \ell B_e / m \quad (1.17)$$

Now, if it is assumed that the motion of the positive ions controls the discharge velocity and that positive ions and molecules have the same diameter, then

$$\ell = (4 \pi r^2 N)^{-1} \quad (1.18)$$

where  $r$  = radius of a molecule (or a positive ion)

$N$  = number of molecules per unit volume.

This equation assumes that an ion and a molecule will collide if their centres pass within  $2r$  of each other. This concept had its origins in the Kinetic Theory of gases, and has been transferred to ion-molecule collisions, it being assumed that the ion and the molecule have the same diameter, and that the ions are moving more rapidly than the molecules (Co 41).

From equations 1.17 and 1.18

$$u' = \frac{eB}{12 \pi r^2 N m} \quad (1.19)$$

The discharge velocity measured at high pressures, where velocity is inversely proportional to pressure, has been used by Guye to calculate  $r$ , using equation 1.19. The values obtained in this way show good agreement with the values of  $r$  for neutral molecules obtained from viscosity measurements. It should be noted that equation 1.19 gives the correct dependence of discharge velocity on magnetic field and pressure, but does not explain the variation of velocity with discharge current.

### 1.7 THE ARC DISCHARGE IN A TRANSVERSE MAGNETIC FIELD: RETROGRADE MOTION

Very little interest has been shown in the motion of a glow discharge under the influence of a T.M.F. since the work of Guye and his co-workers. The opposite is true for the motion of the arc in a T.M.F., which has been studied extensively since World War II. The motion of an arc in a T.M.F. is of interest for two reasons, one technical, the other scientific.

- (1) Many commercial circuit breakers utilize "crossed-fields" geometries.
- (2) Under certain conditions the arc moves in the direction opposite to that of the  $j \times B$  force on the discharge - a phenomenon referred to as "retrograde motion" or "reverse driving".

In 1928 MINORSKY (Mi 28) published a paper describing a study of the motion of a mercury arc in apparatus similar to that

used by Wilson and Martyn (see figure 1.4b). The arc was observed to move in the retrograde direction at low pressures. This was the first observation of the retrograde motion of an arc in an apparatus with a geometry of interest in relation to this thesis, although the tendency of the cathode region of an arc to move in the retrograde direction had previously been reported by STARK (St 03) and WEINTRAUB (We 04).

A few months later TANBERG (Ta 29) reported that an arc struck between straight parallel solid electrodes (i.e., a geometry such as that of figure 1.1a) moved in the retrograde direction at reduced pressure. This work of Minorsky and Tanberg may be considered the beginning of the extensive modern study of the motion of an arc in a T.M.F.

SMITH, who since the early days of World War II has made an extensive study of mercury arcs, has extended the work of Minorsky on the retrograde motion of mercury arcs (Sm 42, Sm 43, Sm 45, Sm 46). He observed that the "wind" of gas from the column of the arc is in the Amperian direction, even when the arc moves in the retrograde direction. This gas blast originates from momentum transferred from the ions and electrons in the discharge to the gas through which the discharge moves. The Amperian sense of this blast indicates that the column is not the seat of the retrograde motion - the force on the column still appears to be in the Amperian

sense. More recent observations by this worker (Sm 57. See also Sm 46) on the retrograde motion of an "anchored" mercury arc in the apparatus shown in figure 1.9, tend to confirm this conclusion, and point to the cathode region as the seat of the retrograde motion. The magnetic field is transverse to the current only at the cathode, so that the cathode region (and part of the positive column) is the only region of the arc driven by the magnetic field.

From immediately after World War II, until the present time, the study of arc motion in a T. M. F. has been extensively pursued by many researchers\*. A stimulus for this work was provided by the World War II observation of retrograde motion of the arc in circuit breakers in high-flying aircraft. (Hi 48).

#### 1.7.1 Arc motion: the experimental facts (Ec 61, Gu 61)

Although there are inconsistencies between some sets of experimental results, the accepted behaviour of an arc moving under the influence of a T. M. F. is as follows:

- (1) Retrograde motion is a low pressure effect. As pressure increases the retrograde velocity decreases, the arc becomes stationary, and, as pressure increases still further, moves off in

---

\* The post-war literature on the motion of an arc in a T. M. F., is very extensive. A list of the papers on this topic published since 1944 is included in the bibliography at the back of this thesis.

FIG 1.9 THE RETROGRADE MOTION OF AN "ANCHORED"  
MERCURY ARC (AFTER SMITH)

- A - Anode.
- B - Molybdenum "stump".
- C - Mercury pool.
- D - "Wetting" line. The cathode spot moves along this line.
- E - Arc column.
- F - Cathode spot. The current flow in the spot is perpendicular to the magnetic field.

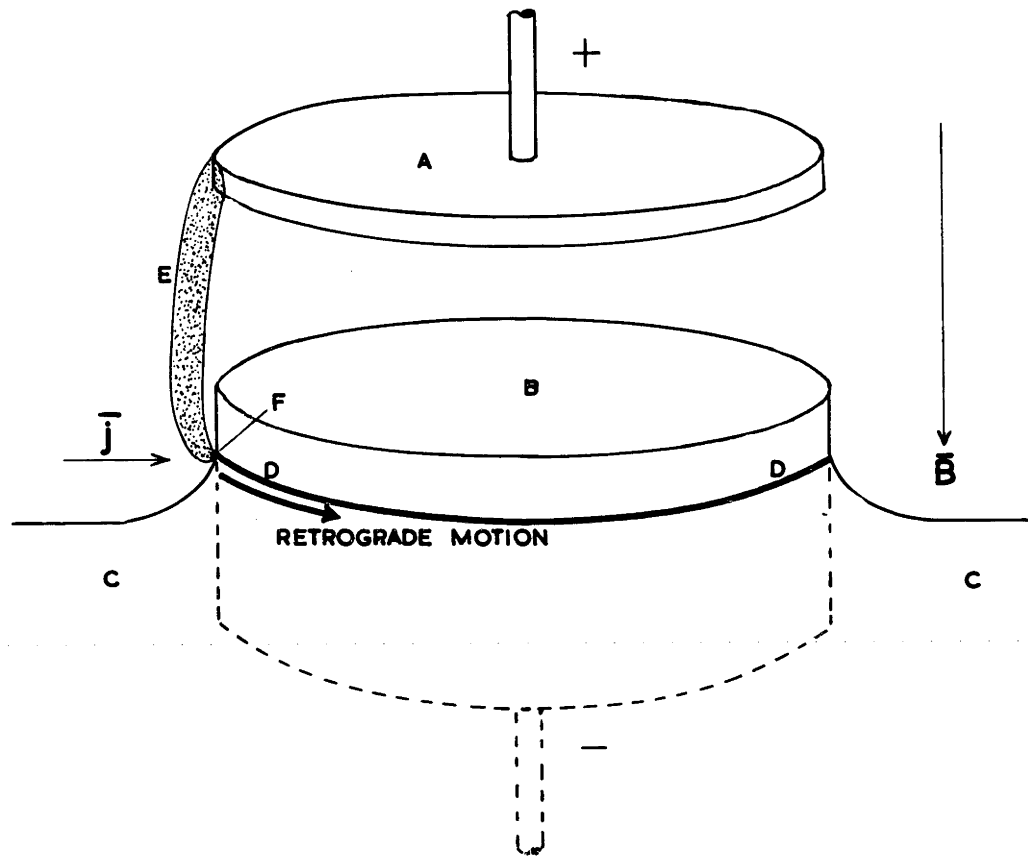


**FIG 1·9 RETROGRADE MOTION OF AN  
"ANCHORED" MERCURY ARC**

the Amperian sense (Ya 50).

(2) The retrograde velocity increases as magnetic field increases. At moderate pressures the forward velocity observed at low magnetic fields decreases through zero to become a retrograde velocity as the magnetic field increases. (St 54)

At high magnetic fields the retrograde velocity is not strongly dependent on the field. However at very high magnetic fields (above 10,000 gauss) the retrograde velocity of a low pressure mercury arc has been observed to increase sharply as the magnetic field increases, to double its previous value.

A forward arc velocity that increases as magnetic field increases is observed near atmospheric pressure. (Se 59)

(3) The arc velocity is not strongly dependent on arc current, except at low currents, provided the current is fed to the arc in such a manner that the magnetic field of the current in the electrodes has a negligible driving effect on the arc (Se 59, Gu 58, St 54, Ga 50). For low current arcs (of the order of amperes) at low pressures, where the motion is in the retrograde direction, and near atmospheric pressure, increasing the arc current increases the magnitude of the velocity (St 54, Gu 58). At moderate pressures and low currents an increase of current decreases the retrograde velocity, and can even give a reversal of the direction of motion.

The occurrence of the sudden doubling of the velocity of low pressure mercury arcs observed at high magnetic fields is dependent on arc current; the higher the current, the lower the magnetic field at which the velocity increases. (Ze 59, St 55)

(4) The velocity and nature of the motion (i.e., smooth, or irregular) depend on the cathode material, and the nature of the cathode surface (i.e., the polish, and the degree of oxidation).

(Gu 61, Le 61)

(5) If the gap between the electrodes is decreased the arc velocity decreases (Se 59). At suitably low pressures its direction may even be reversed (Ro 56). The motion is somewhat more regular for smaller gaps (Se 59).

(6) Retrograde motion does not occur for heated cathodes (Ga 49). (However retrograde motion of the "ball-of-fire" in the "ball-of-fire" mode of a hot cathode mercury arc has been observed by HERNQVIST and JOHNSON (He 55). This unique phenomenon consists of the motion of the ball through a "dark" plasma region, rather than the motion of a discrete discharge. This phenomenon is beyond the scope of this review).

(7) The higher the first excitation potential of the gas in which the discharge runs, the higher the pressure at which the direction of motion reverses (Ga 50, Ga 47).

### 1.7.2 Theories of the motion of an arc in a transverse magnetic field

Many theories, mostly of a highly speculative nature, have been developed to explain the retrograde motion. Most of these theories are only qualitative. At present only one, that of ECKER and MÜLLER (Ec 58, Gu 61) appears to give a satisfactory explanation of the observed forward and retrograde velocities, and the properties of the moving arc. However, the other theories will be mentioned briefly (without discussion) to indicate the wide range of ideas called upon to explain the retrograde motion. It should be noted that every one of these theories involves the cathode region of the arc. Critical discussions of these theories are given in papers by ECKER (Ec 61, Ec 58), ZEI and WINANS (Ze 59), SMITH (Sm 57), St. JOHN and WINANS (St 55), YAMAMURA (Ya 50), and GALLAGHER and COBINE (Ga 49).

1. The MINORSKY theory (Mi 28) Electrons from the arc drift ahead of the arc under the influence of the crossed electric and magnetic fields. (The drift of charged particles in this fashion is discussed by SPITZER (Sp 56), and in section 5.1 of this thesis.) The electrons move around the annular gap in which the arc moves, to build up a negative space charge on the retrograde side of the cathode spot. This charge drags the positive charge above the cathode spot in the retrograde direction.

2. TANBERG (Ta 29) and others (We 04) have suggested that the vapour jet from the cathode spot consists partly of positive ions, which are deflected by the magnetic field to strike the cathode on the retrograde side of the spot, resulting in the initiation of a new spot on the retrograde side of the original spot.

3. Thermoelectric effects (Li 60, pp. 182-184, Wa 54) The Righi-Leduc effect (a flow of heat perpendicular to a magnetic field, and a temperature gradient perpendicular to the field) (Sm 42) and von Ettingshausen's effect (flow of heat in the E  $\times$  B direction) (Wa 54) have both been used to explain retrograde motion.

4. ROTHSTEIN (Ro 50) suggests that the gas density above the cathode spot is so great that it resembles a solid. Energy levels are spread out into "bands". "Holes" in these bands are deflected in the retrograde sense, resulting in the cathode spot moving in this sense.

5. Interaction of the self field of the current in the cathode region of the discharge, with the applied magnetic field gives a very non-uniform magnetic field in the cathode region. PUPKE (Pu 56) suggests that the retrograde motion results from dia - and paramagnetic forces on the cathode region due to this non-uniform field. According to KESAEV (Ke 57), this field assymetry gives rise to an asymmetrical charge distribution in the cathode spot, which results in the cathode region moving in the retrograde direction.

ROBSON and von ENGEL (Ro 54) have proposed that the

arc is sharply bent near the cathode by the Amperian force. Because of this bending, the self field at one side of the cathode region is much stronger than at the other side. The resultant large reverse field on one side of the cathode region drives the arc in the retrograde direction.

6. LONGINI (Lo 49) suggests that the motion of the electrons in the cathode fall region in the Amperian sense results in the electric field in the cathode region - which is the difference between a strong positive ion field and a weaker electron field - moving in the retrograde direction. It is assumed that the cathode spot is centred on this field.

7. YAMAMURA (Ya 50) and HIMLER and COHN (Hi 48) assume that electrons are emitted from the cathode spot in all directions. Those emitted in the Amperian direction are deflected into the cathode by the T.M.F.; those emitted on the other side of the spot are deflected upwards by the field, and produce ionization on the ~~WAD~~ retrograde side of the spot which results in the re-establishment of the spot on the retrograde side of the original spot.

8. St. JOHN and WINANS (St 54, St 55, Ze 59) discuss the motion of charged particles under the influence of the T.M.F., and the charges present in the cathode fall region of the arc. An electron from the cathode spot will produce an ion on the Amperian side of the spot. However, under the influence of the electrostatic forces, the

ion produced will pass through the cathode fall region before being deflected by the T.M.F. to strike the cathode on the retrograde side of the spot. The spot becomes established at the point where the ions strike the cathode - i.e., it moves in the retrograde direction.

9. ECKER and MULLER (Ec 58, Gu 61) have developed a theory of the retrograde motion of arcs at low pressures, based on Ecker's description of the cathode region of the arc (see section 1.4.1). GUILE, LEWIS and SECKER (Gu 61, Se 61) have improved this theory and are extending it in an endeavour to explain the motion of arcs at atmospheric pressure.

According to this theory the retrograde motion occurs only for an arc with extreme contraction of the cathode region, in which the positive ion component of the cathode current is produced by field ionization (i.e., ionization due to electrons accelerated in the electric field of the cathode fall region) at the top of the positive space charge region. Most of the cathode current is carried by electrons in this case. A radial electric field prevents electrons moving from the space charge region. i.e., they are constrained to move along a potential tube that follows the path of the high density stream of positive ions that flows to the cathode from the plasma region, until they reach the top of the space charge region, where they have gained enough energy to escape from this potential well.

A T. M. F. bends the stream of ions that gives rise to the space charge in the Amperian direction as shown in figure 1.10(a). Hence electrons, moving up the potential tube, move initially in the retrograde direction. Their initial retrograde velocity causes them to escape from the retrograde side of the potential tubes (figure 1.10(b)). The ions produced by these electrons strike the cathode on the retrograde side of the original cathode spot, initiating a new spot on the retrograde side the original spot. At higher pressures the electrons lose their original retrograde velocity component in collisions. They drift out of the ion tube on the Amperian side of the space charge region under the influence of the crossed electric and magnetic fields (figure 1.10(c)), resulting in a new cathode spot being formed on the Amperian side of the old spot.

#### 1.8 RECENT WORK ON THE GLOW DISCHARGE IN A TRANSVERSE MAGNETIC FIELD

Since the completion of the work of Guye and his co-workers only two groups have studied the motion of a glow discharge in a T. M. F. GROTH (Gr 25) has reported briefly a repetition of some of the experiments performed previously with de la Rive's apparatus, and, since World War II a group of workers at the University of Michigan have studied the motion of a discharge in high magnetic fields at low gas pressures (Ea 50, Ea 58).

FIG 1.10 THE FORMATION OF NEW ION TUBES

- (a) The structure of an ion tube. The magnetic field causes the ion stream to bend in the Amperian direction as shown.
- (b) The motion of an electron at low pressure. The electron retains its initial retrograde velocity component, and escapes from the potential well on the retrograde side of the cathode spot.
- (c) The motion of an electron at high pressures. The electron loses its retrograde velocity component in collisions, and escapes from the potential well on the Amperian side of the cathode spot.

Fig 1.10 (a) & (b)

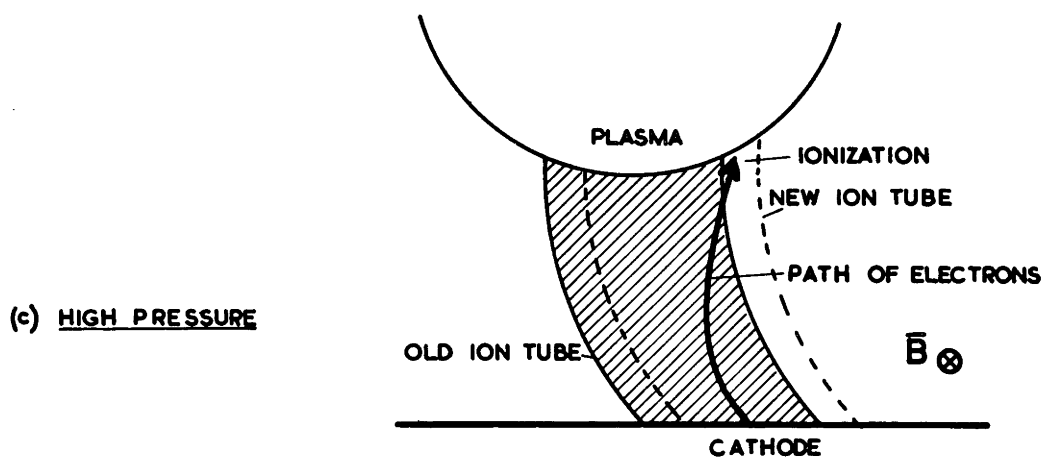
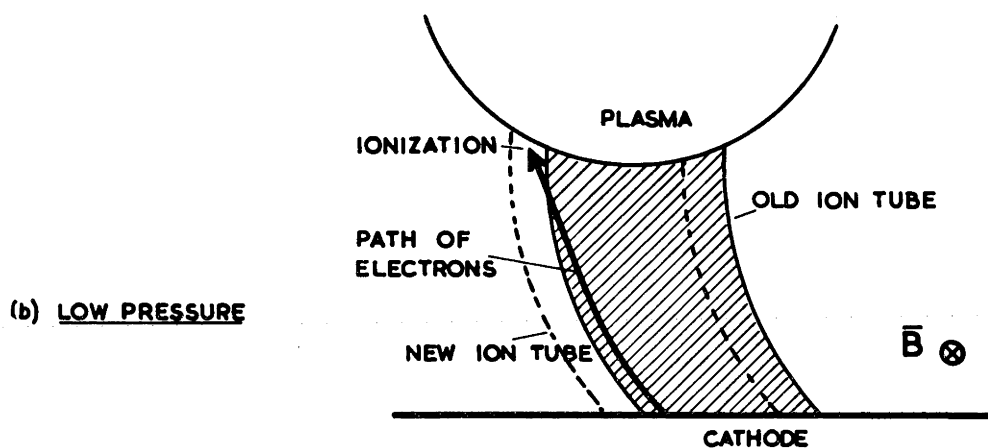
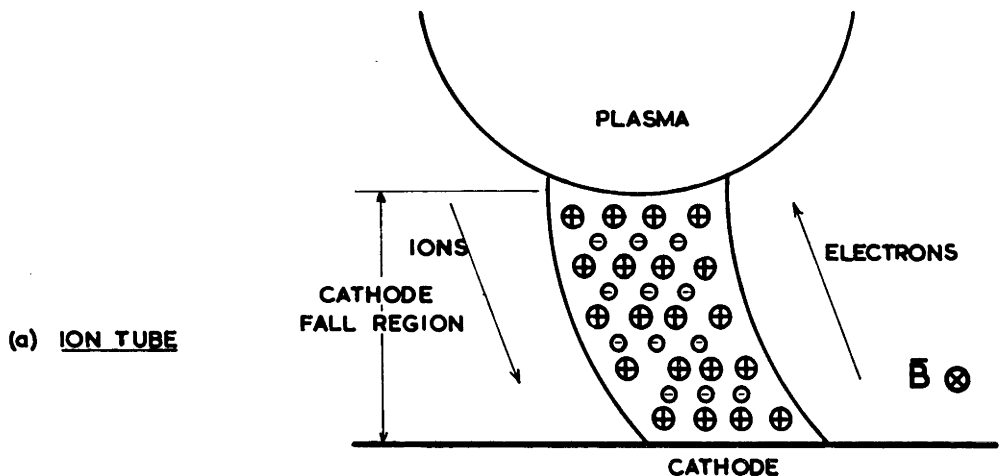


FIG 1-10 FORMATION OF NEW ION TUBES

However much attention has been paid to the "glow discharge" in a T.M.F. at very low pressures (e.g., So 53, So 48, Re 58). The discharge geometry is generally similar to that of figure 1.1(b) - concentric electrodes in an axial magnetic field. The pressure is such that the discharge completely fills the discharge tube. This work is not of interest in relation to this thesis, apart from the descriptions of particle motion contained in two of these papers (So 53, Re 58).

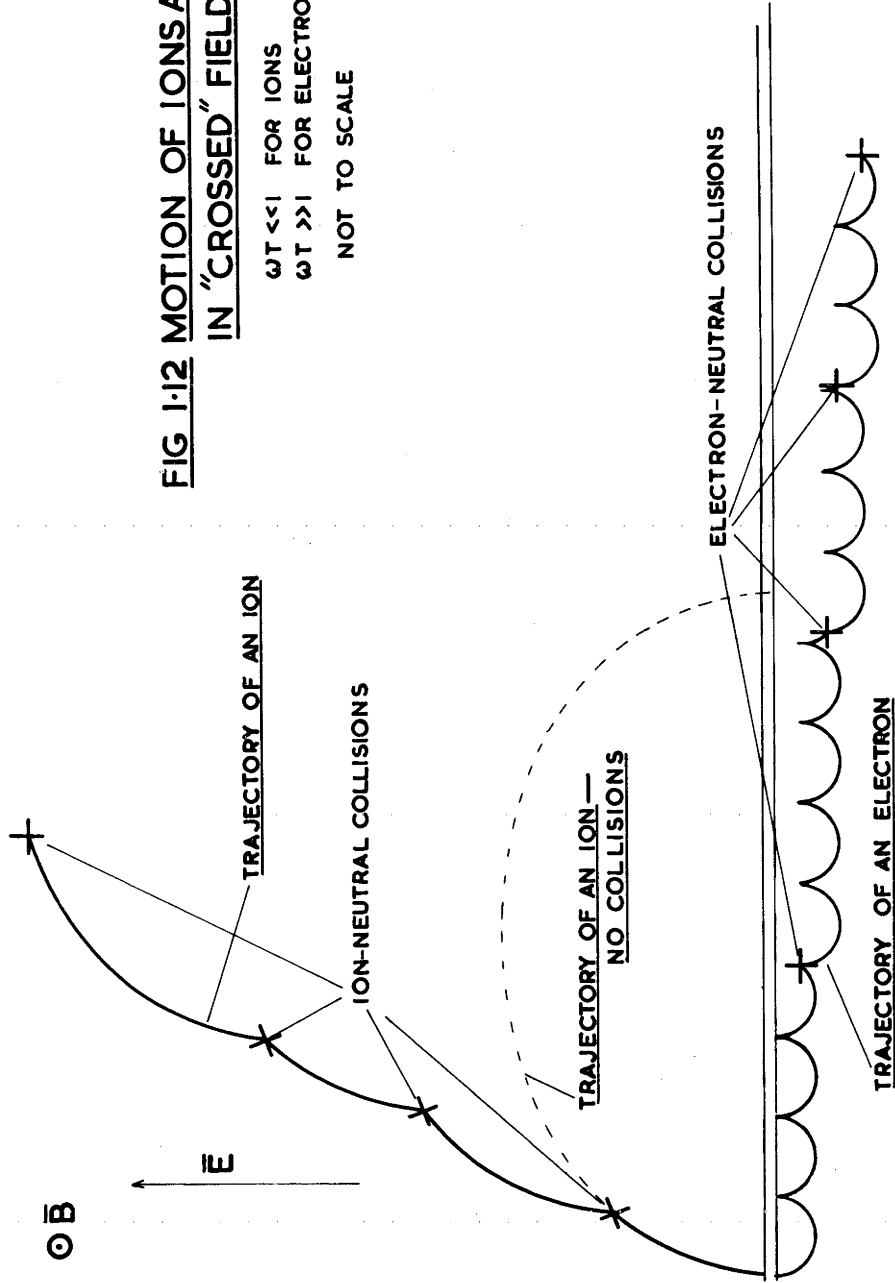
The Michigan group have studied the rotating glow discharge, and an unconfined glow discharge running between small electrodes, so that it cannot rotate (see figure 1.11) (Mc 51, Mc 53). The latter discharge was studied to assist in understanding the behaviour of the rotating discharge.

The stationary discharge is observed to "bow" in the direction of the Amperian force (see figure 1.11). A "wind" of neutral particles from this side of the discharge results from the transfer of transverse momentum from ions and electrons to the neutral gas molecules. A potential gradient exists across the discharge. The "leading edge" (i.e., the edge that would lead if the discharge could move) is negative with respect to the "trailing edge" by up to 500 volts. The discharge voltage is greater than in the absence of a magnetic field.

This behaviour is explained in terms of the motion of ions and electrons in crossed electric and magnetic fields (see section 5.1).

FIG 1.2 MOTION OF IONS AND ELECTRONS  
IN "CROSSED" FIELDS (SCHEMATIC)

$\omega T \ll 1$  FOR IONS  
 $\omega T \gg 1$  FOR ELECTRONS  
NOT TO SCALE



In crossed fields ions and electrons of zero initial energy follow cycloidal paths. The guiding centre of the charged particles moves in the  $\bar{E} \times \bar{B}$  direction with a velocity,

$$\bar{v} = \bar{E} \times \bar{B} / B^2 \quad (1.20)$$

where  $\bar{E}$  = electric field

$\bar{B}$  = magnetic induction.

The height of the arch of the cycloid,

$$h = \frac{2Em}{eB^2} \quad (1.21)$$

where  $e, m$  = charge, mass of the charged particle. Note that the ion's cycloid is much larger than the electron's cycloid.

If  $\omega = Be/m$  = angular frequency of rotation of charged particles in a magnetic field (the cyclotron frequency)

$T$  = mean free time between the collisions of a charged particle with the neutral gas molecules.

Then  $\omega T$  gives a measure of the fraction of a cycloidal (or, for zero electric field, the circular orbit) covered by a particle between collisions. (The motion of charged particles in crossed electric and magnetic fields, and the significance of  $\omega T$  will be discussed more fully in section 5.1).

At pressures where  $\omega T$  is considerably greater than one for electrons, but, because of the greater mass of an ion, considerably less than one for the ions, the electrons can move around several arches of the cycloid between collisions, but the ions move along

only a fraction of an arch between collisions. Thus, as shown in figure 1.12, the electrons tend to move across the electric field, while the ions move along the electric field.

The electric field component transverse to the axis of the discharge is due to electrons drifting to the leading edge of the discharge under the influence of the crossed electric and magnetic fields; the ions are little affected by the magnetic field, and move in the direction of the electric field. The separation of the ions and the electrons gives the transverse field, which prevents the electrons moving away from the discharge region. The increase of the discharge voltage is explained in terms of the reduced electron mobility due to the transverse magnetic field (To 12). This increase is not as great as would be expected from mobility considerations alone. The distortion of the equipotentials due to the separation of the ions and the electrons (see figure 1.12) is such that the electrons may move from the cathode to the anode along the equipotentials (i.e., in the  $\bar{E} \times \bar{B}$  direction). An imaginary mobility which may be greater than the real mobility is used to describe the motion of electrons perpendicular to the electric field. Thus the field distortion results in a discharge voltage that is less than would be expected from simple mobility considerations.

Low frequency electrical oscillations of large amplitude were observed in the presence of the magnetic field. Oscillations

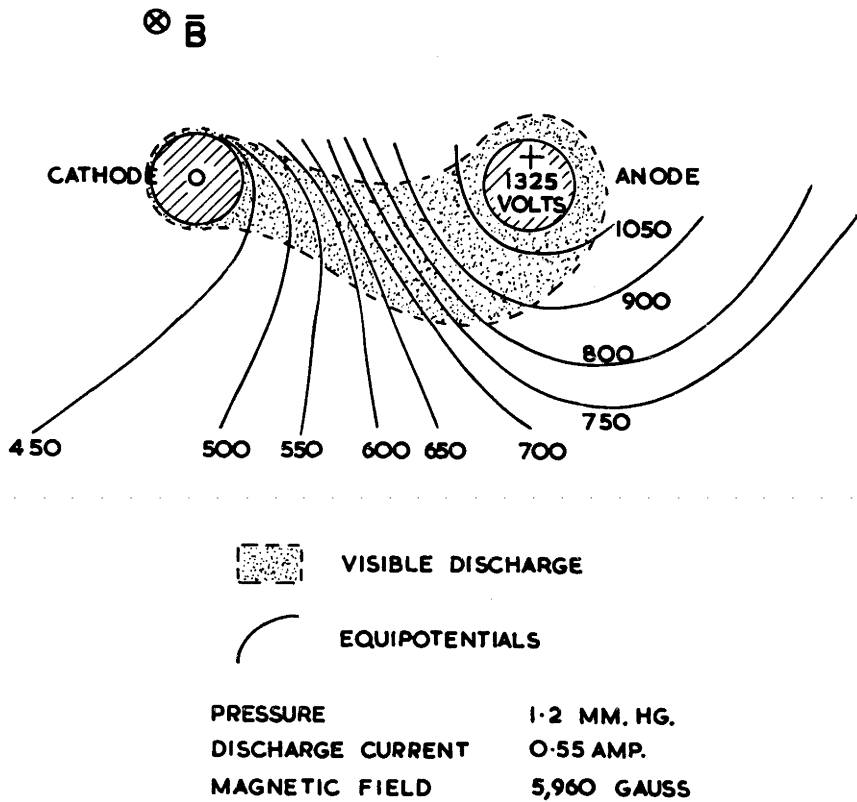


**FIG I-III THE UNCONFINED GLOW DISCHARGE (Ea58)**

have a great influence on the behaviour of a discharge, and it was suggested that the presence of these oscillations may invalidate, to a great extent, the simple model of the behaviour of the discharge described above. No attempt has been made to correlate the oscillations with one of the well known types of oscillations that occur in plasmas (Ro 61).

The rotating discharge was studied as a possible means of efficiently transferring large amounts of electrical energy to the directed motion of a small mass of gas. Hence the velocity of the wind produced by the discharge was a parameter of great interest in relation to experiments with both the rotating and the stationary glow discharges. No systematic measurements of discharge velocity are reported.

### 1.9 A CRITICAL SUMMARY OF THE PREVIOUS WORK ON THE MOTION OF A GAS DISCHARGE IN A TRANSVERSE MAGNETIC FIELD

#### 1.9.1 Experimental studies of the moving glow discharge

The early work was mostly performed at high pressures, and in low magnetic fields, where the rotation is relatively slow. Under these conditions, the characteristics of the discharge are not greatly perturbed by the magnetic field. e.g., appearance, particle densities and temperatures, and the electric fields are substantially the same as they would be in the absence of a magnetic field. In terms of particle motion, this means that conditions are such that the magnetic field does not greatly bend the paths of ions and electrons between

collisions. i.e., conditions are such that  $\omega T \ll 1$  (see section 5.1). Because of the limitations of the methods of velocity measurement - visual observation, or a rotating-disk stroboscope - the velocity of only slowly rotating discharges could be measured.

The Michigan group has extended the study of the rotating glow discharge to high fields and low pressures - i.e., conditions such that  $\omega T$  is of the order of 1 for electrons. Velocity measurements are made with the aid of a probe, and a cathode ray oscilloscope.

The range of the important parameters encountered in the experiments of WILSON and MARTYN, MALLIK, GUYE and his co-workers, and the MICHIGAN group are shown in table 1.1.

WILSON and MARTYN'S experiments are performed in a geometry that is close to ideal for a "radial magnetic field" geometry. The candidate is of the opinion that the geometry of Guye et al, with its uniform axial magnetic field, is preferable to this geometry, where the axial electric field is uniform. There is no advantage in a uniform "zero current" electric field, as the electric field between the electrodes will be greatly distorted by the presence of the discharge. The discharge current was obtained from a d.c. power supply. A rotating disk stroboscope enabled the velocity of relatively high velocity discharges to be measured. MALLIK'S geometry is far from simple. The magnetic field is not radial, and the discharge is not constrained to move around in an annular gap, as is the case

Table 1.1 PARAMETERS ENCOUNTERED IN PREVIOUS STUDIES  
OF THE ROTATING GLOW DISCHARGE

| Workers           | Magnetic Field<br>(Gauss) | Pressure<br>(mm Hg) | Current      | Period of<br>rotation (sec) |
|-------------------|---------------------------|---------------------|--------------|-----------------------------|
| Wilson and Martyn | 0 - 134                   | 4.35 - 11.8         | 10 - 30 mA   | .002 - .016                 |
| Mallik            | Tens of gauss *           | 6.9 - 126           | microamp.    | .515 - 2.4                  |
| Guye et al        | 0 - 440                   | 5.8 - 124           | .14 - .17 mA | .056 - 9.5                  |
| Michigan group ** | 6,000                     | .5                  | 6 amp.       | $6 \times 10^{-5}$          |

\* Magnetic field non-uniform. Not enough data is available to enable the field to be calculated to more than "order of magnitude" accuracy.

\*\* Not extensively reported.

in the above experiment. Most of the work was performed using as a power supply an induction coil, which gives an intermittent current. Wilson and Martyn's use of a direct current power supply, and the simpler geometry of their experiment, make the interpretation of the results of their experiment somewhat simpler than the interpretation of those of Mallik.

GUYE et al have performed a very extensive, systematic, study of the motion of a discharge in "good" geometry. The curved edges to the electrodes could be considered a complication to the geometry (see figure 1.5). However this electrode geometry, rather than a pair of concentric cylinders, was possibly chosen to constrain the discharge to move in a plane (see section 3.8). Care was taken to use pure gas, and run on clean electrodes.

Comparison of the behaviour of the discharge with the centre electrode positive, and negative, indicates that the electrode regions may be of importance in determining the velocity of rotation of the discharge. However these observations of the quite marked change in behaviour on reversing the polarity of the centre electrode were not followed up.

The MICHIGAN group. No extensive measurements are reported. Measurements are made at high currents and fields, where the magnetic wind has a high velocity. The discharge will be moving through a moving gas, rather than the substantially stationary gas of the experiments discussed above.

### 1.9.2 The theory of the motion of the glow discharge.

The theory of WILSON and MARTYN (and MALLIK) is in error. The drag on the charged particles of one kind in the  $\underline{E} \times \underline{B}$  direction, and in the  $\underline{E}$  direction are assumed proportional to the mean particle velocity in the direction concerned, the constant of proportionality being the same for both directions. This implies that the nature of the motion of the particles is the same in both directions, which is not the case. Under low magnetic field conditions, the particles move, on the average, one mean-free-path in the direction of the electric field between collisions. However, as the magnetic field barely deflects the particles between collisions, it moves much less than one mean-free-path in the  $\bar{E} \times \bar{B}$  direction between collisions. Thus the drag, which is the result of collisions, will be different for the two directions.

This theory assumes that conditions are uniform between the electrodes. In particular, no account is taken of the variation of the electric field between the electrodes. (see equation 1.9).

The theory of GUYE. Because of approximations made during its derivation, equation 1.19 is correct only for  $\omega T \ll 1$  for ions. However experimental results in disagreement with this theory are obtained even when conditions are such that  $\omega T \ll 1$ . Again the discharge is assumed to be uniform between the electrodes. This not a great error in this case, as the electric field does not appear explicitly in the equation giving the velocity.

Neither of these theories takes into account the vastly different natures of the three regions of the discharge, and neither explains the variation of discharge velocity with current.

### 1.9.3 The motion of the arc

The extensive experimental work, especially that of Guile et al, reveals the importance of the cathode region of the arc in determining discharge velocity and behaviour. These observations indicate that a study of the influence of the cathode region on the motion of a glow discharge would be of value.

The neglect by earlier workers of the possibility of the electrode regions, particularly the cathode region, influencing the velocity of rotation of the glow discharge, is most surprising. This is particularly so in view of the observation of Guye of remarkable changes of discharge behaviour on reversing the polarity of the centre electrode.

The theory of the rotation of the arc depends on the model chosen for the cathode region of the arc. Indeed a test of a theory of the cathode region of the arc is whether it can explain arc motion, especially retrograde motion. In a similar manner, will a study of the rotating glow discharge give a method of studying the cathode region of the glow discharge? The physics of the cathode region is not understood in detail, as yet. (Fr 56)

1.9.4 The relationship between the work described in this thesis, and the previous work

(a) The work described in this thesis is primarily a survey of the behaviour of the rotating glow discharge under a wide range of conditions. Emphasis will be placed on a study of the rotation under conditions such that  $\omega T$  for electrons is of the order of 1. The rotation of the glow discharge has not been systematically studied under these conditions.

The velocity is measured by a technique involving the use of a photomultiplier and a cathode ray oscilloscope, enabling the accurate determination of angular velocities far greater than could be measured by the early workers (Wilson and Martyn, Mallik, Guye et al). It is only this method of velocity measurement that enables the velocity to be measured under conditions such that  $\omega T$  is of the order of 1 for electrons.

The majority of the measurements will be made at low current, where the wind velocity is negligible compared with the discharge velocity.

(b) The influence of the cathode region on discharge motion will be studied, both experimentally and theoretically.

(c) The motion will be studied in a geometry similar to that of Guye and his co-workers, where the current flows radially between concentric electrodes, and is driven around the gap between these

electrodes by an axial magnetic field - see figure 1.1(b). This geometry was chosen because it gives itself to a more convenient experimental arrangement than the other geometries discussed, because of the simplicity of this geometry compared with other geometries (this is discussed in section 1.9.1), and because this geometry is particularly suitable for a study of the influence of the electrode regions on the motion of the discharge (see Chapters 2 and 3).

## Chapter 2

### INITIAL STUDIES OF THE MOTION OF THE GLOW DISCHARGE IN A TRANSVERSE MAGNETIC FIELD: EXPERIMENTS WITH THE "RACETRACK" CHAMBER

When a study of the glow discharge in a transverse magnetic field was first proposed it was decided to build a discharge chamber of simple design that could readily be constructed in a machine shop. The chamber was initially intended only for a trial series of experiments, using the magnetic field of the A.N.U. Cyclotron, which was available only for a few days. However features of the behaviour of the discharge were of such interest that it was decided to continue the experiments with this chamber in a magnet especially constructed for that purpose. This chapter describes the apparatus used for these latter experiments, and the results of these experiments.

Much of the apparatus was also used for later experiments. For this reason, it will be described here in some detail.

The experimental results will be discussed only briefly. The results do not contribute significantly to the argument of this thesis, but do give information as to where improvements can be made in the design of apparatus to be constructed for later experiments.

#### **2.1 EXPERIMENTAL APPARATUS**

##### **2.1.1 The Discharge Chamber**

A photograph of this chamber is shown in figure 2.1.

FIG 2.1 A PHOTOGRAPH OF THE "RACETRACK" CHAMBER

This photograph was taken after the discharge chamber had been used for a long series of experiments. The electrodes are particularly heavily coated with a dark grey deposit - a mixture of "cracked" oil, and copper oxide. Note the bright marks on the outer electrode. One is on the hard-soldered join of this electrode; the other does not correspond to an obvious irregularity, or change of the surface properties of the electrode.

The top cover has been removed, but the rubber sealing gasket is still in position.

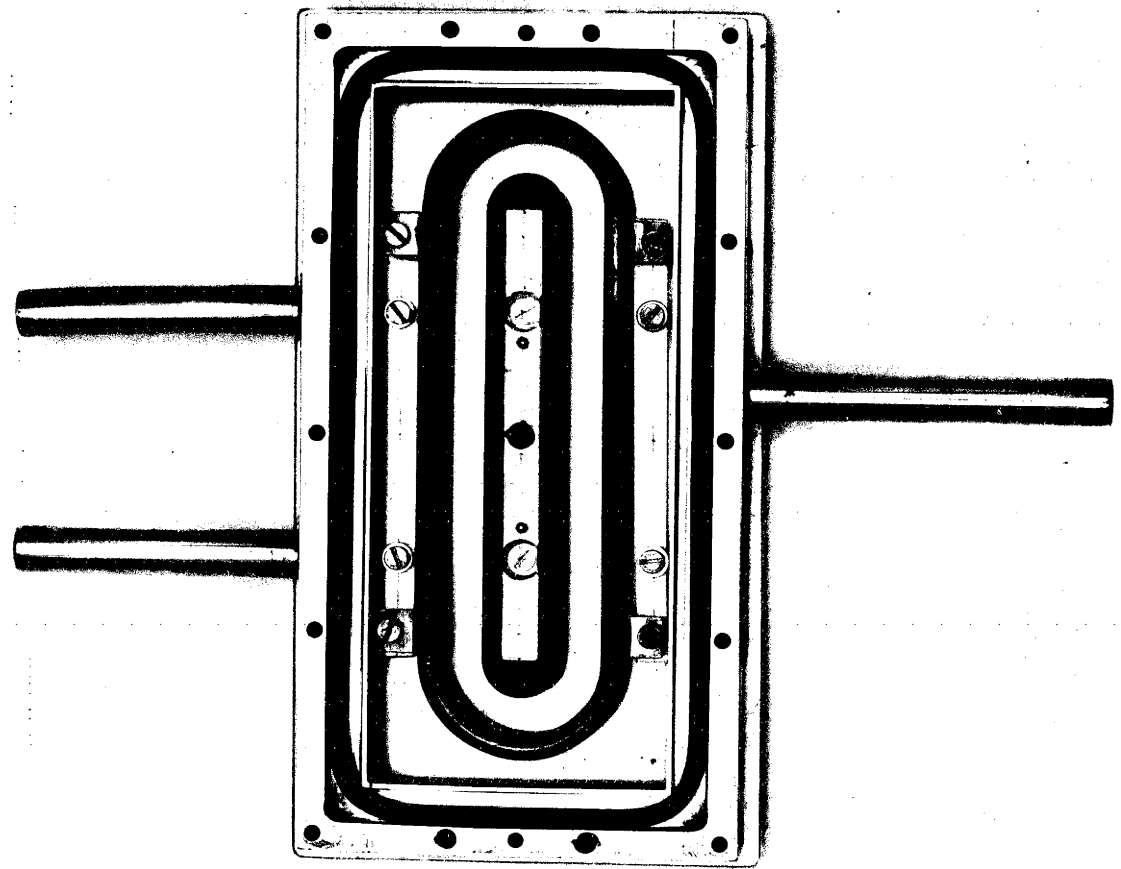


Figure 2.2 shows details of the construction and the important dimensions of this chamber. The "racetrack" electrode geometry - flat concentric electrodes, the gap around which the discharge moves consisting of two straight sections joined by two semi-circular sections - was chosen for two reasons:

- (1) To study the motion of the discharge along straight parallel electrodes.
- (2) To attempt to find the region of the discharge that determines the velocity in a T.M.F. A photomultiplier looks down on two points, 10 cm. apart, at the ends of one of the straight sections. The time the discharge takes to move along 10 cm. of the straight,  $T_{r1}$ , and the time it takes to complete a circuit of the racetrack,  $T_r$ , can be measured by observing the signals from the photomultiplier on a cathode ray oscilloscope.

The cathode region of the discharge is said to control the motion of the discharge if this region moves with a constant velocity,  $v$ , along both the straight and curved sections of its path, the remainder of the discharge being dragged along at, or held back to this velocity by the cathode region. If this is the case

$$v = 10/T_{r1} = \ell/T_r \quad (2.1)$$

i.e.  $T_{r1}/T_r = 10/\ell \quad (2.2)$

where  $\ell$  = total length of the cathode (outer electrode).

Similarly if the anode region or the positive column control

FIG 2.2 THE "RACETRACK CHAMBER - IMPORTANT DIMENSIONS, AND DETAILS OF CONSTRUCTION

- A - Inner electrode - generally the anode.
- B - Discharge gap.
- C - Outer electrode - generally the cathode.
- D,D' - Position of viewing holes of the light detection equipment. D - large hole.  
D' - small hole.
- E - "Perspex" covers.
- F - Pumping lines.
- G - Gasket grooves.

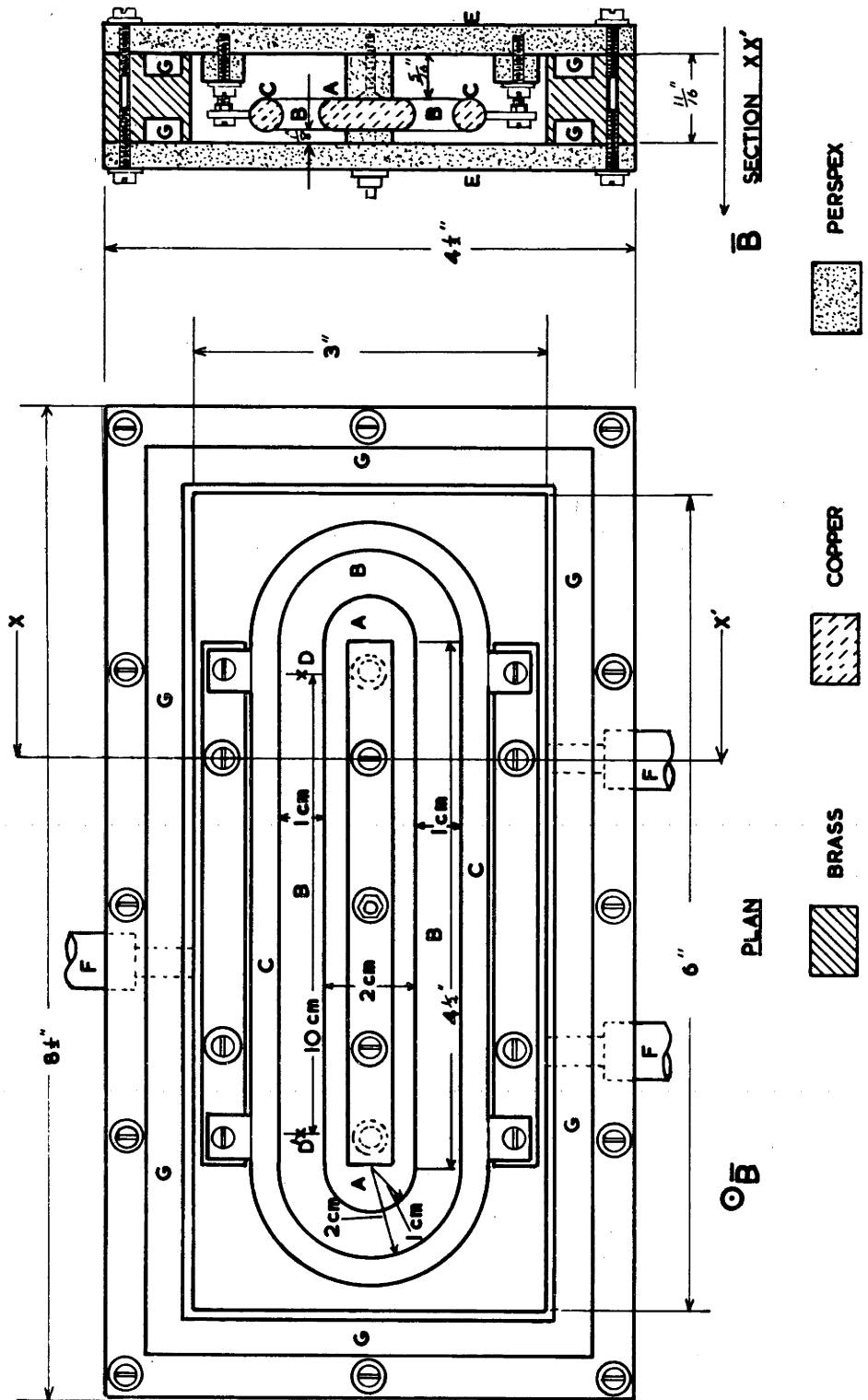


**FIG 2.2 THE RACETRACK CHAMBER - DETAILS OF CONSTRUCTION**

the motion of the discharge, equation 2.1 holds, where  $\mathbf{L}$  is now the perimeter of the anode, or the length of the racetrack measured between the electrodes. Measurement of the ratio  $T_{r1}/T_r$  will enable the determination of the region controlling the velocity of the discharge. The results of these measurements will be discussed later in this chapter.

The outer wall of the discharge chamber,  $\frac{11}{16}$ " in height, was constructed from brass, with silver soldered joins. Square-section rubber gaskets in grooves at the top and bottom of this wall seal "Perspex" cover plates to the wall.

The outer electrode was made from a  $\frac{1}{4}$ " diameter copper rod, bent into the racetrack shape. The ends of the rod were silver soldered together. Mounting lugs are used to screw this electrode to "Perspex" blocks, which are attached to the bottom cover of the chamber. The inner electrode, machined from  $\frac{1}{4}$ " copper sheet, had  $\frac{1}{8}$ " radii machined on the edges. This is also mounted on "Perspex" blocks, screwed to the bottom cover of the chamber. The gap between the electrodes is set to a constant value by means of removable cylindrical spacers of "Bakelite". The gap, nominally 10 mm. is not particularly constant. Because of the tolerances allowed in the construction of the chamber, rough handling during the course of the experiments, and difficulties in adjusting the electrodes to obtain a constant gap, the gap can only be set constant to within  $\pm \frac{1}{2}$  mm.

### 2.1.2 The Power Supply

The power supply of an R.C.A. MI-8167 high frequency radio transmitter was used to supply the discharge current. This supply consists of 4 x 866-A mercury arc rectifiers, connected as a full wave rectifier. The output is filtered by a choke-input LC filter; the filter capacitance is 20 microfarad, and the inductance approximately 8 henrys. Additional filtering is supplied by a similar filter external to the transmitter cabinet. The output voltage may be varied by means of a "Variac" in the primary of the power transformer.

Under low load conditions, the output voltage can be raised to 3.1 K volt. The maximum output current, which is determined by the rated maximum plate current of the rectifiers, is 1 amp at peak voltage. This may be increased at low output voltages. The R.C.A. Tube Handbook (Ra 57) gives data showing that the maximum output current of the supply can be raised to 2 amp at 800 volts. The ripple on the output voltage is less than 0.06% (peak-to-peak) for voltages up to 2.5 K volt, and current up to 0.5 amp.

At load resistance continuously variable from 0 to 110 K ohm is used to stabilize the discharge current and, when necessary, to act as a fine current control.

### 2.1.3 The magnet

A low-cost magnet, with no stringent requirements for field

uniformity and constancy is all that is required for this research project. Consequently the magnet was designed to make maximum use of surplus material available in this laboratory, and to be of simple construction. The gap must be several inches high to accommodate the discharge chamber and light pipes running from the top of the chamber to photomultipliers external to the magnet. A maximum magnetic field of 6 kilogauss was suggested as a basis for the design of the magnet. This is the maximum magnetic field used by the Michigan group (Ea 58, Mc 51) for their experiments.

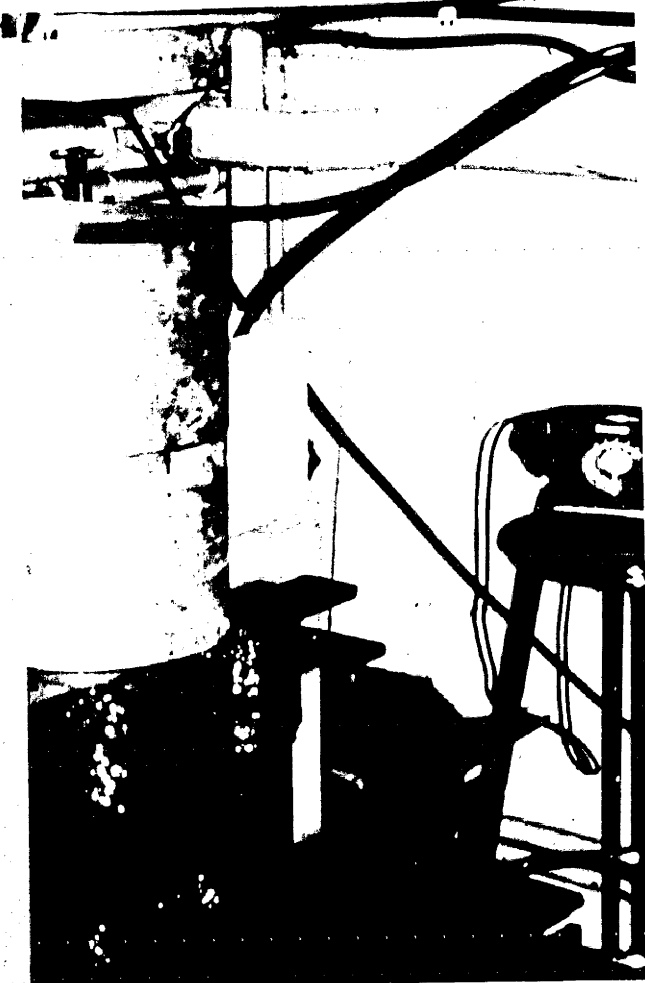
A cee-shaped yoke was decided upon because this shape can be readily constructed from steel available in the laboratory, and allows access to the gap over almost  $360^{\circ}$ . Two cees, each 5" thick were flame-cut from slabs of low carbon steel, and welded together. The cross-section of the yoke is approximately 10" x 10". The completed cee was not machined in any way, apart from removal of rough edges by a portable grinder. Two pole-pieces, each consisting of two sections, 10" in diameter and 7" high, are held to the cee by  $\frac{3}{4}$ " set screws. Shims between the pole pieces and the yoke, and sloppy holes for the holding screws enable the gap to be adjusted for parallelism to within 0.002", and the pole pieces to be set coaxial to within  $\frac{1}{32}$ ". The gap of the assembled magnet (before shimming) is 4.473".

Figure 2.3 shows details of the construction of the magnet.

Power for the magnet is supplied by an Oliver Electric Co.

FIG 2.3 A PHOTOGRAPH OF THE ELECTROMAGNET

This photograph, taken during the assembly of this magnet, shows details of the construction of the magnet. Both sets of pole pieces, and the upper coil (located around the upper pole-pieces), are in position. Iron lugs welded to the yoke (bottom of the photograph) hold the coils in position.



motor generator set designed for electroplating, which supplies 450 amp at 6-8 volts. This generator is self-excited as supplied. Two coils were wound for the magnet from an aluminium conductor, 0.75" x 1.25", with a 0.4" diameter hole for coolant running down the centre. The coils must have a low resistance (approximately 0.008 ohm each) to match the output characteristics of the generator. The coils were wound on a brass former lined with "Armite" insulating paper. Each coil consists of 6 layers, of just over 9 turns of conductor per layer. Because of the small number of turns required the coils were hand wound. The former was mounted on a windlass turned by two men. Winding tension was supplied by screwing two cylinders of paper-filled "Bakelite" hard against the conductor. The gaps at the end of each layer were packed with "Masonite". Strips of "Armite" provided insulation between turns, and a double layer of "Armite" provided insulation between layers. The coils were mounted around the pole pieces.

The generator was separately excited by lead-acid accumulators, excitation current being controlled by series resistors. Field direction is reversed by reversing the excitation current. A trickle of cooling water flows through the cooling channel. This is not essential for the reliable running of the magnet - the conductors only become warm to the touch if the cooling water is left off. However the current stabilizes within a few minutes if the coils are cooled.

The uniformity of the magnetic field was improved by the addition of shims to the pole pieces. Figure 2.4 shows the shim geometry that gave the most uniform field, and the radial variation of the magnetic field (the field "profile") with these shims in position. Curves (i) and (ii) show the measured radial variation of the axial magnetic field in the median plane before and after the installation of the shims. Curve (iii) shows the measured radial variation of the axial magnetic field, and curve (iv) the calculated radial variation of the radial magnetic field,  $\frac{1}{2}$ " above the median plane, with the shims in position. The field is uniform to better than 1% over a cylindrical volume 1" deep and 7" in diameter at the centre of the gap. The uniformity of the magnetic field is such that the drift of particles due to non-uniformity of the field is negligible compared with that likely to result from the action of crossed electric and magnetic fields.

The field measurements were made by a method due to LANE (La 28) modified by MORTON (Mo 58) for field difference measurements. Identical coils, one a reference coil which is located on the axis of the pole pieces, the other a coil that may be moved radially, are connected in opposition. The charge induced by turning these coils through  $180^\circ$  is proportional to the difference between the magnetic fields through the coils. This charge is measured by bucking it against the charge induced in the secondary of a mutual inductance by reversing the primary current.

FIG 2.4 SHIM GEOMETRY AND THE EFFECT OF SHIMS  
ON THE UNIFORMITY OF THE MAGNETIC FIELD

- (a) Shim geometry.
- (b) Radial variation of the axial magnetic field.  
Magnetic field - 2,160 gauss.
  - (i) Field profile in the median plane - no shims.
  - (ii) Field profile in the median plane - shims as in figure 2.4(a).
  - (iii) Field profile  $\frac{1}{2}$ " above the median plane - shims as in figure 2.4(a).
- (c) Radial variation of the radial magnetic field,  $\frac{1}{2}$ " above the median plane. Magnetic field - 2,160 gauss. Shims as in figure 2.4(a).

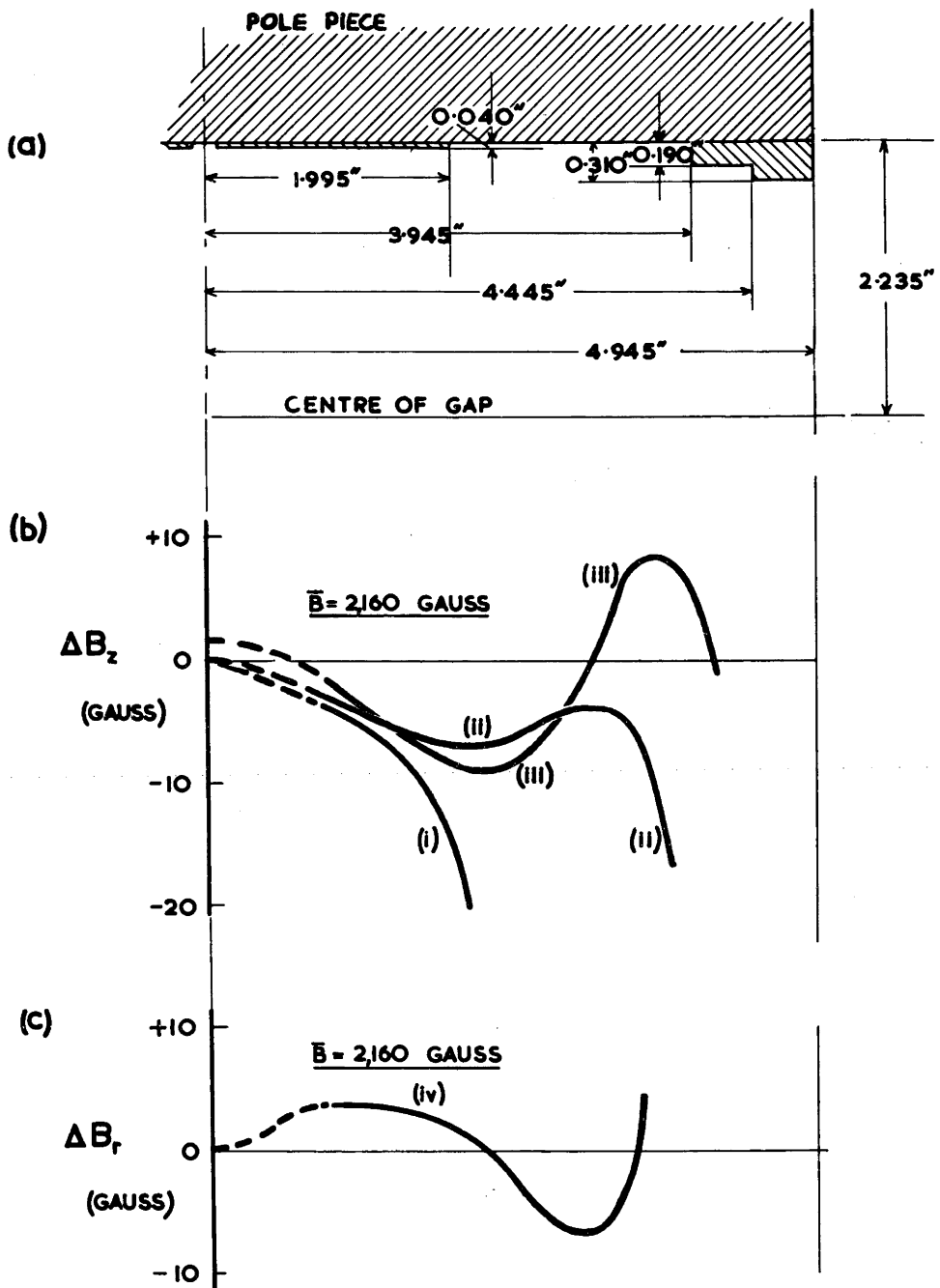


FIG 2.4 THE EFFECT OF THE SHIMS

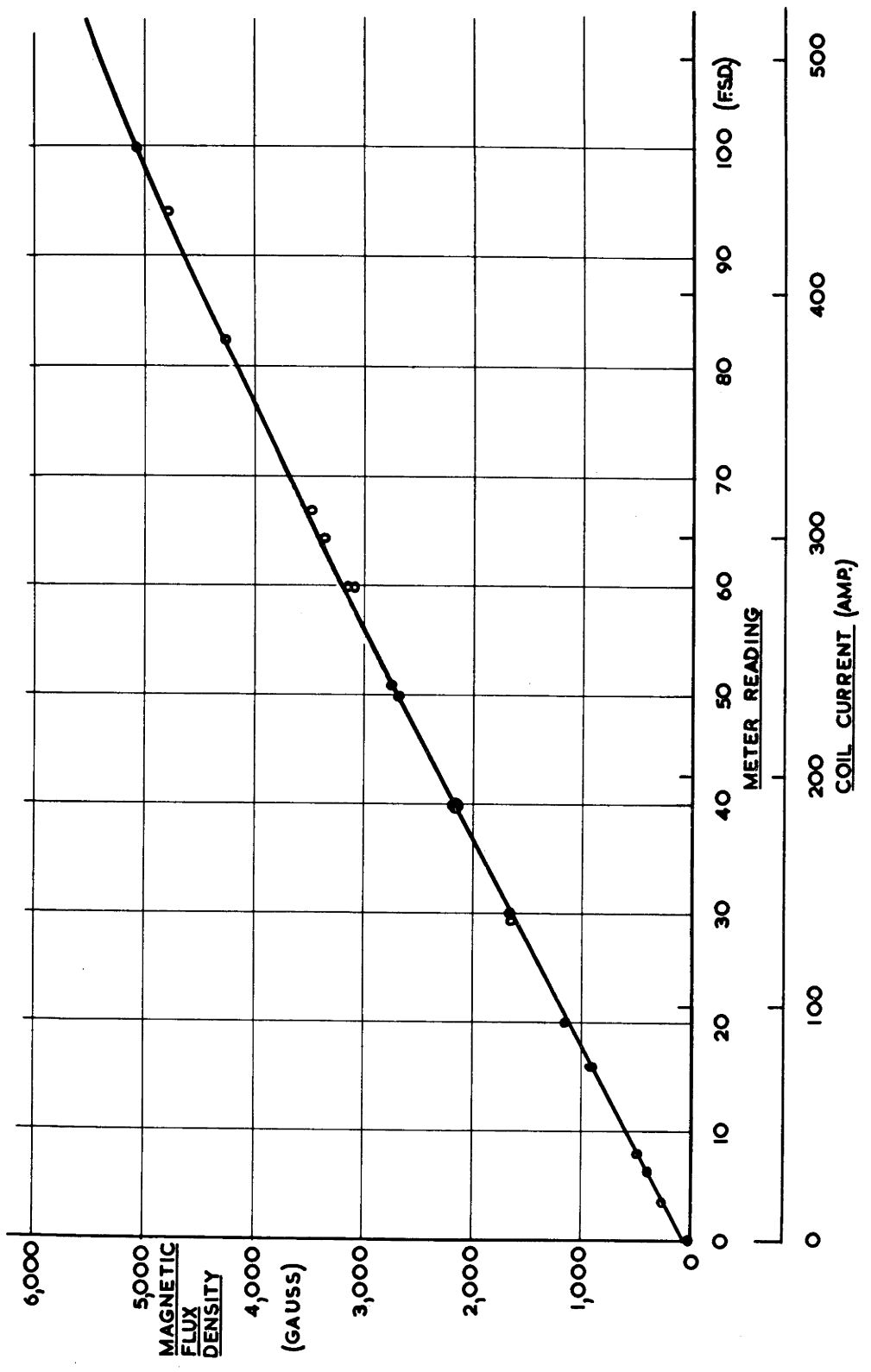
It was thought that magnetic field "lines", "short circuiting" through the back of the yoke, might give a magnetic field that was not cylindrically symmetric. However a series of field measurements made 90° apart, gave identical field profiles. Profiles made in fields of 590, 2,160 and 4,700 gauss have substantially the same shape, indicating that the shimming is satisfactory over the range of magnetic fields used for these experiments.

Figure 2.5 shows the magnetic field at the centre of the gap as a function of the "Coil current" meter reading. This meter reading is the parameter recorded during experiments. It is necessary to draw more than the rated current from the generator to obtain the design field of 6,000 gauss. However, the generator does not appear to have been harmed by overloading for short periods. Measurements indicate that the hysteresis is negligible. (The remanent field is less than 20 gauss).

The performance of the magnet has been most reliable to date. It runs stably, after warming up, at all but the lowest fields (under 1,000 gauss) where the coil current tends to wander.

#### 2.1.4 The vacuum system

The discharge chamber, was initially pumped only with a mechanical backing pump, but experimental studies of the reproducibility of the results indicated that a "cleaner" vacuum system would be required. A diffusion pump, and liquid-air cooled backing-line



**FIG 2.5 CALIBRATION CURVE FOR ELECTROMAGNET**

and diffusion pump cold traps were progressively installed in an attempt to:

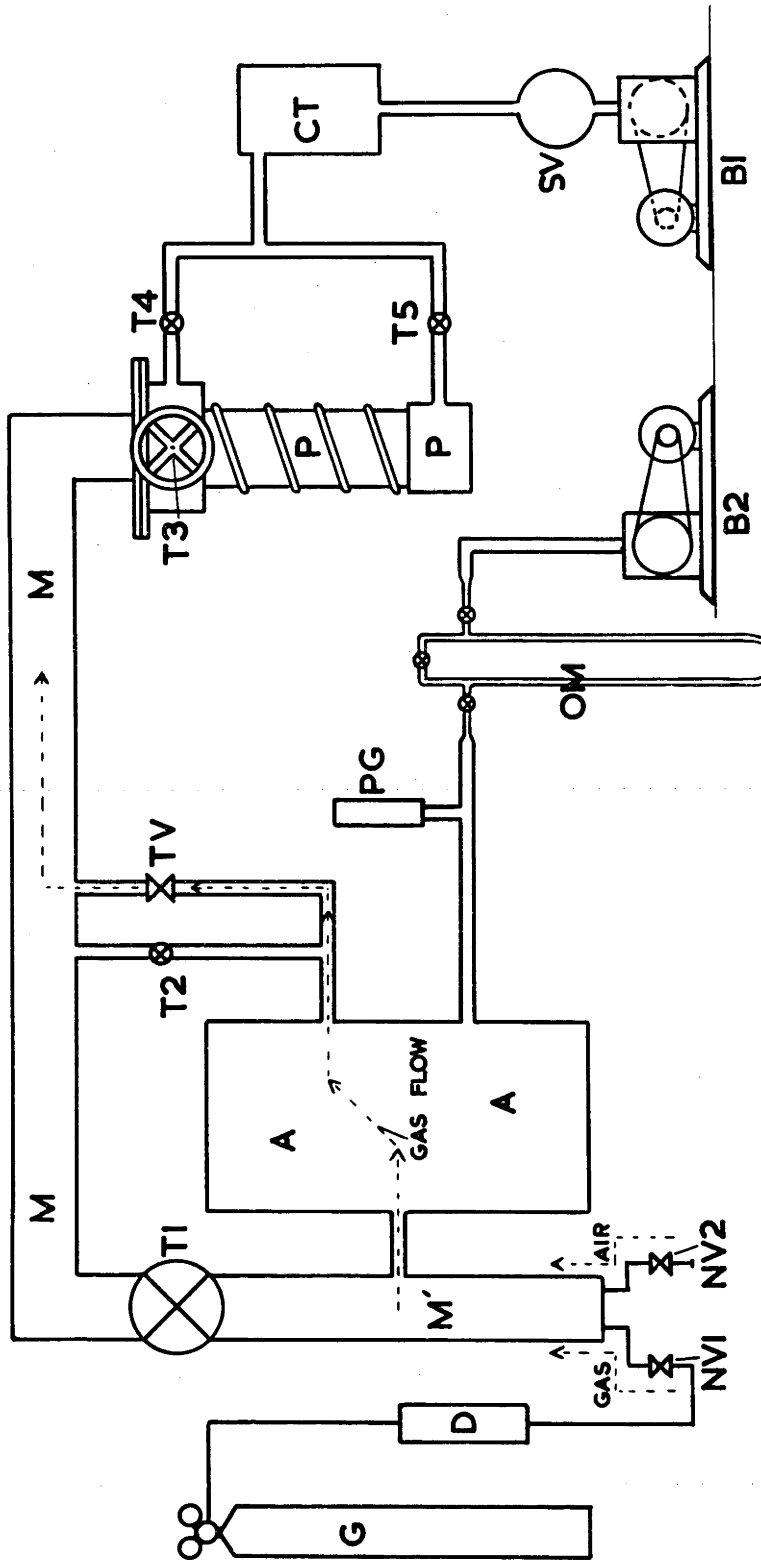
- (a) Reduce the base pressure and, it was hoped, the virtual leak rate into the vacuum system.
- (b) Prevent the migration of oil to the discharge chamber.

Figure 2.6 shows schematically the vacuum system as it was during the experimental study of the shape of the moving discharge described in section 2.4. The main pumping line from the diffusion pump to the discharge chamber, which is made of 2" and 4" brass and copper tubing, has a high conductance. However, the  $\frac{1}{2}$ " o.d. line from the main line to the chamber itself, and the  $\frac{1}{4}$ " hole in the chamber wall (shown in figure 2.1) drastically reduce the pumping speed of the system. This vacuum system was designed for use with other chambers - in particular the chamber described in section 3.1. For this reason, the main line was made from large diameter tubing, in spite of the narrow line into the chamber itself. Demountable vacuum seals using "Neoprene" O-rings were used extensively to enable rapid removal of the discharge chamber from the gap of the magnet.

The Pirani gauge measures the pressure to which the system was pumped prior to an experiment. During experiments, the gas pressure is measured by the oil manometer, which is filled with Apiezon "B" oil. The vapour pressure of this oil is approximately

FIG 2.6 VACUUM SYSTEM AS SET UP FOR PROFILING EXPERIMENTS WITH THE "RACETRACK" CHAMBER  
(SCHEMATIC)

- A - "Racetrack" chamber.
- B1 - Main backing pump.
- B2 - Backing pump for evacuating "reference" arm of the oil manometer.
- CT - Cold trap.
- D - Gas drying tube - packed with Linde "Molecular Sieve".
- G - Gas cylinder.
- M - Main pumping line.
- M' - Gas mixing chamber - main pumping line.
- NV1 - Needle valves - gas is leaked into the system
- NV2 - through these valves.
- OM - Oil manometer.
- P - Diffusion pump.
- PG - Pirani gauge.
- T1-T5 - Vacuum taps. (T3 - baffle valve above diffusion pump).
- TV - Throttle valve. Controls the gas pressure.
- SV - Safety volume. Prevents backing pump oil sucking back into the system in the event of a power failure.



**FIG 2.6 VACUUM SYSTEM—SCHEMATIC**

$10^{-7}$  mm. Hg at room temperature, density = .871 gm/cm<sup>3</sup> at 20° C.

The gas used for the experiments was passed continuously through the discharge chamber. It enters through the needle valve, and is pumped away through the throttle valve by the backing pump. Taps T1 and T2 are opened when pumping down, but closed while experimenting. The pressure in the chamber is controlled by closing the throttle valve, the rate at which the gas enters the system being set at the same value for a series of experiments.

When the gas flows continuously through the system, and the pressure is controlled in this manner, the percentage of impurities in the gas in the system should be substantially independent of pressure and time. It is assumed that the rate at which impurities from both real and virtual leaks leak into the system, does not vary greatly over a series of experiments, and is independent of pressure.

The base leak rate (the rate at which impurities leak into the system) was approximately 0.15 micron litre/sec., the gas leak rate approximately 500 micron litre/sec. for typical experiments. Thus, if a pure gas was fed into the discharge chamber, the discharge would be running in a gas containing 0.03% of impurities.

Industrial grade hydrogen, helium and argon, and air, were used for these experiments. The inert gases and hydrogen were chosen for their relatively simple nature, and their chemical inertness. These gases are not decomposed by the discharge (although

the hydrogen will be dissociated to some extent) and do not react with the materials of which the chamber is constructed. Their molecular weights covered a wide range, and large cylinders were readily obtainable. Although the gas from these cylinders is not particularly pure (approximately 99.9% pure, after drying; the composition varies from cylinder to cylinder), it was assumed that the composition of the gas from a particular cylinder would not change with time. The gases (with the exception of the air) were dried by passing through type 4A "Molecular Sieve" (an artificial zeolite manufactured by the Linde Company) prior to entering the discharge chamber. Because of the relatively large rate at which impurities leak into the discharge chamber, further purification was considered to be of doubtful value, and was not attempted.

The discharge will thus be running in the mixture of gases from an industrial cylinder, contaminated, but not greatly so, by impurities leaking into the discharge chamber. The magnitude and composition of the impurities leaking into the discharge chamber is variable, even though the gas is passed through the chamber in such a manner as to keep the percentage of impurities in the gas at a constant level.

Impurities (including those from the cylinder as well as those leaking into the chamber) can have a major effect on discharge behaviour, even though they make up only a small percentage of the

gas in the chamber. The gases used for these experiments are characterized by high ionization and excitation potentials. For this reason impurity molecules, which in general have lower ionization potentials, will tend to be ionized in preference to the molecules of the experimental gas. The ionization of the impurities frequently occurs in collisions of the second kind (Fr 56), the impurity molecule being ionized in a collision with a metastable excited molecule of the main gas. Approximate calculations indicate that the degree of ionization is of the order of the percentage of impurity molecules present in the chamber. The percentage of the ions that are not ions of the experimental gas will thus be quite large. The effect of a small percentage of an impurity gas on the behaviour of a discharge is discussed by FRANCIS (Fr 56).

The above discussion indicates that:

- (a) The nature of the vacuum system, and the purity of the gas fed into the chamber, are such that the experiments are not performed in a gas that is sufficiently pure for the results to be characteristic only of the experimental gas.
- (b) Variation of the impurity level, and the composition of the impurities could give rise to a lack of repeatability of the experimental results.

The use of relatively impure gases in a "dirty" vacuum system for the experiments described in this chapter, is justified

only because these experiments are in the nature of a preliminary survey.

#### 2.1.5 Light detection and velocity measurement

The light from the moving discharge was detected by DuMont type 6291 photomultiplier tubes placed outside the field of the magnet. The light from the discharge passes through the "Perspex" top cover of the discharge chamber, up a narrow hole that defines the spatial resolution of the light detection equipment (the viewing hole) and enters the side of a cylindrical "Perspex" light pipe. It is totally internally reflected by a polished face at  $45^{\circ}$  to the axis of the pipe, and is reflected 3 feet down the pipe to the photomultiplier.

For velocity measurement the light from two holes 10 cm. apart was reflected down two light pipes to a single photomultiplier. One viewing hole was smaller than the other, enabling the direction of rotation to be determined by the relative position of the small and large pulses on the oscilloscope screen.

The photomultiplier dynode voltages were supplied from a "bleeder chain" of voltage dividing resistors. The current through the bleeder chain is 3 m A, with 1,800 volts (the maximum tube voltage) across the photomultiplier. The bleeder chain current was chosen to be as large as possible consistent with the power supply being used for a number of photomultipliers. (In later experiments three photomultipliers were used simultaneously). The high voltage for the photomultipliers is supplied by a John Fluke Manufacturing

Coy. Inc. Model 405L high voltage supply, which will give 15 mA output current. Heavy filtering of the last two stages of the photomultiplier is accomplished by shunting each bleeder chain resistor with an 8 microfarad electrolytic condenser. This filtering, and the large bleeder chain current, prevent distortion of the photomultiplier output pulses due to current pulses from the dynodes altering the voltage, and hence the gain, of the later stages of the photomultiplier during a pulse.

The anode of the photomultiplier is at earth potential, the photocathode at a negative potential, so that the signal may be directly coupled from the anode of the tube to the input of the cathode ray oscilloscope. This feature allows the light intensity to be measured between pulses, so that it can be determined whether or not the intensity falls to zero between pulses. The signal was fed to the oscilloscope via about 10 feet of unterminated coaxial cable. A low load resistor (1.2 K ohm) was chosen so that the load impedance time constant, which determines the frequency response of the light detection system, was suitably low (approximately .2 microsec.) The use of an unterminated cable enables a suitably large oscilloscope input signal to be obtained without using a d.c. preamplifier.

A Tektronix Type 545-A cathode ray oscilloscope was used for signal display and time measurement. A Type CA plug-in preamplifier assisted with the comparison of signals from two sources.

This preamplifier has facilities for:

- (a) The display of signals from each of two input channels on alternate sweeps of the electron beam across the screen.
- (b) "Chopping" between the two channels at a frequency of approximately 100 Kc/sec.
- (c) "Adding" the signals from each channel. Polarity reversal switches enable the CA plug-in preamplifier to act as a differential amplifier when operated in this mode.
- (d) Individual display of the two input signals.

The gain of the CA preamplifier (maximum sensitivity of the oscilloscope = 50 m Volt/cm. with this amplifier) and the bandwidth of the equipment have proved satisfactory for the experiments described in this thesis.

## 2.2 EARLY EXPERIMENTS: LACK OF REPRODUCIBILITY AND ITS CAUSES

The observed variation of the velocity of the discharge as a function of magnetic field, discharge current, and the pressure and composition of the gas will not be discussed. The results obtained are not inconsistent with the more reliable and more significant results discussed in Chapters 3 and 4 which describe experiments performed in discharge chambers of improved design.

The direction of motion of the discharge, as indicated by the relative positions on the oscilloscope screen of the signals due to light passing through the small and large holes, was always in the

Amperian direction. This result is not unexpected because of the high pressure at which the observations were made (at lower pressures the discharge occupies the entire region between the electrodes, so that the light intensity does not fall to zero) and the entirely different natures of the cathode region of the glow discharge, and the arc discharge.

In these studies of the repeatability of the experimental results the time the discharge took to make a circuit of the racetrack (the period of rotation of the discharge) was measured as a function of gas pressure at fixed discharge current and magnetic field. Experiments in argon, helium, and hydrogen showed that the results were not repeatable. At a fixed pressure the times obtained over a series of measurements would vary by up to  $\pm$  60% of the mean value.

For most measurements, this scatter of the experimental points is perhaps not as bad as it would appear at first sight. The period of rotation is varying rapidly with pressure where conditions are such that the spread of the times is large, so that the scatter of the points about a mean curve through the points is somewhat less than this figure would indicate.

After much experimental work using this chamber, the following conclusions were reached regarding the lack of reproducibility, and its sources.

1. The scatter of the periods of rotation is greatest for helium

(ionization potential = 24.58 volts. Potential of lowest excited state (metastable) = 20.96 volts), somewhat less for argon (ionization potential = 15.755 volts. Potential of lowest excited state (metastable) = 11.55 volts) and still less for hydrogen (ionization potential = 13.595 volts. Potential of lowest excited state = 10.15 volts.) This result is consistent with the lack of reproduceability resulting from the presence of a small percentage of impurity in the gas. Generally the higher the ionization and excitation potentials, the greater should be the effect of an impurity. Hence, because the nature and percentage of the impurity is not entirely controlled, the scatter of the measured periods of rotation will be greater, the higher the ionization and excitation potentials of the gas. Experiments in air showed that the curves would be repeated to within a few percent. However not enough measurements were made with air to come to a definite conclusions as to the reproduceability of the results of measurements obtained with air.

2. The velocity can be particularly sensitive to the presence of impurities. For example, in one experiment, the presence of 0.3% of air in argon caused the velocity to increase by a factor of approximately 4, at pressures between 10 and 20 mm. Hg. (The highest pressure at which measurements were made). The increase was somewhat less marked below 10 mm. Hg. Above 10 mm. Hg the velocity of a discharge in pure air is 20 to 40 times that of the

discharge in argon. The presence of a small percentage of argon in air, however, does not greatly affect the velocity of the discharge. This again indicates that the presence of a small amount of an impurity of low ionization potential in a gas with high ionization and excitation potentials has a major effect on the behaviour of a discharge in this gas.

3. The velocity, and the regularity of the motion depend on the condition of the electrodes. This is particularly true at higher pressures. A dark grey deposit resulting from the cracking of diffusion pump oil by the discharge soon builds up on the electrodes, causing the discharge to move in a jerky fashion and even, at higher pressures, to become stationary, rather than move round the race-track at constant velocity, as it does on clean electrodes.

4. At high pressures (15-20 mm. Hg), the discharge tends to "stick" at projections and irregularities in the discharge chamber. It has been observed to stick at the silver soldered join in the outer electrode, and the "Perspex" blocks on which the outer electrode is mounted. These blocks become covered with a thin film consisting of a mixture of cracked oil, and copper sputtered from the cathode. It is of interest to note that the silver solder of the joins was bare while the remainder of the electrode was covered with the dark grey deposit resulting from the cracking of the diffusion pump oil.

5. The deposit on the electrodes, and the walls of the chamber

originates almost entirely from the cracking of diffusion pump oil. The rate at which the deposit grew was quite low when only a backing pump was used to pump down the vacuum system. The rate-of-growth was exceedingly high when a silicone oil was used in the diffusion pump. Spectrographic analysis (performed by the Department of Geophysics of this University) showed the presence of large amounts of silicon in the deposit on the electrodes.

The tendency of silicone diffusion pump oils to migrate to the discharge chamber by "creeping" over surfaces, is fairly well known (Ri 61). For this reason, the silicone pump oil was replaced by Apiezon "B" oil, which appeared to reduce the rate-of-growth of the deposit. A significant reduction in the rate-of-growth resulted from the installation of a cold trap above the diffusion pump.

The deposit still observed after the installation of this trap could come from three sources:

- (a) The level of the liquid air in the cold trap was not automatically controlled, so that as level of the liquid air dropped, oil trapped at the top of this trap would evaporate off, and enter the discharge chamber.
- (b) Unpolymerized methyl methacrylate from the "Perspex" covers of the box could enter the chamber, and be cracked by the discharge.
- (c) The vacuum system could not be cleaned thoroughly prior

to installing the cold trap. Traces of oil remaining above the cold trap could diffuse to the chamber, and be cracked.

6. The improvements to the vacuum system described above have not significantly improved the reproduceability of the results, except in so far as the deposit on the electrodes affects reproduceability. The improved vacuum system has improved the base pressure to which the system may be pumped, but has not significantly changed the rate at which impurities leak into the system.

7. The results summarized above, and the discussion of section 2.1.4 emphasize the necessity for the construction of a vacuum system of a much more sophisticated design to enable the discharge to run between "clean" electrodes in gases of very high purity. Care must be taken to maintain gas purity and electrode cleanliness during experiments. The design of, and experiments performed in such a system, are described in Chapter 4.

### 2.3 THE SOURCE OF THE MOTION

As mentioned in section 2.1.1, the racetrack design was chosen primarily for attempting to determine the source of the motion of the discharge from the measurement of the ratio  $T_{r1}/T_r$ . It is assumed that the velocity is controlled by the region of the discharge that moves around the racetrack at constant velocity, the remainder of the discharge being dragged along at this velocity.

Experimental values of  $T_{r1}/T_r$  for argon, air and argon/air

mixtures were plotted against pressure. Lines were drawn on this graph corresponding to the values of  $T_{r1}/T_r$  that would be obtained if the discharge moved with constant velocity along the cathode and anode surfaces. The experimental values of  $T_{r1}/T_r$  tended to cluster about the line corresponding to a constant velocity along the cathode. However experimental errors are of such a magnitude that all that can be concluded is that the discharge appears to move with constant velocity along the cathode (the outer electrode). The lengths of the anode and the cathode are not sufficiently different to give a more significant result.

The ratio  $T_{r1}/T_r$  was plotted only for signals where the jitter and noise on the light pulse was not excessive, and where the discharge was so narrow that the pulses corresponding to the discharge passing under the small and large viewing holes were so narrow that the pulses were well resolved. Such signals only occurred at higher pressures. Hence the above conclusion only holds for pressures above approximately 10 mm. Hg.

It is assumed that the velocity at which the velocity-controlling region of the discharge moves around the curved section of the gap between the electrodes, is the same as that at which it moves along the straight sections. This is probably a satisfactory assumption if the anode and cathode regions control the velocity. These regions are thin compared with the radius of the curved sections of the electrodes.

and the cross-sectional area of the discharge (this is particularly true at high pressures, where these measurements were made) i.e., from geometrical considerations the electric field, and other parameters describing these regions will be substantially the same at the curved sections as along the straight sections.

However this is not the case if the positive column controls the discharge velocity. In the absence of a discharge, the electric field distribution at the curved sections is markedly different from that along the straight sections. Hence the electric field distribution and the structure of the positive column may be markedly different for a discharge moving around the curved sections than for one moving along the straights. The above measurements do not exclude the possibility of the positive column controlling the velocity of the discharge, a change in the structure of the positive column causing the velocity to drop as the discharge moves around the curved sections of the racetrack.

Because of the suggestive, but not conclusive, result of this experiment, the determination of the source of the motion of the discharge will be further pursued using a discharge chamber of somewhat different design. (See sections 3.1.1 and 3.4).

#### 2.4 THE SHAPE OF THE MOVING DISCHARGE

It is of importance for a complete description of the motion of a discharge in a T.M.F. to determine not only the region of the

discharge controlling the motion, but the spatial relationship of the various parts of the discharge. e.g., does the cathode region lead, or lag behind, the positive column of the discharge. This section describes observations of the shape of the moving discharge looking down on the discharge in the direction of the magnetic field.

The racetrack chamber is ideal for observation of the shape of the moving discharge, because the discharge runs close to the flat top cover of the discharge chamber. Because of the proximity of the discharge to the viewing hole of the light detection equipment (which determines the spatial resolution of this equipment), a high spatial resolution may be obtained without reducing the photomultiplier output pulse to an amplitude such that the noise from the light detection system becomes excessive, or difficulty is experienced in triggering the oscilloscope.

The spatial resolution of this apparatus is such that the photomultiplier sees the light originating from a circle of 4.8 mm. diameter in the median plane of the discharge. (See figure 2.7(a)). The resolution of the equipment is not as poor as this diameter would suggest. If a "step" light pulse with a straight edge (as shown in figure 2.7(b)) should move across this circle, the amplitude of the photomultiplier output signal will have increased to only 19% of the peak amplitude when the step has moved across a quarter of the diameter of the circle. The radius of this circle would give a better

FIG 2.7 RESOLUTION OF THE LIGHT DETECTION SYSTEM

(a) Geometry of the light detection system

- V - Viewing hole. This hole limits the area of the discharge seen by the photomultiplier.
- P - "Perspex" light pipe.
- E - Electrodes.

(b) Response of the system to a "step" of light moving across the viewing hole

- (i) - Light pulse.
- (ii) - Response of the photomultiplier.

(c) Response of the system to a dark strip moving across the viewing hole. Width of strip - radius of the circle of resolution

- (i) - Dark strip.
- (ii) - Response of the photomultiplier.

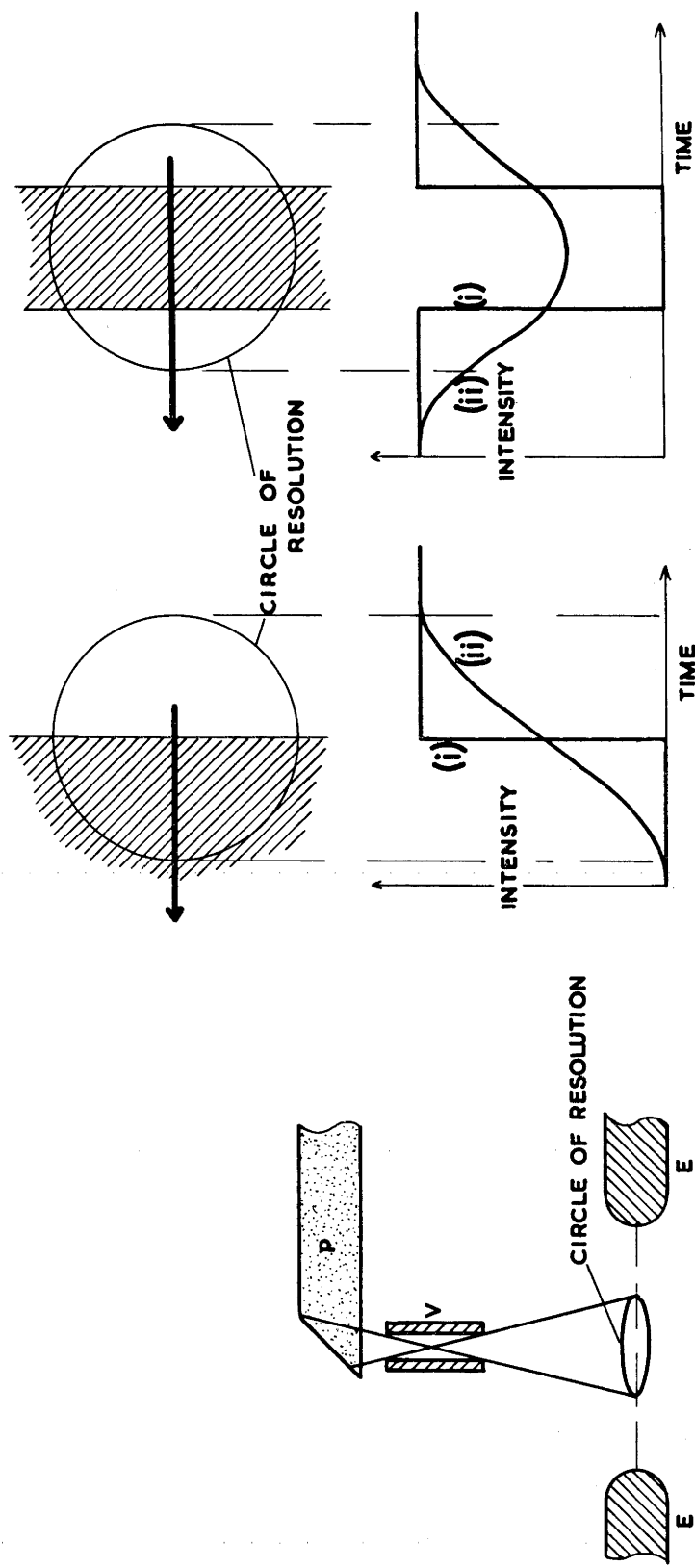


**FIG 2.7 RESOLUTION OF LIGHT DETECTION SYSTEM**

measure of the resolution. If a dark strip, a radius wide, should move across this circle, the amplitude of the photomultiplier output signal would fall to approximately 40% of the peak amplitude as the dark strip moves across the circle. (See figure 2.7(c)).

A schematic diagram of the apparatus used for determining the shape of the discharge is shown in figure 2.8. Two photomultipliers look down on the discharge through "Perspex" light pipes. The signal from the "upstream" photomultiplier (Photomultiplier A) is fed into the "trigger" input of the cathode ray oscilloscope. The viewing hole of the other photomultiplier can be moved across the gap between the electrodes (i.e., perpendicular to the direction of motion of the discharge) by means of an 8 B.A. lead screw. The signal from this photomultiplier (Photomultiplier B) is displayed on the oscilloscope.

Photomultiplier A, which is stationary, provides a time reference signal. The oscilloscope time base always starts when the discharge is at a certain position, irrespective of the position of Photomultiplier B. A series of photographs of the oscilloscope trace are taken as the viewing hole of Photomultiplier B is moved across the discharge. The time taken by the various parts of the discharge to move from the datum position to the viewing hole may be read from these photos. e.g., the leading edge near the cathode may be under the viewing hole 1 millisecond after the discharge is at the datum position; the leading edge at the anode 0.5 millisecond after the discharge

FIG 2.8 THE APPARATUS USED FOR THE DETERMINATION  
OF THE SHAPE OF THE DISCHARGE (SCHEMATIC)

- C - Bearing
- D - Discharge
- E - Electrodes
- K - Knurled knob
- MC - Moveable carriage
- N - Fixed nut
- P - "Perspex" light pipes
- VF - Fixed viewing hole
- VM - Moveable viewing hole
- PM - Photomultiplier.

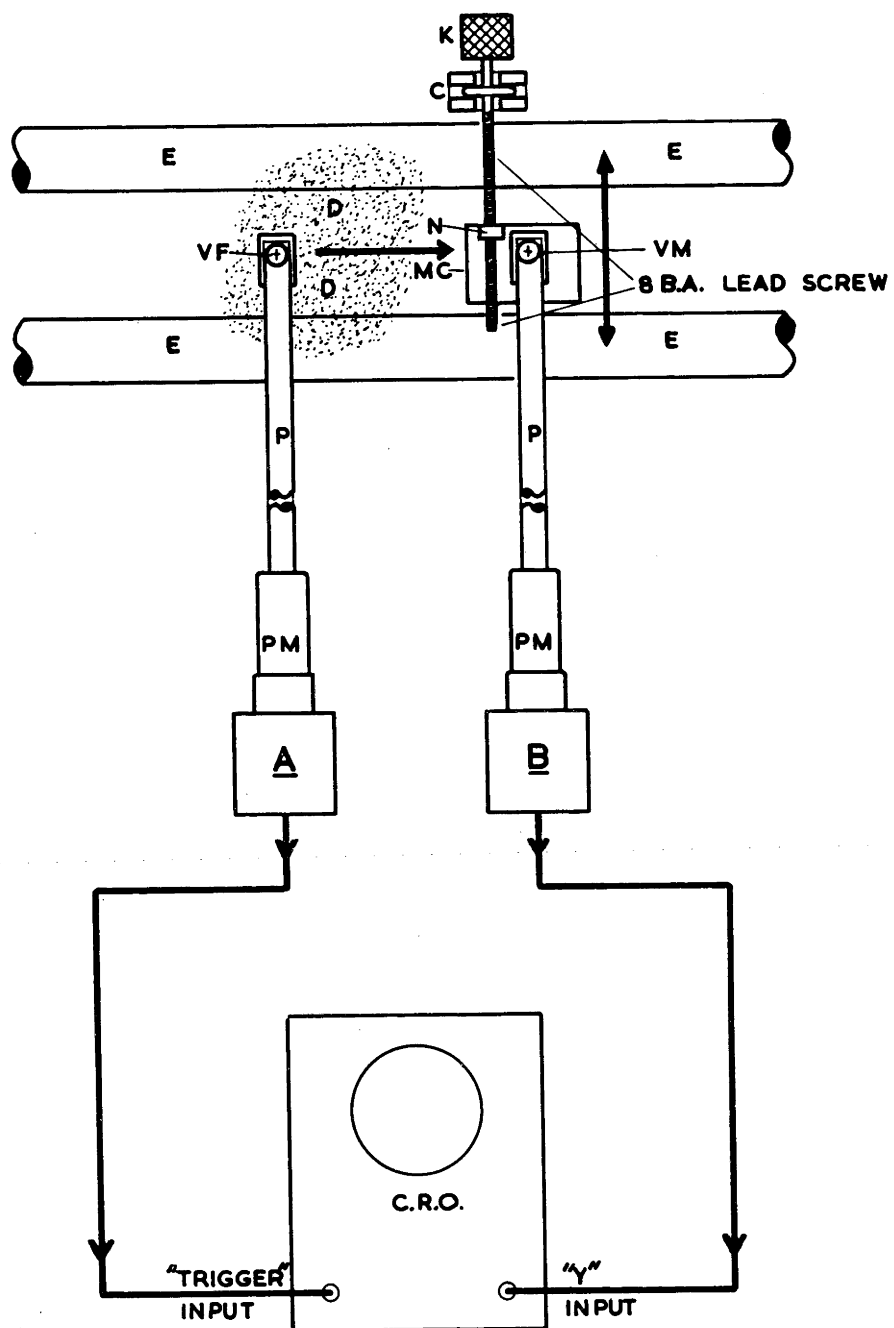


FIG 2·8 THE APPARATUS USED FOR THE DETERMINATION OF THE SHAPE OF THE DISCHARGE

is at the datum position. This shows that the anode region moves ahead of the cathode region. From a knowledge of the velocity of the discharge (obtained by measuring the time the discharge takes to move between the viewing holes  $T_{r1}$ , or the time the discharge takes to move around the racetrack,  $T_r$ ) the distance the anode region lies ahead of the cathode region may be calculated.

In a similar manner diagrams showing light intensity contours - i.e., the shape of the discharge - may be prepared from these photographs, which are profiles of the light intensity across the discharge. The collector current of a photomultiplier is proportional to the intensity of the light striking the photocathode. No attempt has been made to correct these photos for the different spectral distributions of the light from different regions of the discharge.

Because the photomultiplier scans the discharge as it moves past the viewing hole, these contour diagrams are strictly not "snapshots" of the moving discharge, such as would be obtained from a high-speed camera. However the intensity of the light from the discharge was so low that the discharge possibly could not have been recorded by a high-speed camera, had one been available.

For this reason the determination of discharge shape in this manner is only satisfactory if the discharge does not change shape as it moves along the electrodes, and moves with a constant

velocity, rather than with an irregular motion. This can be checked by removing the light pipe of the photomultiplier from its support, and moving the viewing hole back and forth in the direction of motion of the discharge. The stability of the signals on the oscilloscope screen, which shift smoothly as the light pipe is moved, and do not jitter or change shape, indicates that the discharge does not change shape, and moves with a constant velocity.

There is a small uncertainty in the shape of the contour diagrams due to errors in making measurements from the oscillograms. The error is magnified by noise on the signal from the photomultiplier, which increases the width, and reduces the sharpness of the trace. For some of the later experiments the noise was reduced by shunting a small filter condenser across the input of the oscilloscope.

The oscilloscope screen was photographed by a Du Mont Type 302 Oscilloscope Recording Camera, fitted with a Polaroid Land back. Ten exposures could be accommodated on two frames of the film used. The first exposure shows the signal from the velocity measuring photomultiplier, from which  $T_{r1}$  or  $T_r$  can be determined. For exposures 2 to 9, which show the signal from photomultiplier B, the viewing hole was advanced by 5 turns of the lead screw between exposures, moving from the "5 turns" position to the "40 turns" position. For the final exposure the viewing hole was returned to

the "5 turns" or "10 turns" position. This photograph was compared with that taken earlier at the same position, to check if conditions had changed during the measurement to such an extent as to render this particular set of photographs valueless. In addition pressure, magnetic field, discharge voltage and  $T_r$  were monitored before and after measurement to check that conditions had not changed excessively during the measurements.

A series of photographs of the signal from photomultiplier B, from which contour diagrams were prepared, were taken for discharges in air, argon, helium, hydrogen and argon plus  $1\frac{1}{2}\%$  air. A discharge in this gas mixture moved with a constant velocity, whereas a discharge in argon under equivalent conditions would often move in an irregular manner, and even "stick".

For air, argon, helium and the argon/air mixture, determinations of the shape of the discharge were made with magnetic fields between 590 and 5,700 gauss, and pressures between 3.8 and 24.4 mm. Hg. The majority of the measurements for argon, and the argon/air mixture, were made at pressures greater than 6.8 mm. Hg, and for helium at pressures above 12.9 mm. Hg. Below these pressures, the discharge becomes excessively noisy. Triggering difficulties, and the noisy signals from photomultiplier B prevent the construction of an accurate contour diagram at these low pressures. At pressures above 25 mm. Hg, it was extremely difficult to obtain a useful series of oscilloscopes. At these pressures the motion of

the discharge became irregular, and the discharge tended to extinguish. The discharge current was set at 5 mA or 15 mA.

A discharge that moves with constant velocity in hydrogen can be obtained only at low pressures and magnetic fields. Indeed it is difficult to establish a discharge in hydrogen at higher pressures and magnetic fields. For this reason, measurements were made in hydrogen only in fields of 320 and 590 gauss, at pressures between 0.8 and 2.7 mm. Hg. At pressures below 0.8 mm. Hg the discharge is not constricted, but continuous, i.e., it occupies the entire space between the electrodes.

Figures 2.9 and 2.11 show oscillograms obtained during two determinations of the shape of the discharge, and figures 2.10 and 2.12 contour diagrams prepared from these oscillograms. Other contour diagrams are shown in Appendix 1.

From these, and similar diagrams, the following observations were made.

1. The anode region leads the cathode region in all the gases studied.

The slope of the leading edge of the discharge gives a measure of the degree to which the anode region leads the cathode region. It is difficult to give a definition of slope that can satisfactorily be used with all contour diagrams. The leading edge of the discharge is not straight; the shape of the discharge, and the relative

FIGS 2.9 and 2.10 THE SHAPE OF A DISCHARGE AT  
LOW PRESSURE

Gas - argon with 1.6% air  
Gas pressure - 10.1 mm. Hg  
Magnetic field - 590 gauss  
Discharge current - 5 mA.

FIG 2.9 OSCILLOGRAMS FROM WHICH THE SHAPE OF THE  
DISCHARGE WAS DETERMINED

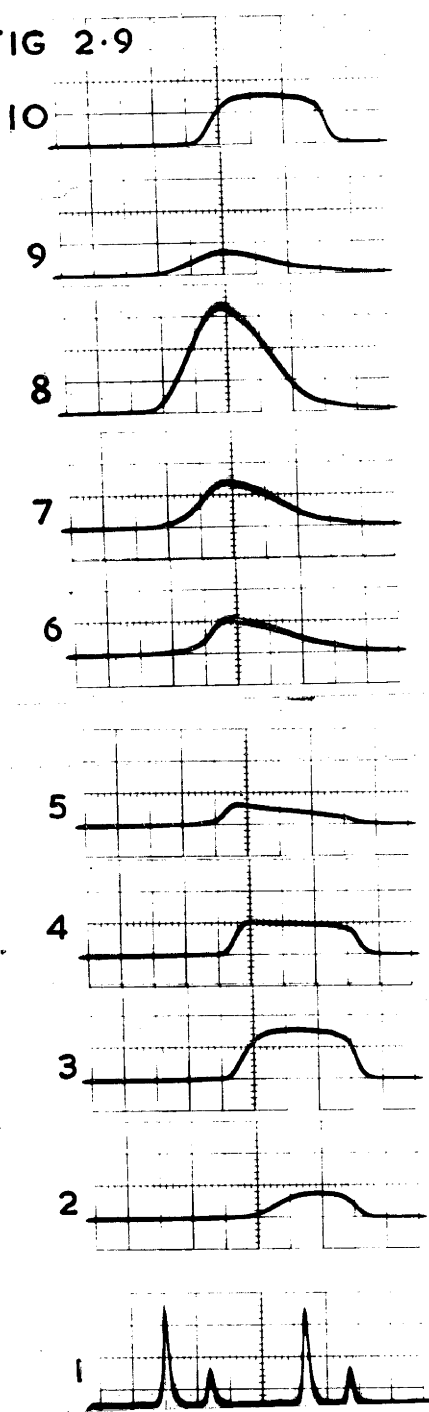
Electron beam moves from left to right of photo.

| <u>Frame</u> | <u>Signal</u>           | <u>Time base</u> | <u>Vertical Sensitivity</u> |
|--------------|-------------------------|------------------|-----------------------------|
| 1            | Velocity signal         | 1 m sec/cm       | 2 volt/cm                   |
| 2            | Discharge profile 5 tns | 0.1 m sec/cm     | 0.2 volt/cm                 |
| 3            | " 10 tns                | "                | "                           |
| 4            | " 15 tns                | "                | "                           |
| 5            | " 20 tns                | "                | 0.1 volt/cm                 |
| 6            | " 25 tns                | "                | "                           |
| 7            | " 30 tns                | "                | "                           |
| 8            | " 35 tns                | "                | "                           |
| 9            | " 40 tns                | "                | "                           |
| 10           | Check photo 10 tns      | "                | 0.2 volt/cm                 |

FIG 2.10 THE SHAPE OF THE DISCHARGE

Light intensity contours: arbitrary units - the output of the photomultiplier in millivolts.

**FIG 2·9**



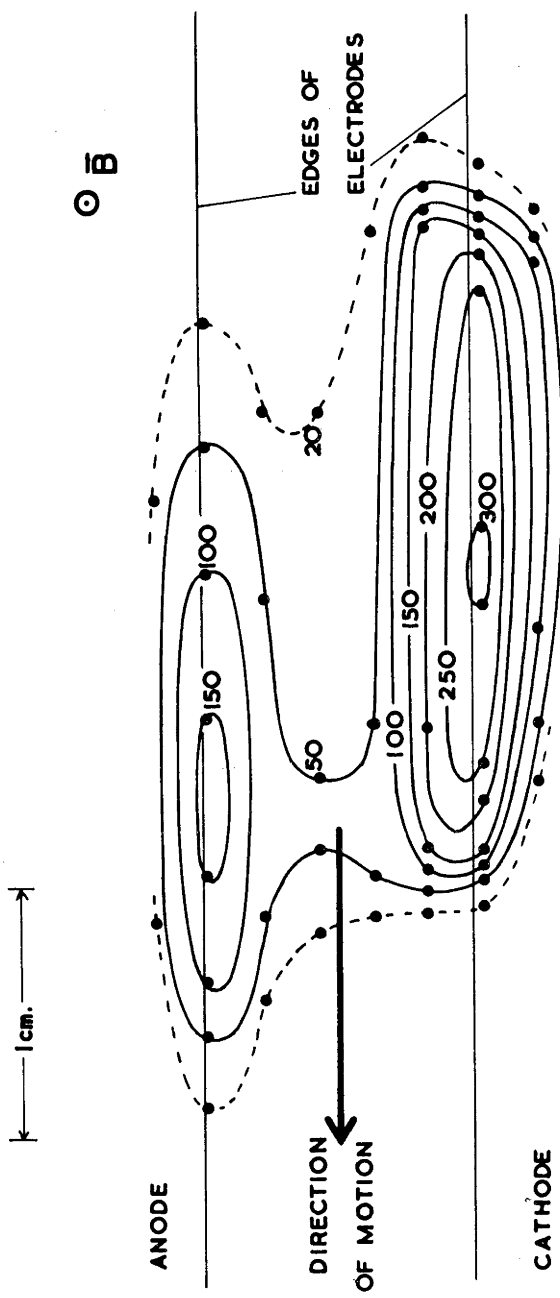


FIG 2·10 THE SHAPE OF THE DISCHARGE AT LOW PRESSURES<sub>2,6</sub>

FIGS 2.11 and 2.12 THE SHAPE OF A DISCHARGE AT HIGH PRESSURE

Gas - argon with 1.5% air  
Gas pressure - 23.3 mm. Hg  
Magnetic field - 2,160 gauss  
Discharge current - 5 mA.

FIG 2.11 OSCILLOGRAMS FROM WHICH THE SHAPE OF THE DISCHARGE WAS DETERMINED

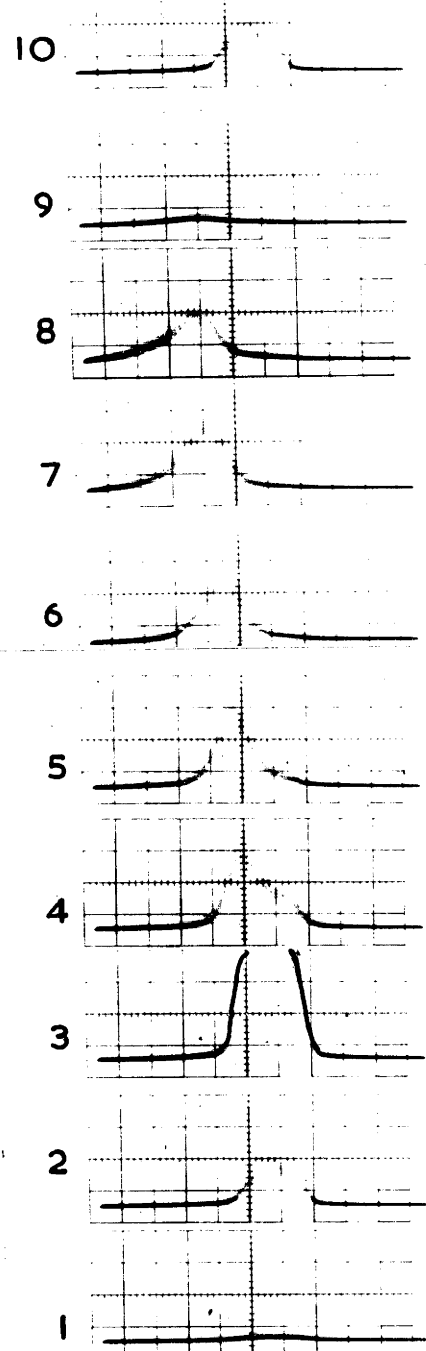
Electron beam moves from left to right of photo.

| <u>Frame</u> | <u>Signal</u>     | <u>Time base</u> | <u>Vertical Sensitivity</u> |
|--------------|-------------------|------------------|-----------------------------|
| 1            | Discharge profile | 0 tns            | 0.05 m sec/cm               |
| 2            | "                 | 5 tns            | "                           |
| 3            | "                 | 10 tns           | "                           |
| 4            | "                 | 15 tns           | "                           |
| 5            | "                 | 20 tns           | "                           |
| 6            | "                 | 25 tns           | "                           |
| 7            | "                 | 30 tns           | "                           |
| 8            | "                 | 35 tns           | "                           |
| 9            | "                 | 40 tns           | "                           |
| 10           | Check photo       | 5 tns            | "                           |

FIG 2.12 THE SHAPE OF THE DISCHARGE

Light intensity contours: arbitrary units - the output of the photomultiplier in millivolts.

**FIG 2·11**



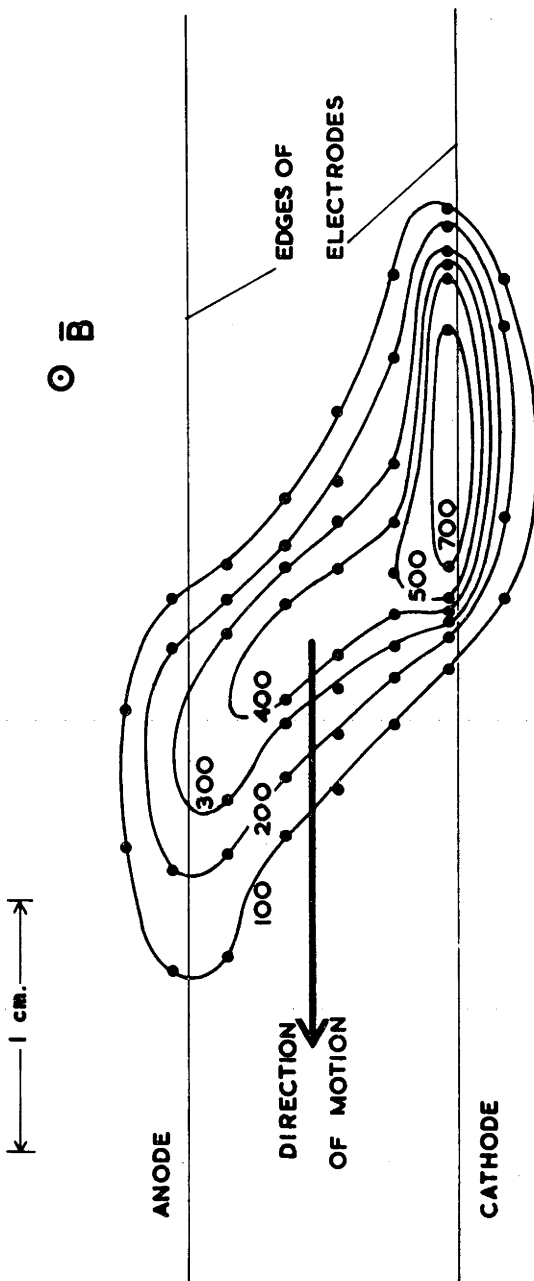
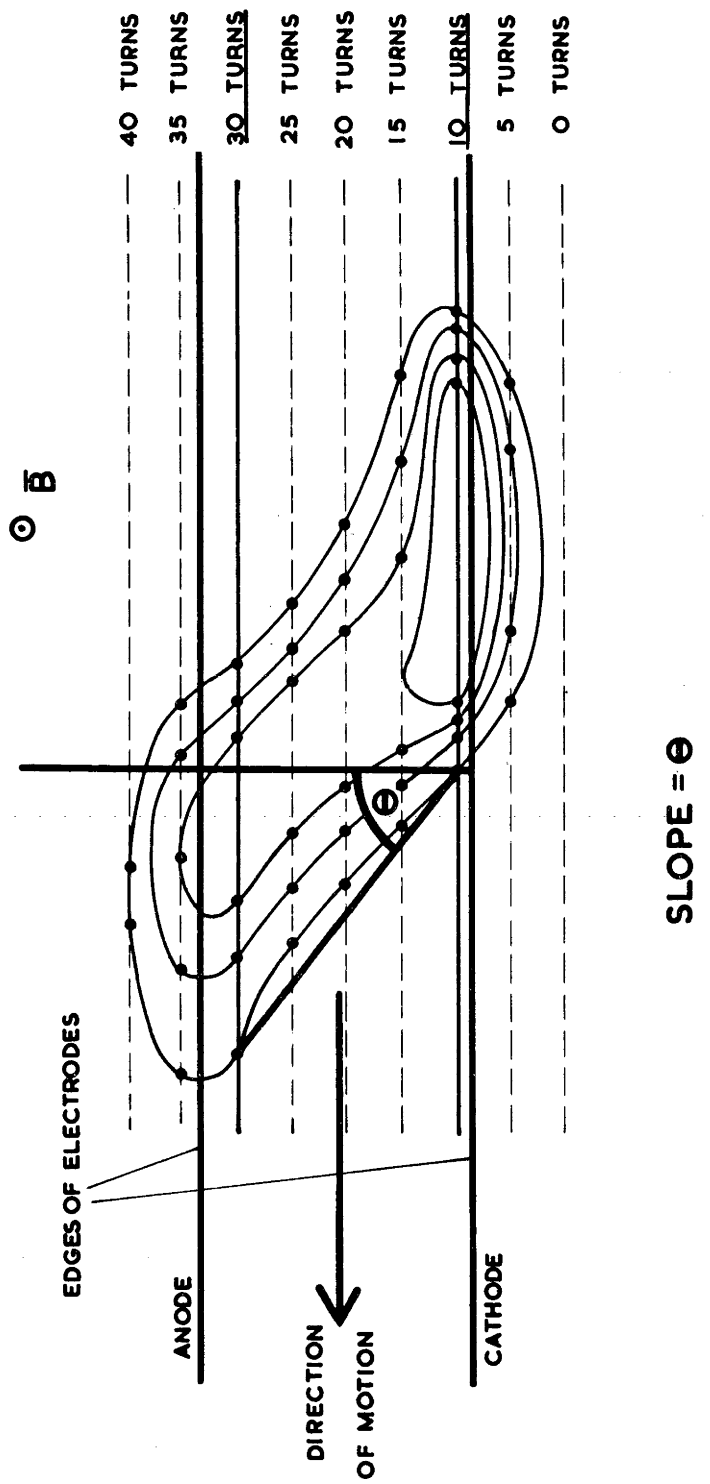


FIG 2.12 THE SHAPE OF THE DISCHARGE AT HIGH PRESSURES,

intensities of various parts of the discharge may be much different for discharges running under different conditions. The following arbitrary definition of slope will be used in relation to the work described in this section: The slope is the angle between a line perpendicular to the edge of the electrode, and the line joining points on a suitable contour at the "10 turns" and "30 turns" positions.

This definition is demonstrated in figure 2.13. The suitable contour is generally the lowest contour, although a higher contour will be chosen if this does not have a slope and shape similar to that of the other leading edge contours. The "10 turns" and "30 turns" positions were chosen as points close to the edges of the electrodes.

The slope of the leading edge is greatest for argon, and the argon/air mixture. For the air discharge, where the slope is not so great, but the discharge narrower, the separation of the anode and cathode regions is most striking (see figure A1.1, Appendix 1). There is no doubt about the anode region leading the cathode region for air, argon, and the argon/air mixture. Measurements with helium and hydrogen are not so conclusive. Not only is the slope less, but uncertainties in the measurements were much greater for these gases. The discharges were much broader, so that when the pulse from photomultiplier B was squeezed on to the oscilloscope screen, the leading edge region occupied only a small fraction of the screen, increasing the errors in measurement from an already noisy oscillosgram.



**FIG 2.13 MEASUREMENT OF THE SLOPE OF THE DISCHARGE**

2. The slope of the discharge in the argon/air mixture increases as the magnetic field increases. This is demonstrated in Table 2.1, in which are tabulated slopes obtained from contour diagrams for gas discharges in this mixture. The two values of slope given in this table are the maximum and minimum values calculated for the slope, when allowance is made for the estimated errors in taking readings from the profile oscillograms.

Not enough data is available to come to any conclusion regarding the variation of slope with magnetic field in the other gases.

3. Nothing conclusive can be said about the variation of the slope of the discharge with pressure, except that it tends to be independent of pressure (see table 2.1).

The appearance of a discharge in the argon/air mixture changes quite markedly with pressure. This is demonstrated in figures 2.10 and 2.12. At low pressures a line through the points of the maximum intensity in the positive column of the discharge (i. e., the peaks of the profile photographs) tends to be perpendicular to the electrodes. The centres of the bright regions in the vicinity of the electrodes, which are assumed to correspond to the anode glow and the negative glow, lie on either side of this line. The edges of the discharge (the lowest contours) are far from straight. (See figure 2.10).

At high pressures, the glowing regions above the electrodes lie at the ends of the line through the points of maximum intensity,

Table 2.1 SLOPE OF THE DISCHARGE IN AN ARGON/AIR MIXTURE

| Magnetic Field<br>(Gauss) | 590 | 1,100             | 2,160             | 4,420 - 4,600     |
|---------------------------|-----|-------------------|-------------------|-------------------|
| Slope<br>Pressure (mm Hg) |     |                   | 46° - 57°<br>10.0 | 48° - 61°<br>10.7 |
| Slope<br>Pressure (mm Hg) |     | 12° - 22°<br>17.9 | 37° - 47°<br>18.0 | 46° - 56°<br>18.0 |
| Slope<br>Pressure (mm Hg) |     |                   |                   | 49° - 56°<br>23.3 |

which is now at an angle to the perpendicular. The glowing regions are smaller than at lower pressures, and the contours tend to be straight and parallel. This is shown in figure 2.12.

4. The slope does not result from the cathode region lagging behind the anode region because it has a longer path over which to travel. Experiments with the polarity of the centre electrode reversed, (the inner electrode becoming the cathode) give contour diagrams that show that the anode region still leads the cathode region, the shape being the same as for the measurements made with the outer electrode the cathode. If the path length was an important factor, the cathode region would be expected to lead the anode region when the polarity was reversed.

5. The width of the discharge (in the direction of motion of the discharge) as observed from the contour diagrams, decreases as the pressure increases. However, it does not change significantly as the magnetic field increases, even at the lowest pressures, where the T.M.F. will have its greatest effect on the behaviour of the discharge.

6. The higher the magnetic field, the noisier the light signals from the photomultipliers.

## 2.5 CONCLUSIONS

The more important conclusions resulting from the work described in this Chapter are:

- (1) The anode region of the discharge leads the cathode region,

the slope increasing as the magnetic field increases.

(2) The cathode region of the discharge probably controls the velocity of the discharge. (The study of the influence of the cathode region on the motion of the discharge will be further pursued with the discharge chamber described in section 3.1.1).

(3) The reproduceability of experimental results is strongly influenced by gas purity, and the condition of the surfaces of the electrodes.

---

### Chapter 3

#### THE EFFECT OF THE LENGTH OF THE DISCHARGE, AND THE ELECTRODE GEOMETRY, ON THE MOTION OF THE DISCHARGE

A demountable discharge chamber in which electrodes of different sizes and shapes could be readily installed was designed in order to ascertain the effect of varying the length of the discharge, the diameter and shape of the electrodes, and the material from which they are constructed, on the motion of the discharge. Attempts were made to incorporate in the design of the chamber improvements suggested by the experiments with the "Racetrack" chamber, described in Chapter 2. The experiments described in this chapter, however, are in no manner the "ultimate" experiments as far as gas purity and electrode cleanliness are concerned.

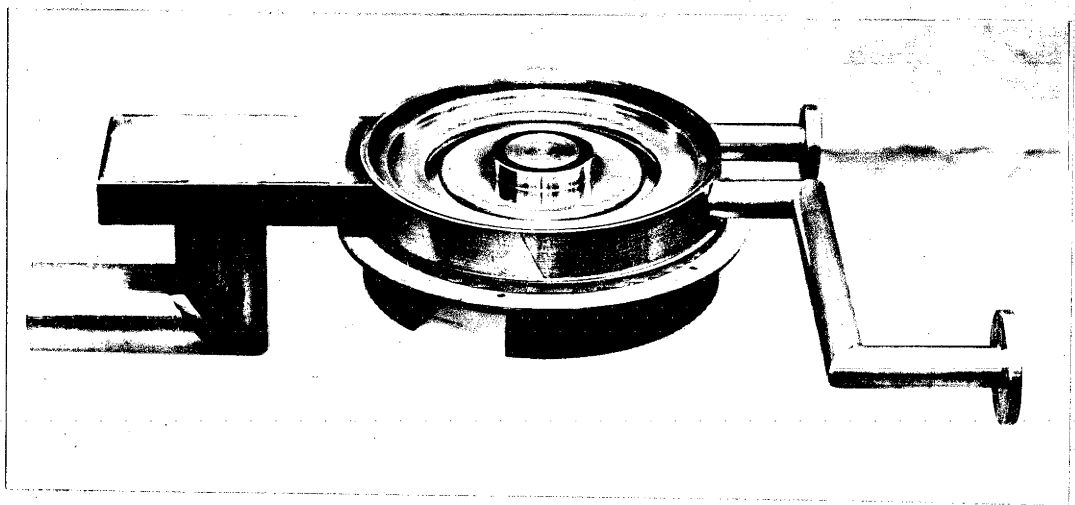
This chapter also describes a study (involving the same discharge chamber) of a sharp change in the nature of the motion of the discharge that occurs when  $\omega T$  for electrons is of the order of 1 ( $\omega$  - electron cyclotron angular frequency.  $T$  - mean time between collisions of an electron with a neutral molecule).

#### 3.1 THE EXPERIMENTAL APPARATUS

##### 3.1.1 The discharge chamber

A photograph of this chamber - the Mk. II chamber - is shown in figure 3.1 and a drawing showing the more important

FIG 3.1 A PHOTOGRAPH OF THE MK II CHAMBER



dimensions, in figure 3.2. A circular electrode geometry was chosen for ease of machining the electrodes and adjustment for a constant discharge gap. The experimental results may be readily interpreted if this simple geometry is used.

The outer wall of the chamber, 1" high, was machined from 7" o.d. brass tubing. Glass cover plates,  $\frac{1}{4}$ " thick were sealed to the top and bottom of the wall by  $\frac{1}{16}$ " diameter O-rings. The cover plates and the outer wall are sandwiched together by brass clamping rings. The flat glass covers enable the viewing holes of the light detection equipment to be positioned over any part of the discharge gap. This feature enables the shape of the discharge to be determined by the method described in section 2.4.

The electrodes used for the majority of the experiments were  $\frac{1}{4}$ " deep, with  $\frac{1}{8}$ " radii machined on the edges along which the discharge will run. These are shown in figure 3.2. The outer electrodes are screwed to a brass ring hard soldered to the inside of the outer wall. A raised step at the outside of this electrode, the same size as the mounting ring, gives an electrode geometry that is symmetrical about the mid plane of the electrodes, out to the edge of the electrodes. (This ring also shields the pumping ports from the discharge region.) The inner electrode consists of a  $\frac{1}{4}$ " thick copper disk, and a massive centre post (of 2" diameter for most experiments). This electrode helps to hold the gas in the

FIG 3.2 MK II CHAMBER - DETAILS OF CONSTRUCTION

- A - Glass cover plates.
- C - Clamping rings.
- D - Discharge gap.
- E - Electrodes.
- G - Gas inlet and outlet lines.
- O - O-ring grooves.
- P - Main pumping line.

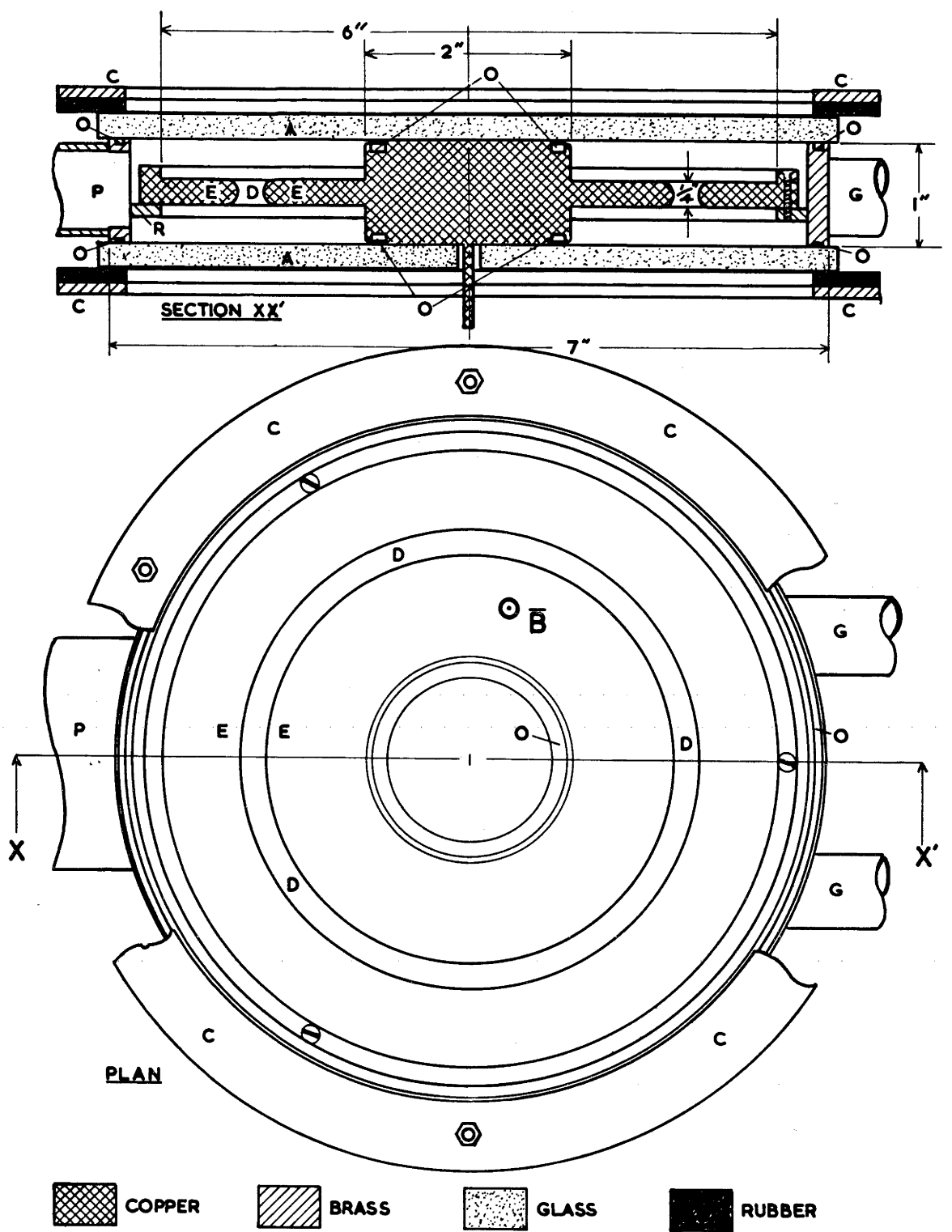


**FIG 3·2 MK II CHAMBER - DETAILS OF CONSTRUCTION**

discharge chamber down to a temperature not greatly in excess of room temperature by virtue of its large heat capacity, and the large area through which heat may be transferred to the surrounding atmosphere. The centre post provides a support for the centre of the glass cover plates. O-rings set in grooves at the top and bottom of the outer wall provide vacuum seals, and a cushion for the glass plates. The cushion reduces the stresses that would build up if the glass plates were supported on a rigid edge. The electrodes were adjusted for concentricity by means of a removable annular spacing ring constructed of "Bakelite".

A short flat rectangular pumping line (cross-section  $2\frac{1}{2}$ " x  $\frac{3}{4}$ ") leads from this chamber to the main pumping line. It should be noted that, even though this line is partially blocked by the outer electrode, the conductance is much greater than that of the pumping line into the "Racetrack" chamber.  $\frac{3}{4}$ " o.d. brass tubing takes the gas into, and from, the discharge chamber.

This chamber is an improvement on the "Racetrack" chamber because:

- (1) The pumping line is designed to have a high conductance, facilitating the rapid removal of gas and vapour from the discharge chamber.
- (2) The cover plates are of glass, not "Perspex".
- (3) The geometry is "clean". There are no projections,

irregularities, or soldered joins in the vicinity of the discharge gap.

### 3.1.2 The vacuum system

The vacuum system, shown schematically in figure 3.3, is substantially that used for the "Racetrack" experiments. (See section 2.1.4). Additions to the system are:

- (1) Two ionization gauge heads,
- (2) A cold trap above the diffusion pump, and
- (3) A cold trap packed with Linde Type 4A "Molecular Sieve" (an artificial zeolite), that is used to purify the gas prior to entering the discharge chamber.

The gas is still passed continuously through the chamber while experimenting, but along a slightly different path.

Ionization gauge No. 1 (IG 1), above the diffusion pump cold trap, gives a base pressure reading of approximately  $10^{-6}$  mm.Hg. Ionization gauge No. 2 (IG 2), which is near the oil manometer along approximately one foot of narrow ( $\frac{3}{4}$ " o.d.) tubing from the discharge chamber, gives a base pressure reading of approximately  $10^{-5}$  mm.Hg.

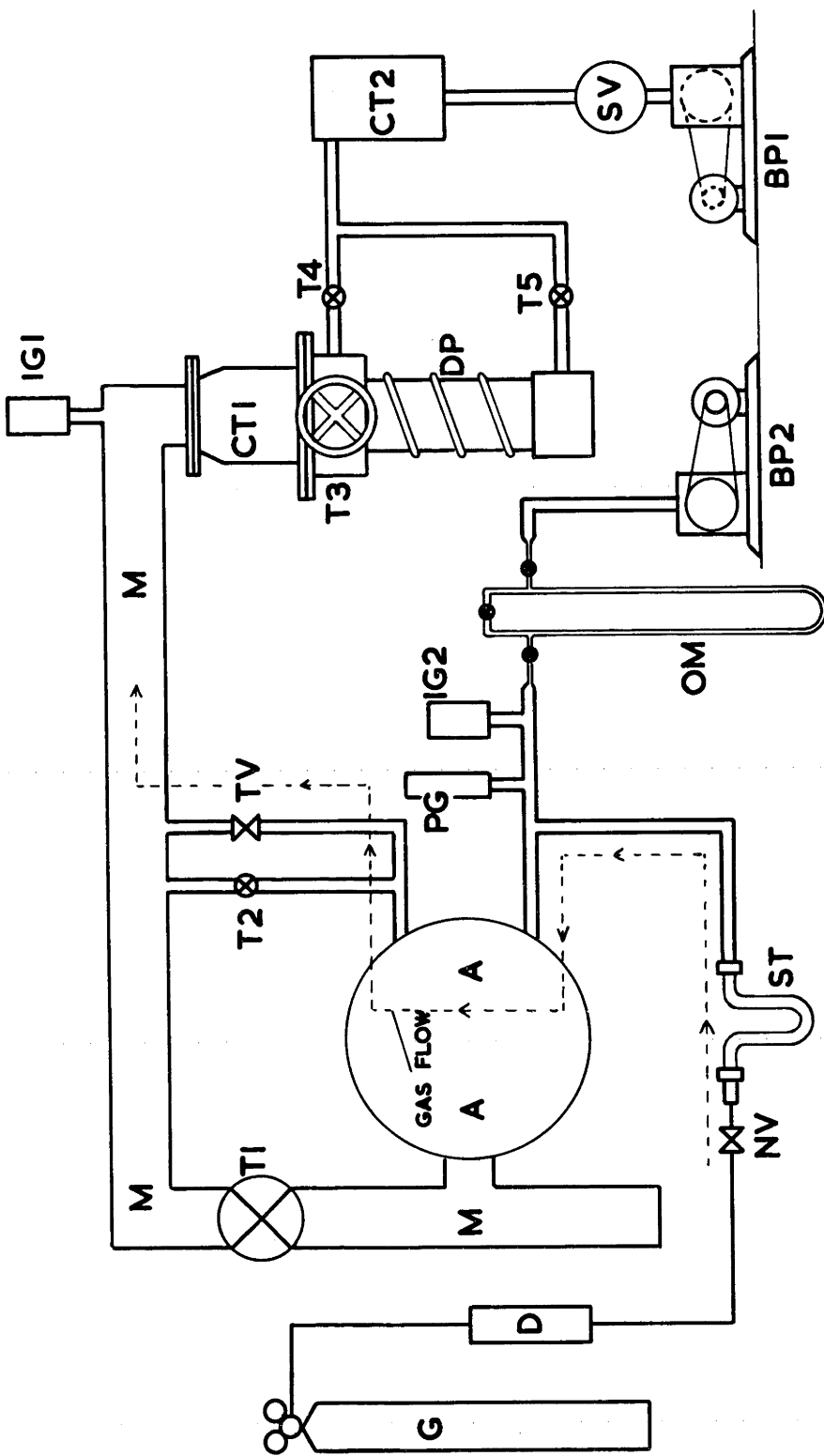
The level of the liquid air in the diffusion pump cold trap was maintained at a constant value by means of a liquid air level controller developed in this laboratory. This liquid air level controller is described in Appendix 2.

The gas used for these experiments was dried by passing through "Molecular Sieve", and then treated as follows:

FIG 3.3 THE VACUUM SYSTEM USED WITH THE MK II CHAMBER (SCHEMATIC)

- A - Mk II chamber.
- BP1 - Main backing pump.
- BP2 - Backing pump for evacuating "reference" arm of the oil manometer.
- CT1 - Main cold trap.
- CT2 - Backing line cold trap.
- D - Gas drying tube - packed with Linde "Molecular Sieve".
- DP - Diffusion pump.
- G - Gas cylinder.
- IG1 - Ionization gauge heads.  
IG2
- M - Main pumping line.
- NV - Needle valve. Gas is leaked into the system through this valve.
- OM - Oil Manometer.
- PG - Pirani gauge.
- ST - Sorption trap - a cold trap packed with "Molecular Sieve".
- SV - Safety volume. Prevents backing pump oil sucking back into the system in the event of a power failure.
- T1-T5 - Vacuum taps (T3 - baffle valve above diffusion pump).
- TV - Throttle valve - controls gas pressure.

**FIG 3.3 VACUUM SYSTEM USED WITH THE MK II CHAMBER (SCHEMATIC)**



Argon, helium, hydrogen were passed through "Molecular Sieve" cooled to liquid air temperature. "Molecular Sieve", like activated charcoal, adsorbs most gases strongly when cooled to liquid air temperature (Br 56, El 61). Hydrogen and helium are not adsorbed, so that these gases may be purified to some extent by passing through chilled "Molecular Sieve". Argon is only slightly adsorbed by the "Molecular Sieve", so that this gas may be satisfactorily purified by this method.

Nitrogen was obtained from a cylinder of industrial grade "Dry, Oxygen-Free Nitrogen", a very pure gas that contains less than 25 p. p. m. of impurities when dry. Water is the main impurity. It is estimated that the water level is reduced from approximately 0.025% (the average level) to substantially less than that of the other impurities by passing over the drying bed of "Molecular Sieve", so that no additional treatment will be required.

The impurity leak rate was initially such that the percentage of impurity in the experimental gas that results from leaks, both virtual and real, was between 0.02% and 0.05%. However during the course of the experiments a small leak was located. On sealing this leak, the leak rate fell so that the impurity level fell below 0.02%, being below 0.01% for the majority of the experiments. These latter experiments include all those in which the discharge runs in nitrogen, with the exception of those where the discharge

runs between electrodes of 11.3 cm. and 14.0 cm. diameter.

### 3.1.3 The power supply, the magnet and the velocity measuring equipment

These are all substantially as they were for the experiments described in Chapter 2. The power supply is electrically the same as that described in section 2.1.2. However the supply has been modified so that outputs of both polarities are available. This is necessary if the polarity of the centre electrode of the discharge chamber is to be reversed, because the construction of the chamber is such that the outer electrode must be at earth potential.

The photomultiplier of the light detection equipment looks down on the discharge through a single viewing hole, rather than through two viewing holes as was the case with the light detection equipment used for the majority of the experiments with the "Racetrack" chamber. The resolution of the light-detection equipment is somewhat less than that of the equipment described in section 2.1.5, the diameter of the circle of resolution being 6.25 mm. in the former case, as compared with 4.8 mm. in the latter case. This results because the viewing holes are further from the mid-plane of the discharge with the present experimental equipment, than they were with the equipment used with the "Racetrack" chamber. The discharge runs further below the cover of the Mk. II chamber than it did in the "Racetrack" chamber, and, to simplify the design of the light detection equipment, it was necessary to arrange the

light pipes so that the viewing holes were approximately  $\frac{3}{8}$ " above the cover plate. The intensity of the light falling on the photomultiplier tubes was such that attempts to increase the resolution by decreasing the size of the viewing holes would reduce the amplitude of the signals from the photomultiplier to such an extent that noise could become a problem, and difficulty would be experienced in triggering the oscilloscope.

### 3.2 LACK OF REPRODUCEABILITY - FURTHER OBSERVATIONS

The results are not reproduceable. Indeed there has been little improvement in the repeatability of the results compared with those obtained from experiments with the "Racetrack" chamber. However, in spite of this difficulty valuable observations could be made from the results of experiments with this chamber. Most of the measurements were made at fixed magnetic field and discharge current, the period of rotation,  $T_r$ , being measured as a function of gas pressure.

The following procedure was adopted when making measurements, in order to obtain significant results from this work:

Each "run" consists of a series of measurements made while the pressure was increased between measurements, followed immediately by a series made with the pressure decreasing between measurements. Similar runs were made at different currents or magnetic fields, or with the polarity of the centre electrode changed.

These measurements were then repeated. This procedure guards against spurious results due to a gradual change of conditions over a series of experiments. Thus, during a series of experiments, four (and sometimes more) series of measurements of  $T_r$  as a function of gas pressure, with other parameters unchanged, were obtained. For further calculations the mean value of  $T_r$  was obtained from graphs of  $T_r$  as a function of pressure. A curve that differed greatly from the rest of a series was discarded if there was reasonable justification of this action. e.g., the first run of a series would often differ from those obtained from the later runs for two reasons:

- (a) When a discharge is first run on a newly installed electrode the electrode will outgas strongly, so that the impurity level in the gas is higher than for later runs of the series of experiments.
- (b) The sputtering action of the discharge "cleans" the cathode. i.e., removes traces of grease, oxide, or impurities remaining from the final polishing of the electrode. The secondary emission coefficient of the surface will change during the cleaning process. Thus, insofar as the velocity of the discharge depends on the processes occurring at the surface of the cathode, the velocity with a dirty cathode will be different from that of a discharge moving along a clean cathode.

The complete data obtained from a series of experiments

will only be plotted where this is of importance to the argument of this thesis. Typical curves, or a shaded area in which all the points obtained in a series of experiments lie, will be plotted under other circumstances, in order to simplify the presentation of the data.

The following observations, based on the results of experiments in the Mk. II chamber, can be made about the causes of the lack of repeatability of the experimental results.

1. The results obtained with this chamber are not significantly more reproduceable than those obtained with the "Racetrack" chamber. However this is not entirely unexpected. The level of the impurities in the gas resulting from leaks into the vacuum system is not much less than the impurity level due to leaks into the "Racetrack" chamber. Under these conditions the purification of the gas by passing through "Molecular Sieve" at liquid air temperature will not be of great value.

2. As for the "Racetrack" chamber, helium gave by far the greatest scatter of the experimental points. The scatter was somewhat less for hydrogen and a little less for argon than for hydrogen, with nitrogen giving by far the most repeatable results.

3. A regularly rotating discharge in argon was obtained in the Mk. II chamber up to the highest pressure at which measurements were made (23 mm. Hg). The discharge in argon in the "Racetrack" chamber becomes stationary, or extinguishes, at pressures well below this value. This is attributed to the greater cleanliness of

the electrodes, and the lack of irregularities in the vicinity of the discharge gap of the Mk. II chamber.

The electrodes were relatively deposit-free, even after hours of running at a discharge current of 15 mA. The copper cathodes used for the majority of the experiments were polished by the sputtering action of the discharge where the ion current enters the electrode, this zone being bordered by narrow strips of a dark deposit that is almost certainly copper oxide (see figure 3.24). The anode was lightly oxidized where the current flowed from this electrode.

4. Values of  $T_r$  reproduceable to within less than  $\pm 10\%$  of the mean value were obtained when a discharge was run in nitrogen on specially prepared clean gold surfaces. This is considerably better than the repeatability of the results obtained with a nitrogen discharge on polished copper electrodes. The gold surface was prepared by the vacuum evaporation of gold on to polished copper electrodes. The electrodes were degreased, and cleaned by ion bombardment in a low pressure hydrogen glow discharge prior to the evaporation.

This result indicates quite markedly the importance of the condition of the surface of the electrode on the behaviour of the discharge, especially in relation to the reproduceability of the results.\*

---

\* An evaporating unit was available only when the majority of the experiments performed in the Mk. II chamber had been completed. Had the above results been obtained earlier, most of the experiments described in the later sections of this thesis, would have been performed with evaporated gold electrodes.

5. It was observed quite regularly that the values of  $T_r$  measured during the first part of a "run" (measurements made with pressure increasing) were greater than those obtained during the second part of the "run" (measurements made with pressure decreasing). This observation could be explained in terms of the heating of the gas during the course of the experiment. The important parameter describing the behaviour of the discharge is not the pressure, but the density of the neutral molecules, which falls as the temperature increases, at fixed pressure. Inspection of curves of the period of rotation as a function of pressure revealed that the period,  $T_r$ , increased as the density of the neutral molecules increased. (These curves are given in the later sections of this chapter). Thus the heating of the gas will result in a decrease of  $T_r$  at fixed pressure. However calculations indicate that this effect should be much smaller than the observed effect.

The experiments with the gold electrodes (which do not reveal this effect), and additional experiments using a water cooled centre electrode constructed of copper as the cathode (which reveal this effect), show that this effect does not result from the heating of the gas. It is suggested that the velocity increases as the cathode becomes "conditioned" - probably due to the cleaning of the surface by positive ion bombardment.

### 3.3 THE TWO MODES OF ROTATION OF THE DISCHARGE

The rotation of the discharge could be observed in the Mk. II chamber at much lower pressures than it could in the "Racetrack" chamber, noisy but discrete pulses appearing on the screen of the oscilloscope at pressures down to 1 - 2 mm. Hg. This is attributed to the use of a single viewing hole in the light detection equipment and the longer path around which the discharge moves. Because of the "clean" geometry, and the low pressures at which the rotation could be observed in this chamber, it was used to study a sharp change between two modes of rotation that occurs as the pressure of the gas is increased. (This transition was observed in the "Racetrack" chamber, but it is more rapid, and the changes of the behaviour are more marked in the Mk. II chamber).

At low pressures a discharge of 15 mA in nitrogen in a magnetic field of 2,160 gauss occupies the entire gap between the electrodes. At a pressure in the vicinity of 1 mm. Hg., the discharge contracts to occupy only a fraction of the annulus between the electrodes and is driven around this gap by the transverse magnetic field (although at lower pressures a wave of light intensity was often observed to move around the gap). Above 1 mm. Hg, the signal from the photomultipliers is noisy and "jittery" - i.e., the time interval between pulses varies in an irregular fashion from pulse to pulse. At approximately 10 mm. Hg (the transition pressure)

the nature of the photomultiplier signal undergoes a sudden change. The noise and jitter disappear, and the pulses become narrower, and increase in amplitude. Curves of the period of rotation as a function of pressure show a sharp break at this pressure. The low pressure mode of rotation is called the J (for "jittery") mode, the high pressure mode, the R (for "regular") mode. Transitions of this type occur for all the gases studied in this chamber, the transition in helium being most marked.

### 3.31 The nature of the transition

The transition was studied for discharges in various gases, between electrodes of 10.2 and 14.0 cm. diameter. The magnetic field was 2,160 gauss for helium, nitrogen and argon, and 590 gauss for hydrogen. The following observations were made regarding the transition in the various gases studied:

Helium Curves showing the period of rotation of the discharge,  $T_r$ , and the discharge voltage plotted against gas pressure are given in figure 3.4. These curves show a sharp decrease in  $T_r$  and the discharge voltage as the pressure increases through the transition. These decreases are characteristic of the transition in this gas.

Figure 3.5 shows oscillograms of

- (i) Photomultiplier signals obtained with the viewing hole looking down on the cathode and anode regions of the discharge, both below and above the transition, and

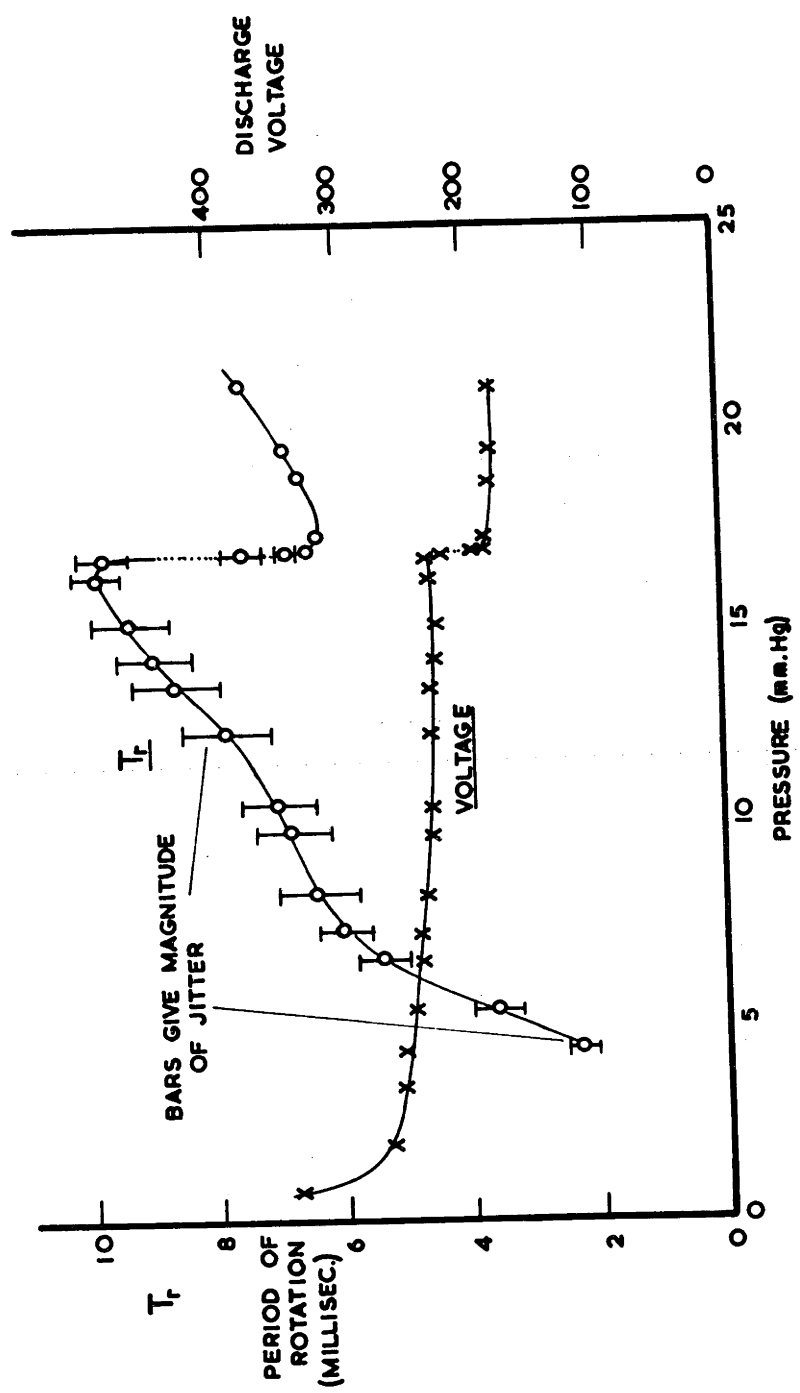


FIG 3·4 THE TRANSITION IN HELIUM

MAGNETIC FIELD - 2,60 GAUSS. DISCHARGE CURRENT - 5mA. CENTRE NEGATIVE  
DIAMETERS OF ELECTRODES - 10·3, 14·0 cm.

FIG 3.5 OSCILLOGRAMS - HELIUM TRANSITION

Magnetic field - 2,160 gauss  
Discharge current - 5 mA

- (a) Photomultiplier signal and discharge noise voltage - ABOVE the transition. Pressure - 12.1 mm. Hg. Time base - 2 m sec/cm.

Upper trace

Signal from a photomultiplier looking down on the cathode region. Vertical sensitivity - 0.2 v/cm.

Lower trace

Alternating component of the discharge voltage. Vertical sensitivity - 20 volt/cm.

- (b) Photomultiplier signal and discharge noise voltage - BELOW the transition. Pressure - 11.8 mm. Hg. Time base - 2 m sec/cm.

Upper trace

Signal from a photomultiplier looking down on the cathode region. Vertical sensitivity - 0.1 v/cm.

Lower trace

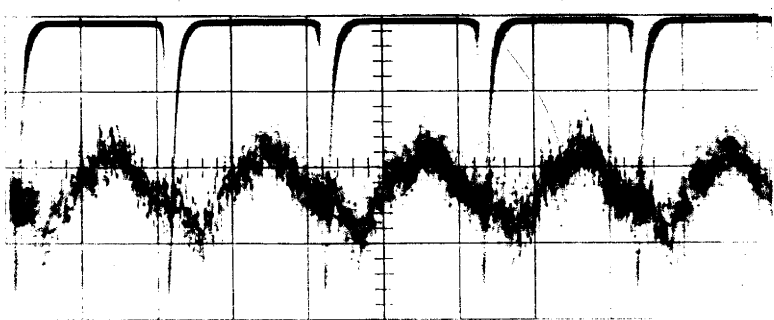
Alternating component of the discharge voltage. Vertical sensitivity - 20 volt/cm.

- (c) Photomultiplier signal looking down on the anode region - ABOVE the transition. Pressure - 11.7 mm. Hg. Time base - 2 m sec/cm.

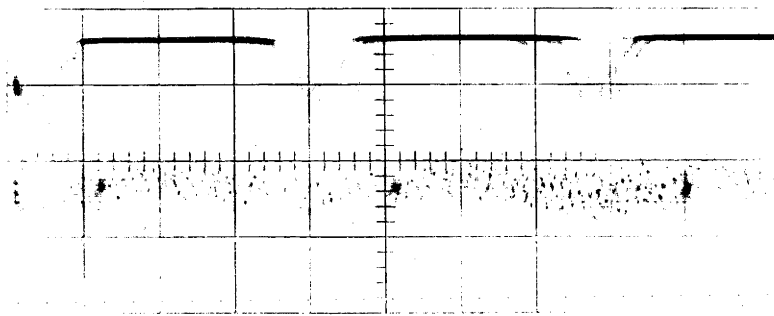
Vertical sensitivity - 0.05 volt/cm.

- (d) Photomultiplier signal looking down on the anode region - BELOW the transition. Pressure - 10.4 mm. Hg. Time base - 2 m sec/cm.

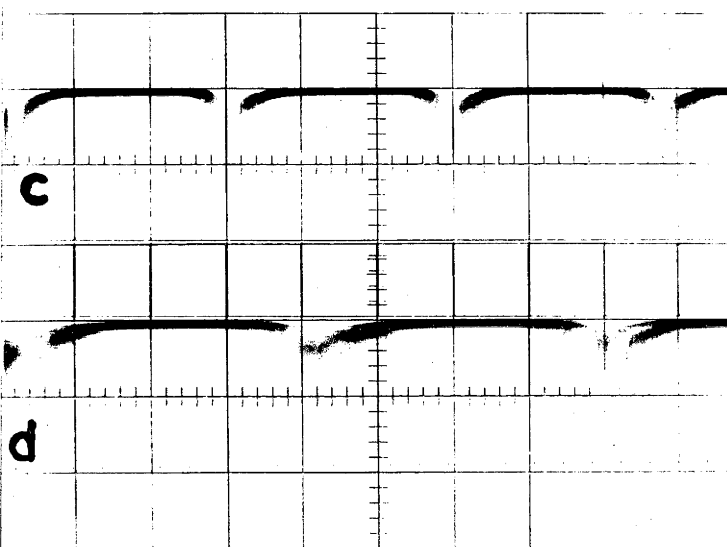
Vertical sensitivity - 0.05 volt/cm.



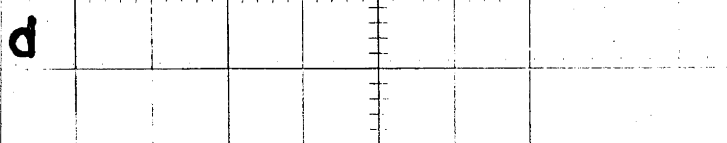
D



b



c

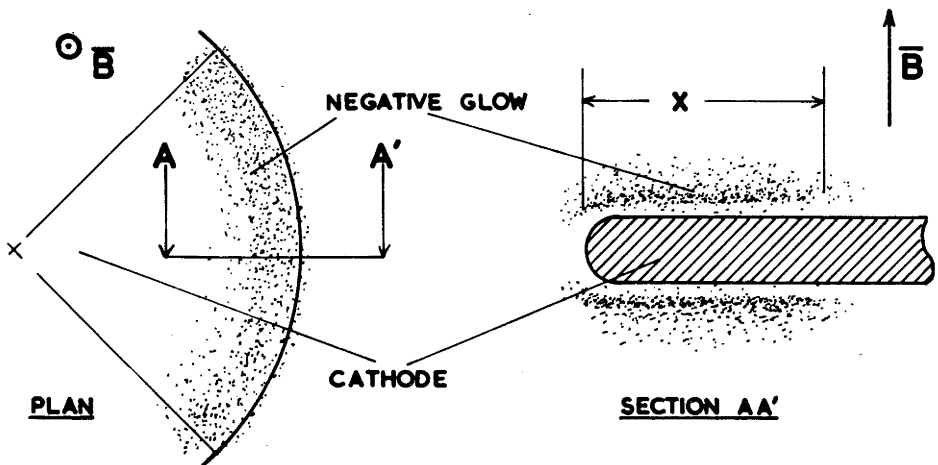


d

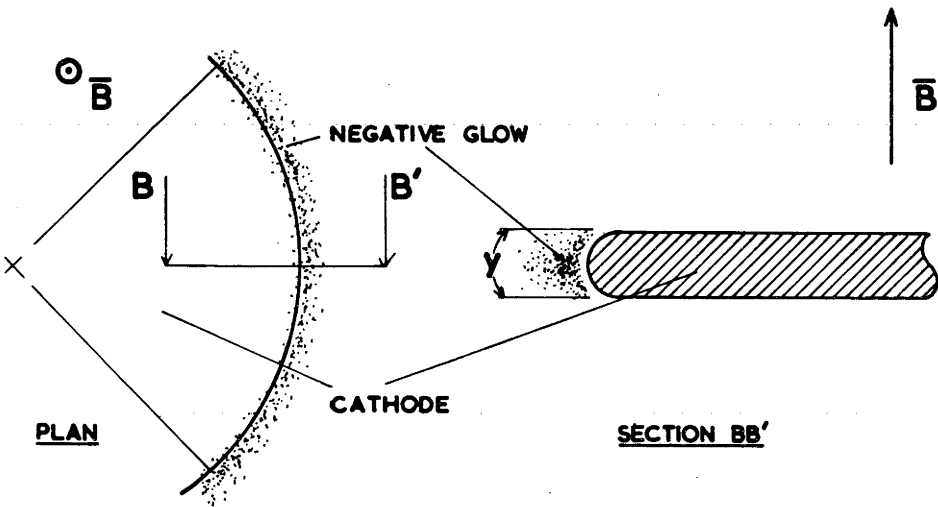
(ii) The noise voltage across the discharge tube, below and above the transition.

Figures 3.5(a) and (b) (upper traces), photomultiplier signals obtained with the viewing hole looking down on the cathode region, show the characteristic decrease in noise and jitter, and the decrease in the width of the discharge, that occurs where the pressure increases so that the discharge passes through the transition. When the viewing hole is over the anode, the photomultiplier signals (figures 3.5(c) and (d)) do not show quite as marked a change in appearance. The jitter and noise, and the width decrease, but not to the same extent as was the case when the photomultiplier looked down on the cathode.

Visual observation of the discharge revealed that, below the transition, the negative glow of the discharge was over the flat top and bottom surfaces of the cathode, as shown in figure 3.6(a). Above the transition the negative glow is on the curved edge of the cathode, as shown in figure 3.6(b). The observed width of the negative glow, which gives a measure of the width of the cathode fall region of the discharge perpendicular to the direction of motion of the discharge, is greater below the transition than above the transition. i.e., referring to figure 3.6, x is greater than y. This observation, coupled with the decrease in the width of the discharge in the direction of motion, as observed from the photomultiplier signals, reveals a sharp increase in the cathode current density



(a) BELow THE TRANSITION



(b) ABOVE THE TRANSITION

FIG 3·6 THE POSITION OF THE NEGATIVE GLOW

when the pressure is increased through the transition.

It was thought that the jitter observed on the photomultiplier signal would be associated with fluctuations of the electric fields in the discharge. If this was so, then fluctuations on the discharge voltage would be expected to decrease on passing through the transition. Observations of the noise on the voltage across the discharge tube show that the noise level does not change at the transition pressure. However just above the transition a regular variation of the discharge voltage of the same fundamental frequency as the frequency of the rotation of the discharge, was also observed. This variation which will be called the synchronized component (because it "locks" to the signal from the photomultiplier) is often of an approximately sinusoidal or "ramp" shape. Sometimes, however, much more complex patterns were observed. Characteristic voltage signals are shown in figures 3.5(a) and (b) (lower traces). (The synchronized component of low amplitude observed below the transition is not commonly present).

The synchronized component, and the noise component of the discharge voltage are both of the order of 20 volts peak-to-peak. (The amplitude of the synchronized component of the discharge voltage shown in figure 3.6(b) is exceptionally large). The amplitude of the synchronized component falls rapidly as the pressure is increased above the transition.

The voltage across the discharge will change as the discharge

moves around the gap if the length of the discharge changes as it moves around the gap. The length may change because:

- (1) The gap between the electrodes is not constant.
- (2) The discharge may tilt at an angle to, or move off the plane of symmetry of the electrodes.
- (3) The slope of the discharge may change.

The electric field in the positive column is estimated to be of the order of 10 volts/cm. Thus the length of the discharge would be required to vary by approximately 2 cm. to explain the observed synchronized component. The spacing of the electrodes was checked on completing the experiments, and the electrodes were found to be concentric. The discharge does not appear to move far from the plane of symmetry of the electrodes. Hence a change of length due to (1) or (2) above would be too small to be a possible explanation of the synchronized component. Possibility (3) was not checked, but there is no evidence in other measurements of the remarkable change of slope that would be required to give a change of the length of the discharge of 2 cm. This discussion suggests that the synchronized component may result from changes in the discharge itself; a likely explanation is a change of the cathode fall voltage due to a change in the condition of the surface of the cathode around this electrode.

The estimated value of the electric field was calculated from the voltage obtained by subtracting from the measured discharge

voltage, the value of normal cathode fall voltage given by BROWN (Br 59) for the glow discharge in zero magnetic field. It is assumed that the cathode fall voltage is not changed greatly by the magnetic field. GÜNTHERSCHULZE (Gu 24) has observed that, under similar conditions the cathode fall voltage is not changed by a magnetic field. This calculation is undoubtedly crude, but even a considerable error in the estimated field will not invalidate the above conclusions.

The dependence of the transition pressure on the magnetic field and the discharge current cannot be studied for this gas because of the poor repeatability of the experimental results. It has been found that increasing the current results in a transition from the R mode of rotation to the J mode.

Nitrogen. The transition in this gas is more gradual than that in helium, but is still quite marked. Figure 3.7 shows plots of the period of rotation of the discharge, and the discharge voltage, against pressure. Below the transition  $T_r$  is substantially independent of pressure.  $T_r$  rises steeply at the transition, and then less steeply at higher pressures.

It should be noted that the increase of  $T_r$  with increasing pressure at the transition is in marked contrast with the sudden decrease of  $T_r$  with increasing pressure, at the transition in helium. This behaviour is characteristic of the moving discharge in nitrogen, except for very short discharges. The discharge voltage shows a

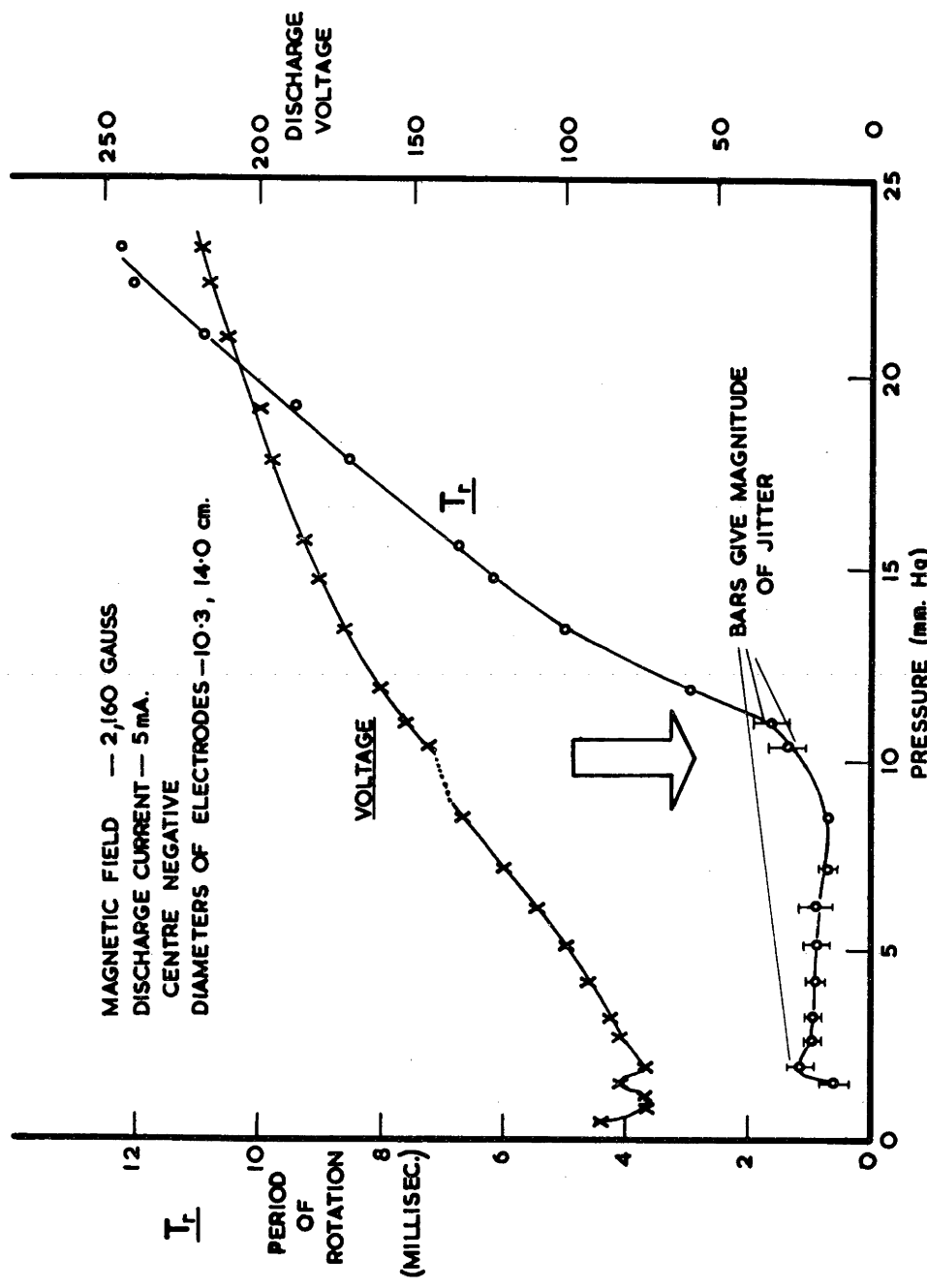


**FIG 3.7 THE TRANSITION IN NITROGEN**

break, but not a sharp break, at the transition. The negative glow of the discharge is at the edge of the cathode (as was the case for the R mode in helium) both above and below the transition. The negative glow is observed above and below the cathode (as was the case for the J mode in helium), only at pressures of the order of 1 - 2 mm. Hg.

The alternating component of the discharge voltage shows a remarkable change at the transition. Below the transition the signal is very noisy, and shows no synchronized component, whereas above the transition, the noise disappears to be replaced by a signal synchronized with the rotation of the discharge. The signals from the photomultiplier, and a high-voltage probe across the discharge below, and above the transition, are shown in figures 3.8(a), (b) and (c). Figures 3.8(d) and (e) show the photomultiplier signal and the voltage at pressures well above the transition pressure.

Signals from the voltage probe similar to those shown in figures 3.8(b) and (c) are observed just above (but not necessarily immediately above) the transition. These signals, which have the appearance of a series of regularly spaced pulses standing on a simple signal of the type observed at higher pressures, (see figures 3.8(d) and (e)) are not fully understood. This phenomenon will be discussed in section 3.9.

At high pressures, and in the narrow pressure range between the transition and the appearance of the complex signal just described,

FIG 3.8 OSCILLOGRAMS - NITROGEN TRANSITION

Magnetic field - 2,150 gauss. Discharge current - 15 mA.

- (a) Photomultiplier signal and discharge noise voltage - BELOW the transition. Pressure - 4.6 mm. Hg. Time base - 0.5 m sec/cm.

Upper trace Photomultiplier signal looking down on the cathode region. Vertical sensitivity - 0.5 volt/cm.

Lower trace Alternating component of discharge voltage. Vertical sensitivity - 100 volt/cm.

- (b) and (c) Photomultiplier signal and discharge noise voltage - complex signals observed JUST ABOVE the transition.

(b) Pressure - 6.2 mm. Hg. Time base - 0.5 m sec/cm.

Upper trace Photomultiplier signal. Vertical sensitivity - 0.5 volt/cm.

Lower trace Alternating component of discharge voltage. Vertical sensitivity - 20 volt/cm.

(c) Pressure - 12.2 mm. Hg. Time base - 0.5 m sec/cm.

Upper trace Photomultiplier signal. Vertical sensitivity - 1 volt/cm.

Lower trace Alternating component of discharge voltage. Vertical sensitivity - 100 volt/cm.

- (d) and (e) Photomultiplier signal and discharge noise voltage - simple signals observed ABOVE the transition.

(d) Pressure - 9.9 mm. Hg. Time base - 2 m sec/cm.

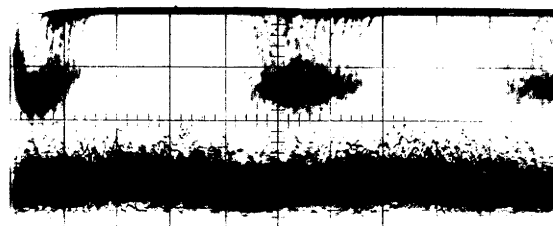
Upper trace Photomultiplier signal. Vertical sensitivity - 1 volt/cm.

Lower trace Alternating component of discharge voltage. Vertical sensitivity - 10 volt/cm.

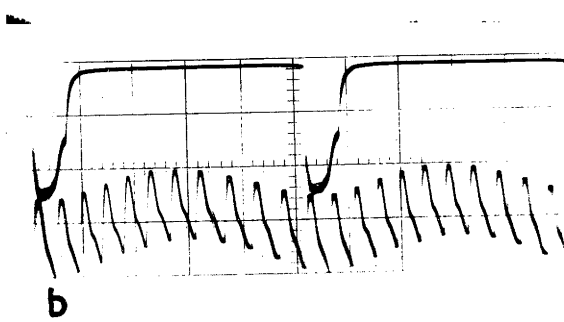
(e) Pressure - 22.3 mm. Hg. Time base - 5 m sec/cm.

Upper trace Photomultiplier signal. Vertical sensitivity - 1 volt/cm.

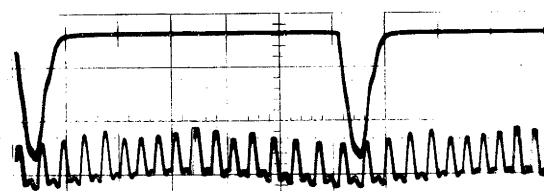
Lower trace Alternating component of discharge voltage. Vertical sensitivity - 20 volt/cm.



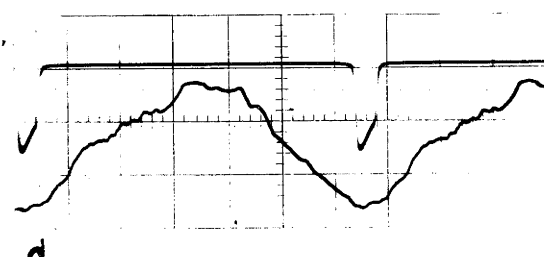
a



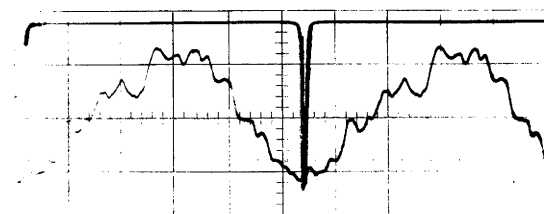
b



c



d



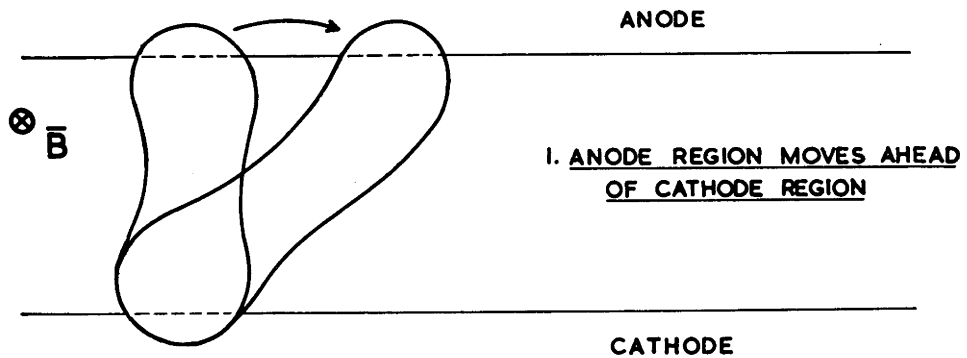
e

the synchronized component is of a relatively simple nature (see figures 3.8(d) and (e)). The electric field is very high in the positive column of the discharge in nitrogen ( $\sim 500$  volts/cm. This figure was calculated from the difference between the voltages across two discharges of different lengths - see section 3.7). It is so high that the synchronized component in this case could be explained if the length of the discharge changed by the order of 0.04 cm. The measured increase in the electric field as pressure increases (see section 3.7) would give the increase of the amplitude of the synchronized component observed as the pressure increases.

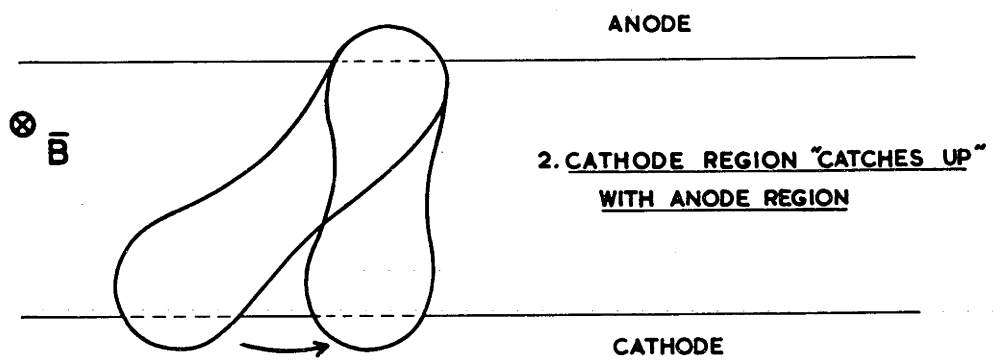
The separation between the electrodes changes by less than 0.002 cm. around the gap, so that a change in the separation cannot explain the synchronized component. The second possibility, that the discharge does not run in the plane of symmetry of the electrodes for part of its path around the electrodes, is supported by the appearance of the track left on the cathode, and, to a lesser extent, the appearance of the negative glow. The cathode track and the negative glow frequently move off the plane of symmetry for part of the circumference of the cathode. Similarly irregular "bumps" on the discharge voltage signals may often be correlated with irregularities in the negative glow (and marks on the cathode). The position of the irregularity relative to the viewing hole is the same as that of the "bump" on the voltage-signal in relation to the signal

from the photomultiplier. These irregular "bumps" on the signal from the voltage probe are not present and the amplitude of this signal is much reduced for the nitrogen discharge moving on evaporated gold electrodes, indicating that the discharge may move off the plane of symmetry due to non-uniform electrode surface conditions. The negative glow is symmetrical, and of a uniform appearance for the discharge on the gold electrodes.

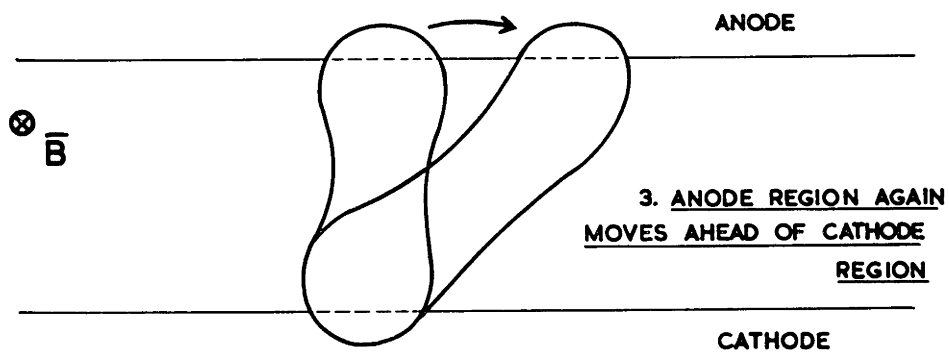
It was thought that the jitter observed below the transition might indicate that the discharge moves in the manner indicated in figure 3.9: the anode region moves ahead of the cathode region, the length and "slope" of the discharge increasing. The cathode region then moves up to the anode region, and then the anode region again moves ahead of the cathode region. i.e., the discharge "walks" along the electrodes. The signal from two photomultipliers, so arranged that they looked down on the anode and cathode regions of the discharge, were displayed simultaneously on an oscilloscope operating in the "single shot" mode. The time interval between the pulses from the two photomultipliers changes very little from "shot" to "shot", even though  $T_r$  may change due to the jitter, indicating that the shape of the discharge does not change greatly from revolution to revolution - i.e., the discharge does not "walk" along the electrode as indicated in figure 3.9.



I. ANODE REGION MOVES AHEAD OF CATHODE REGION



2. CATHODE REGION "CATCHES UP" WITH ANODE REGION



3. ANODE REGION AGAIN MOVES AHEAD OF CATHODE REGION

FIG 3·9 THE "WALKING" DISCHARGE

Hydrogen. Discharges in this gas show a change of photomultiplier signal and the alternating component of the discharge voltage similar to that observed in nitrogen. However, the synchronized component is more irregular than that observed for nitrogen discharges, and the signal is not entirely noise-free. (See figure 3.10). The  $T_r$ /pressure curves (shown in figure 3.11), do not show a sharp break at the transition, but the voltage across the discharge drops slightly as the pressure is increased through the transition. The transition is neither sudden nor reproduceable.

The negative glow is more extensive and diffuse than in the other gases. There is no sharp change in the appearance of the negative glow at the transition, the discharge covering the edge of the cathode, and extending on to the flat top and bottom surfaces of the cathode both above and below the transition.

Argon. The transition is neither marked nor sharp in argon, the most pronounced characteristic being a large change in the slope of the  $T_r$ /pressure curve at the transition (see figure 3.12).  $T_r$  does not vary greatly with pressure below the transition, but increases rapidly as the pressure is increased through the transition - i.e., the dependence of  $T_r$  on pressure is similar to that observed for the discharge in nitrogen. The jitter on  $T_r$  is not great, and decreases only gradually at the transition. (The change in the alternating component of the discharge voltage was not studied for this gas). There

FIG 3.10 OSCILLOGRAMS - HYDROGEN TRANSITION

Magnetic field - 590 gauss  
Discharge current - 15 mA.

(a)

Photomultiplier signal and discharge noise-ABOVE  
the transition.

Pressure - 6.05 mm. Hg. Time base - 0.2 m sec/cm.

Upper trace Photomultiplier signal.  
Vertical sensitivity - 0.1 volt/cm.

Lower trace Alternating component of discharge current.  
Vertical sensitivity - 5 mA/cm.

(b)

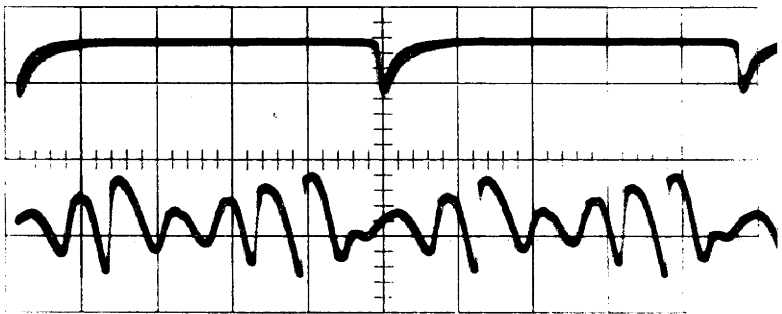
Photomultiplier signal and discharge noise-BELOW  
the transition.

Pressure - 1.7 mm. Hg. Time base - 0.1 m sec/cm.

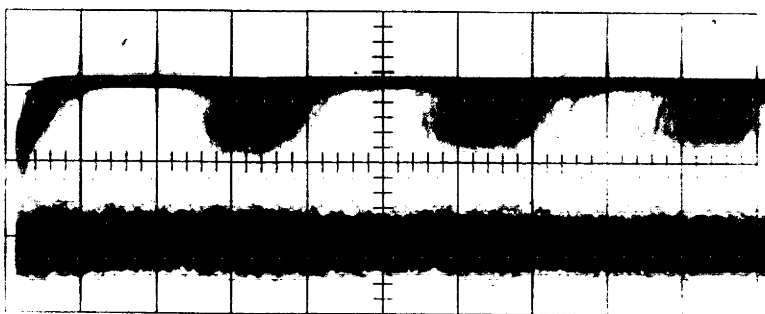
Upper trace Photomultiplier signal  
Vertical sensitivity - 50 volt/cm.

Lower trace Alternating component of discharge voltage.  
Vertical sensitivity - 50 volt/cm.

(Corresponding current sensitivity - 0.75 mA/cm.)



a



b

FIG 3.11 PERIOD OF ROTATION vs. PRESSURE FOR HYDROGEN

The broad arrow marks approximately, the transition pressure. Below this pressure the vertical bars give the magnitude of the jitter on the signal from the photo-multiplier. Above the transition, the bars indicate a slower "drift" of  $T_r$ .

Points obtained for three runs, each run consisting of a series of measurements with the pressure increasing, and a series of measurements with the pressure decreasing between measurements, have been plotted, to show the extent of the lack of the reproduceability of the experimental curves.

Magnetic field - 590 gauss  
Discharge current - 15 mA  
Diameters of electrodes - 10.2, 14.0 cm.

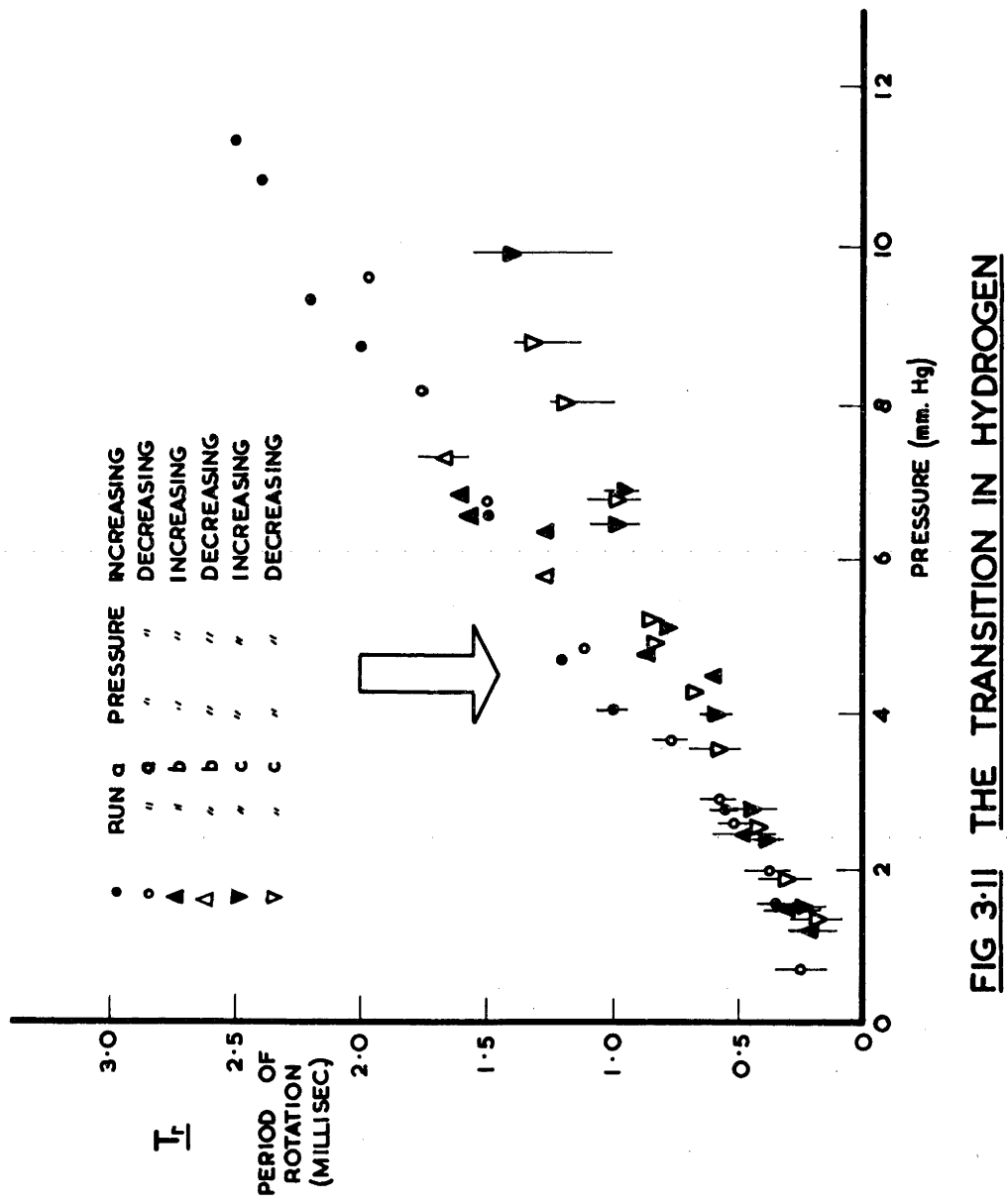
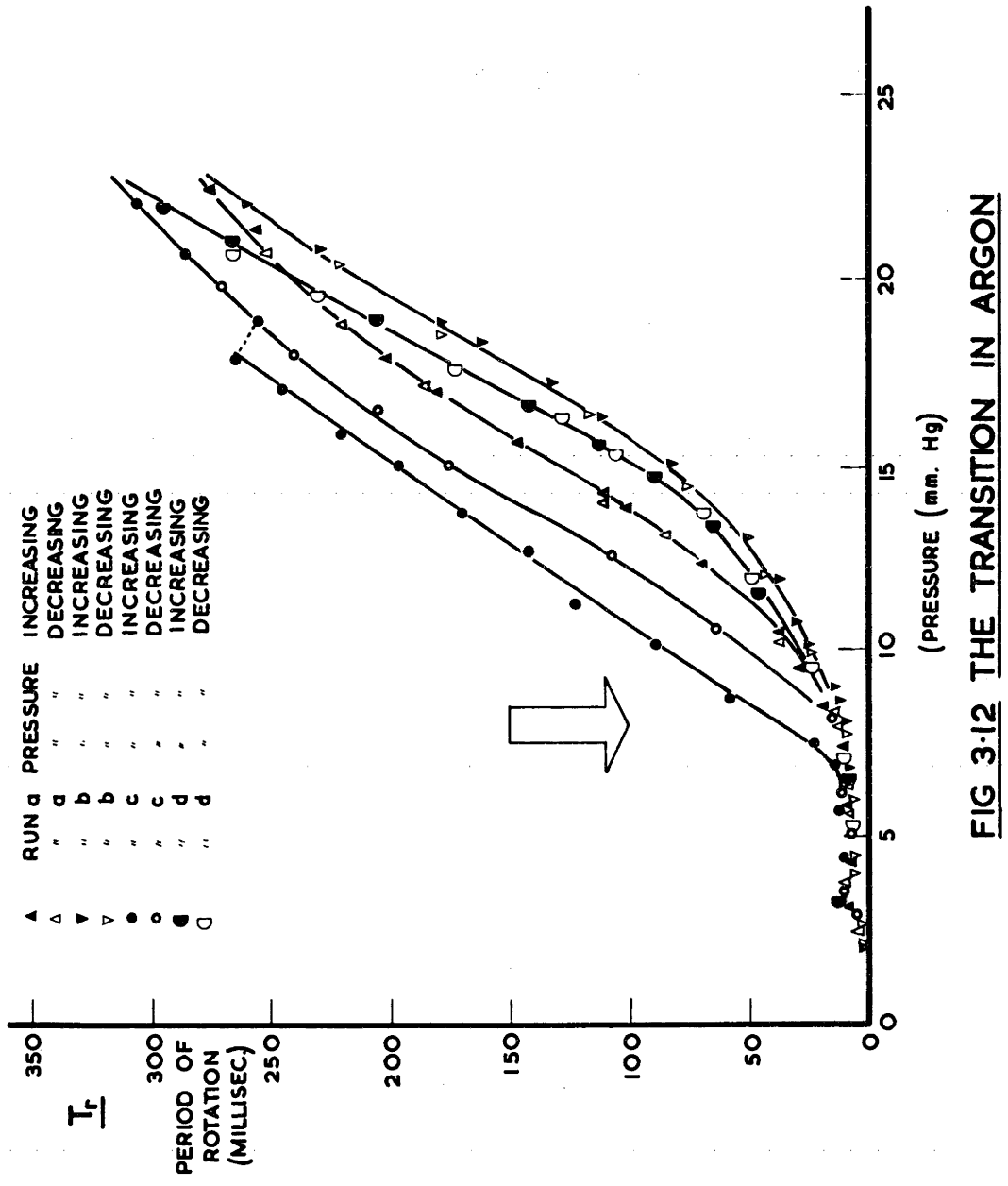


FIG 3.12 PERIOD OF ROTATION vs. PRESSURE FOR ARGON

The broad arrow marks, approximately, the transition pressure. The jitter observed below the transition is not particularly great - it is too small to be marked on this graph.

The results of four runs are plotted to show the extent of the lack of reproduceability of the experimental results.

Magnetic field - 2,160 gauss  
Discharge current - 15 mA  
Diameters of electrodes - 10.2, 14.0 cm.



**FIG 3-12 THE TRANSITION IN ARGON**

is no remarkable change in position of the negative glow at the transition.

### 3.3.2 Dependence of the transition pressure on the experimental gas (Br 59)

Table 3.1 shows the range of pressures at which the transition occurred in the various gases in which the discharge has been studied. Also shown is the pressure at which  $\omega T = 1$  for electrons ( $\omega$  = electron cyclotron frequency,  $T$  = mean time between the collisions of an electron with a neutral gas molecule) in a magnetic field of 2,160 gauss (590 gauss for hydrogen) for electrons of energies of 1, 4, 9 and 25 eV.

Now,

$$T = \ell/v = (p_0 P_c v)^{-1} \quad (3.1)$$

where  $\ell$  = mean free path of an electron

$v$  = velocity of the electrons

$p_0$  = gas pressure, "reduced" to 0°C

$P_c$  = probability of an electron colliding with a neutral molecule in passing through 1 cm. of the gas at a pressure of 1 mm. Hg.  $P_c$  is a function of electron energy

and  $\omega = Be/m$  (3.2)

where  $B$  = magnetic field

$e, m$  = charge, mass of an electron.

Therefore

$$\omega T = Be/(mp_0 P_c v) \quad (3.3)$$

Table 3.1 TRANSITION PRESSURE, AND PRESSURE AT WHICH  $\omega T = 1$

| <u>Gas</u>  | Hydrogen | Helium    | Nitrogen   | Argon  |
|---|----------|-----------|------------|--------|
| <u>Magnetic Field</u><br><u>(Gauss)</u>                           | 590      | 2,160     | 2,160      | 2,160  |
| <u>Experimental transition</u>                                    | 4 - 7    | 10.5 - 18 | 9.5 - 11.5 | 7 - 11 |
| <u>Pressure for <math>\omega T = 1</math></u><br><u>(mm. Hg.)</u> |          |           |            |        |
| Electron energy = 1 eV  | (3.8)    | (36)      | (23)       | (200*) |
| Electron energy = 4 eV  | 2.0      | 20        | 10.4       | 12     |
| Electron energy = 9 eV  | 1.9      | 16        | 6.4        | 3.1    |
| Electron energy = 25 eV   | 2.0      | 17        | 3.4        | 2.9    |

\* Probably not significant because collision cross section is very small at 1 eV for Argon.

Now, for

$$\omega T = 1$$

$$p_0 = Be/(m P_c v) \quad (3.4)$$

The pressure at which  $\omega T = 1$  was calculated from (3.4) for monoenergetic electrons, no account being taken of the distribution of the velocities of the electrons in the discharge. Inclusion of the distribution of the velocities of the electrons in the calculation of the pressure at which  $\omega T = 1$  would reduce the effect on this calculation of deep "valleys" (such as occurs for argon at low electron energies) and sharp resonances (observed for nitrogen) in the curves of  $P_c$  as a function of electron energy. (See BROWN (Br 59)). It is the low value of  $P_c$  at low energies that gives rise to the extremely high value of the pressure shown in the table for 1 eV electrons in argon.

Table 3.1 shows that the transition occurs for all the gases studied at a pressure of the order of that at which  $\omega T = 1$  for electrons.

(The pressures calculated for 1 eV electrons are not of great importance, as it is doubtful if the mean energy of the electrons in the discharge is this low).

The agreement is worst for hydrogen, where measurements were made in a low magnetic field.

3.4 THE INFLUENCE OF THE RADII OF THE ELECTRODES,  
AND THE POLARITY OF THE CENTRE ELECTRODE, ON  
THE BEHAVIOUR OF THE DISCHARGE

The results discussed in section 2.3 indicate that the cathode region may control the velocity of the discharge. A study in the Mk. II chamber of the motion of the discharge around electrodes of widely different radii can be used to confirm this observation.

It is assumed that electrodes of diameters  $d_1$  (the inner electrode) and  $d_2$  (the outer electrode) are installed in this chamber, the inner electrode being negative with respect to the outer. i.e., it is the cathode (see figure 3.13(a)).

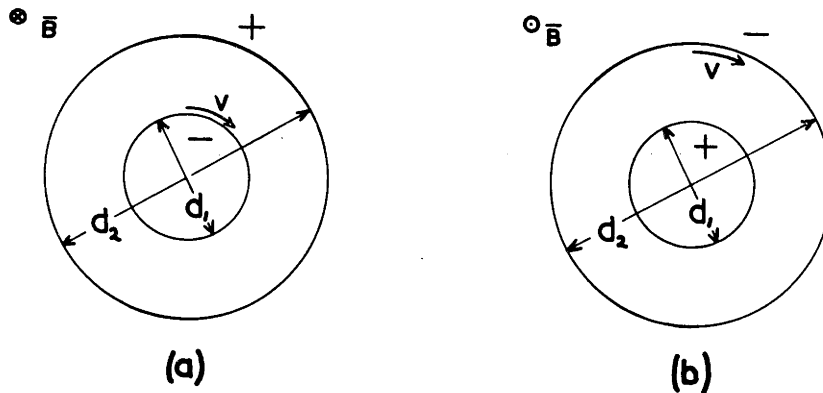


FIG 3.13 REVERSAL OF THE POLARITY OF THE  
CENTRE ELECTRODE

If the velocity is controlled by the cathode region of the discharge, then the period of rotation of the discharge,

$$T_{r1} = \pi d_1 / v \quad (3.5)$$

where  $v$  = velocity of the discharge along the cathode.

Now, if the polarity of the electrodes is reversed so that the outer electrode is now the cathode (see figure 3.13(b)), the period of rotation,

$$T_{r2} = \pi d_2 / v \quad (3.6)$$

$v$  being the same as when the inner electrode was the cathode if the cathode region alone determines the velocity of the discharge.

Thus, if the cathode region controls the velocity of the discharge,

$$T_{r1}/T_{r2} = d_1/d_2 \quad (3.7)$$

The period of rotation was measured as a function of pressure for a discharge in nitrogen between electrodes of 5.08 cm. (2") and 11.4 cm. ( $4\frac{1}{2}$ ") diameter, with the inner electrode both positive and negative. Above the transition  $T_{r1}$  was quite markedly less than  $T_{r2}$  (see section 3.4.1), (indicating that the cathode region does indeed control the velocity of the discharge), but not to the extent expected from equation (3.7).

This discrepancy could occur for three reasons:

- I      The controlling region of the discharge is not at the surface of the cathode, but some distance  $\Delta r$  beyond the surface.

If this is the case then equation (3.7) must be modified to read

$$T_{r1}/T_{r2} = (d_1 + 2 \Delta r)(d_2 - 2 \Delta r). \quad (3.8)$$

II     The properties of the cathode region, and the velocity at which it moves may be different when the cathode is the outer electrode, than when it is the inner electrode. The curvature of the electrodes, and the "vacuum" electric field at the surface of the electrodes are different for the two cases.

III    The discharge may not move with a velocity determined solely by the cathode region. This region may receive an increment of velocity over that which it would have if it alone controlled the velocity of the discharge determined by the other regions of the discharge. i.e., it is "dragged along" by the positive column or cathode region of the discharge. This increment could possibly be greater when the cathode is the outer electrode, than when it is the inner electrode.

If the cathode region moved with a velocity  $v$ , if it was not dragged along by the remainder of the discharge, and the positive column moved with a velocity  $u$ , if it was not constrained by the cathode region, then:

If the centre electrode of radius  $r_1$ , was negative, the cathode region would move with an angular velocity  $v/r_1$ . (See figure 3.14(a)). The positive column would move with an angular velocity  $u/r$ , where  $r$  is between  $r_1$  and  $r_2$ , the radius of the outer electrode.

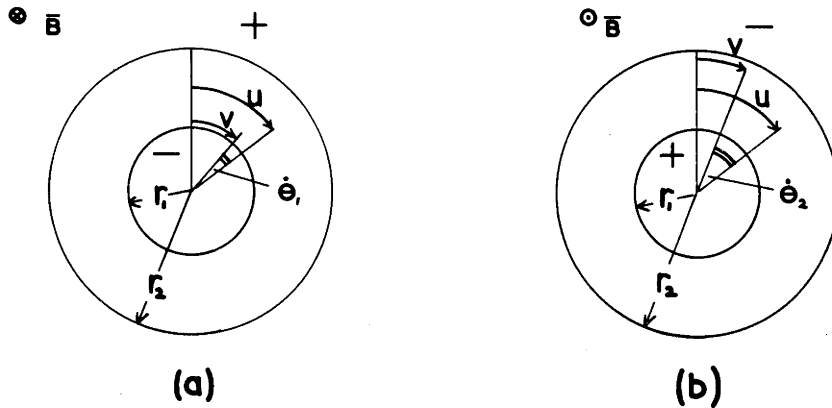


FIG 3.14 THE AUGMENTATION OF THE VELOCITY  
OF THE CATHODE REGION

The rate-of-change of the angle between these regions,

which gives a measure of the rate at which these regions separate,

$$\dot{\theta}_1 = u/r - v/r_1 \quad (3.9)$$

Similarly, if the centre electrode was positive, the rate at which these regions would separate,

$$\dot{\theta}_2 = u/r - v/r_2 \quad (3.10)$$

(See figure 3.14(b)).

Now, if it is assumed that

$$u/r > v/r_1 \quad (3.11)$$

then

$$\dot{\theta}_1 < \dot{\theta}_2 \quad (3.12)$$

because  $r_1 < r_2$

i.e., the positive column would move ahead of the cathode region at a greater rate if the centre electrode was negative, than if it was positive.

Now obviously the positive column does not continue moving ahead of the cathode region, but either (i) it is slowed down to the velocity of the cathode region, (ii) the cathode region is accelerated to the velocity of the positive column, or (iii) the positive column is slowed down, and in addition, the velocity of the cathode region is increased to a velocity greater than that at which it would move if it alone controlled the velocity of the discharge. i.e., the velocity of the cathode region is augmented because this region is dragged along by the remainder of the discharge.

The experimentally observed difference between  $T_{r1}$  and  $T_{r2}$  excludes the possibility of the cathode region being accelerated to the velocity of the positive column,  $u$ , (possibility (ii) above), in which case  $T_{r1}$  and  $T_{r2}$  would be equal. However the experimental results are not those that would be expected if the cathode region alone controlled the velocity of the discharge (possibility (i)).

It is suggested that the velocity of the cathode region is augmented by the positive column of the discharge, the augmentation being greater, the greater the degree to which the angular velocity of the positive column must be reduced to be equal to that of the

cathode region. i.e., the greater the rate at which these regions would separate if they were able to move independently.

Now, as

$$\dot{\theta}_1 < \dot{\theta}_2 \quad (3.12)$$

then, if this is the case, the augmentation will be greater for the centre electrode positive, than for the centre electrode negative. If this is so, then the augmentation of the velocity will explain why the observed ratio  $T_{r1}/T_{r2}$  is larger than the ratio  $d_1/d_2$  (see section 3.4.1).  $T_{r1}$  (centre negative) and  $T_{r2}$  (centre positive) will both be reduced over the values given by the simple theory involving pure cathode control. (See equations (3.5) and (3.6)), but because the augmentation is greater for a positive centre electrode,  $T_{r2}$  will be reduced by more than  $T_{r1}$ .

Arguments that would apply if the anode region was the region of the discharge that must be prevented from moving ahead of the cathode region, give a similar result.

The weaknesses of this argument are:

- (i) It is assumed that, if the various regions of the discharge could move independently, the remainder of the discharge would move ahead of the cathode region. The only justification for this assumption is the observed shape of the discharge, the determination of which is described in section 2.1.4. The light intensity contour diagrams show that the anode region and positive column are ahead

of the cathode region, suggesting that the cathode region is dragged along by the remainder of the discharge or the remainder of the discharge is held back by the cathode region.

(ii) There is no sound basis for the assumptions that (a) the remainder of the discharge augments the velocity of the cathode region, and (b) the augmentation is greater, the greater the rate at which these regions would separate if they could move independently.

(iii) Although a change of charge density, or electric field distribution would give a mechanism whereby the velocity of the cathode region could be augmented, and the remainder of the discharge slowed down, this theory is not based on a specific mechanism of this type.

#### 3.4.1 The motion of a long discharge

Figure 3.15 shows period of rotation/pressure curves obtained for a discharge in nitrogen rotating around the gap between electrodes of 5.08 cm. (2") and 11.4 cm. ( $4\frac{1}{2}$ ") in a field of 1,100 gauss. Above the transition,  $T_{r1}$  (the period of rotation with the centre electrode negative) is less than  $T_{r2}$  (the period with the centre electrode positive). This indicates that the cathode region controls the velocity of the discharge.

$$\text{However } T_{r1}/T_{r2} > d_1/d_2 \quad (3.13)$$

$$\text{not } = d_1/d_2 \quad (3.7)$$

as would be expected if a region at the surface of the cathode moved with constant velocity in both cases.

FIG 3.15 PERIOD OF ROTATION vs. PRESSURE FOR NITROGEN  
LONG DISCHARGE

Magnetic field - 1,100 gauss  
Discharge current - 15 mA.

Each set of points consists of the results of two runs, each run consisting of a series of measurements made with the pressure increasing, and a series made with the pressure decreasing.

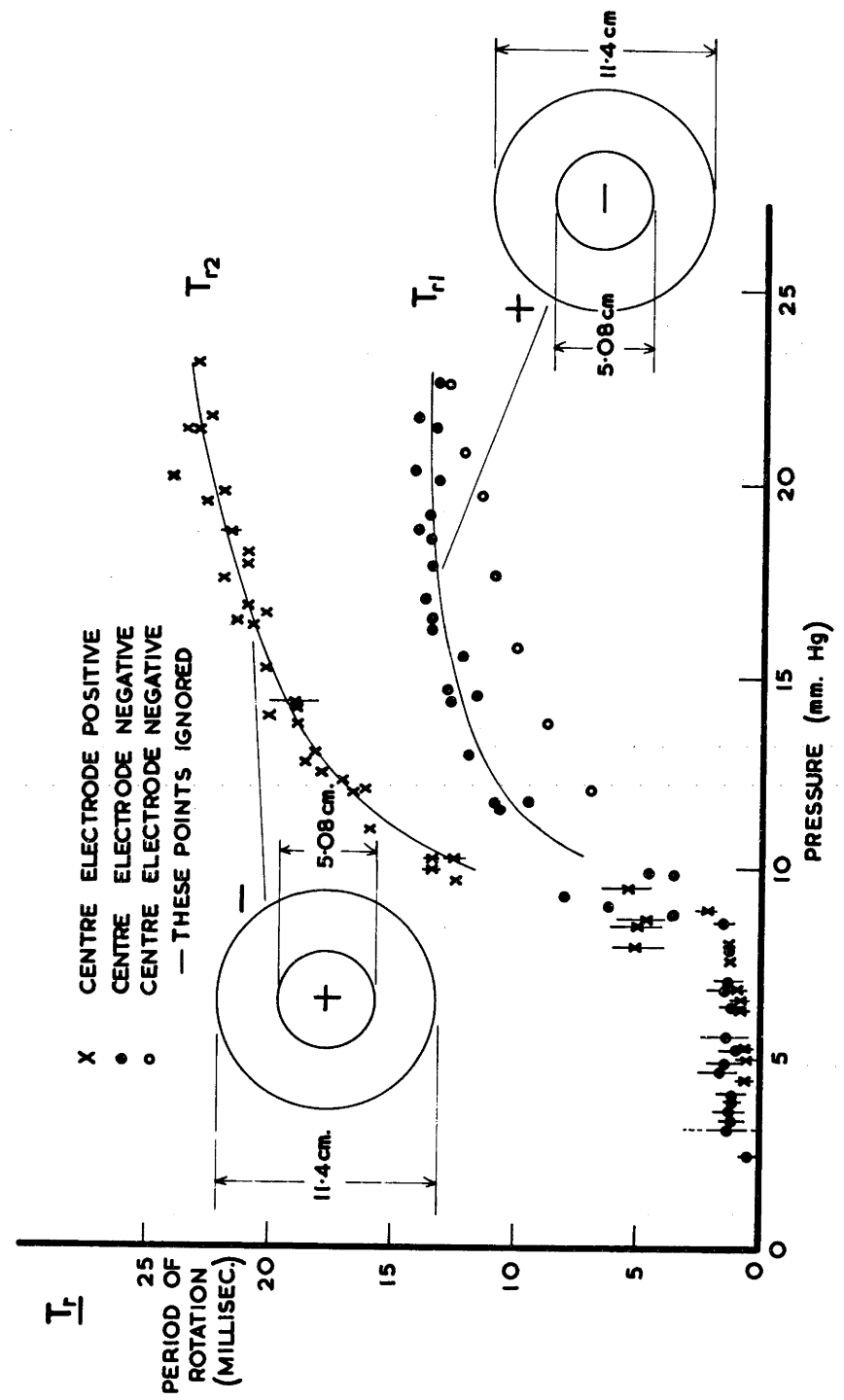


FIG 3.15  $T_r$  vs. PRESSURE IN NITROGEN – LONG DISCHARGE

Table 3.2 gives values of the ratio  $T_{r1}/T_{r2}$  obtained from the above curves, and  $\Delta r$  calculated from  $T_{r1}/T_{r2}$  (see equation 3.8). The values of  $T_{r1}$  obtained for one run of the series were excluded when making calculations, because these values differ greatly from those obtained for other runs of the series (see figure 3.15). Had these points been included, the ratio  $T_{r1}/T_{r2}$  would have been slightly closer to the ratio  $d_1/d_2$ .

The length of the cathode region of a normal glow discharge, and the length of the negative glow, are also tabulated. The former was obtained from BROWN (Br 59) for a nitrogen glow discharge on an iron cathode. (Values for copper were not available. Iron gives a longer cathode fall for nitrogen than the other cathode materials for which this parameter is tabulated). Measurements by GÜNTHERSCHULZE (Gu 24) indicate that, at the pressure at which these measurements were made, the magnetic field will cause only a minor decrease of the length of the cathode fall region. The length of the negative glow was computed from data given by BREWER and WESTHAVER (Br 37, Fr 56) by making use of the Similarity Principle (Fr 56). No reference has been found in the literature to the influence of a magnetic field on the length of the negative glow. Measurements of the distance from the cathode to the far edge of the negative glow of a glow discharge driven along parallel electrodes by a T. M. F. (The Rail Discharge. This work

Table 3.2

CHANGE OF THE PERIOD OF ROTATION ON REVERSING THE ELECTRIC FIELD

| Pressure<br>(mm. Hg.)               | $\frac{T_{r1}}{(m \text{ sec})}$ | $\frac{T_{r2}}{(m \text{ sec})}$ | $\frac{T_{r1}/T_{r2}}{(CentrePositiveNegative)}$ | $\frac{\Delta r}{(cm)}$ | $\frac{r_c}{(cm)}$ | $\frac{r_n}{(cm)}$ |
|-------------------------------------|----------------------------------|----------------------------------|--|-------------------------|--------------------|--------------------|
| <u>Magnetic field = 1,100 gauss</u> |                                  |                                  |  |                         |                    |                    |
| 12                                  | 10.7                             | 16.7                             | 0.64   | 0.67                    | 0.035              | 0.083              |
| 14                                  | 12.2                             | 19.1                             | 0.64   | 0.67                    | 0.030              | 0.072              |
| 16                                  | 12.9                             | 20.6                             | 0.63   | 0.65                    | 0.026              | 0.062              |
| 18                                  | 13.5                             | 21.7                             | 0.62   | 0.61                    | 0.023              | 0.056              |
| 20                                  | 13.6                             | 22.6                             | 0.60   | 0.55                    | 0.021              | 0.050              |
| 22                                  | 13.7                             | 23.2                             | 0.59   | 0.54                    | 0.019              | 0.045              |
| <u>Magnetic field = 590 gauss</u>   |                                  |                                  |  |                         |                    |                    |
| 12                                  | 18.6                             | 37.8                             | 0.49   | 0.2                     | 0.035              | 0.083              |
| 18                                  | 20.2                             | 40.2                             | 0.50   | 0.2                     | 0.023              | 0.056              |

$r_c$  - length of cathode fall region

$r_n$  - length of negative glow

is described briefly in Appendix 3) indicate that the length is decreased, but not greatly, by the magnetic field.

Table 3.2 reveals that  $\Delta r$ , the distance of the controlling region from the cathode, is much greater than the distance from the cathode to the boundary between the negative glow and the F.D.S. Therefore, if the assumption of the existence of a controlling region  $\Delta r$  from the cathode is correct, the controlling region must be beyond the negative glow - i.e., in the F.D.S., or the positive column. No data is available on the length of the F.D.S. However, in the absence of a magnetic field, it is not much greater than the length of the negative glow. Thus it appears that the above assumption is not correct. The controlling region would almost certainly be in the positive column if this was so, in which case the difference in the period of rotation on reversing the polarity of the centre electrode cannot be explained. (Even if the F.D.S. was of such a length that the controlling region was in the F.D.S., it is doubtful if this result would be of significance. The nature of the F.D.S. - a region with properties midway between those of the negative glow and the positive column - is such that it is difficult to conceive the velocity being controlled by this region of the discharge).

This discussion shows that it could not be unreasonable to discard the assumption of the existence of a controlling region at a distance  $\Delta r$  from the cathode, in favour of the assumption that

the velocity of the cathode region is augmented due to this region being dragged along by the remainder of the discharge.

Experiments in a magnetic field of 590 gauss give a similar result. These measurements are of lower accuracy than those described above, because of the instability of the magnet encountered at low fields. The results are also tabulated in table 3.2.

A similar change of the period of rotation when the polarity of the centre electrode was reversed was found for a field of 2,160 gauss. However, the presence of another phenomenon - the slowly rotating "spokes" discussed in section 3.9 - prevents a significant comparison of  $T_{r1}$  and  $T_{r2}$ .

Below the transition, the two sets of points are close together (see figure 3.15). i.e., the discharge moves at essentially the same velocity, independent of the polarity of the centre electrode. There are few experimental points below the transition, because the discharge becomes constricted at higher pressures for the small (5.08 cm.) centre electrode used for these experiments. Because of the scarcity of experimental points, and the large jitter that occurs when the gap is long,  $T_{r1}$  and  $T_{r2}$  cannot be accurately compared. However the data indicates that the period for a negative centre electrode,  $T_{r1}$ , is greater than that for a positive centre electrode,  $T_{r2}$ . This is the opposite to the result observed above the transition, and indicates that the anode region may have an

important influence on the velocity of the discharge below the transition.

### 3.4.2 The motion of short discharges

The experimental period/pressure curve for a nitrogen discharge between electrodes of diameters of 5.08 cm. and 6.35 cm. is compared with that for a nitrogen discharge between electrodes of 5.08 and 11.4 cm. in figure 3.16. The centre electrodes, of the same diameter, were negative in both cases.

The most significant difference is in the shape of the curves at low pressures. The curve for the narrow gap does not fall sharply as the pressure falls to the transition pressure, but flattens out just above a less marked transition. The jitter on the photomultiplier signal is far less than for wider gaps.

The period of rotation,  $T_{r1}$ , is smaller above the transition for the discharge across the narrow gap, than for that across the wide gap, indicating that the augmentation of the velocity is greater in the former case than in the latter case. This is in keeping with the model developed in the introduction to this section (3.4), of the cathode region being dragged along by the remainder of the discharge. If the cathode region alone controlled the velocity of the discharge,  $T_{r1}$  would be the same in both cases.

The angular velocity at which the remainder of the discharge would move if not constrained by the cathode region will be greater

FIG 3.16 PERIOD OF ROTATION vs. PRESSURE IN NITROGEN  
COMPARISON OF CURVES FOR SHORT AND  
LONG DISCHARGES - 1

Magnetic field - 1,100 gauss  
Discharge current - 15 mA

Each set of points consists of the results of two runs.  
The arrow marks, approximately, the transition  
pressure for the short gap.

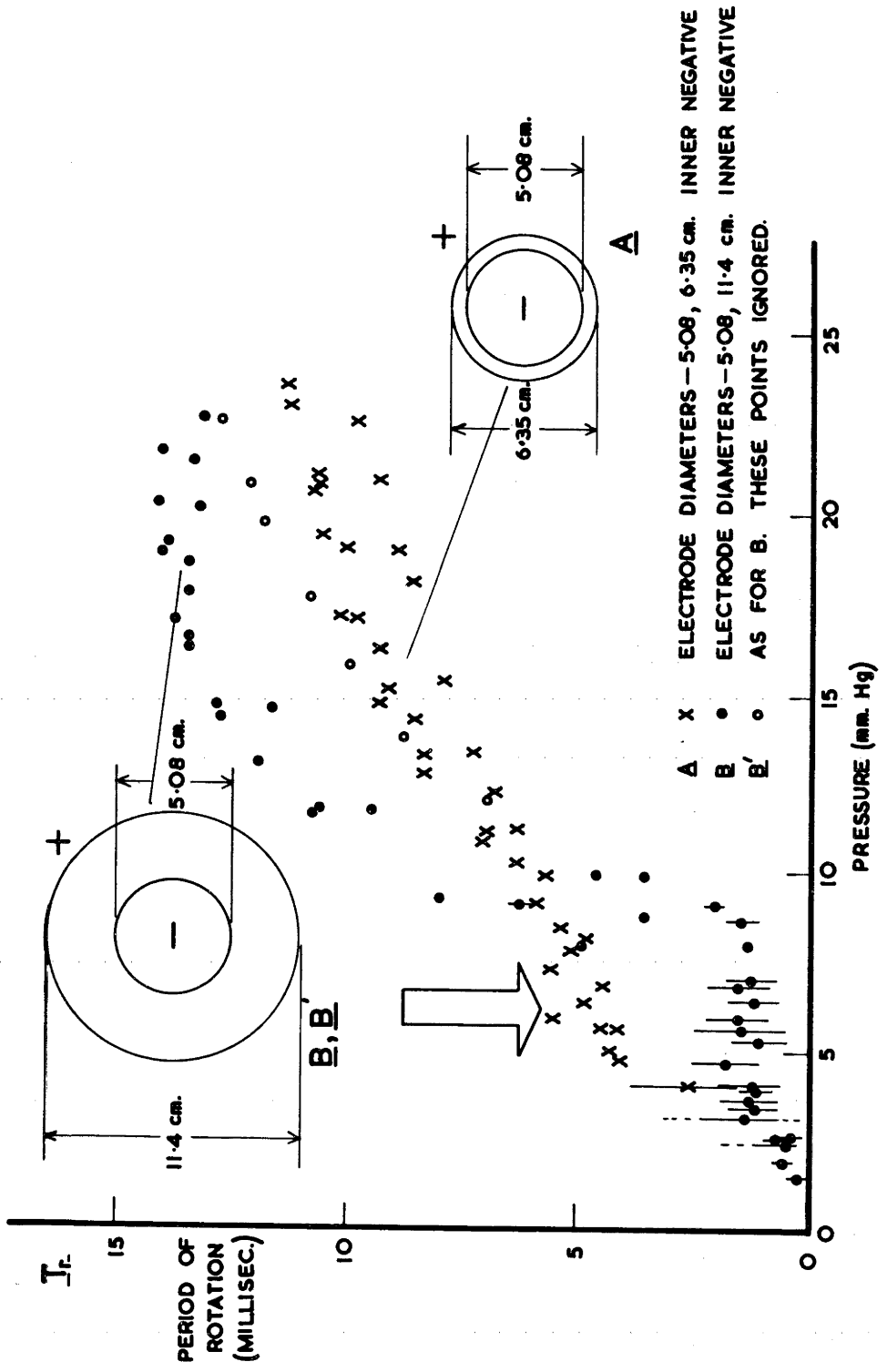


**FIG 3.16  $T_r$  vs. PRESSURE IN NITROGEN - SHORT & LONG DISCHARGES-I**

for the small gap, because of the smaller distance from the centre of the electrode system, to the centre of the discharge. The radius of the cathode is the same in both cases. Hence the angular velocity of the cathode region, would be the same in both cases if the motion of this region was not influenced by the remainder of the discharge. The augmentation is assumed to be greater, the greater the difference between the angular velocity of the remainder of the discharge, if it could move ahead of the cathode region, and the angular velocity of the cathode region, if it was not influenced by the remainder of the discharge. This difference, and hence the augmentation, will be greater for the small gap.

These results show without any doubt that the motion of the discharge may be influenced by regions other than the cathode region. The observed difference between  $T_{r1}$  for the two gap lengths, the size and geometry of the cathode being unchanged, cannot be explained in terms of:

I      The region of the discharge that controls the velocity being  $\Delta r$  from the cathode,  $\Delta r$  being different in both cases.

II      The properties and velocity of the cathode region being different for the two cases.

Another observation not inconsistent with this picture is:

For electrodes as above, but with the outer electrode the cathode in the case of the narrow gap, the periods of rotation are

substantially the same, above the transition, for both the wide and the narrow gaps. This is shown in figure 3.17. This observation can be explained if the augmentation is greater for the narrow gap, for reasons similar to those discussed above. Were there no augmentation the period of rotation would be greater for the narrow gap, because of the greater diameter of the cathode in this case - see figure 3.17.

### 3.4.3 The motion of a discharge of medium length

The period/pressure curve obtained when a nitrogen discharge was run between electrodes of 10.2 and 14.0 cm. in diameter with the centre electrode negative, is shown in figure 3.18. The shape of this curve is similar to those for a nitrogen discharge across a long gap, but the jitter on the signal from the photomultiplier observed when the discharge was rotating in the J mode, was considerably reduced.

A comparison of this curve with that obtained for a discharge between electrodes of 5.08 and 11.4 cm. in diameter, with the centre electrode positive (this curve is also shown in figure 3.18) reveals that the period is slightly shorter in the latter case. If the cathode region alone controlled the velocity of the discharge, the period of rotation would be smaller for the medium length gap, because the diameter of the cathode is less in this case (see figure 3.18). The observed result can be explained in terms of a greater augmentation

PARAGRAPH 3.17

FIG 3.17 PERIOD OF ROTATION vs. PRESSURE IN NITROGEN  
COMPARISON OF CURVES FOR SHORT AND  
LONG DISCHARGES - II

Magnetic field - 1,100 gauss  
Discharge current - 15 mA

Each set of points consists of the results of two runs.

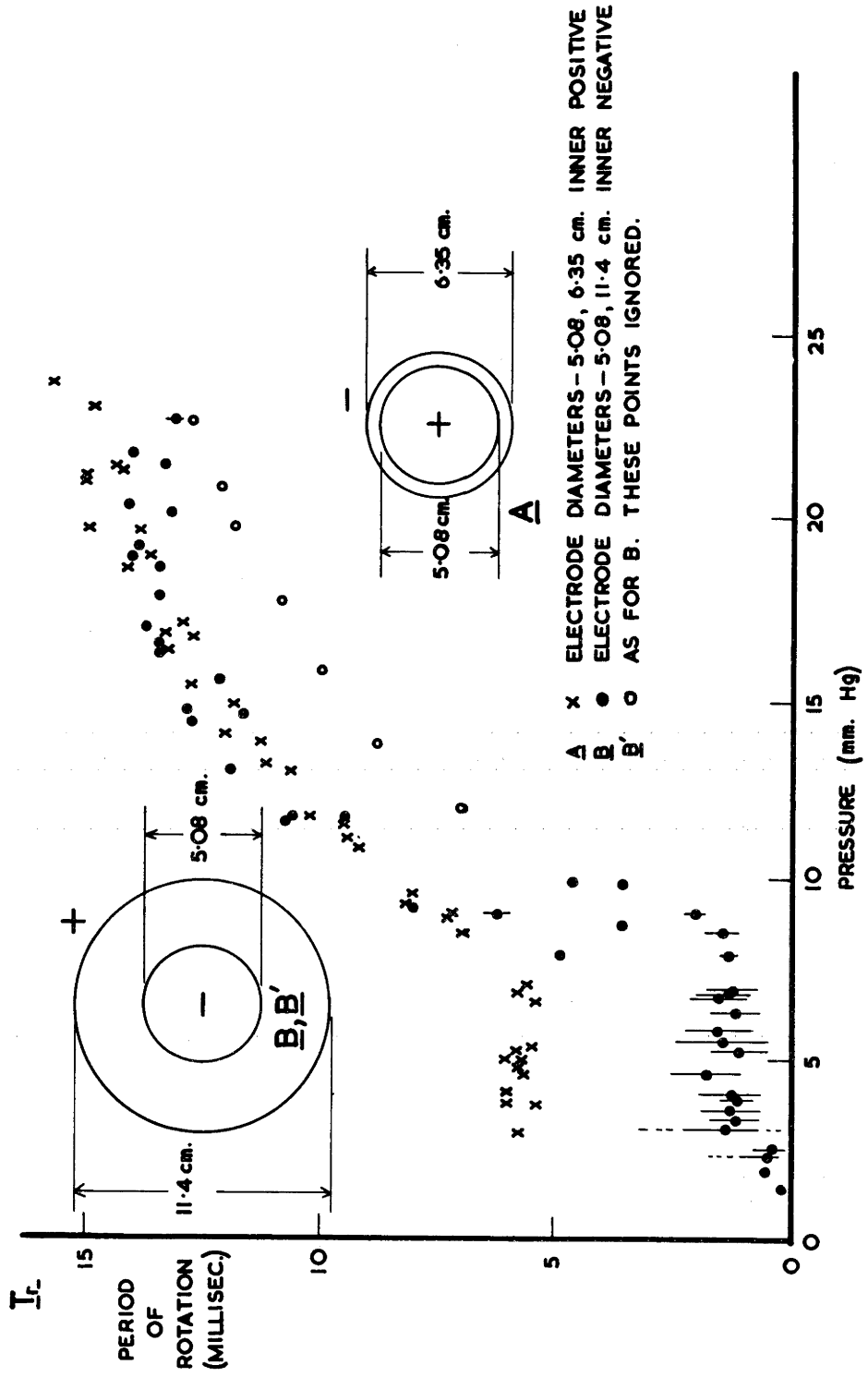
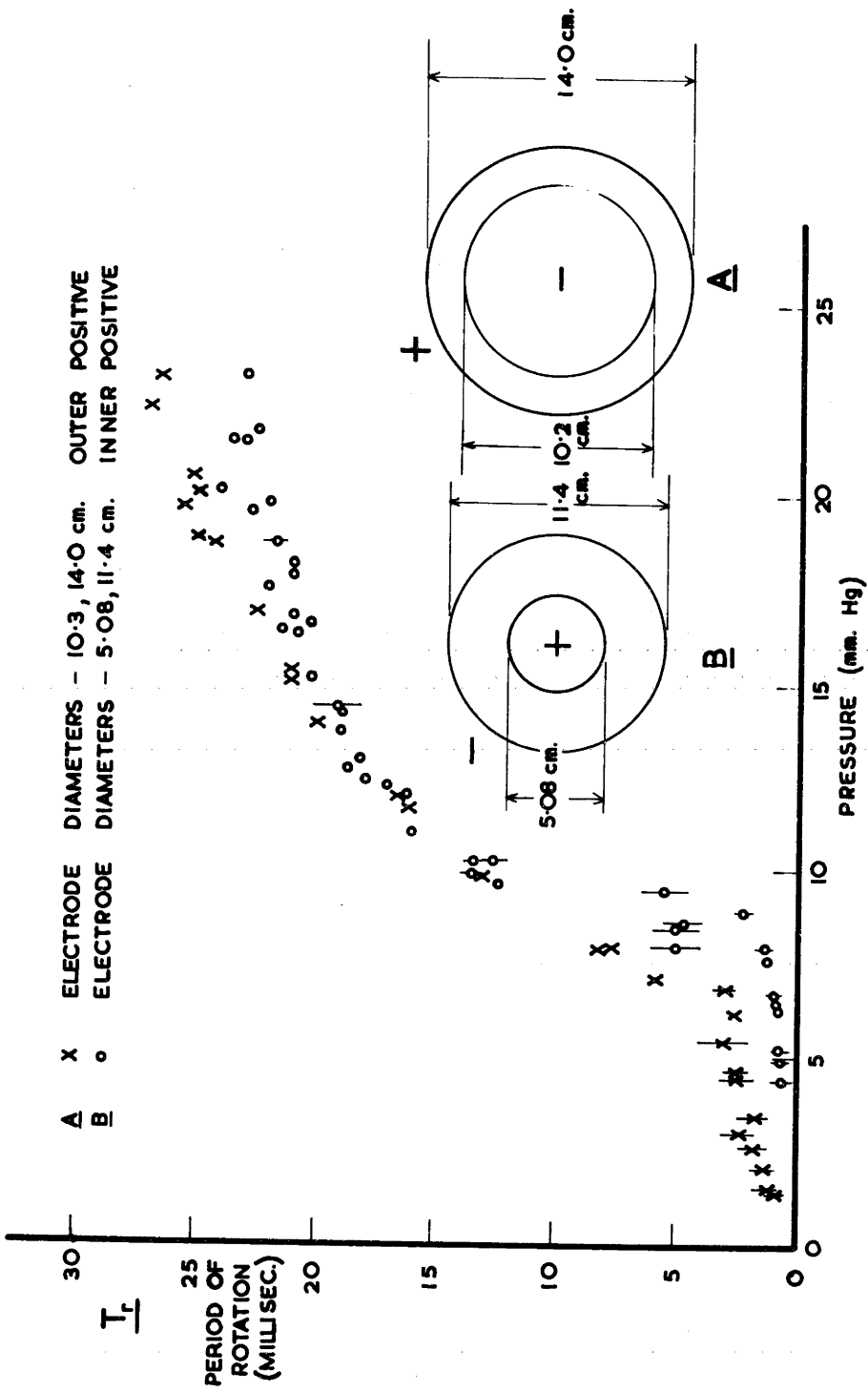


FIG 3.18 PERIOD OF ROTATION vs. PRESSURE IN NITROGEN  
COMPARISON OF CURVES FOR MEDIUM-LENGTH  
AND LONG DISCHARGES

Magnetic field - 1,100 gauss  
Discharge current - 15 mA

Curve "A" consists of the result of one run only.

Curve "B" consists of the results of two runs.



**FIG 3·18**  $T_r$  vs. PRESSURE IN NITROGEN-MEDIUM & LONG DISCHARGES.

of the velocity for the long discharge. The distance to the centre of the discharge from the centre of the electrode system is smaller for the long gap, and hence, for reasons discussed in section 3.4.2, the augmentation of the velocity of the cathode region will be greater.

When rotating in the J mode, the period for the medium length discharge is approximately three times that for the long discharge. A comparison of this ratio, with the ratio of the mean diameters of the gaps, and the diameters of the anodes for the two geometries, indicates that below the transition, the anode region controls the velocity of the discharge - see table 3.3.

#### 3.4.4 The shape of a long discharge

The concept of the augmentation of the velocity of the cathode region, introduced in this section, implies that the positive column and the anode region of the discharge move around the gap ahead of the cathode region. These regions were observed to move ahead of the cathode region in the "Racetrack" chamber, this being one of the reasons for the introduction of this concept.

In cases where the augmentation of the velocity is different, it would be expected that the degree to which the remainder of the discharge is ahead of the cathode region would be different. This is demonstrated in figure 3.19, which shows two pairs of light intensity contour diagrams obtained by means of the apparatus described in

Table 3.3

THE INFLUENCE OF THE ANODE REGION ON THE VELOCITY OF THE DISCHARGE

| Pressure<br>(mm. Hg.) | $\frac{T_a}{T_b}$<br>(m sec) | $\frac{T_a}{T_b}$ | $\frac{d'_a}{d_b}$<br>(Ratio of mean<br>diameters) | $\frac{d''_a}{d_b}$<br>(Ratio of anode<br>diameters) |
|-----------------------|------------------------------|-------------------|--|--|
| 4.5                   | $2.5 \pm 0.7$                | $0.7 \pm 0.3$     | $3.6 + 4.4$<br>$- 1.8$                             | 1.46   |
| 7.0                   | $3.0 \pm 0.5$                | $1.0 \pm 0.2$     | $3.0 + 1.4$<br>$- 0.9$                             | 2.75   |

Subscripts "a" and "b" refer to the medium length gap, and the long gap, respectively.

$d'$  - diameter of the centre of the gap.

$d''$  - diameter of the anode.

FIG 3.19 THE SHAPES OF LONG DISCHARGES IN THE MK II CHAMBER

Magnetic field - 1,100 gauss  
Discharge current - 15 mA.  
Gas - Nitrogen  
Diameters of electrodes - 5.08, 11.4 cm.

The distance of travel of the movable viewing hole was such that it was not possible to move the carriage so that this viewing hole could look down on both electrodes.

(a) Centre Electrode Positive

Pressure - 14.2 mm. Hg.

(b) Centre Electrode Negative

Pressure - 14.1 mm. Hg.

(c) Centre Electrode Positive

Pressure - 19.5 mm. Hg.

(d) Centre Electrode Negative

Pressure - 19.5 mm. Hg.

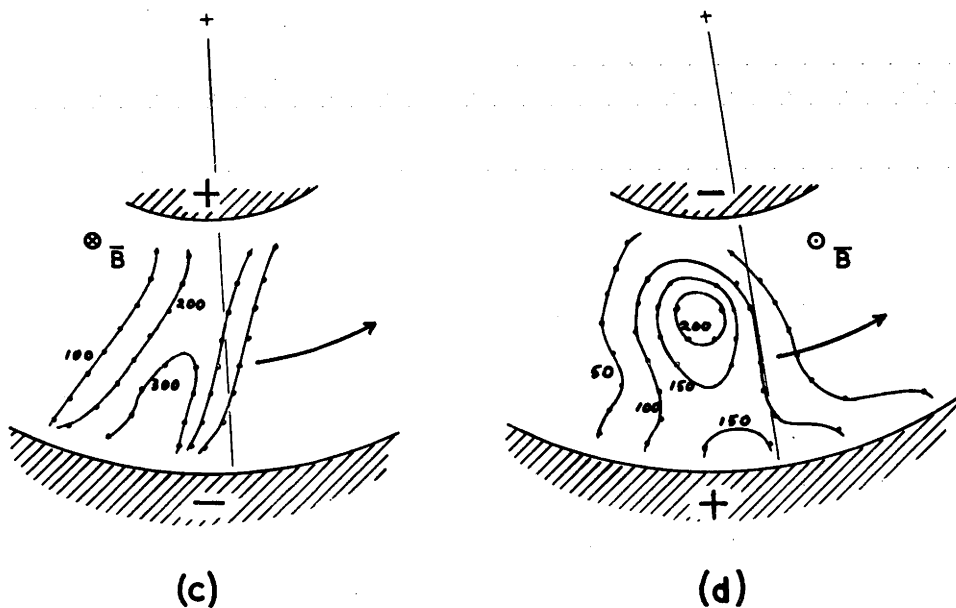
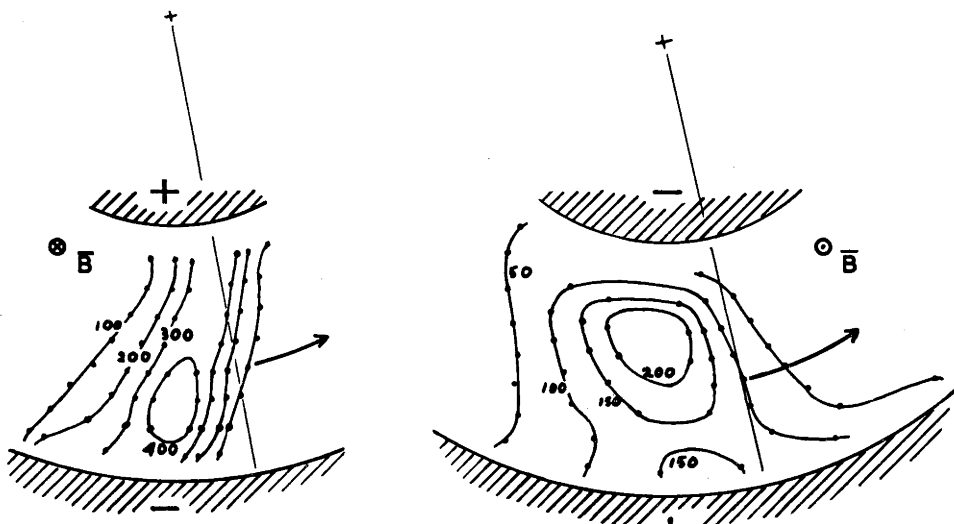


**FIG 3·19 SHAPES OF DISCHARGES IN Mk II CHAMBER**

section 2.4. The shape of a discharge between electrodes of 5.08 and 11.4 cm. diameter, was determined with the centre electrode both positive and negative. Figures 3.19 (a) and (c) which are contour diagrams obtained when the centre electrode was positive, show, in the positive column region of the discharge, a much greater slope at the leading edge than 3.19 (c) and (d), which give the shape for the centre electrode negative. The measured values of  $T_{r1}$  and  $T_{r2}$  for a nitrogen discharge moving around this gap (these measurements are discussed in section 3.4.1), revealed that the augmentation of the velocity of the cathode region was greater with the centre electrode positive, than with the centre electrode negative. Thus the observation of a greater slope in the former case is in keeping with the assumption that the remainder of the discharge moves ahead of the cathode region, and drags this region behind it.

Although the slope of the positive column is less for the centre electrode negative, the anode region lies further ahead of the positive column in this case, than for the centre electrode positive. This does not invalidate the above discussion, as the anode region can only influence the cathode region by its effect on the positive column of the discharge.

### 3.5 THE DEPENDENCE OF TRANSITION PRESSURE ON THE MAGNETIC FIELD

It was suggested in section 3.3 that the transition occurs at pressures near that at which  $\omega T = 1$ . This was checked by

determining the transition pressure as a function of magnetic field for discharges in nitrogen of various lengths. The results - obtained from a number of experimental curves - are tabulated in Table 3.4.

As the magnetic field increases,  $\omega$  will increase, and hence the pressure at which  $\omega T = 1$  will increase. Equation 3.4 shows that the pressure at which  $\omega T = 1$  is proportional to the magnetic field. Thus it would be expected that the transition pressure would be proportional to the magnetic field. This is true only for the discharge across the narrow gaps (see Table 3.4), (and, for the long gap, where measurements were made in a field of 590 gauss, for the lower magnetic fields).

### 3.6 THE DEPENDENCE OF THE PERIOD OF ROTATION ON THE DISCHARGE CURRENT

Measurements of the period of rotation of a nitrogen discharge between electrodes of 10.2 and 11.4 cm. were made in a field of 2,160 gauss. Much of the energy dissipated in a glow discharge is transferred to the cathode, and the gas in the cathode fall region (Fr 56). For this reason the centre electrode - the cathode for these experiments - was water cooled, to reduce the change of gas density due to heating of the gas in the vicinity of this electrode.

Curves of the period of rotation,  $T_r$ , as a function of discharge current,  $I$ , are plotted in figure 3.20. Also shown is the curve

$$T_r = k/I \quad (3.14)$$

(where  $k$  is a constant) normalized to the measured value of  $T_r$  at

Table 3.4 DEPENDENCE OF THE TRANSITION PRESSURE ON THE MAGNETIC FIELD

(TRANSITION PRESSURE IN mm. Hg.)

| Diameter of electrodes<br>(cm) | 5.08/6.35 | 10.2/11.4 | 5.08/11.4 | 10.2/14.0 |
|--------------------------------|-----------|-----------|-----------|-----------|
| Magnetic field (gauss)         |           |           |           |           |
| 590                            | -         | 5 + 1     | -         | -         |
| 1,100                          | 5 + 1.5   | 5 - 1     | 9 + 2     | 7 + 1.5   |
| 2,160                          | 9 + 2     | 8 - 2     | 10 + 3    | 10 - 2    |

Note: The figure tabulated is the mean transition pressure.

The "error" gives the range over which transitions were observed.

FIG 3.20 PERIOD OF ROTATION vs. DISCHARGE CURRENT  
FOR NITROGEN

Magnetic field - 2,160 gauss  
Diameters of electrodes - 10.2, 11.4 cm.

Curve "A" consists of points obtained from one run (with measurements made both with the current increasing, and the current decreasing, between measurements).

Curves "B" and "C" consist of points obtained from two runs.

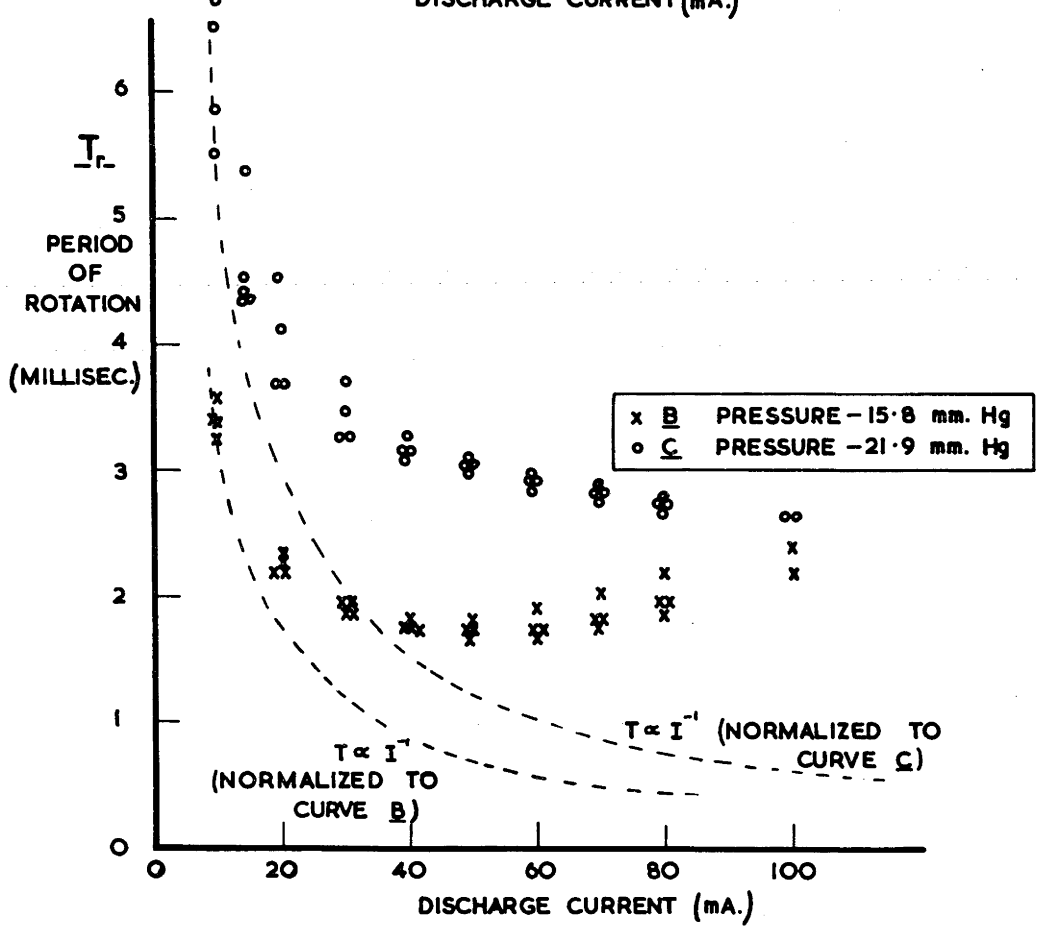
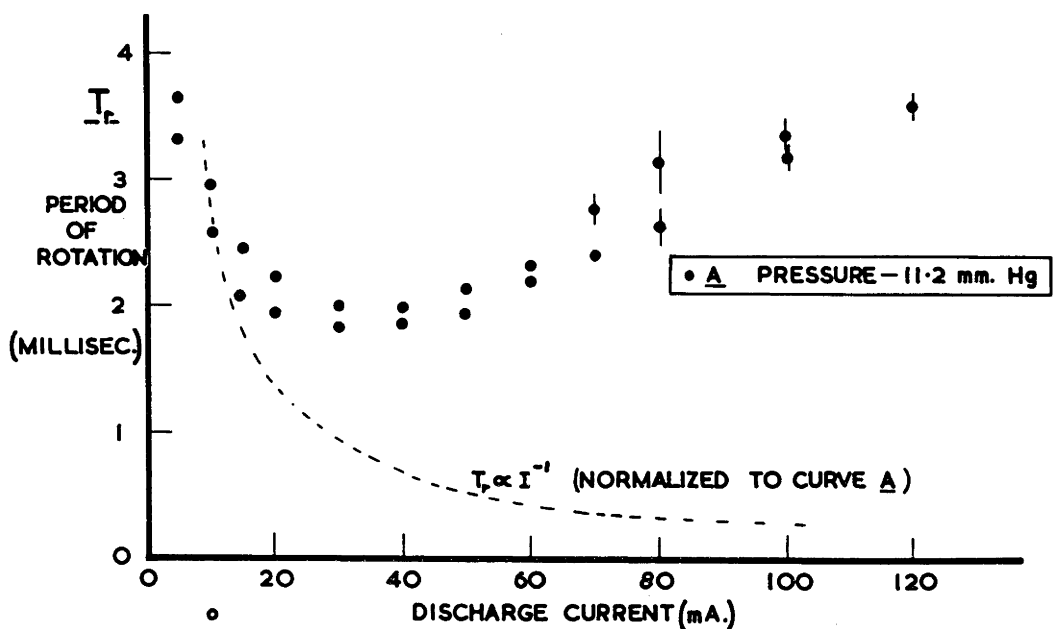


FIG 3.2O  $T_r$  vs. DISCHARGE CURRENT

10 mA. GUYE (Gu 21 a) observed that, at lower currents than those for which these measurements were made, the velocity was proportional to the discharge current, i.e., equation 3.14 holds. The present experiments show that  $T_r$  does not decrease this rapidly with increasing current.  $T_r$  initially decreases rapidly, and then more slowly, as the current is increased from 10 mA. At a pressure of 21.9 mm. Hg,  $T_r$  continues decreasing as the current is increased to 100 mA, but at lower pressures it increases slightly at the higher currents. This result is contrary to the observation of Wilson and Martyn, for currents of the order of tens of milliamperes of a ~~decrease of discharge velocity as the current is increased.~~

The discharge would not rotate regularly for current below 10 mA (possibly due to dirty electrodes - running at high currents accelerates the rate of formation of the deposit on the electrodes). At pressures below 11.2 mm. Hg excessive jitter at high currents (where the discharge switches from R mode to J mode) prevents accurate measurement of the period of rotation.

The width of the discharge in the direction of its motion increases as the current is increased, rather than the depth of the discharge - i.e., the signal from the photomultiplier becomes broader. The visually observed width of the negative glow increases as the current is increased, but does not extend on to the flat top and bottom surfaces of the cathode, even at the highest currents.

### 3.7 THE ELECTRIC FIELD IN THE POSITIVE COLUMN OF THE DISCHARGE

The voltage across a discharge in nitrogen between electrodes of 10.2 and 14.0 cm. in diameter, plotted as a function of gas pressure, is shown in figure 3.21, for zero magnetic field, and magnetic fields of 1,100 and 2,160 gauss. The T.M.F. gives rise to a large increase of the voltage across the discharge. Figure 3.22 shows the same series of curves for a discharge between electrodes of 10.2 and 11.4 cm. diameter. The T.M.F. gives rise to a less marked increase of the voltage in this case. This indicates that the T.M.F. increases the electric field in the positive column, rather than the cathode fall voltage of the discharge, in which case the voltage increase would be large for both the short discharge, and the medium length discharge.

The electric field in the positive column of the discharge may be calculated from the difference between the voltages across the discharge for the two gaps between the electrodes. Figure 3.23 shows the electric field, computed in this manner, plotted as a function of pressure. The electric field increases as the pressure increases and as the magnetic field increases. The linear dependence of the electric field on pressure, observed between 4 and 22 mm. Hg. for zero magnetic field, is observed above the transition pressure in the presence of a magnetic field. The electric field/period curves show a break at the transition.

The increase of the electric field with magnetic field is not

FIG 3.21    DISCHARGE VOLTAGE vs. PRESSURE FOR A  
MEDIUM-LENGTH DISCHARGE

Discharge current - 15 mA  
Diameters of electrodes - 10.2, 14.0 cm.

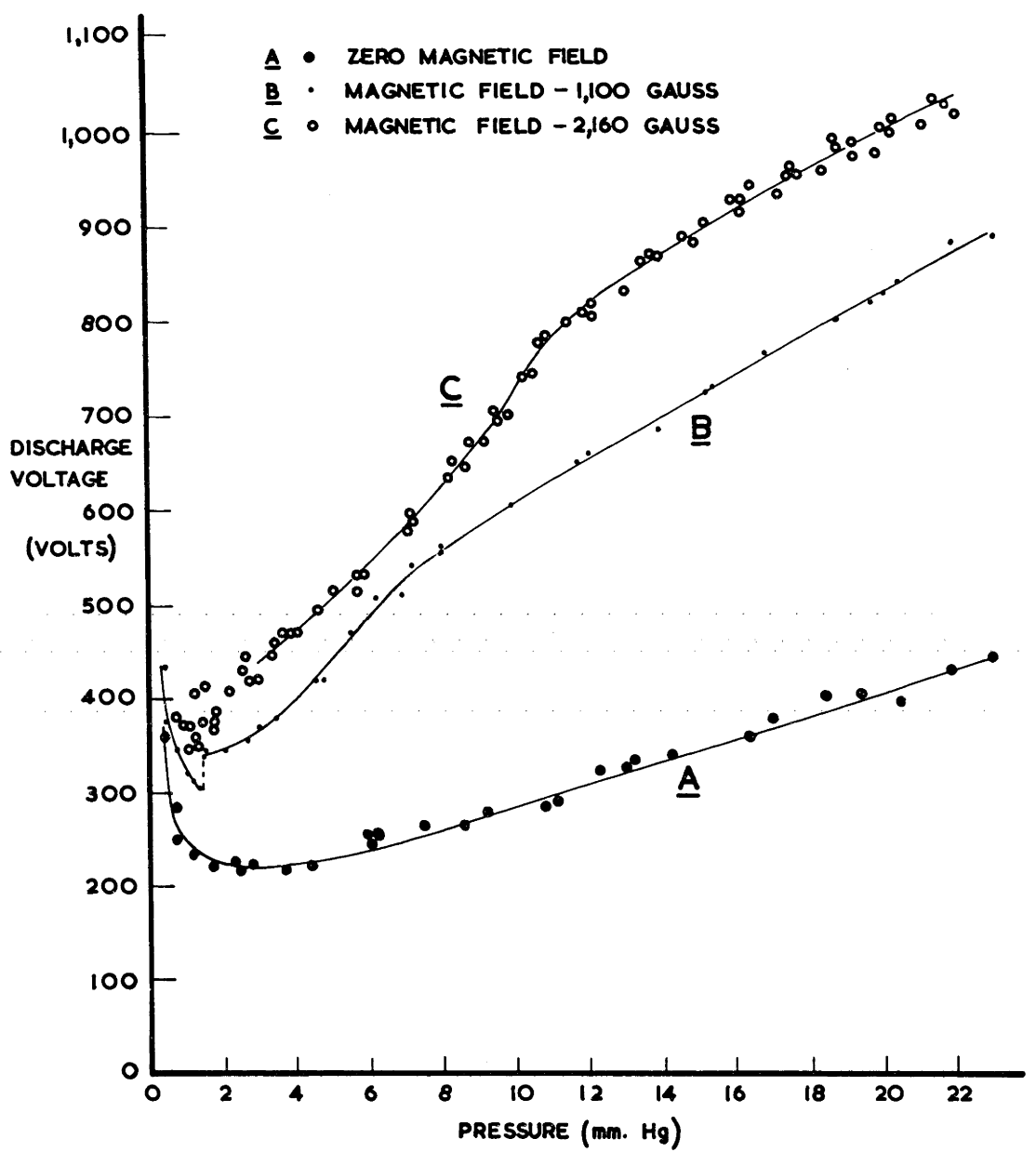


FIG 3·2I DISCHARGE VOLTAGE vs. PRESSURE —  
MEDIUM LENGTH DISCHARGE

FIG 3.22 DISCHARGE VOLTAGE vs. PRESSURE FOR A  
SHORT DISCHARGE

Discharge current - 15 mA

Diameters of electrodes - 10.2, 11.4 cm.

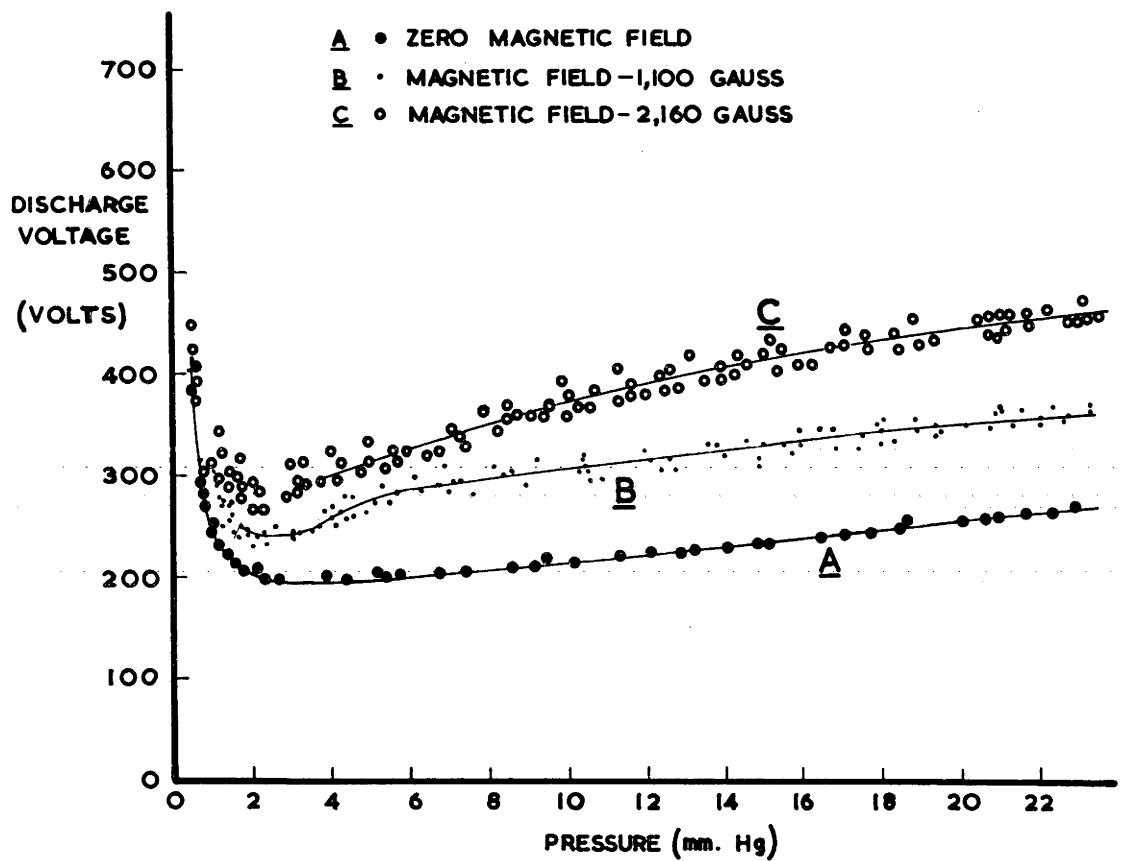
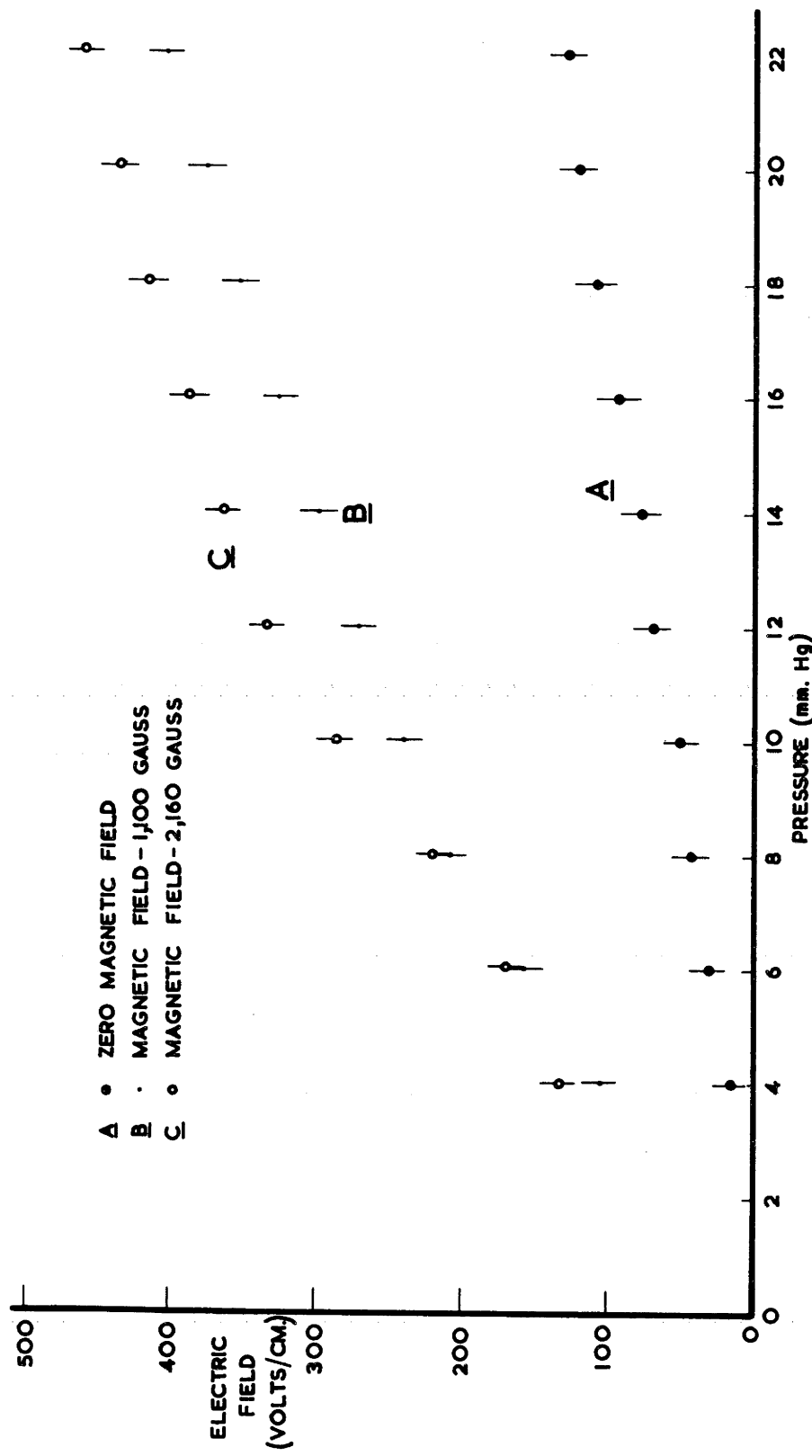


FIG 3·22 DISCHARGE VOLTAGE vs. PRESSURE —  
SHORT DISCHARGE

FIG 3.23    ELECTRIC FIELD IN THE POSITIVE COLUMN  
vs. PRESSURE FOR A NITROGEN DISCHARGE

Discharge current - 15 mA

The points plotted in this diagram were derived  
from the voltage curves given in figures 3.21  
and 3.22.



**FIG. 3·23 ELECTRIC FIELD vs. PRESSURE-NITROGEN DISCHARGE**

the result of a generated e.m.f., which, under these conditions, will increase the voltage across the discharge by less than a volt.

Because of the slope of the discharge, the path along which the current flows will be greater than the gap between the electrodes. The electric field in the direction of current flow - which is a more significant parameter than the "field" as measured by the above method - will therefore be less than the measured "electric field".

This method of determination of the electric field in the positive column of the discharge assumes that the electric field and the cathode and anode falls, are the same for discharges of both lengths.

These assumptions, true for a glow discharge in the absence of a magnetic field, need not necessarily be true for the rotating discharge. At pressures near the transition pressure, where the discharges across the two gaps may be rotating in different modes (see table 3.4), the measured values of the electric field should be regarded as suspect, because these assumptions may not be true.

### 3.8 THE INFLUENCE OF ELECTRODE SHAPE ON THE MOTION OF THE DISCHARGE

The majority of the experiments were performed with discharges running between flat electrodes similar to those shown in figure 3.2, the edges on which the discharge runs being curved. A criticism of this geometry is that, because the electrode surface is not parallel to the magnetic field, the current flow in the cathode

fall region is not everywhere perpendicular to the magnetic field.  
(The current flow in this region is perpendicular to the cathode surface (En 55)).

Experiments performed with a cylindrical centre electrode that extended the full depth of the discharge chamber as the cathode, gave period/pressure curves not dissimilar to those obtained with flat electrodes of the standard design. Above the transition the reproduceability is not particularly good, but below the transition, results of moderately good reproduceability were obtained.

This indicates that satisfactory results can be obtained with the flat electrodes, which localize the discharge so that it moves in the plane of symmetry of the electrodes. Figure 3.24(a), photographs of the markings on the cylindrical cathode due to the action of the discharge, shows that the discharge does not remain in this plane. (The markings towards the top and bottom edges result from the action of the discharge at pressures of the order of 1 mm. Hg. At higher pressures the discharge does not move this far off the plane of symmetry).

Some experiments were performed with flat electrodes similar to those used for the majority of the experiments, but with the cylindrical surfaces of the centre electrode - the cathode - covered with "Teflon", so that the cathode region must move over a surface perpendicular to the magnetic field. (See figure 3.24(b)).

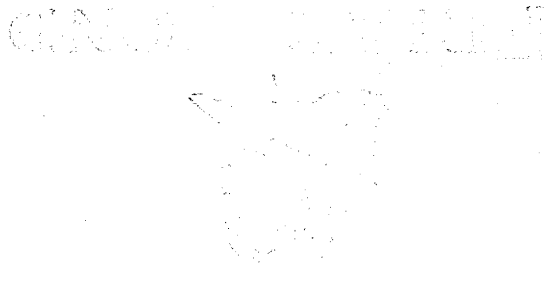
FIG 3.24    MARKINGS ON THE CATHODE

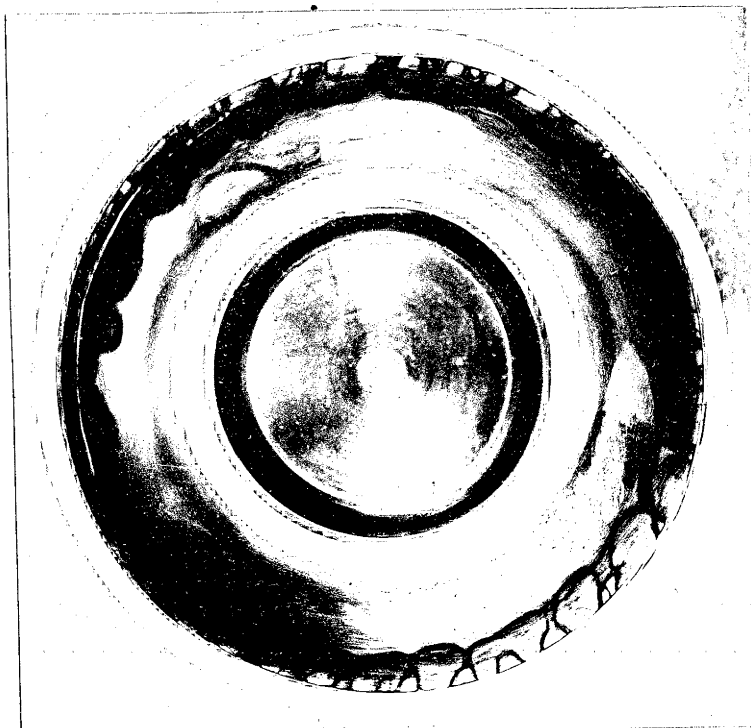
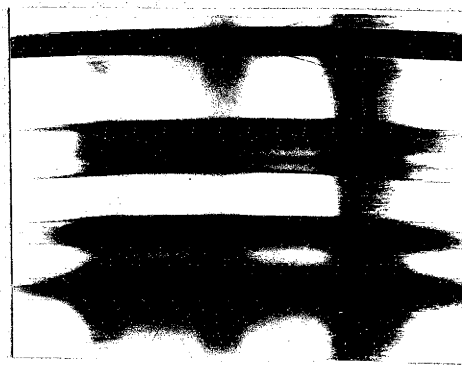
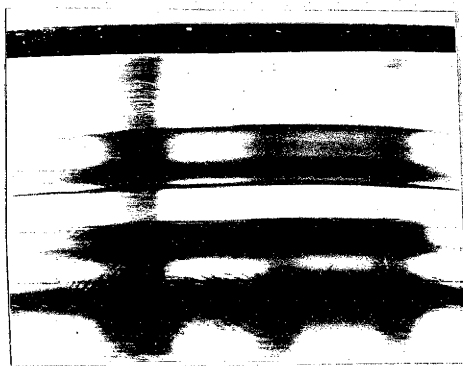
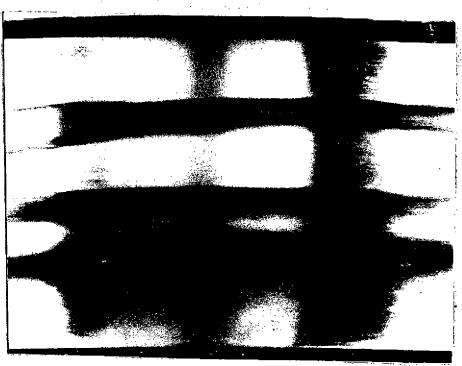
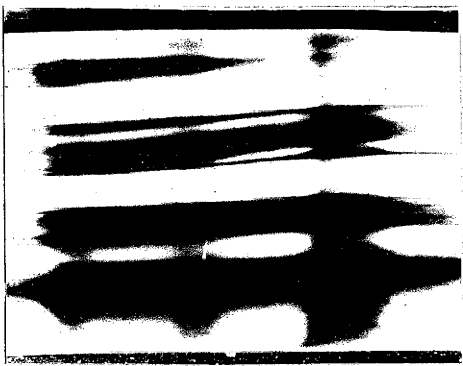
(a) (Four photographs at the top of the page)

Markings on the cylindrical cathode. These four photographs show the markings at different points on the circumference of this electrode. The discharge moves across the page, the cathode extending the full depth of each photo.

(b) (Large photograph at the bottom of the page)

Markings on the "Teflon" edged electrode.





Measurements give period/pressure curves that are far from reproduceable. The period/pressure curves are substantially those obtained for the standard electrodes under similar conditions. The nature of the transition is unchanged, and it occurs at substantially the same pressure as it did on the standard electrodes.

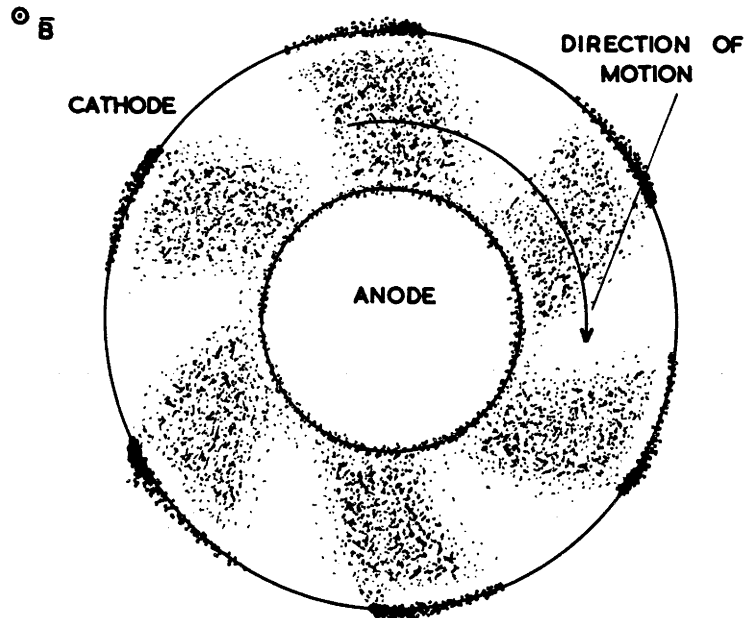
The results of section 3.4.1 show that, above the transition, some part of the cathode region must control the velocity of the discharge. In the cathode fall region the current flow is perpendicular to the surface of the cathode, so that for the "Teflon"-edged electrodes the charge carriers will move in the direction of the magnetic field, and will not be deflected by the magnetic field to move along the cathode, as they would if the current flowed perpendicular to the field, as it does when the discharge runs between electrodes of standard design. The insignificant change of the behaviour of the discharge when the cathode region is constrained to move along the flat surfaces of the electrode, indicates that the negative glow region, and not the cathode fall region, may be the region controlling the velocity of the discharge. The current in the negative glow is able to flow parallel to the surface of the electrode, so that it can be influenced by the magnetic field. The above results should not be regarded as conclusive evidence, but merely as evidence suggesting that the negative glow controls the velocity.

The marks on the cathode surface are not streaks, such

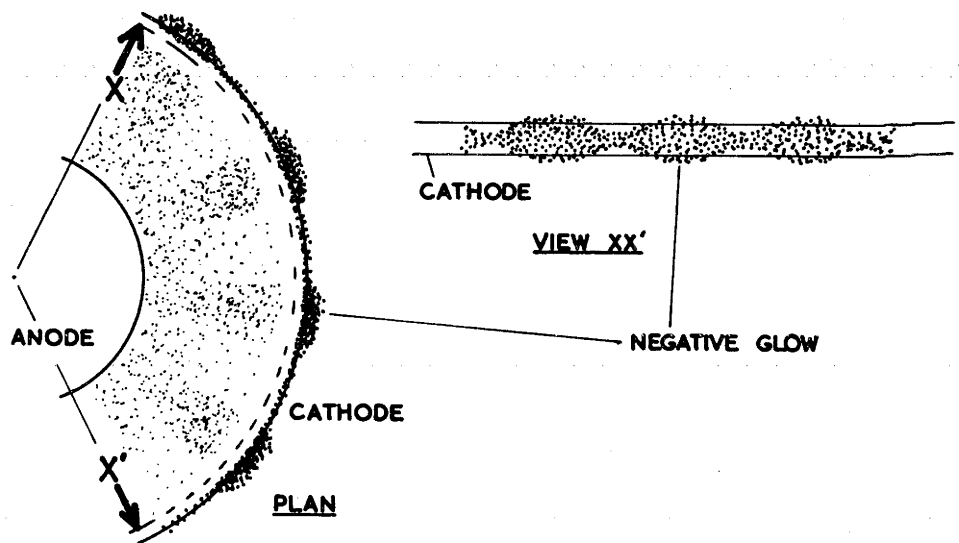
as were observed for the cylindrical cathode (figure 3.24(a)), or the standard cathode, but a series of overlapping marks of irregular shape, approximately twice as long as they are broad (see figure 3.24(b)). This pattern indicates that the cathode fall region, dragged along by the remainder of the discharge as it moves under the influence of the magnetic field, moves in "jumps" across the cathode surface, being stationary at each point for a short time before moving on. This suggests that the cathode fall region is not driven around the electrodes by the magnetic field but, as the negative glow moves away from the point where the electrons are extracted from the cathode, a new cathode fall region is established under the negative glow and the original cathode fall region extinguishes.

### 3.9 "SPOKES"

The rotating discharge normally appears as a uniform disk of light between the electrodes. However, for a discharge in nitrogen across the long gap (electrode diameters - 5.08 and 11.4 cm.) with the centre electrode positive in a magnetic field of 2,160 gauss, the discharge breaks up into five or six slowly rotating "spokes" as shown in figure 3.25(a). The period of rotation of the spokes which is in the Amperian sense, is of the order of 30 seconds. The anode region of the discharge is continuous around the gap. The width of a spoke, and the dark space between spokes are of the order of the width of the rotating discharge. The spokes occur just above, but not



(a) SLOWLY ROTATING "SPOKES"



(b) REGULAR VARIATION OF THE WIDTH OF THE NEGATIVE GLOW

FIG 3·25 "SPOKES" & RELATED PHENOMENA

immediately above, the transition, and are observed for a pressure range of less than 1 mm. Hg.

Two photomultipliers were positioned so that they looked down on the discharge at the same radius, but were just less than the width of the discharge apart, around the gap. Signals from these photomultipliers showed that the discharge was still rotating at high speed. Comparison of the time the rotating discharge took to move between the two viewing holes when a spoke was between the holes, and the time the discharge took to move around the gap, showed that the discharge moves through a spoke, and then jumps to the next spoke. Inspection of the alternating component of the discharge voltage showed that the discharge current does not cut off when this jump occurs. Above and below the pressure range in which this phenomenon is observed the negative glow flickers as if waves of light were moving around the cathode at high speed. This flickering is also observed just above the transition, for smaller gaps and lower magnetic fields, with the centre electrode of either polarity, and is often accompanied by a modulation of the amplitude of the signal from the photomultiplier.

It is suggested that the unusual signal from the voltage probe observed just above the transition for a nitrogen discharge between electrodes of 10.2 and 14.0 cm. diameter in a field of 2,160 gauss (this signal consists of a series of pulses superimposed

on the more simple synchronized component observed at higher pressures - see section 3.3.1 and figure 3.8(b) and (c)), is another manifestation of this phenomenon. The visually observed width of the negative glow often shows a regular variation around the circumference of the electrode (see figure 3.25(b)), when this signal is observed. It is not difficult to explain this variation - if the voltage across the discharge changes, the discharge current must change; hence, for a constant cathode current density the cross sectional area of the cathode region of the discharge must change.

### 3.10 CONCLUSIONS

The more important conclusions reached as a result of the experiments described in this chapter are:

- (1) A change occurs in the mode of rotation of the discharge at a pressure near that at which  $\omega T = 1$  for electrons. This change is apparently related to the difference in the nature of the motion of an electron in a magnetic field at high and low pressures,  $\omega T = 1$  giving a measure of the pressure at which this change occurs. (See section 5.1).
- (2) Above this transition, the cathode region has an important influence on the velocity of the discharge. However the velocity is not determined by the cathode region alone; the remainder of the discharge drags the cathode region along at a velocity greater than that at which it would move if it alone controlled the velocity of

the discharge.

(3) There is some evidence that the negative glow, and not the cathode fall region, is the part of the cathode region that controls the velocity of the discharge.

(4) Below the transition, the anode region controls the velocity of the discharge.

---

## Chapter 4

### EXPERIMENTS WITH SPECTROSCOPICALLY PURE GASES

The experimental observations of Chapters 2 and 3 demonstrate the necessity for studying the rotation of the discharge in very pure gases around pure, clean electrodes. This chapter describes briefly the development of a discharge chamber and vacuum system suitable for experiments of this nature, and some experiments performed in this apparatus. Unfortunately the breakage of a glass cold trap prevented the completion of the experimental program planned for this equipment.

#### 4.1 EXPERIMENTAL APPARATUS

##### 4.1.1 The discharge chamber

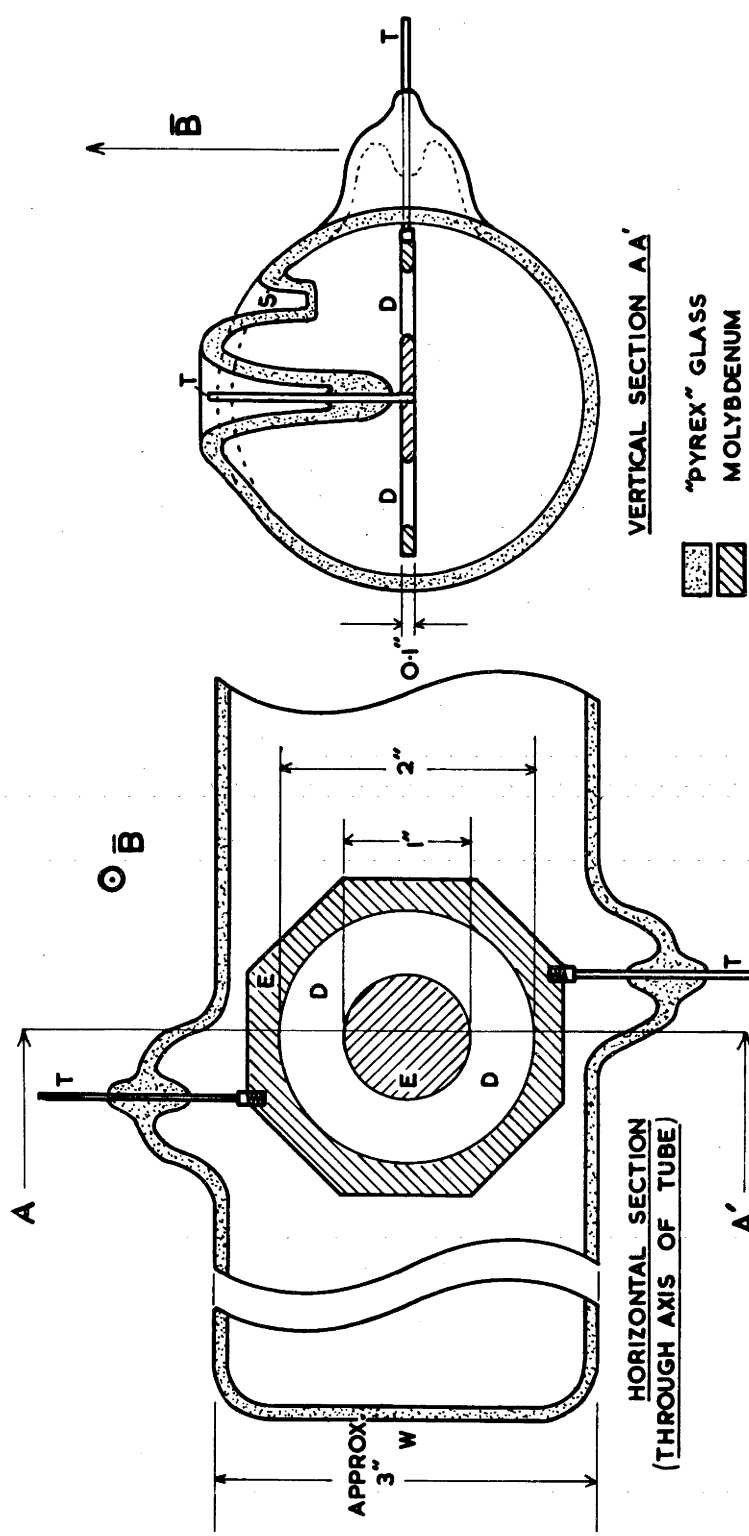
An all-glass construction was used for this piece of apparatus, the electrodes being permanently sealed into the walls of the vacuum system. Figure 4.1 shows details of the construction of the discharge chamber, which is little more than an extension of the main pumping line. The electrodes, machined from molybdenum, are 0.1" thick, and 1" and 2" in diameter. 0.05" radii are machined on the edges of these electrodes on which the discharge will run. Tungsten wires, silver-soldered into the electrodes, are sealed into the glass walls of the vacuum chamber. These wires support the electrodes, and provide a lead-through for the discharge current.

FIG. 4.1

THE ALL-GLASS DISCHARGE TUBE USED FOR THE  
EXPERIMENTS WITH SPECTROSCOPICALLY PURE  
GASES - DETAILS OF CONSTRUCTION

Two sections through the tube are shown: a vertical section perpendicular to the axis of the pumping tube, and a horizontal section on the axis of the tube.

- D - Discharge gap.
- E - Electrodes.
- S - Glass "stalk" in which the light pipe is inserted. This stalk locates the light pipe close to the discharge.
- T - Tungsten wires sealed into the glass walls of the tube.
- W - Flat window.



**FIG 4·I ALL-Glass DISCHARGE TUBE - DETAILS OF CONSTRUCTION**

#### 4.1.2 The vacuum system

Because of the high pressures at which the experiments are performed, it was decided to use conventional vacuum-producing techniques - i.e., a diffusion pump, rather than an ion pump, or a getter pump.

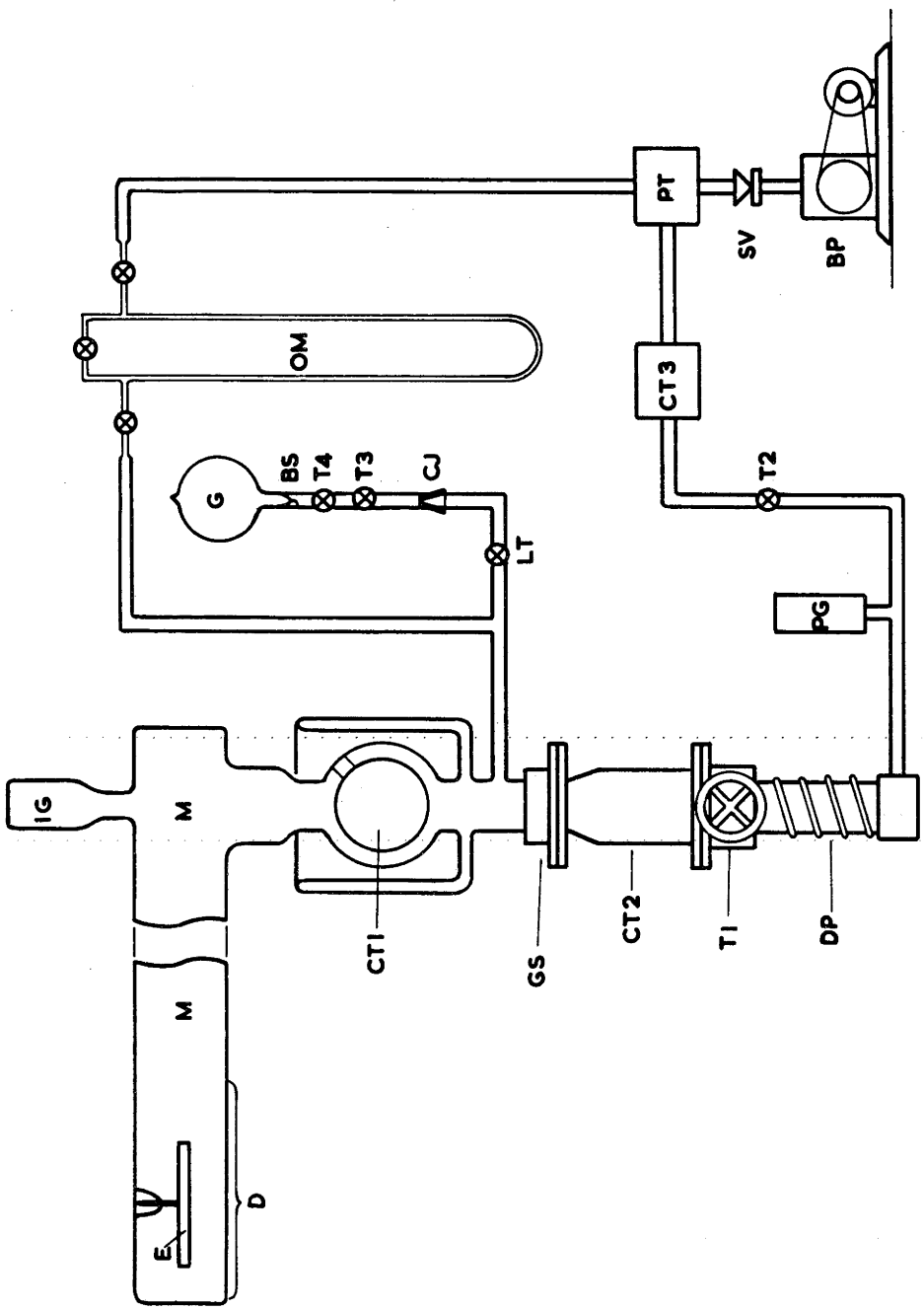
The vacuum system is shown schematically in figure 4.2. The diffusion pump, an Edwards High Vacuum Ltd., 2" metal pump, was filled with Apeizon "C" oil. This oil has a very low vapour pressure at room temperature ( $\sim 10^{-8}$  mm. Hg), but is more readily decomposed than the more commonly used "A" and "B" oils. Two cold traps reduce the migration of the pump oil and other vapours to the discharge region. The lower trap is a conventional Edwards High Vacuum Ltd., stainless steel cold trap, the upper trap a high conductance, high efficiency glass trap of the type designed by Venema (Ve 49). Both the inner and outer walls of this trap are surrounded by a jacket of liquid air, a feature that not only improves the efficiency of the trap as a vapour trap, but prevents the migration of oil to the discharge region by creeping over surfaces. A 3" glass pumping line 3' long, leads from the trap to the discharge region.

The base pressure in the system, and the leak rate were measured by an Edwards IG-2H ionization gauge, mounted above the top cold trap - this is the closest the gauge could be mounted to the discharge region without fouling on the magnet. The gas

FIG 4.2 THE "CLEAN" VACUUM SYSTEM (SCHEMATIC)

|     |   |   |
|-----|---|---|
| BP  | - | Two stage backing pump.   |
| BS  | - | "Breakoff" seal.  |
| CJ  | - | Conical glass joint.  |
| CT1 | - | Glass cold trap (Venema's design).  |
| CT2 | - | Stainless steel cold trap.  |
| CT3 | - | Backing line cold trap.   |
| D   | - | Discharge tube - see figure 4.1.  |
| DP  | - | Diffusion pump.   |
| E   | - | Electrodes.   |
| G   | - | Cylinder of spectroscopically pure gas.   |
| GS  | - | Demountable glass-to-metal seal - sealing accomplished by "Viton-A" O-rings.  |
| IG  | - | Ionization gauge.   |
| LT  | - | Leak tap. (A glass tap with a groove scratched on the key).   |
| M   | - | Main pumping line.  |
| OM  | - | Oil manometer.  |
| PG  | - | Pirani gauge.   |
| PT  | - | Phosphorus pentoxide moisture trap.   |
| SV  | - | Safety valve. Isolates system from the backing pump in the event of a power failure, preventing the backing pump oil from being sucked back into the vacuum system. |
| T1  | - | Baffle valve above diffusion pump.  |
| T2  | - | Metal vacuum tap (with O-ring seals).   |
| T3  | - | Glass taps.   |
| T4  | - |   |

**FIG 4.2 THE "CLEAN" VACUUM SYSTEM—SCHEMATIC**



pressure was measured during experiments by an oil manometer, which was also filled with Apiezon "C" oil. This oil was heated gently between experiments to drive off any dissolved gases.

To reduce the virtual leak rate into the system resulting from the outgassing of gaskets and metal parts above the diffusion pump, O-rings of "Viton-A" (a Dupont fluoroelastomer) were used for the gaskets (Ad 60) and the metal parts were made of stainless steel (Ri 61). The O-rings were degassed prior to assembling the system by heating under vacuum for two days.

The line from the oil manometer and the gas bottle enters the main pumping line below the Venema cold trap, so that vapour from the manometer oil and stopcock grease will be prevented by this trap from migrating to the discharge region.

The discharge region, the main pumping line, and the glass cold trap were "baked" at a temperature of over 300°C for about twelve hours prior to filling the glass cold trap. The "bakeout" oven was constructed from "Miscolite" (a bonded asbestos board) and asbestos, the heat required being supplied by heating elements for domestic bar radiators, and "Infraphil" infra-red lamps. The entire vacuum system was mounted on a trolley so that it could be rolled out of the magnet for baking.

A base pressure reading of  $6 \times 10^{-8}$  mm. Hg was obtained after the ionization gauge head had been outgassed. (The X-ray limit

of the gauge is  $5 \times 10^{-8}$  mm. Hg). The rate-of-rise of the pressure in the system was of the order of  $10^{-6}$  mm. Hg/minute before the cold trap was filled; it fell to the order of  $1.5 \times 10^{-7}$  mm. Hg/minute on filling this cold trap.

The spectroscopically pure gases used for these experiments (supplied by the British Oxygen Company) contain approximately 3 - 4 p.p.m. of impurities. The leak rate into the system is such that, for a "charge" of gas at a pressure of 10 mm. Hg in this system, it would take approximately seven hours for the impurity level to rise to 1 part in  $10^5$ . This calculation indicates that the vacuum system is satisfactory to the extent that, after experimenting for several hours, the impurity level will not be much greater than the intrinsic impurity level of the spectroscopically pure gas.

Two factors that have not been taken account of are:

- (1) The loss of efficiency of the cold traps at the high pressures at which the experiments were performed.
- (2) The evolution of gas from the electrodes, (and, to a lesser extent, the walls of the discharge region) under the action of the discharge.

The charge of gas in the system was changed more frequently than the above discussion would indicate was necessary, to compensate for these additional sources of impurities. It is difficult to assess the extent to which the purity will be affected by these factors. However

the satisfactorily reproduceable results obtained from experiments in argon indicate that these factors do not result in an embarrassing increase of the level of the impurities in the gas.

#### 4.1.3 The magnet, power supply, and light-detection equipment

The magnet, power supply, and light-detection equipment are those described in Chapter 2, as modified for the experiments described in Chapter 3 (apart from a minor modification of the "discharge" end of the light pipe).

#### 4.2 THE CLEANLINESS OF THE ELECTRODES

Although the impurity content of the gas has been reduced to a satisfactory level, the electrodes are still not "clean". They were bright when made, but during the assembly of the glassware, and the baking of the vacuum system, became covered with oxide. Attempts to remove this layer of oxide by positive ion bombardment in both hydrogen and argon discharges were not successful. Parts of the electrodes - especially the edges - were partially cleaned, but the oxide and metal sputtered off were deposited elsewhere on the electrodes, and on the glass walls in the vicinity of the electrodes. The end of the "stalk" in which the end of the light pipe is inserted, was particularly heavily coated with a black deposit, considerably reducing the intensity of the light falling on the photomultiplier. This deposit made measurement of the period of rotation rather difficult.

#### 4.3 EXPERIMENTAL RESULTS

The period of rotation,  $T_r$ , was measured as a function of magnetic field only for argon and helium before the breaking of the cold trap. The discharges in both gases misbehaved rather badly; they frequently became stationary, especially at higher pressures, and low magnetic fields. The tendency to "stick" was particularly marked for the argon discharge. This result is not surprising, as the electrodes were covered with a film of oxide.

Satisfactory measurements of  $T_r$  could be made only at fairly high pressures. At pressures below approximately 7 mm. Hg for argon, and even as high as 20 mm. Hg for helium, the discharge was frequently not constricted, but occupied the entire annulus between the electrodes (for discharge currents for the order of milliamperes). This occurs because of the small diameter of the electrodes, especially the centre electrode, and was not unexpected. The problem of the construction of a suitable discharge chamber would have been much greater had larger electrodes been used.

The results obtained for helium were not reproduceable, but those for argon were repeatable to better than  $\pm 20\%$ , except for magnetic fields below 2,160 gauss (see figure 4.3).

Figure 4.3 shows  $T_r$  plotted as a function of magnetic field at pressures of 9.4 and 15.4 mm. Hg; the discharge current was set at 5 mA at 9.4 mm. Hg, and at both 5 mA and 15 mA at 15.4 mm. Hg.

These curves fall more steeply than would be the case if,

$$T_r \propto B^{-1} \quad (4.1)$$

They do not follow a power law.

Because of the dirty electrodes these results should be treated with caution.

It is proposed to rebuild the discharge region of this apparatus so that the electrodes may be cleaned by heating under vacuum to a very high temperature by means of an induction heater. The electrodes will be of larger diameter and depth, and the gap between them will be reduced. With this apparatus, it is hoped to obtain reproduceable results for a discharge that rotates regularly for a wide range of pressures and magnetic fields.

---

FIG 4.3 PERIOD OF ROTATION vs. MAGNETIC FIELD  
IN PURE ARGON

Experiments performed in the all-glass system.

Electrode diameters - 2.54 cm., 5.08 cm.

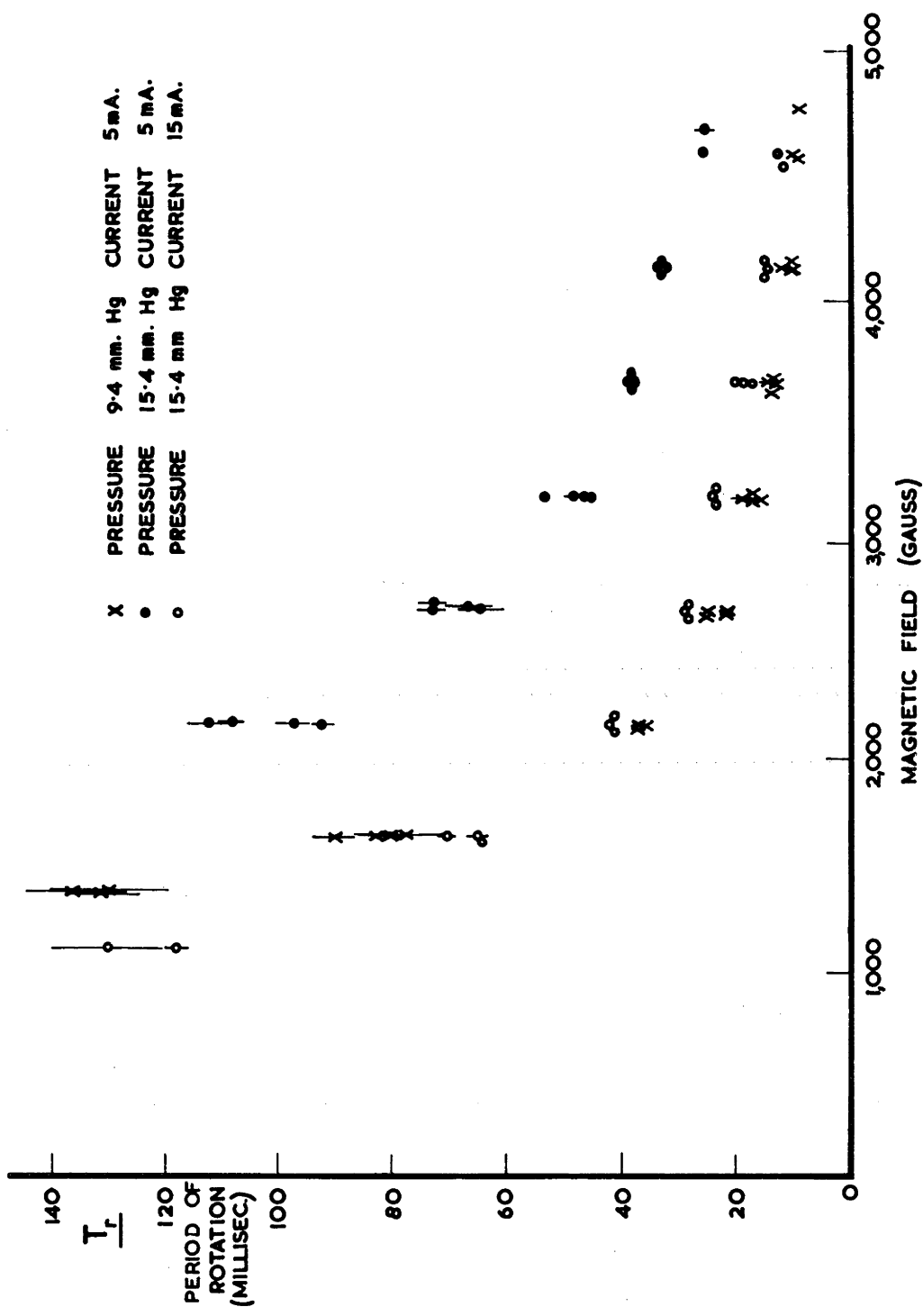


**FIG 4·3  $T_r$  vs. MAGNETIC FIELD IN PURE ARGON**

## Chapter 5

### SOME THEORETICAL ASPECTS OF THE MOTION OF A GLOW DISCHARGE IN A TRANSVERSE MAGNETIC FIELD

#### 5.1 THE MOTION OF CHARGED PARTICLES IN STEADY ELECTRIC AND MAGNETIC FIELDS

##### 5.1.1 Motion in a magnetic field - no collisions (Sp 56)

A particle of charge,  $e$ , moving with a velocity,  $\underline{v}$  constitutes a current,  $ev$ , which can interact with a magnetic field. The magnitude of the velocity of the particle moving in a uniform magnetic field is unchanged by the field, the electromagnetic force acting in a direction perpendicular to the direction of motion of the particle.

The particle is constrained by this force to move in circles around the direction of the field, the radius of these circles (the radius of gyration),

$$a = mv/Be \quad (5.1)$$

where  $B$  = magnetic flux density

$e, m$  = charge, mass of the particle.

The angular frequency of rotation of the particle (the cyclotron frequency)

$$\omega = Be/m \quad (5.2)$$

The radius of gyration is larger, and the cyclotron frequency smaller, for ions than for electrons, and these particles

rotate in opposite directions. The component of the velocity of a particle parallel to the field is not affected by the field.

5.1.2 Motion in crossed electric and magnetic fields -  
no collisions (Sp 56, To 12, Do 37 pp. 66-70)

The circular motion is modified by the presence of the electric field, E, so that the particles move in cycloidal or trochoidal paths; the guiding centre - the instantaneous centre of gyration of the particles - drifts in a direction perpendicular to both the electric and magnetic fields. See figure 5.1. The drift velocity (Sp 56), the velocity of the guiding centre, is given by

$$V_d = (\underline{E} \times \underline{B}) / B^2 \quad (5.3)$$

Physically the cycloidal path results because, as the energy of the particle is increased as it moves in the direction of the electric field, the radius of gyration increases (see figure 5.1). When the particle moves into the second half of the arch of the cycloid the energy decreases, and the orbit of the particle "tightens up" again.

The equations describing the motion of charged particles in crossed fields are:

$$x = \frac{E}{B^2 e} m (\omega t - \sin \omega t) \quad (5.4)$$

$$y = \frac{E}{B^2 e} m (1 - \cos \omega t) \quad (5.5)$$

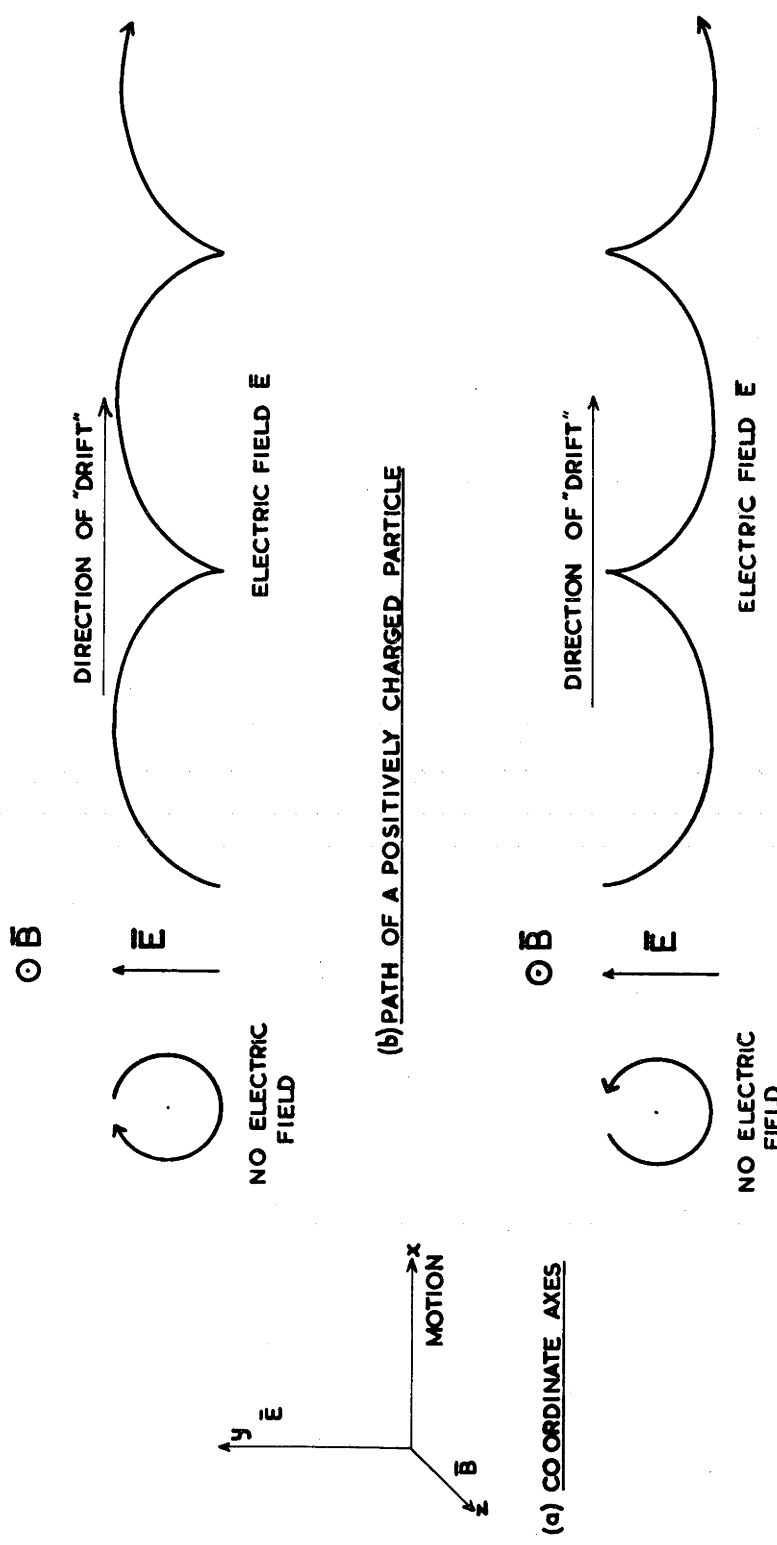


**FIG 6.1 THE MOTION OF CHARGED PARTICLES IN "CROSSED" FIELDS**

where the particles have zero initial velocity - see figure 5.1.

$\omega$  is the cyclotron frequency, defined by equation 5.2.

The path of a particle is not a cycloid, but a trochoid, when the particle has an initial velocity, the roll circle being the same as that of the cycloid if the electric and magnetic fields are unchanged. Equations 5.4 and 5.5 show that the arch of the cycloid is larger for ions than for electrons, and, because  $\omega$  is smaller for ions, the time an ion will take to move around the arch of its cycloidal path, is much greater than the time an electron would take to move around an arch of its cycloidal path.

### 5.1.3 The effect of collisions

Inspection of equations 5.4 and 5.5 reveals that the product  $\omega t$  gives a measure of the fraction of an arch of a cycloid around which a charged particle will move in a time,  $t$ . When  $\omega t = 2\pi$  the particle has moved around an arch of the cycloid. Similarly this product gives the fraction of the circumference of a circle around which a particle will move in a time,  $t$ , the particle moving around a complete circle when  $\omega t = 2\pi$ .

Thus, if  $T$  is the mean time between the collisions of a charged particle with a neutral gas molecule, then  $\omega T$  gives a measure of the degree to which a charged particle is deflected by a magnetic field between collisions, both in a magnetic field, and in crossed electric and magnetic fields. When  $\omega T \ll 1$

the charged particle will have moved around only a small fraction of a circle, or an arch of a cycloid, between collisions, so that the magnetic field will not have changed its direction greatly from that it had immediately after the preceding collision. i.e., the behaviour of a charged particle will not differ greatly from that in zero magnetic field. Under these conditions the properties of a discharge will be similar to those of a discharge in zero magnetic field. However, when  $\omega T \gg 1$  the particle will cover many circles (or cycloidal arches) between collisions, i.e., the motion of the charged particle, and hence the behaviour of the discharge, is influenced strongly by the magnetic field.

Now the ion cyclotron frequency,  $\omega_i$ , is considerably less than the electron cyclotron frequency,  $\omega_e$ , and the mean free times of the ions and electrons ( $T_i$  and  $T_e$ , respectively) do not differ greatly.

Therefore, when

$$\omega_e T_e \sim 1 \quad (5.6)$$

$$\text{then } \omega_i T_i \ll 1 \quad (5.7)$$

i.e., the magnetic field influences the motion of electrons more readily than that of ions.

In crossed fields, where

$$\omega_i T_i \ll 1 \quad (5.8)$$

$$\text{but } \omega_e T_e \gg 1 \quad (5.9)$$

the ions will move substantially along the electric field, as they are little affected by the magnetic field between collisions, whereas the electrons will move across the field (i.e., in the E  $\times$  B direction) - see figure 5.2.

#### 5.1.4 Drift velocity

Charged particles moving in an electric field are accelerated by that field until they reach an equilibrium condition such that, over a large number of collisions, they gain as much energy between collisions, as they lose per collision. This terminal velocity is called the drift velocity of the particles. The drift velocity per unit electric field is called the mobility.

For electrons moving in a magnetic field through a gas where the mean time between collisions with neutral molecules is independent of electron energy

$$v_{dm} = v_d (1 + \omega_e^2 T_e^2)^{-1} \quad (5.10)$$

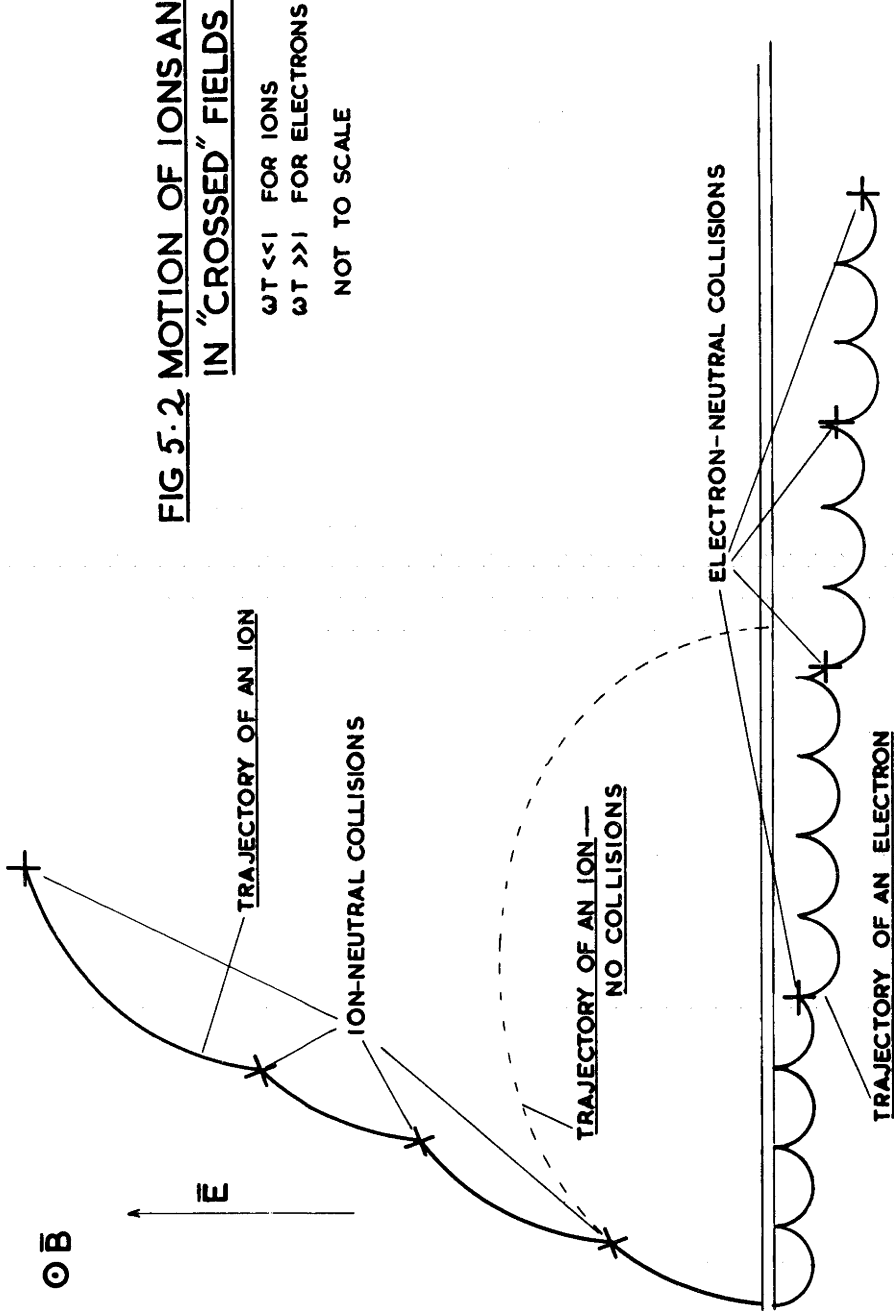
where  $v_{dm}$  = drift velocity in the magnetic field

$v_d$  = drift velocity in zero magnetic field.

This relation has been derived by TOWNSEND (To 12), who neglected the electrons' velocity distribution, and more rigorously by HUXLEY (Hu 57), and BLEVIN and HAYDON (Bl 58). The expression derived by Townsend applies equally for ions.

Because of the greater mass of an ion, the drift velocity of ions is much less than that of electrons moving at the same

FIG 5.2 MOTION OF IONS AND ELECTRONS  
IN "CROSSED" FIELDS (SCHEMATIC)



gas pressure in the same electric field (En 55). The current in the positive column of a glow discharge is carried primarily by electrons, the ions making only a minor contribution to the total current. However in the presence of a magnetic field, such that

$$\omega_e T_e \gg 1 \quad (5.9)$$

$$\text{and} \quad \omega_i T_i \ll 1 \quad (5.8)$$

equation 5.10 shows that the electrons' mobility is greatly reduced. The individual electrons do not move in the direction of the electric field, but across the field, as described in section 5.1.3. Under these conditions, the ions, moving along the field, can carry a large fraction of the discharge current, in spite of their low drift velocity in zero magnetic field.

## 5.2 THE VELOCITY OF AN UNCONSTRAINED POSITIVE COLUMN

The motion of a positive column, unconstrained by the electrode regions of the discharge, will be discussed in this section, even though the positive column has little influence on the velocity of the discharge. It is necessary to have a knowledge of the velocity of an unconstrained positive column in order to discuss the augmentation of the velocity of the cathode region by the remainder of the discharge. However, more important, the results of this section may be applied to the

other plasma regions of the discharge - the F.D.S., and, especially the negative glow.

### 5.2.1 Theory of the motion of a positive column

The external force acting on a volume element,  $dv$ , of a discharge

$$\underline{dF} = (\underline{j} \times \underline{B}) dv \quad (1.2)$$

where       $\underline{j}$  = current density

$\underline{B}$  = magnetic flux density.

The mechanism by which the momentum supplied by this force to the moving discharge is transferred to the ionized gas, is as follows: The  $(\underline{j} \times \underline{B})dv$  force acts on the electrons, the current being primarily an electron current. The electrons, accelerated by this force, would tend to move away from the positive ions. However the electrostatic field set up as the electrons move away from the ions prevents the separation of these two species.

The momentum supplied to the electrons is transferred to the positive ions by this electrostatic coupling. As the electrons and ions move around the gap between the electrodes with the same velocity, most of the momentum of the discharge will be carried by the heavier ions.

When the discharge is moving at a constant velocity, the  $(\underline{j} \times \underline{B})dv$  force is equal to the rate at which momentum is transferred from the discharge to the neutral molecules, i.e., the

"frictional" force on the discharge

$$\text{i.e., } \int_{A,1.0} (j \times B) dv = \frac{1}{2} n_i \bar{U} M v_i + n_e \bar{U} m v_e \quad (5.11)$$

where  $\int_{A,1.0}$  signifies integration over the cross-section

of the discharge, along unit length of the discharge

$n_i = n_e$  = number of charged particles per unit  
length of the discharge.

$M, m$  = mass of an ion, and an electron, respectively.

$\bar{U}$  = nett velocity of the discharge.

$v_i$  = ion-neutral collision frequency

$v_e$  = electron-neutral collision frequency.

It is assumed that (averaging over a large number of collisions), the electrons lose all their nett momentum (i.e., the momentum  $m\bar{U}$ ) in one collision, the massive ions only half their nett momentum in a collision. The factor " $\frac{1}{2}$ " in equation 5.11 accounts for this persistence of velocity.

The second term in equation 5.11 may be neglected, as  
 $m v_e \ll M v_i$ .

From 5.11

$$i B = \frac{1}{2} n_i \bar{U} M v_i \quad (5.12)$$

$$\text{Now } v_i = v_i N \sigma \quad (5.13)$$

where  $v_i$  = thermal velocity of the ions

$\sigma$  = ion-neutral collision cross section

N = density of neutral molecules.

(See Brown (Br 59) - Chapter 1).

Therefore, from 5.12,

$$\bar{U} = \frac{2iB}{n_i MN \langle \sigma v_i \rangle} \quad (5.14)$$

$\langle \rangle$  indicates that  $\sigma v_i$  is averaged over the ions' velocity distribution.

Now, if it is assumed that

$$T_{ion} = T_g \text{ and } M = M_g$$

where

$T_{ion}$  = ion temperature

$T_g$  = gas temperature

$M_g$  = mass of a neutral molecule,

then, if the neutral particle densities and the ionic thermal velocity in equation 5.14 are expressed in terms of gas pressure and temperature

$$\bar{U} = \frac{2iB}{n_i \rho \sigma} \sqrt{\frac{k T_g}{3 M_g}} \quad (5.15)$$

All the parameters on the R.H.S. of equation 5.15 may be estimated, with the exception of  $n_i$ .

Now  $i = n_e v_{dm}$  (5.16)

the contribution to the current of the positive ions being neglected,

where  $n_e$  = number of electrons per unit length  
of the discharge

$v_{dm}$  = electron drift velocity in a magnetic  
field.

Therefore,  $n_i = n_e = i / e v_d$  (5.17)

Hence  $\bar{U} = \frac{2 Be v_{dm}}{p\sigma} \sqrt{\frac{kT_g}{3M_g}}$  (5.18)

### 5.2.2 Comparison of this theory with experiment

Equation 5.18 may be used to obtain an estimate of the velocity at which the positive column of a nitrogen discharge would move in a magnetic field, if not influenced by the electrode regions. The electric field,  $E$ , has been measured for a rotating nitrogen discharge (see section 3.7, for the values of the electric field, and a discussion of an error in the measured field due to the slope of the discharge). The drift velocity in zero magnetic field, a function of  $E/p$  was obtained from the experimental curves of TOWNSEND (To 21), ( $p$  = gas pressure), more recent values being available for the high values of  $E/p$  encountered in these experiments.

The drift velocity in a magnetic field was calculated from these values by means of equation 5.10, the electrons being assumed to have an energy of 4 eV. This correction is <sup>of</sup> doubtful accuracy for nitrogen. The exact derivations of HUXLEY (Hu 57), and BLEVIN and HAYDON (Bl 58) assume that  $T_e$  is independent of electron energy

$$\text{i.e., } \sigma(v) v = \text{Constant} \quad (5.19)$$

where  $\sigma(v)$  = electron-neutral collision cross section,

$v$  = velocity of an electron,

which is far from the case for nitrogen. (See BROWN (Br 59), Chapter 1).

The ion-neutral collision cross section has not been measured for nitrogen. The neutral-neutral collision cross section was used for these calculations, this being a fair approximation to the ion-neutral collision cross section (Co 41). This cross-section was calculated from the mean-free-path at 0°C given in von ENGEL'S book (En 55), Sutherland's formula (Co 41) being used to correct for the decrease in cross section at the higher gas temperature assumed for the calculations (300°K).

It was assumed in the derivation of equation 5.18 that the nitrogen ion present was  $N_2^+$ . There is evidence in the ionic

mobility measurements of VARNEY (Va 53) of the existence of the  $N_4^+$  ion, for  $E/p$  of the order of the values encountered in these experiments. If the ion present was  $N_4^+$ , the velocity would be 70% of that calculated from equation 5.18.

Values of  $T_r$  for a magnetic field of 2,160 gauss, obtained using equation 5.18 are plotted in figure 5.3. It will be noted that the velocity of an unconstrained positive column is greater than the observed velocity of the discharge. This is a further indication of the correctness of the assumption, made in section 3.4, that the unconstrained positive column would move at a velocity greater than that of the cathode region of the discharge.

---

The electric field in the positive column, above the transition, is given approximately, by the empirical relation

$$E = 0.09B + 12p \quad (5.20)$$

where

$E$  = electric field in volts/cm

$B$  = magnetic field in gauss

$p$  = pressure in mm. Hg.

This expression is derived from the measured values of the electric field. See section 3.7, and particularly figure 3.23 in this section.

There is no doubt about the linear dependence of  $E$  on  $p$ ; however the assumed linear dependence of  $E$  on  $B$  is extremely

FIG 5.3 COMPARISON OF EXPERIMENTAL AND THEORETICAL  
VALUES OF  $T_r$

Magnetic field - 2,160 gauss

Gas - Nitrogen

A Experimental curve. Electrode diameters - 10.2, 14.0 cm.  
Centre electrode negative

Discharge current - 15 mA.

B Experimental curve. Electrode diameters - 10.2, 11.4 cm.  
Centre electrode negative

Discharge current - 15 mA.

C Theoretical curve: positive column control

Mean diameter of gap - 10.8 cm.

D Theoretical curve: negative glow control

$T_r$  is ten times the value of  $T_r$  calculated for curve C.

E Theoretical curve: cathode fall region control

Diameter of cathode - 10.2 cm.

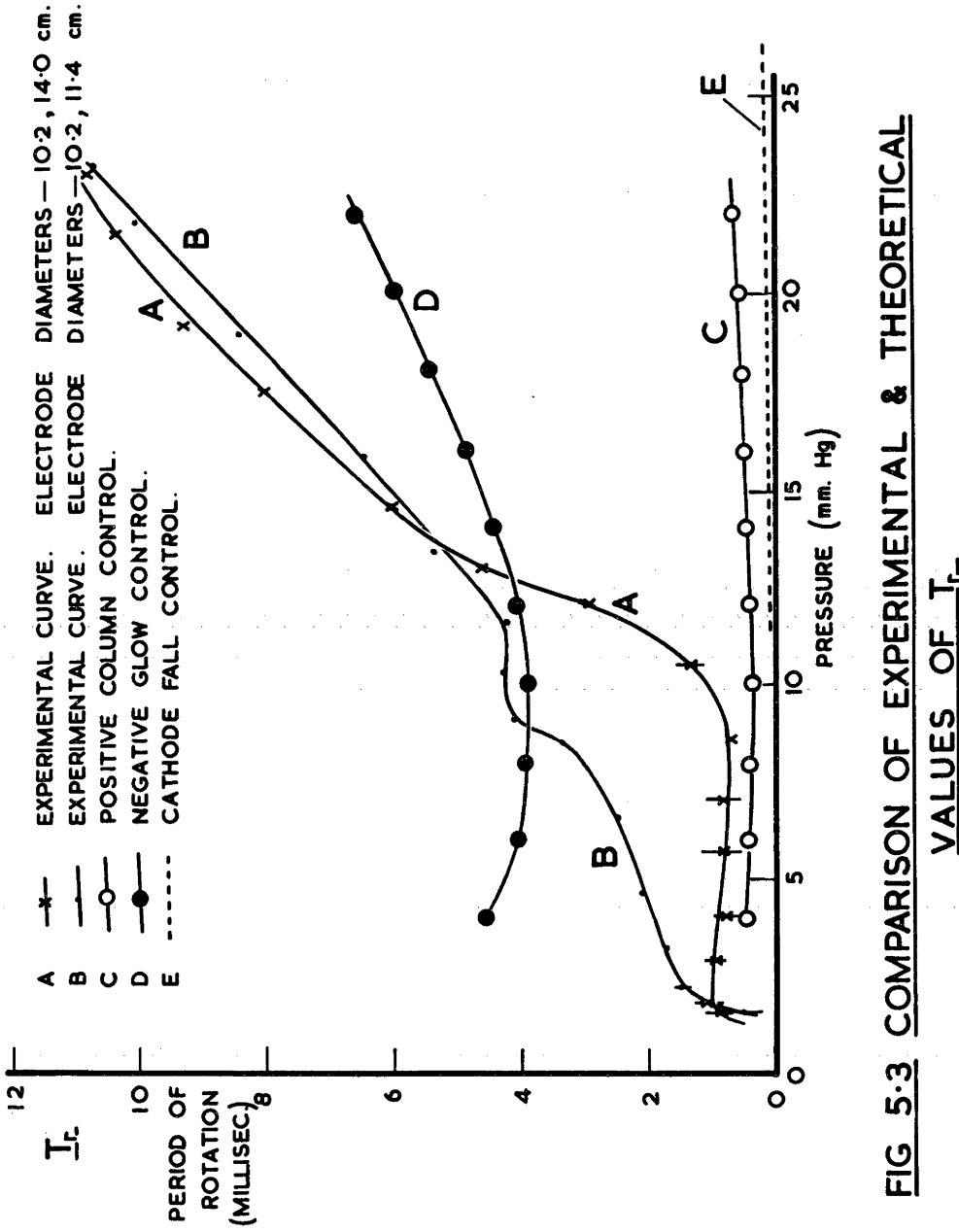


**FIG. 5.3 COMPARISON OF EXPERIMENTAL & THEORETICAL VALUES OF  $T_r$**

uncertain. The electric field was only measured for magnetic fields of 1,100 gauss, and 2,160 gauss (and zero magnetic field).

Now from TOWNSEND'S curves of drift velocity as a function of  $E/p$  (To 21)

$$v_d \propto E/p \text{ approximately} \quad (5.21)$$

Thus, the drift velocity in a magnetic field

$$v_{dm} \propto (E/p) \left\{ 1 + C(B/p)^2 \right\}^{-1} \quad (5.22)$$

where  $\omega_e T_e$  is expressed in terms of  $p$  and  $B$ .  $C$  is a constant.

Hence, from 5.20, and 5.22

$$v_{dm} \propto \frac{1}{p} (0.09 B + 12 p) \left/ \left\{ 1 + C \left( \frac{B}{p} \right)^2 \right\} \right. \quad (5.23)$$

and, substituting for  $v_{dm}$  in 5.18

$$T_r = k \frac{(p/B)^2 + C}{0.09 + 12 p/B} \quad (5.24)$$

where  $k$  is a constant.

This expression does not give the experimentally observed dependence of  $T_r$  on  $p$  and  $B$ . However  $T_r$  increases as  $p$  increases, and as  $B$  decreases, as observed experimentally.  $T_r$  is given as a function of  $p/B$ . The experimentally observed values of  $T_r$  are not a function of  $p/B$ . (See figures 3.7 and 3.18).

---

The discrepancy between this theory, and the experimental results indicates that there is something seriously wrong

with the above theory. The approximations used in deriving equation 5.18 would not give an error of this magnitude in the calculated velocity.

Two possible explanations of this discrepancy are:

(i) In equation 5.15, the basic equation from which equation 5.18 was derived, the only parameter that is not well known is  $n_i$ , the number of ions per unit length of the discharge. The method of calculating  $n_i$  may be incorrect, possibly due to the use of an over-simplified model for the positive column of the discharge. No account has been taken of the transverse electric field, or the shape of the discharge, and the positive column has been assumed uniform along its length.

(ii) The ions and electrons move through the discharge, to re-combine at the leading edge of the discharge. These particles will move at a velocity,  $\bar{u}$ , given by equation 5.18. This drift of charged particles through the discharge would mean that the rate of loss of charged particles from the discharge column is greater for a T. M. F., than in the absence of a T. M. F. The rate of production of charged particles, and hence the electric field in the positive column, must be higher in a magnetic field, in order to replace this loss. Thus the high electric field observed for a discharge in a T. M. F. (see section 3.7), is not inconsistent with this idea.

### 5.3 THE NEGATIVE GLOW AS THE VELOCITY-CONTROLLING REGION OF THE DISCHARGE

Equation 5.15, the basic equation from which the velocity of the positive column was calculated, can be applied to any plasma region of the discharge. i.e., it can be used to calculate the velocity at which an unconstrained negative glow would move. However this calculation necessitates a knowledge of the positive ion density in this region. The charge density in the positive column was calculated from a knowledge of the electric field in the column, and the electron mobility in a magnetic field. This method is not applicable to the negative glow, where the charge density is determined by the rate of ionization, and diffusion.

It is well known that, in zero magnetic field, the electron density (and hence the positive ion density) in the negative glow is an order of magnitude, or more, greater than that in the positive column (Fr 56, Ud 52). If it is assumed in this case that the positive ion density is an order of magnitude greater than in the positive column, then equation 5.15 shows that the velocity will be correspondingly less, as the velocity is inversely proportional to the positive ion density. The velocity at which an unconstrained negative glow would move, assuming the positive ion density is ten times that in the positive column (i.e., a value of  $T_r$  ten times that calculated from equation 5.18), is also plotted in figure 5.3.

This curve shows that negative glow control offers a reasonable explanation of the velocity of the discharge observed at pressures where the cathode region has been shown to control the velocity of the discharge - i.e., above the transition. (The theoretical curves are compared with experimental curves in figure 5.3).

#### 5.4 CONTROL OF THE VELOCITY OF THE DISCHARGE BY THE CATHODE FALL REGION

Although negative glow control offers a credible explanation of the observed velocity of the discharge, a study of the motion of the particles in the cathode fall region of the discharge is required to show that this region would not also move at approximately the observed velocity. What follows is a first crude attempt to explain the observed velocity of the discharge in terms of the motion of ions and electrons in the cathode fall region.

For a first attempt at estimating the velocity of the cathode fall region, it will be assumed that a uniform electric field  $V_n/d_n$  extends a distance  $d_n$  from the cathode, where

$V_n$  = normal cathode fall voltage

$d_n$  = normal cathode fall thickness.

It is assumed that an electron moves from the cathode to a point at a distance  $ad_n$  from the cathode ( $a \leq 1$ ), where ionization occurs, and the ion produced moves back to the cathode, where it ejects another electron from the cathode. The distance from the

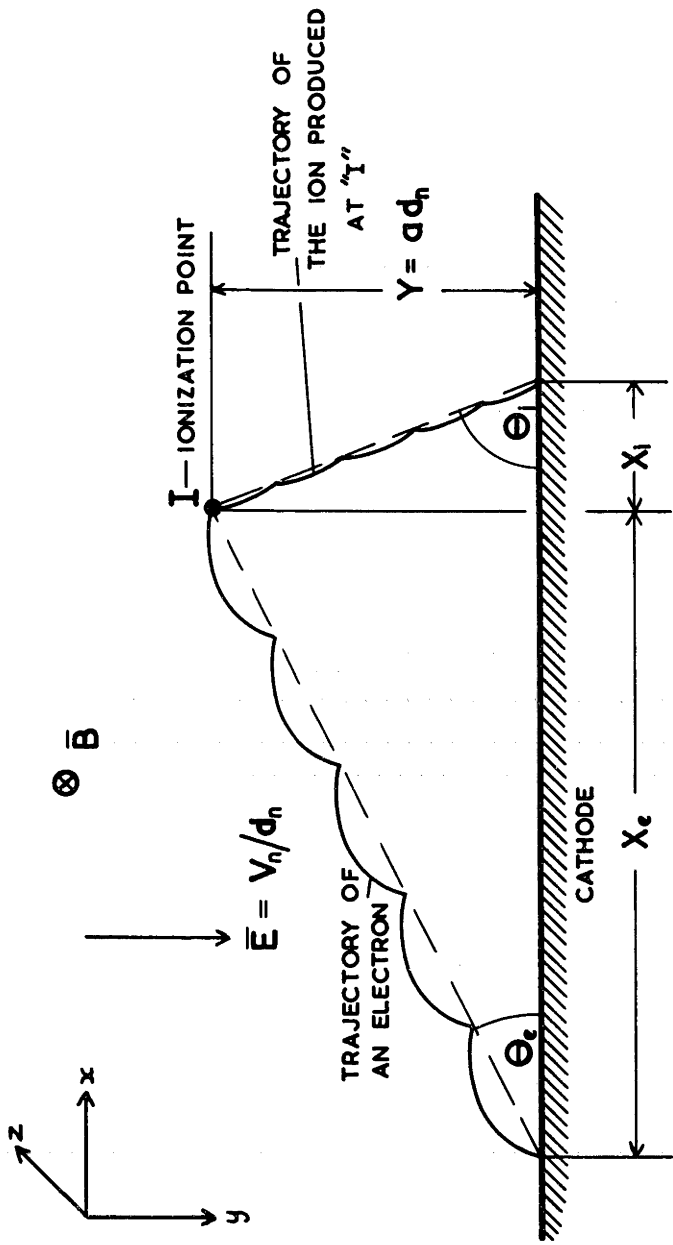


FIG 5-4 THE MOTION OF IONS & ELECTRONS IN  
THE CATHODE FALL REGION

point of origin of the first electron, to the point where the second is produced, divided by the time the electron and the ion take to move between these points, is assumed to give a measure of the velocity of the discharge. (See figure 5.4).

It is assumed that the electrons lose all their energy in a collision. This assumption is not as drastic as it would first appear. The direction of motion of the electrons is randomized in a collision, so that this particular path (a cycloidal path, rather than the range of trochoidal paths that would occur for an elastic collision) will give a measure of the mean path of the particles between collisions.

Now, from equations 5.4 and 5.5, in a time  $t$ , an electron will move distances in the  $x$  and  $y$  directions, given by

$$x = \frac{V_n m_e}{d_n B_e^2} (\omega_e t - \sin \omega_e t) \quad (5.25)$$

$$y = \frac{V_n m_e}{d_n B_e^2} (1 - \cos \omega_e t) \quad (5.26)$$

Now, if the times between collisions are distributed according to the law

$$\frac{dn}{n} = - \frac{1}{T_e} \exp\left(-\frac{t}{T_e}\right) dt \quad (5.27)$$

where  $\frac{dn}{n}$  = fraction of the collisions that occur in the time interval between  $t$ , and  $t + dt$ .

$T_e$  = mean time between collisions, then the mean

distance a group of electrons will move in the x direction between collisions

$$\bar{x} = \int_0^{\infty} \frac{V_n m_e}{d_n B^2 e} (\omega_e t - \sin \omega_e t) \exp\left(-\frac{t}{T_e}\right) dt \quad (5.28)$$

$$= \frac{V_n m_e}{d_n B^2 e} \frac{(\omega_e T_e)^3}{1 + (\omega_e T_e)^2} \quad (5.29)$$

Similarly, the mean distance a group of electrons will move in the y direction between collisions

$$\bar{y} = \frac{V_n m_e}{d_n B^2 e} \frac{(\omega_e T_e)^2}{1 + (\omega_e T_e)^2} \quad (5.30)$$

Similar equations hold for the motion of ions in crossed fields.

The assumed distribution of the free times (equation 5.22) is equivalent to that used by TOWNSEND in his study of the diffusion of charged particles in a magnetic field (To 12). Townsend assumed that the free paths of the electrons had an exponential distribution, and that the charged particles had a constant velocity. This distribution function is not strictly applicable in the present case, where the motion of particles accelerated to high energies in an electric field is under consideration, but will be adopted as a reasonable assumption in view of the crudity of some of the other assumptions.

Number of collisions an electron will make in moving from the cathode to the ionization point, I (see figure 5.4),

$$n_c = ad_n \sqrt{\frac{y}{y}} \quad (5.31)$$

$$= \frac{a d_n^2 B^2 e}{V_n m_e (\omega_e T_e)^2} \left\{ 1 + (\omega_e T_e)^2 \right\} \quad (5.32)$$

Therefore, time required for an electron to move to the ionization point

$$T_e' = \frac{a d_n^2 B}{V_n \omega_e T_e} \left\{ 1 + (\omega_e T_e)^2 \right\} \quad (5.33)$$

Similarly, the time for an ion to move from the ionization point to the cathode,

$$T_i' = \frac{a d_n^2 B}{V_n \omega_i T_i} \left\{ 1 + (\omega_i T_i)^2 \right\} \quad (5.34)$$

The distance between the point of origin of the first electron, and the point where the ion produced strikes the cathode,

$$X_e + X_i = Y \left\{ (\tan \theta_e)^{-1} + (\tan \theta_i)^{-1} \right\} \quad (5.35)$$

where  $X_e, X_i, Y (= a d_n)$ ,  $\theta_e$  and  $\theta_i$  are defined in figure 5.4.

Now from equations 5.24 and 5.30, and the equivalent equations for ions

$$\tan \theta_e = (\omega_e T_e)^{-1} \quad (5.36)$$

$$\tan \theta_i = (\omega_i T_i)^{-1} \quad (5.37)$$

Therefore the velocity of the discharge,

$$\bar{u} = \frac{X_e + X_i}{T_e + T_i} \quad (5.38)$$

$$= \frac{\frac{a d_n}{V_n} (\omega_e T_e + \omega_i T_i)}{\frac{a d_n^2 B}{V_n} \left\{ \frac{1 + (\omega_e T_e)^2}{\omega_e T_e} + \frac{1 + (\omega_i T_i)^2}{\omega_i T_i} \right\}} \quad (5.39)$$

Now,  $\omega_i T_i \ll \omega_e T_e$ ,

and, at pressures of interest

$$\omega_i T_e \ll 1$$

Therefore, simplifying equation 5.39,

$$\bar{u} = \frac{V_n}{d_n B} \omega_i T_i \left\{ \frac{\omega_i T_i}{(\omega_e T_e)^2} \left[ 1 + (\omega_e T_e)^2 \right] + \frac{1}{\omega_e T_e} \right\}^{-1} \quad (5.40)$$

Now, provided  $\omega_e T_e \lesssim 3$ , which is the case for the present experiments, except at the lowest pressures,

$$\bar{u} = \frac{V_n}{d_n B} \omega_e T_e \omega_i T_i \quad (5.41)$$

Now, if it is assumed that the thickness of the cathode fall region is the same as the thickness for zero magnetic field (a fair enough assumption under the present experimental conditions -

see discussion in section 3.4.1), so that  $d_n$  is inversely proportional to pressure, then

$$\bar{u} = KB/p \quad (5.42)$$

as  $\omega_e, \omega_i \propto B$

and  $T_e, T_i \propto p^{-1}$

where K is a constant.

---

A curve showing the value of  $T_r$  calculated from equation 5.41 is shown in figure 5.3. The ions and electrons were assumed to have an energy of 10 eV for the calculation of  $T_e$  and  $T_i$ .  $T_i$  was obtained by applying Sutherland's mean-free path correction (Co 41) to the neutral-neutral mean-free-path given by von ENGEL (En 55), although it is doubtful if this formula will give the correct mean-free-path for ions of this high energy.

This curve is well below the experimental curves, and the curve obtained from the theory of positive column control. In spite of the crudity of the assumptions used in deriving equation 5.36, this curve indicates that this single particle model does not satisfactorily describe the motion of the discharge.

A more sophisticated model that takes into account the linear decreasing electric field and the nature of the multiplication process in the cathode fall region (the Townsend avalanche), the maintenance condition, and probably the diffusion of charged

particles from the cathode fall region, must be studied before a satisfactory theory of the motion of the cathode fall region of a discharge can be developed.

---

## APPENDICES

Appendix 1

THE SHAPE OF THE DISCHARGE - FURTHER  
CONTOUR DIAGRAMS

This appendix contains further examples of the contour diagrams obtained while experimenting with the "Racetrack" chamber. See section 2.4 for further details of the experimental apparatus, and the method by which these diagrams were obtained.

FIG A 1.1 THE SHAPE OF A DISCHARGE IN AIR

|                   |   |              |
|-------------------|---|--------------|
| Gas               | - | dry air      |
| Gas pressure      | - | 18.8 mm. Hg. |
| Magnetic field    | - | 1,100 gauss  |
| Discharge current | - | 15 mA.       |

Light intensity contours: arbitrary units - the output of the photomultiplier in millivolts. Note that for this diagram the height of the contours varies approximately logarithmically, rather than linearly as it does for the other contour diagrams.

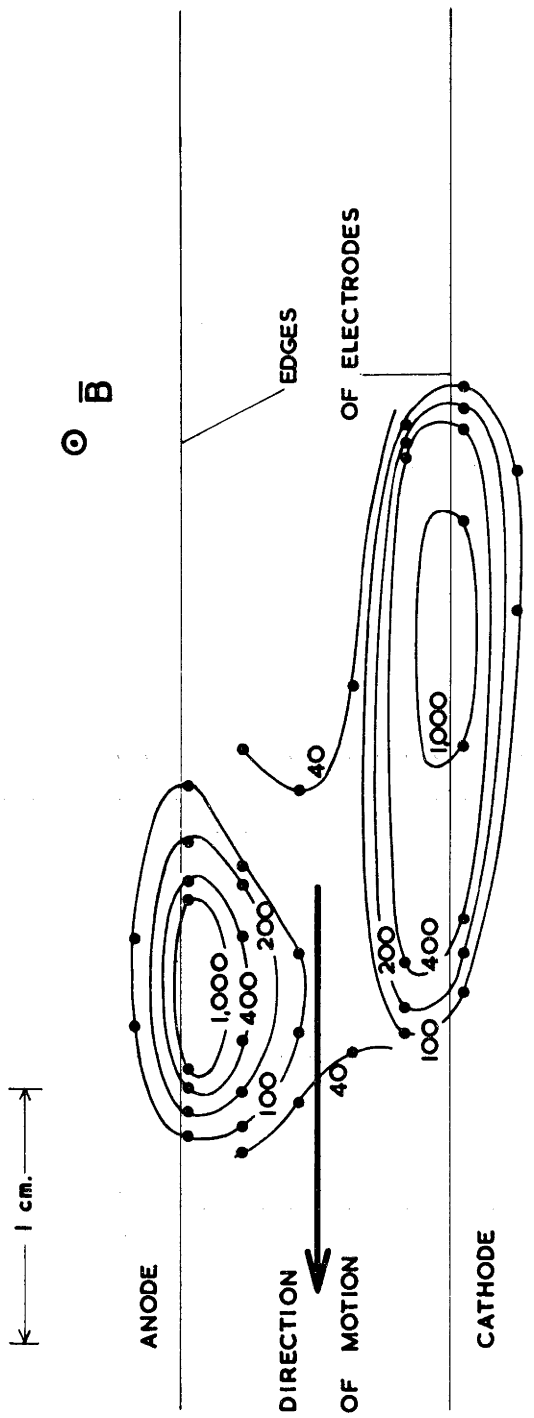


FIG A.I THE SHAPE OF A DISCHARGE IN AIR

FIG A 1.2 THE SHAPE OF A DISCHARGE AT MODERATE PRESSURE IN THE ARGON/AIR MIXTURE

Gas - argon with 1.5% air.  
Gas pressure - 10.0 mm. Hg.  
Magnetic field - 1,100 gauss.  
Discharge current - 5 mA.

Light intensity contours: arbitrary units - the output of the photomultiplier in millivolts.

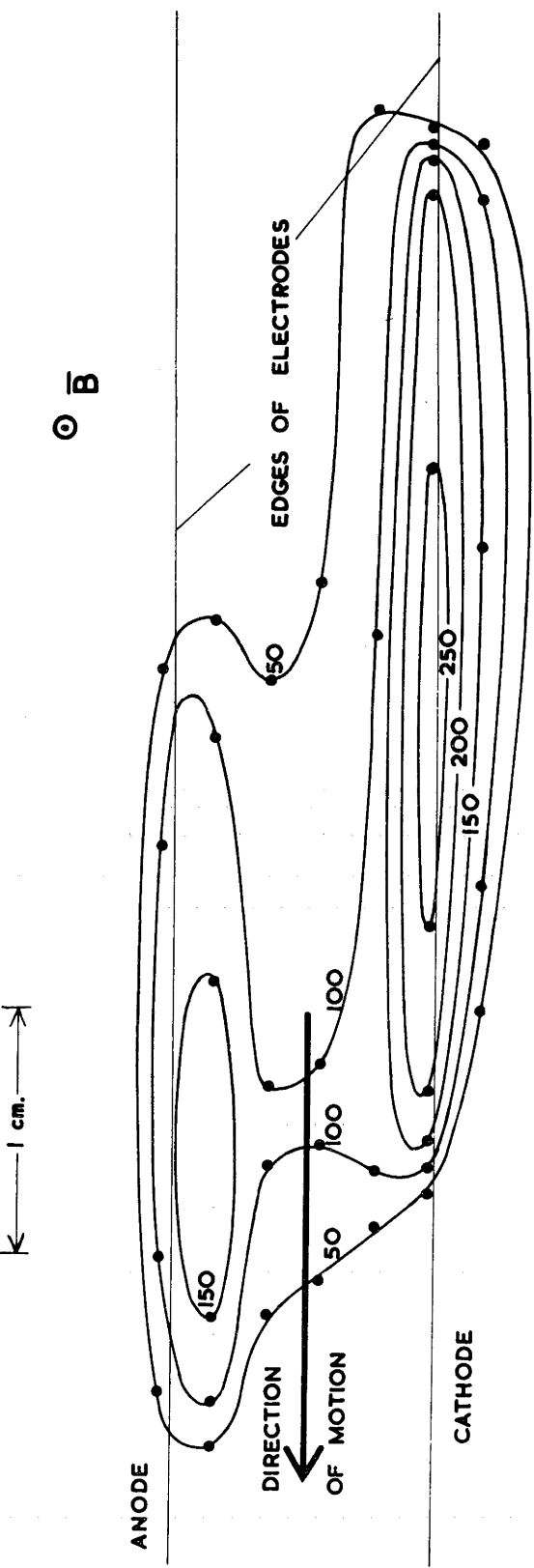


FIG A1.2 ARGON/AIR DISCHARGE AT A MODERATE PRESSURE

FIG A 1.3 THE SHAPE OF A DISCHARGE AT HIGH PRESSURE  
IN THE ARGON/AIR MIXTURE

Gas - argon with 1.6% air  
Gas pressure - 17.9 mm. Hg.  
Magnetic field - 2,160 gauss  
Discharge current - 5 mA.

Light intensity contours: arbitrary units - the output of the photomultiplier in millivolts.

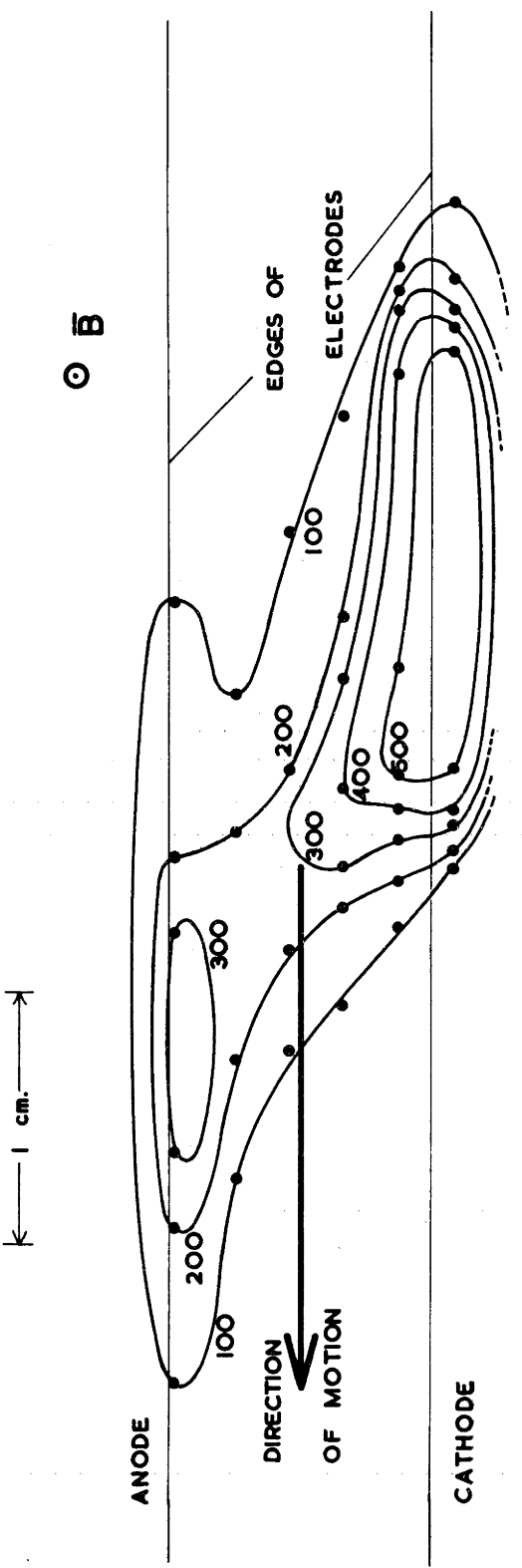


FIG A 1.3 ARGON / AIR DISCHARGE AT HIGH PRESSURE

Appendix 2

LIQUID AIR LEVEL CONTROLLER

The level sensor of this device is similar to that described by PURSER and RICHARDS (Pu 59) of this laboratory. It consists of a brass bulb, which is located in the cold trap, connected to a metal bellows by a length of nickel capillary tubing. The sensor is filled with oxygen to a pressure of two atmospheres. When the liquid air is in contact with the bulb, the oxygen is liquified. However, when the level of the liquid air falls below the bulb, the oxygen evaporates, and the increasing pressure expands the bellows, which closes a microswitch. The microswitch activates a solenoid valve, allowing dried compressed air to enter the liquid air storage flask, and pump liquid air into the cold trap. The solenoid valve is a Skinner quick-exhaust 3-way valve, which allows a rapid release of the excess pressure in the storage flask on de-activation of this valve.

The microswitch, mounted rigidly above the bellows, is of a directly actuated type, rather than the type actuated by a springy lever. The latter type showed a "hysteresis" in the switching position, resulting in unreliable operation of the controller.

When the controller was first put into operation, the rate of consumption of liquid air was particularly high, and the liquid air line regularly iced up. These troubles resulted from the high frequency of operation of the controller, due to the short time during which liquid air flowed into the cold trap. (Much liquid air is lost in cooling the liquid air line during the first second or so of the transfer process). The sensor would switch off the compressed air almost immediately the liquid air came into contact with the bulb. Indeed it was suspected that the sensor was triggered by splashes of liquid air, rather than the surface of the liquid air in the cold trap rising to come into contact with the bulb. An RC timing circuit was arranged so that the liquid air would flow for a set period of time whenever the microswitch was actuated, even though the microswitch switched off during this period. A suitable circuit for this purpose is shown in figure A 2.1. The frequency of operation of the controller was reduced, and because of this, air economy was improved, and trouble due to icing reduced. The "on" time was generally set at 11 seconds. (The "on" time could have been controlled by a more simple method than the RC circuit used for the present controller. In later models, it is proposed to use a Hotwire Vacuum Switch (made by Sunvic Controls), with reduced heater current, as the timing element).

FIG A 2.1 THE TIMING CIRCUIT OF THE LIQUID AIR LEVEL  
CONTROLLER

Components

- CONT - 240 Volt A.C. contactor
- RELAY - Sigma 22RJCC 1,000 G-SIL 22 Volt relay.
- 
- C1 - Timing capacitors - 3 x 12 microfarad electrolytic condensers in parallel.
- C2 - Filter capacitors.
- D - Silicon rectifiers
- F - Fuse
- MC - Manual control switch
- N1, N2 - Neon indicator lamps. N1 - "Power on"  
N2 - "Solenoid valve on".
- R1 - 2.5 kohm potentiometer.
- R2 - 1 kohm
- S - Mains switch
- T - Power transformer.

Relay contacts

- N.C. - Normally closed.
- N.O. - Normally open.

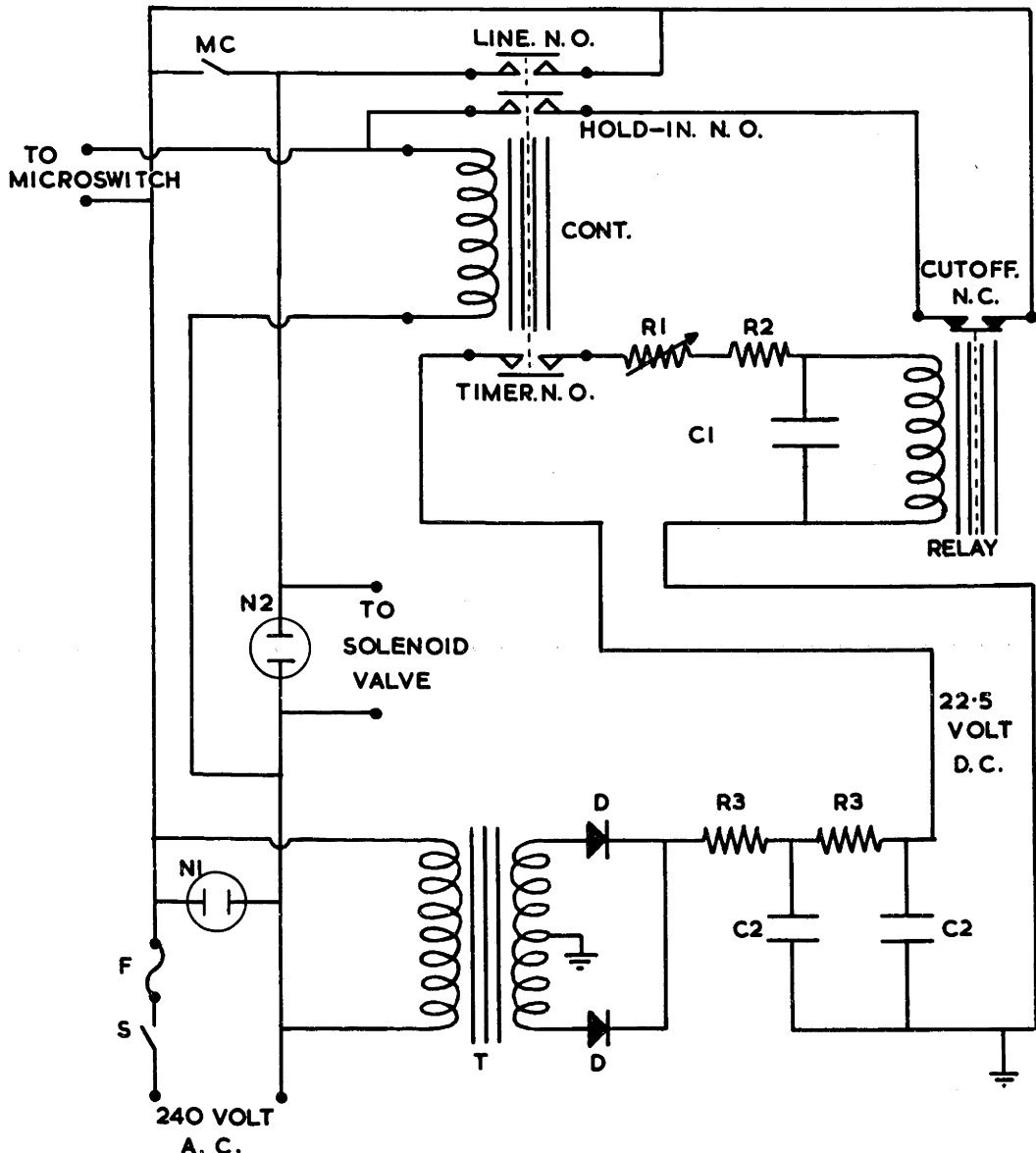


## FIG A2-1 LIQUID AIR LEVEL CONTROLLER

This device has the advantage over a commonly used economy device in which the controller is only sensitive for short periods of time, in that it is continuously sensitive. i.e., this device will control the level at all times, which is particularly important for experiments of the type described in this thesis. The consumption of liquid air can be very high during the experiments, because of the high pressure of the gas in the cold trap.

### Appendix 3

#### THE RAIL DISCHARGE EXPERIMENT

In order to further investigate the structure of the discharge, particularly the structure of the electrode regions of the discharge, a study was made of a glow discharge driven along straight parallel rails by a transverse magnetic field.

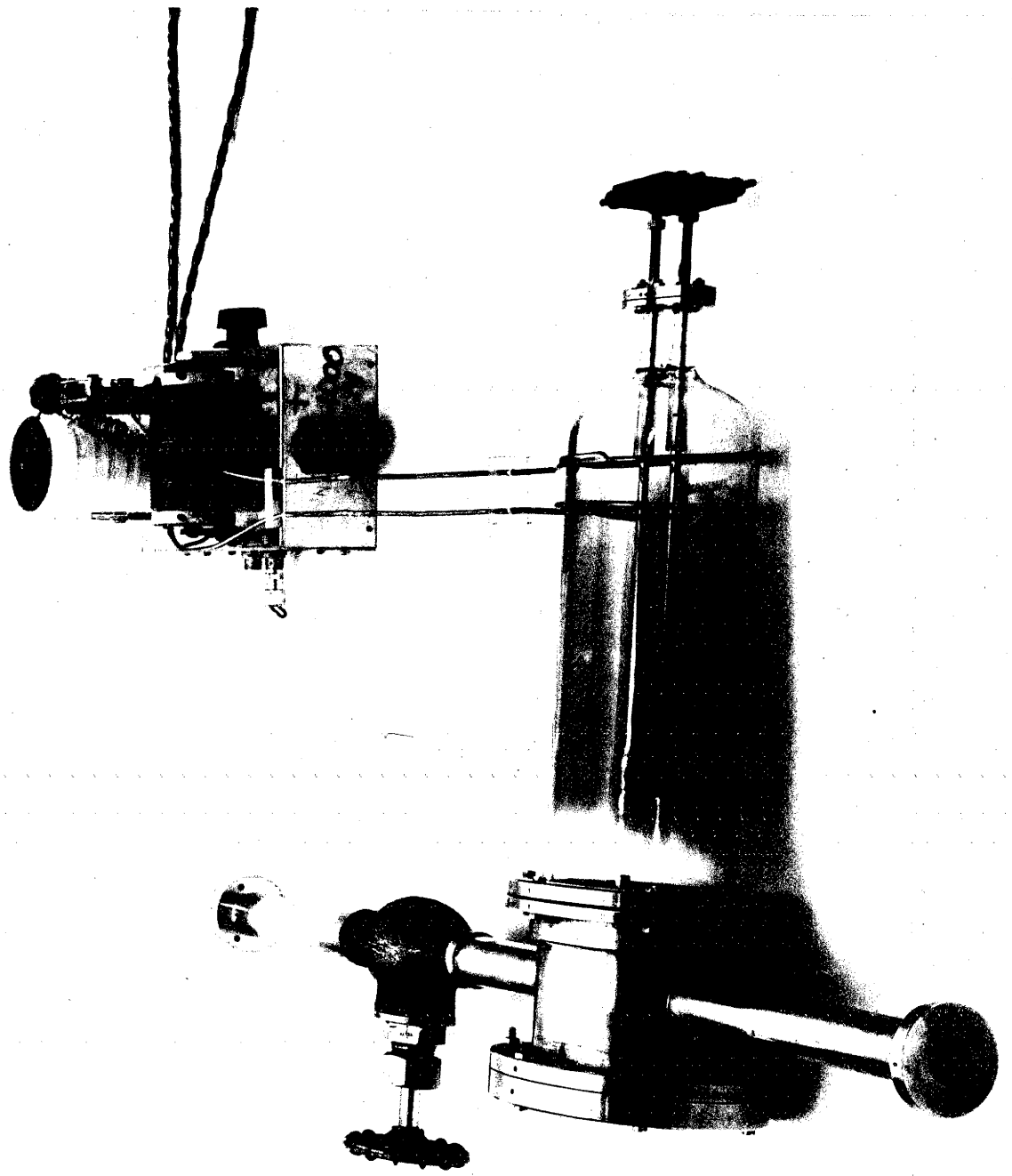
The discharge tube used for these experiments is shown in figure A 3.1. The discharge current flows between  $\frac{1}{4}$ " diameter copper rods whose centres are approximately 2.4 cm. apart. The electrodes are supported by flanges that are clamped to short glass tubes at one end of the main glass tube. (See figure A 3.1). The flanges are held in place on the outside ends of the tubes by O-rings, which also provide a vacuum seal. A flat glass viewing port at the other end of the discharge tube, enables the discharge to be inspected as it is driven along the rails towards an observer. Thus this piece of apparatus complements the "Racetrack" chamber and the Mk II chamber, in that it enables the observation of the structure of the discharge, looking along the direction of motion of the discharge. The other chambers are suitable only for the observation of the discharge, looking along the direction of the magnetic field.

FIG A 3.1 A PHOTOGRAPH OF THE RAIL DISCHARGE CHAMBER

Top R.H. Corner - "Squegging" Oscillator.

R.F. applied to copper ring at the R.H. end of the tube.

Viewing port at L.H. end of discharge tube.



The discharge was initiated by a pulse of 5 Mc/sec. radio frequency energy from a "squegging" oscillator, applied to two copper rings around the outside of the discharge tube. The gas broke down at the end of the rails at which the copper rings are located (near the O-ring seals - see figure A 3.1), the discharge being driven along the rails towards the viewing port by the T. M. F.

The discharge was "pulsed" by means of a resistance-capacitance circuit. A capacitor,  $C$ , was charged through a resistance  $R_1$ , and, when the gas broke down, discharged through another resistance,  $R_2$ . The time constants  $R_1C$  and  $R_2C$  were so arranged that the rate at which the capacitor discharged was greater than the rate at which it was charged. The capacitor thus discharged until the glow discharge extinguished, and then charged until breakdown occurred, on a pulse of r.f. This method of pulsing the discharge was not very satisfactory; it is difficult to vary both the discharge current, and the duration of the flow of current. The electrode regions were driven the length of the rails, and often a short discharge back towards the starting point, along the outside of the rails during the period of current flow.

These experiments were not successful, as the positive column of the discharge was only rarely observed to be constricted. The electrode regions were bright, yet the remainder of the discharge tube often appeared to be quite dark. i.e., the "positive

"column" must occupy the entire space surrounding the electrodes.

This is not so very surprising. The r.f. breakdown produces ionization primarily at the outer walls of the discharge tube, near the rings. It is thought that there was not enough time for the current carrying region to "contract" before the discharge extinguished.

Some measurements were made of the thickness of the cathode fall region, and the distance from the cathode of the junction between the negative glow, and the Faraday dark space. The current was adjusted so that the negative glow surrounded a large part of the circumference of the cathode, and the period of current flow was adjusted so that the discharge travelled to the end of the rails. Measurements of these distances were made by means of a Wild level, focussed on the end of the rails. This instrument can only measure vertical distances - i.e., distances parallel to the direction of the magnetic field. Visual observation indicated that the cathode fall region and the negative glow were somewhat thinner in a direction perpendicular to the magnetic field, than in the direction parallel to the field. The difference in the thicknesses was only marked at pressures below about 8 mm. Hg, for a field of 2,160 gauss.

From measurements made at zero magnetic field, and in magnetic fields of up to 5,000 gauss for air, argon, helium,

and hydrogen, it is estimated that the thicknesses of these regions in a direction perpendicular to the magnetic field are not reduced to less than 70% of the zero field value at pressures above 10 mm. Hg. This indicates that, for pressures above 10 mm. Hg, the assumption that the transverse magnetic field does not influence the thickness of the negative glow, or the cathode fall region, is not a bad assumption.

---

## BIBLIOGRAPHY

### B. 1 PAPERS REFERRED TO IN THIS THESIS

- Ad 60 ADDISS, R.R.Jr., PENSAK, L., and SCOTT, Nancy J. - "Seventh National Symposium on Vacuum Technology - Transaction." Ed. C. Robert Meissner, pp. 39-44. Pergamon Press; Oxford, London, New York, Paris, 1960.
- Al 54 ALLIS, W.P., and ROSE, D.J. - Phys. Rev. Vol. 93, p. 84 (1954).
- Al 56 ALLIS, W.P., et al. - "Series of Lectures on the Physics of Ionized Gases." U.S.A.E.C. Report LA-2055 (1955).
- B1 58 BLEVIN, H.A., and HAYDON, S.C. - Australian J. Phys. Vol. 11, pp. 18-34 (1958).
- Br 37 BREWER, A.K., and WESTHAVER, J. - J. Appl. Phys. Vol. 8, p. 779 (1937).
- Br 56 BRECK, D.W., EVERSOLE, W.G., MILTON, R.M., REED, T.B., and THOMAS, T.L. - J. Am. Chem. Soc. Vol. 78, pp. 5963-5971 (1956).
- Br 59 BROWN, S.C. - "Basic Data of Plasma Physics". Technology Press of M.I.T., and John Wiley & Sons. Inc., New York. Chapman and Hall Ltd., London (1959).
- Co 27(a) COMPTON, K.T. - A.I.E.E. Transactions. Vol. 46, p. 868 (1927).
- Co 27(b) COMPTON, K.T., and MORSE, P.M. - Phys. Rev. Vol. 30, p. 305 (1927).
- Co 41 COBINE, J.D. - "Gaseous conductors: theory and engineering applications". Dover Publications, Inc., New York. Constable & Co. Ltd., London (1958). A re-issue of the book first published by McGraw-Hill, New York, in 1941.

- Da 21 DAVY, Sir Humphrey - Phil. Trans Roy. Soc. Pt. I,  
p. 425 (1821).
- Do 37 DOW, W.G. - "Fundamentals of Engineering electronics."  
John Wiley & Sons Inc., New York. Chapman and  
Hall Ltd., London (1937).
- Dr 40 DRUYVESTEYN, M.J., PENNING, F.M. - Revs.  
Modern Phys. Vol. 12, pp. 87-174 (1940).
- Ea 50 EARLY, H.C., and DOW, W.G. - Phys. Rev. Vol. 79,  
p. 186 (1950).
- Ea 58 EARLY, H.C., and DOW, W.G. - "Conference on  
Extremely High Temperatures". Ed. Fischer, H.  
and Mansur, L.C. pp. 187-193. John Wiley &  
Sons Inc., N.Y. Chapman and Hall Ltd., London  
(1958).
- Ec 54 ECKER, G. - Z. Physik. Vol. 136, p. 556 (1954).
- Ec 58 ECKER, G., and MULLER, K.G. - Z. Physik. Vol. 151,  
pp. 577-594 (1958).
- Ec 59(a) ECKER, G., and MULLER, K.G. - J. Appl. Phys.  
Vol. 30, p. 1466 (1959).
- Ec 59(b) ECKER, G., and MULLER, K.G. - Z. Naturforsch.  
Vol. 14, p. 511 (1959).
- Ec 61 ECKER, G. - Ergeb. exakt. Naturwiss. Vol. 33,  
pp. 1-104 (1961).
- El 51 ELENBAAS, W. - "The high pressure mercury vapour  
discharge". North Holland Publishing Co.  
Amsterdam (1951).
- El 61 ELFORD, M.T. - Private Communication. (1961).
- Em 51 EMELEUS, K.G. - "The conduction of electricity through  
gases". Methuen & Co. Ltd., London. John Wiley  
& Sons Inc., N.Y. (3rd Ed. revised, 1951).
- En 34 Von ENGEL, A., and STEENBECK, M. - "Elektrische  
Gesentladungen", Vol. 2. Springer-Verlag, Berlin,  
(1932).

- En 55 Von ENGEL, A. - "Ionized Gases". Oxford University Press, Oxford (1955).
- Fi 56 FINKELNBURG, W., and MAECKER, H. - "Handbuch der Physik". (Ed. S. Flugge). Vol. 22, pp. 254-444. Springer-Verlag, Berlin (1956).
- Fo 55 FOWLER, R.G. - Proc. Phys. Soc. (London). Vol. B 68, pp. 130-136 (1955).
- Fr 56 FRANCIS, G. - "Handbuch der Physik". (Ed. S. Flugge). Vol. 22, pp. 53-208. Springer-Verlag, Berlin (1956).
- Ga 47 GALLAGHER, C.J., and COBINE, J.D. - Phys. Rev. Vol. 71, p. 481 (1947).
- Ga 49 GALLAGHER, C.J. and COBINE, J.D. - Elec. Eng. Vol. 68, p. 469 (1949).
- Ga 50 GALLAGHER, C.J. - J. Appl. Phys. Vol. 21, pp. 768-771 (1950).
- Gr 25 GROTH, W. - Ann. Physik. Vol. 78, (Folge 4), pp. 680-696 (1925).
- Gu 21(a) GUYE, C.-E. and ROTHEN, A. - Arch. des Sci. Phys. Nat. Vol. 3, pp. 441-470 (1921).
- Gu 21(b) GUYE, C.-E. and ROTHEN, A. - Arch. des Sci. Phys. Nat. Suppl. Vol. 3, pp. 87-88 (1921).
- Gu 23(a) GUYE, C.-E. and RUDY, R. - Arch. des Sci. Phys. Nat. Vol. 5, pp. 182-196; 241-251 (1923).
- Gu 23(b) GUYE, C.-E - Arch. des Sci. Phys. Nat. Suppl. to Vol. 5, pp. 121-123 (1923).
- Gu 23(c) GUYE, C.-E - Comptes Rendus Acad. Sci. Vol. 177, pp. 1104-1106 (1923).
- Gu 23(d) GUYE, C.-E. - Comptes Rendus Acad. Sci. Vol. 177, pp. 1282-1285 (1923).
- Gu 27 GUYE, C.-E. and LUYET, B. - Arch. des Sci. Phys. Nat. Vol. 9, pp. 191-217; 247-263 (1927).

- Gu 17 GUYE, C.-E. - Arch. des Sci. Phys. Nat. p. 489 (1917).
- Gu 24 GÜNTHERSCHULZE, A. - Z. Physik. Vol. 24, p. 140 (1924).
- Gu 49 GUTHRIE, A. and WAKERLING, R.K. - "Characteristics of Electrical Discharges in Magnetic Fields". Vol. 5 of Section I of the National Nuclear Energy Series. McGraw Hill, N.Y. (1949).
- Gu 58 GUILE, A.E., and SECKER, P.E. - J. Appl. Phys. Vol. 29, p. 1662 (1958).
- Gu 61 GUILE, A.E., LEWIS, T.J., and SECKER, P.E. - Proc. (Brit.) I.E.E. Pt. C., Vol. 108, pp. 463-470 (1961).
- He 55 HERNQVIST, K.G. and JOHNSON, E.O. - Phys. Rev. Vol. 98, pp. 1576-1583 (1955).
- He 58 HERNQVIST, K.G. - Phys. Rev. Vol. 109, p. 636 (1958).
- Hi 48 HIMLER, G.J. and COHN, G.I. - Elec. Eng. Vol. 67, pp. 1148-1152 (1948).
- Hu 62 HULL, A.W. - Phys. Rev. Vol. 126, pp. 1603-1610 (1962).
- Hu 57 HUXLEY, L.G.H. - Aust. J. Phys. Vol. 10, pp. 240- (1957).
- Jo 48 JOHNSON, G.W. - Phys. Rev. Vol. 73, (1948).
- Ke 57 KESAEV, J.G. - Soviet Physics - "Doklady", Vol. 2, pp. 60-63 (1957).
- La 28 LANE, C.T. - J. Sci. Instr. Vol. 5, p. 214 (1928).
- Le 57 LEE, T.H. - J. Appl. Phys. Vol. 28, p. 920 (1957).
- Le 59 LEE, T.H. - J. Appl. Phys. Vol. 30, pp. 166-171 (1959).
- Le 61 LEWIS, T.J. and SECKER, P.E. - J. Appl. Phys. Vol. 32, pp. 54-64 (1961).

- Li 54 LITTLE, P.F., and Von ENGEL, A. - Proc. Roy. Soc. (London), A. Vol. 224, pp. 209-227 (1954).
- Li 60 LINHART, J.G. - "Plasma Physics". North Holland Publishing Company, Amsterdam (1960).
- Ll 53 LLEWELLYN-JONES, F. - Repts. Prog. Phys. Vol. 16, pp. 217-165 (1953).
- Lo 39 LOEB, L.B. - "Fundamental processes of Electrical Discharges in Gases". John Wiley & Sons Inc., N.Y. (1939).
- Lo 49 LONGINI, R.L. - Phys. Rev. Vol. 71, pp. 642-643 (1949).
- Lo 55 LOEB, L.B. - "Basic Processes of Gaseous Electronics". University of California Press, Berkeley and Los Angeles, Calif. (1955).
- Ma 08 MALLIK, D.N. - Phil. Mag. Vol. 16, pp. 531-550 (1908).
- Ma 51 MAECKER, H. - Ergeb. exakt. Naturwiss. Vol. 25, pp. 293-358 (1951).
- Mi 28 MINORSKY, M.N. - J. Phys. Radium. Vol. 9, (6th series), pp. 127-136 (1928).
- Mo 28 MORSE, P.M. - Phys. Rev. 31, p. 1003 (1928).
- Mo 46 MORTON, P.L. - Phys. Rev. Vol. 79, p. 388 (1946).
- Mo 58 MORTON, A.H. - "A cyclotron injector for a proton synchrotron". A.N.U. Ph.D. Thesis. (1958).
- Mc 51 McBEE, W.D. - "A study of the influence of a strong transverse magnetic field on an unconfined glow discharge in air at about 1 mm. pressure". University of Michigan Ph.D. Thesis. (1951).
- Mc 53 McBEE, W.D., and DOW, W.G. - Trans. I.E.E. Commun. and Electronics, No. 7, pp. 229-239 (1953).

- Pe 57 PENNING, F. M. - "Electrical Discharges in Gases".  
Philips Technical Library. (N.V. Philips'  
Gloeilampenfabrieken) Eindhoven, Holland (1957).
- Pu 56 PUPKE, H. - Naturwissenschaften. Vol. 43, p. 222 (1956).
- Pu 59 PURSER, K. H., and RICHARDS, J. R. - J. Sci. Instr.  
Vol. 36, pp. 142-143 (1959).
- Ra 57 RADIO CORPORATION OF AMERICA TUBE HANDBOOK -  
Radio Corporation of America, Electron Tube Division  
Commercial Engineering. Harrison, New Jersey.
- Re 58 REDHEAD, P. A. - Canad. J. Phys. Vol. 36, pp. 255-  
270 (1958).
- Ri 66 De la RIVE, A. - Arch. des Sci. Phys. Nat. Vol. 27,  
p. 289 (1866).
- Ri 71 De la RIVE, A., and SARASIN, E. - Arch. des Sci. Phys.  
Nat. Vol. 41 (1871).
- Ri 72 De la RIVE, A., and SARASIN, E. - Arch. des Sci. Phys.  
Nat. Vol. 45 (1872).
- Ri 61 RICHARDS, J. - Private Communication (1961).
- Ro 32 ROGOWSKI, W. - Arch. Elektrotech. Vol. 26, p. 643  
(1932).
- Ro 39 ROGOWSKI, W. - Z. Physik. Vol. 114, p. 1 (1939).
- Ro 50 ROTHSTEIN, J. - Phys. Rev. Vol. 78, p. 331 (1950).
- Ro 54 ROBSON, A. E., and Von ENGEL, A. - Phys. Rev. Vol. 93,  
pp. 1121-1122 (1954).
- Ro 55 ROBSON, A. E., and Von ENGEL, A. - Nature, Vol. 175,  
p. 646 (1955).
- Ro 56 ROBSON, A. E., and Von ENGEL, A. - Phys. Rev. Vol. 104,  
pp. 15-16 (1956).

- Ro 57 ROBSON, A. E. , and Von ENGEL, A. - Proc. Roy. Soc. (London) Vol. 243, p. 217 (1957).
- Ro 61 ROSE, D. J., and CLARK, M. Jr. - "Plasmas and Controlled Fusion". M.I.T. Press, Cambridge, Mass. John Wiley & Sons Inc., N.Y., London (1961).
- Sc 24(a) SCHOTTKY, W. - Z. Physik. Vol. 25, p. 343 (1924).
- Sc 24(b) SCHOTTKY, W. - Z. Physik. Vol. 25, p. 635 (1924).
- Se 53 SEELIGER, R. - Z. Naturforsch. Vol. 8a, p. 74 (1953).
- Se 59 SECKER, P.E., and GUILE, A.E. - Proc. (Brit.) I.E.E. Vol. 106, Pt. A. pp. 311-320 (1959).
- Se 61 SECKER, P.E., and GUILE, A.E. - Nature. Vol. 190, pp. 428-429 (1961).
- Sl 26(a) SLEPIAN, J. - Phys. Rev. Vol. 27, p. 249 (1926).
- Sl 26(b) SLEPIAN, J. - Phys. Rev. Vol. 27, p. 407 (1926).
- Sm 42 SMITH, C G. - Phys. Rev. Vol. 62, pp. 48-54 (1942).
- Sm 43 SMITH, C.G. - Phys. Rev. Vol. 64, p. 40 (1943).
- Sm 45 SMITH, C.G. - Phys. Rev. Vol. 67, p. 201 (1945).
- Sm 46 SMITH, C.G. - Phys. Rev. Vol. 69, pp. 96-100 (1946).
- Sm 50 SMITH, C.G. - Phys. Rev. Vol. 83, p. 194 (1950).
- Sm 51 SMITH, C.G. - Phys. Rev. Vol. 84, p. 1075 (1951).
- Sm 57 SMITH, C.G. - J. Appl. Phys. Vol. 28, pp. 1328-1331 (1957).
- So 48 SOMERVILLE, J. M. , CHAMPION, K.S.W., and BIGG, E.K. - Aust. J. Sci. Res. A. Vol. 1, pp. 400-411 (1948).
- So 53 SOMERVILLE, J. M. - "Electrical Discharges in a Magnetic Field". University of Sydney D.Sc. Thesis. Sydney (1953).

- So 59 SOMERVILLE, J. M. - "The Electric Arc". Methuen & Co. Ltd., London. John Wiley & Sons Inc., New York. (1959).
- Sp 50 SPENKE, E. - Z. Physik. Vol. 127, p. 221 (1950).
- Sp 56 SPITZER, Lyman Jr. - "Physics of Fully ionized gases". Interscience Publishers, Inc., New York (1956).
- St 03 STARK, J. - Z. Physik. Vol. 4, p. 440 (1903).
- St 32 STEENBECK, M. - Z. Physik. Vol. 33, p. 809 (1932).
- St 54 St. JOHN, R. M. and WINANS, J.G. - Phys. Rev. Vol. 94, pp. 1097-1102 (1954).
- St 55 St. JOHN, R. M., and WINANS, J.G. - Phys. Rev. Vol. 98, pp. 1664-1671 (1955).
- Ta 29 TANBERG, R. - Nature, Vol. 124, pp. 371-372 (1929).
- To 12 TOWNSEND, J.S. - Proc. Roy. Soc. (London) A. Vol. 86, pp. 571-577 (1912).
- To 21 TOWNSEND, J.S. - Phil. Mag. Vol. 42, pp. 873-891 (1921).
- Ud 52 UDELSON, B.J., and CREEDON, J.E. - Phys. Rev. Vol. 88, p. 145 (1952).
- Va 53 VARNEY, R.N. - Phys. Rev. Vol. 89, p. 708 (1953).
- Ve 59 VENEMA, A. - Vacuum, Vol. 9, pp. 54-57 (1959).
- Wa 54 WARE, A.A. - Proc. Phys. Soc. (London) Vol. A 67 pp. 869-880 (1954).
- Wa 58 WARD, A.L. - Phys. Rev. 112, p. 1852 (1958).
- Wa 62 WARD, A.L. - J. Appl. Phys. Vol. 33, pp. 2789-2794 (1962).
- We 04 WEINTRAUB, E. - Phil. Mag. Vol. 7 (6th Series) pp. 95-124 (1904).

- We 39(a) WEIZEL, ROMPE, R., and SCHON, M. - Z. Physik.  
Vol. 112, p. 339 (1939).
- We 39(b) WEIZEL, ROMPE, R., and SCHON, M. - Z. Physik.  
Vol. 113, p. 87 (1939).
- We 39(c) WEIZEL, ROMPE, R., and SCHON, M. - Z. Physik.  
Vol. 112, p. 730 (1939).
- We 40 WEIZEL, ROMPE, R., and SCHON, M. - Z. Physik.  
Vol. 115, p. 179 (1940).
- Wi 07 WILSON, H.A., and MARTYN, G.H. - Proc. Roy. Soc.  
(London). A. Vol. 79, pp. 417-427 (1907).
- Ya 50 YAMAMURA, S. - J. Appl. Phys. Vol. 21, pp. 193-196  
(1950).
- Ze 59 ZEI, Dino, and WINANS, J.G. - J. Appl. Phys. Vol. 30,  
pp. 1813-1819 (1959).

BIBLIOGRAPHY

B.2 THE MOTION OF AN ARC IN A TRANSVERSE MAGNETIC FIELD - PAPERS PUBLISHED SINCE 1944

BABAKOV, N.A. - Elektrichestvo. Vol. 1, p. 74 (1948).

DUNKERLEY, H.S., and SCHAEFER, D.L. - J. Appl. Phys. Vol. 26, p. 1834 (1955).

EARLY, H.C., and DOW, W.G. - Phys. Rev. Vol. 79, p. 186 (1950).

EARLY, H.C., and DOW, W.G. - "Conference on Extremely High Temperatures". ed. Fischer and Mansur. pp. 187-193. John Wiley, N.Y.; Chapman & Hall, London. (1958).

ECKER, G., and MÜLLER, K.G. - Z. Physik. Vol. 151, pp. 577-594 (1958).

ECKER, G. - Ergebni. exakt. Naturwiss. Vol. 33, pp. 1-104 (1961).

EIDINGER, A., and RIEDER, W. - Physk. Verhandl. Vol. 5, p. 227 (1954).

EIDINGER, A., and RIEDER, W. - Arch. Elektrotech. Vol. 43, p. 94 (1957).

FÉCHANT, M.D. - Revue Générale de l'Electricité. Vol. 68, p. 519 (1959).

GALLAGHER, C.J., and COBINE, J.D. - Phys. Rev. Vol. 71, p. 481 (1947).

GALLAGHER, C.J., and COBINE, J.D. - Elec. Eng. Vol. 68, p. 469 (1949).

GALLAGHER, C.J. - J. Appl. Phys. Vol. 21, pp. 768-771 (1959).

GUILE, LEWIS, and MEHTA - Nature, Vol. 179, pp. 1023-1024 (1957).

- GUILE, A.E., and MEHTA, S.F. - Proc. (Brit.) I.E.E. Vol. 104, p. 533 (1957).
- GUILE, A.E., LEWIS, T.J., and MEHTA, S.F. - Brit. J. Appl. Phys. Vol. 8, pp. 444-448 (1957).
- GUILE, A.E., and SECKER, P.E. - Nature, Vol. 181, p. 1615 (1958).
- GUILE, A.E., and SECKER, P.E. - J. Appl. Phys. Vol. 29, pp. 1662-1667 (1958).
- GUILE, A.E., LEWIS, T.J., and SECKER, P.E. - Proc. (Brit.) I.E.E. Pt. C., Vol. 108, pp. 463-470 (1961).
- HERNQVIST, K.G., and JOHNSON, E.O. - Phys. Rev. Vol. 98, pp. 1576-1583 (1955).
- HESSE, D. - Arch. Electrotech. Vol. 45, p. 188 (1960).
- HIMLER, G.J., and COHN, G.I. - Elec. Eng. Vol. 67, pp. 1148-1152 (1948).
- HOCHRainer, A. - Elin. Z. Vol. 1, p. 61 (1949).
- KESAEV, J.G. - Soviet Physics - "Doklady". Vol. 2, pp. 60-63 (1957).
- LEWIS, T.J., and SECKER, P.E. - J. Appl. Phys. Vol. 32, pp. 54-64 (1961).
- LONGINI, R.L. - Phys. Rev. Vol. 71, pp. 642-643 (1949).
- McBEE, W.D. - "A study of the influence of a strong transverse magnetic field on an unconfined glow discharge in air at about 1mm. pressure". University of Michigan Ph.D. Thesis. (1951).
- McBEE, W.D., and DOW, W.G. - Trans. I.E.E. Commun. and Electronics, No. 7, pp. 229-239 (1953).
- MILLER, C.G. - Phys. Rev. Vol. 93, p. 654 (1954).
- PUPKE, H. - Naturwissenschaften. Vol. 43, p. 222 (1956).

ROBSON, A.E., and Von ENGEL, A. - Phys. Rev. Vol. 93, pp. 1121-1122 (1954).

ROBSON, A.E., and Von ENGEL, A. - Phys. Rev. Vol. 104, pp. 15-16 (1956).

ROBSON, A.E. - "The motion of an arc in a magnetic field". "Proceedings of the 4th International Conference on Ionization Phenomena in Gases." pp. 346-349. North Holland Publishing Company - Amsterdam. (1960).

ROTHSTEIN, J. - Phys. Rev. Vol. 78, p. 731 (1950).

St. JOHN, R.M., and WINANS, J.G. - Phys. Rev. Vol. 94, pp. 1097-1102 (1954).

St. JOHN, R.M., and WINANS, J.G. - Phys. Rev. Vol. 98, pp. 1664-1671 (1955).

SECKER, P.E., and GUILE, A.E. - Proc. (Brit.) I.E.E. Vol. 106, Pt. A. pp. 311-320 (1959).

SECKER, P.E. - "The influence of cathode surface conditions on arc movement." "Proceedings of the 4th International Conference on Ionization Phenomena in Gases". pp. 350-354. North Holland Publishing Company - Amsterdam (1960).

SECKER, P.E. - Brit. J. Appl. Phys. Vol. 11, pp. 385-388 (1960).

SECKER, P.E., and GUILE, A.E. - Nature. Vol. 190, pp. 428-429 (1961).

SECKER, P.E., GUILE, A.E., and CATON, P.S. - Brit. J. Appl. Phys. Vol. 13, pp. 282-287 (1962).

SMITH, C.G. - Phys. Rev. Vol. 62, pp. 48-54 (1942).

SMITH, C.G. - Phys. Rev. Vol. 64, p. 40 (1943).

SMITH, C.G. - Phys. Rev. Vol. 57, p. 201 (1945).

SMITH, C.G. - Phys. Rev. Vol. 69, pp. 96-100 (1946).

SMITH, C.G. - Phys. Rev. Vol. 83, p. 194 (1950).

SMITH, C.G. - Phys. Rev. Vol. 84, p. 1075 (1951).

SMITH, C.G. - J. Appl. Phys. Vol. 28, pp. 1328-1331 (1957).

WARE, A.A. - Proc. Phys. Soc. (London). Vol. A67, pp. 869-880 (1954).

WINSOR, L.P., and LEE, T.H. - Elec. Eng. Vol. 75, p. 408 (1956).

WINSOR, L.P., and LEE, T.H. - Commun. and Electronics (A.I.E.E.), No. 24, pp. 143-148 (1956).

YAMAMURA, S. - J. Appl. Phys. Vol. 21, pp. 193-196 (1950).

YAMAMURA, S. - J. Fac. Eng. Univ. Tokyo. Vol. 25, p. 57 (1957).

ZEI, D., and WINANS, J.G. - J. Appl. Phys. Vol. 30, pp. 1813-1819 (1959).

ZEI, D., St. JOHN, R. M., and WINANS, J.G. - Phys. Rev. Vol. 100, p. 1232 (1955).